HIGH PRECISION RELOCATION OF EARTHQUAKES IN THE SOCORRO SEISMIC ANOMALY, NEW MEXICO

by

John Morton

Submitted in Partial Fulfillment
of the Requirements for the

Master of Science in Geophysics

New Mexico Institute of Mining and Technology
Department of Earth and Environmental Science

Socorro, New Mexico

May, 2008

Abstract

Improved source locations for earthquakes within the Socorro Seismic Anomaly have resulted from the addition of two broadband seismic stations to the existing Socorro (SC) network and application of waveform cross-correlation (WCC) methods to improve picking consistency among events within earthquake clusters for a catalogue of all locatable events from September, 2004 through May, 2007. Data from these new stations lead to more accurate earthquake locations and can aid in the identification of additional events falling under a quality threshold using only data from the permanent SC network. WCC allows comparison of seismic waveforms to eliminate inconsistencies in user-defined picks, thus reducing hypocentral scatter. Use of these relocation techniques aids in the identification of structures that may be responsible for anomalous uplift attributed to the Socorro Magma Body. Local seismicity is characterized by earthquake clusters, closely related events in space, with nearly half of events falling within this category. Earthquake clusters may be due to magmatic injection in the upper crust or due to a mixture of uplift and instability in the upper crust. Currently active areas of cluster activity within the Socorro Seismic Anomaly include the area around Socorro Peak, a group of clusters running southeast from Ladron Peak, a southeast striking structure east of SC network station CAR, and a recurring center of cluster activity near Bernardo. Seismicity patterns suggest that uplift and seismicity correlate spatially. Anomalously

shallow earthquake depths and elevated seismicity near San Acacia may be caused by a shallow (<6 km) magma body or by migration of hydrothermal fluids.

ACKNOWLEDGEMENTS

I would like to thank my advisor, Sue Bilek, and my committee members Rick Aster and Dave Love. Additional thanks go to Los Alamos National Laboratory, which funded this project, and IRIS/PASSCAL for their aid in setting up the temporary seismic network and archiving the data.

LIST OF FIGURES

Figure 1.1: Map of New Mexico with Sanford catalogue of seismicity above Md 1.3 between the years 1962 and 2004 (Sanford et al., 2002; Sanford et al., 2006). The Socorro Magma Body of Balch et al. (1997) is illustrated in the center of the figure (shaded). The Socorro Seismic Anomaly is clear from accentuated seismicity above the Magma Body. Earthquake locations are red dots. 59

Figure 1.2: General geographic provinces in New Mexico showing locally important features such as the Socorro Fracture Zone, Datil-Mogollon Volcanic Field, and Rio Grande Rift. Lines separate geographic provinces. Shaded area is Socorro Magma Body of Balch et al. (1997). 60

Figure 1.3: Fault map of the Socorro Area with major faults labeled. Red line shows boundaries of available 1:24000 quadrangles (See references for citations). Outside of this area, dashed lines are faults from New Mexico State Geologic Map (NMBGMR, 2003). Socorro Accommodation Zone (SAZ) and boundaries of Socorro Caldera from Chamberlin et al. (2004) are displayed in white. 61

Figure 1.4: A more detailed view of geographic features, towns, and roads in and around the Socorro Seismic Anomaly. Dashed lines separate physiographic provinces. A solid black line delineates the Socorro Magma Body of Balch et al. (1997). Red lines are main roads. White boxes are seismic stations. 62

Figure 1.5: Map of Socorro area with Sanford catalogues superimposed. Events from Sanford et al. (2002) catalogue from 1962-1998 are green squares. Events from Sanford et al. (2006) catalogue from 1998-2004 are blue squares. Historical swarms are highlighted. A is a 1989-90 swarm resulting in four events about 4.3. B is proposed historical source for the large events of 1906. C is an early 1990 swarm resulting in 6 events above M_d 3.2, the largest of which was an M_d 3.9 event. All of these areas are present locations of continued seismicity. 63

Figure 1.6: Boundary of the Socorro Magma Body from previous studies. Dashed outline is developed from Sanford et al. (1977) and Rinehart et al. (1979). Solid outline is from Balch et al., 1997. SC (Socorro) network stations and YN (temporary) network stations are white squares. 64

Figure 1.7: Map showing suspected area for a shallow source of magma within the Socorro Seismic Anomaly. The suspect area is the dashed outline. Seismic stations are white squares. 65

Figure 2.1: Seismic waveform from an $M_d = 0.62$ event occurring on November 1, 2005 recorded at station LEM. P, S, SzP, and SzS waves are shown. PzP is not seen in the waveform. 66

Figure 2.2: Stack of interferograms modified from Fialko and Simons (2001) for period from 1992-1999. Redundancy of data results in a cumulative time span of 29.3 years. Scale bar on the left is in cm for 29.3 year stack. Solid line is magma body outline from Balch et al. (1997). Dashed line is from Rinehart et al. (1979). Dashed circles are best fitting model of inflating cracks at ~19km depth. SC and YN stations are white squares.....67

Figure 2.3: Campaign GPS measurements in the Socorro area between 2002 and 2004. A) Map showing GPS stations and horizontal movement from 2002-2003. B) Vertical movement from November, 2002 through November 2003. Uplift of ~2 cm occurs at stations VVRS and BOWL, with all stations in middle transect except SLVR showing uplift. C) Vertical movement from November, 2003 through November, 2004. Subsidence of ~1 cm occurs at stations VVRS and BOWL, with all stations in middle transect except SLVR showing subsidence. Notice anomalously high values near center of second transect in both B and C.....68

Figure 2.4: Map of the Socorro area with heat flow measurements of Barroll and Reiter, (1990) color coded by value in mW/ m^2. Socorro Caldera and Socorro Accomodation Zone are labeled. Coarsely dashed line is area of proposed shallow source.....69

Figure 3.1: Velocity model used for earthquake location originally from Hartse (1991). P and S velocities (Vp and Vs) and Poisson's ratio (v) are displayed for dual layer model. Notice SMB reflector at 18.75 km depth. Raypaths for direct P and S, SzP, PzP, and SzS are shown. P waves are illustrated as solid. S waves are dashed.....70

Figure 3.2: Similar waveforms from a cluster of events associated with the March 29th, 2007 earthquake swarm (cluster 1). Waveforms are from station SNKE. Flat lines near the end of the waveforms are due to zero padding which occurs after shifting a waveform. Event numbers correspond to event numbers in Appendices A and D..71

Figure 3.3: The same cluster from Figure 3.2 displayed in imagesc format, a MATLAB plotting format that represents values as colors. In this format, positive values corresponding to upward movement are displayed as light colors while negative values corresponding to downward movement are displayed as dark colors. Events are displayed prior to (left) and post (right) waveform cross-correlation. Each seismogram is displayed vertically down with time on the y-axis. Of the nine events in the cluster, eight events correlated while one was thrown out of the dataset.....72

Figure 3.4: Waveform stacks after cross-correlation. A) Stacked seismograms of 8 events from Cluster 1 at station SNKE. No discernible lag exists. B) Stacked seismograms of 21 events from Cluster 14 at station CAR. A 0.02 second lag seems to exist, however inclusion of somewhat dissimilar waveforms in stack may be a contributor.....73

Figure 3.5: Figure clearly showing Socorro (SC) network and temporary (YN) network stations PETR and SNKE. Azimuthal gaps above 180° can be noted for stations CAR, BAR, SMC, SBY, BMT, and LPM (excluding ANMO).....74

Figure 3.6: Map with imagesc plot overlay of maximum azimuthal gap within the Socorro SC seismic network. The smallest azimuthal gap (61°) occurs between LEM and WTX. 75

Figure 3.7: Same as Figure 3.6 with addition of YN seismic network stations PETR and SNKE. Minimum azimuthal gap (54°) is now immediately southwest of PETR. ... 76

Figure 3.8: Waveform comparison for an $M_d = 0.62$ event occurring on Nov 1, 2005 at 09:27 GMT. Labelled are P, S, and identifiable reflections. Note clear presence of magma body reflection SzS in both waveforms. 77

Figure 3.9: Basic focal mechanism showing compression (circles) and dilation (triangles). Stations in SC network are labeled. This event is the M 2.3 Oct. 29th 2005 event (Appendix C event 200510300257) 78

Figure 4.1: Map of original locations of all 346 events in catalogue from September, 2004 through May, 2007. SC and YN stations are white squares. Events are red squares. 81

Figure 4.2: Map illustrating clusters used in this study as black rectangles. Catalogue events prior to relocation are red squares. Stations are white squares. 82

Figure 4.3: Relocated earthquakes from clusters displayed as red squares. Seismic stations are white squares. 83

Figure 4.4: a) Waveform comparison aligned on P pick before and after cross-correlation at SC Network station CAR for a cluster of events east of that station. b) Comparison of cluster before and after WCC relocation. White squares are prior to WCC. Orange circles are after WCC. c) Comparison of hypocentral location on 3-d plots before WCC and after WCC. 84

Figure 4.5: Events relocated with YN data as red squares. White squares are SC network stations. 85

Figure 4.6: Events relocated with YN data and waveform cross-correlation. 86

Figure 4.7: Focal mechanisms for all events without alternative interpretations. Date stamp is given in year-month-day-hour-minute. Notice predominance of normal events and presence of dextral strike-slip and oblique strike-slip events. 87

Fig 5.1: Fully relocated catalogue. YN relocations and waveform CC relocations replace original locations where appropriate. If no CC relocation with YN data exists, original location with YN data is used. If no original location with YN data exists, CC relocation without YN data is used. If no YN data or CC relocation exists, original location is used. 88

Figure 5.2: Fully relocated catalogue with superimposed faults from New Mexico 1:24000 quadrangle maps and New Mexico state map. Red line is the boundary of mapped quadrangles. Outline of Socorro Caldera and Socorro Accomodation Zone are labeled. 89

Figure 5.3: Fully relocated catalogue plotted with Sanford catalogues (Sanford et al., 2002; Sanford et al., 2006). Events from this catalogue are in red. Sanford events

are in green (1962-1999) and blue (2000-2004). SC and YN stations are white squares....90

Figure 5.4: Fully relocated catalogue and Sanford catalogues with faults from New Mexico 1:24000 quadrangle maps and New Mexico state map superimposed. Colors are same as Figure 5.3. Red line is the boundary of mapped quadrangles...91

Figure 5.5: Events from the Sanford catalogue from 1962-1998 study superimposed on the InSAR measurements of Figure 2.3....92

Figure 5.6: Events from the Sanford catalogue from 1999-2004 superimposed on the InSAR measurements of Figure 2.3. 93

Figure 5.7: Events from the catalogue of earthquakes from this study superimposed on the InSAR measurements of Figure 2.3....94

Figure 5.8: All earthquake catalogues used in this study superimposed on the InSAR measurements of Figure 2.3. 95

Figure 5.9: Imagesc histogram plot overlaid on shaded relief map. Map is divided into 1 minute bins, and events occurring within each bin are represented by color bar on the right. This map shows events occurring within waveform catalogue. Solid line is outline of Socorro Magma Body. Finely dashed circles are regions of maximum uplift as modeled by Fialko and Simons (2001). Coarsely dashed circle is proposed shallow source. 96

Figure 5.10: Same as figure 5.9 with histogram from waveform catalogue as well as Sanford et al. catalogues. 97

Figure 5.11: Uplift of Fialko and Simons (2001) overlaid by a histogram representing number of events from waveform catalogue occurring within 1 minute bins. Notice the clear relationship between the modeled uplift (dashed lines) and elevated seismicity. 98

Figure 5.12: Maps of Sanford catalogue events for the periods between GPS campaigns led by Newman (Newman et al., 2004). 99

Figure 5.13: Map of events color coded by depth. Only events for which a depth was determined are used in this plot. Of note is the lack of deep events (>6 km) between stations LEM, PETR, and SNKE. 100

LIST OF TABLES

Table 3.1: Example focmec.dat and focmec.out files. The focmec.dat file includes an arbitrary header line and then lines with station name, azimuth, takeoff angle, and polarity of an event at each station. The focmec.out file contains a number of different parameters used in the solution, then a list of possible solutions..... 79

Table 4.1: Latitude, longitude, and elevation of seismic stations from SC and YN networks..... 80

TABLE OF CONTENTS

Chapter 1: Background *1*

1.1 Introduction 1

1.2 Problem 1

1.3 Geological Setting 3

1.4 Local Seismicity 5

1.5 Socorro Magma Body 6

1.6 Uplift 7

1.8 Shallow magma sources, magma injection, and hydrothermal migration 8

1.7 Analogous Features 9

Chapter 2: State of Research *14*

2.1 Mapping the extent of the Socorro Magma Body 14

2.2 Magma Body Uplift 15

2.3 Campaign GPS Measurements 17

Chapter 3: Methods *19*

3.1 Earthquake location 19

3.2 Waveform Cross-correlation 20

Waveform Cross-Correlation in the time domain 21

Waveform Cross-Correlation Scripts 24

3.3 Addition of New Station Data 25

3.4 Focal Mechanisms 27

Chapter 4: Data Catalogue and Results *30*

4.1 Socorro Seismic Network 30

4.2 Catalogue 31

4.3 Waveform Cross-Correlation of Catalogue 32

4.4 YN Data Addition 33

4.5 Focal Mechanisms 34

Chapter 5: Discussion *36*

5.1 Relocation techniques 36

5.2 Seismic structures 38

Individual Clusters 39

5.3 Forces driving seismicity 45

Chapter 6: Conclusions *49*

References *51*
Figures & Tables *59*
Appendix A: Earthquake Catalogue – Initial Locations *101*
Appendix B: Individual event clusters *113*
Cluster 1 114
Cluster 2 117
Cluster 3 120
Cluster 4 123
Cluster 5 126
Cluster 6 129
Cluster 7 132
Cluster 8 135
Cluster 9 138
Cluster 10 141
Cluster 11 143
Cluster 12 146
Cluster 13 149
Cluster 14 152
Appendix C: Focal Mechanism Solutions *155*
Appendix D: Fully Relocated Earthquake Catalogue *170*

This thesis is accepted on behalf of the
Faculty of the Institute by the following committee:

Susan Welsh
Advisor

Carl C Cook

David W. Love

May 9, 2008
Date

I release this document to the New Mexico Institute of Mining and Technology.

Student's Signature

05/09/2008
Date

Chapter 1: Background

1.1 Introduction

The Socorro Seismic Anomaly sits at the intersection of the Rio Grande Rift and the Precambrian Socorro Fracture Zone (Sanford and Lin, 1998). The 5000 km^2 area representing 2% of the state of New Mexico is responsible for ~45% of earthquakes above magnitude 2.5 as determined by duration (Sanford et al., 1995) (Fig. 1.1). Studies using reflected seismic arrivals have determined that this area is underlain by a 3400 km^2 sill-like intrusion of magma residing at 19 km depth (Sanford et al., 1973; Balch et al., 1997). Leveling data (Larsen et al., 1986), and potential geologic evidence (Ouchi, 1983) have suggested that significant uplift is taking place. More recently, Fialko and Simons (2001) used InSAR measurements to determine an average uplift of ~2 mm/yr. Campaign GPS measurements for 2002-2004 have also shown significant uplift and subsidence in the area (Newman et al., 2004).

1.2 Problem

The problem addressed in this research is the determination of structures that may be accommodating uplift in the area. While seismicity is very common in this area, the structures, focal mechanisms, and underlying stresses associated with this seismicity are not clearly understood. In order to answer this question, it is necessary to determine where seismicity is taking place, what characterizes this seismicity in terms of focal mechanisms and clustering of events, and how it is related to uplift of the magma body,

Rio Grande Rift extensional processes, and due to the transition from a well defined Rio Grande Rift in the north into the beginning of the Basin and Range province to the south.

Seismicity in this area should be expected to exhibit several interesting features due to the variety of processes constrained within a relatively small area. Important among the driving forces of seismicity is the Socorro Magma Body. Imprinted over this driving force are the effects of Rio Grande Rift extension, Basin and Range transition, and the Socorro Accommodation Zone. Structures related to Rio Grande Rift extension (Fig. 1.2) are expected to be the most prominent structures observed in this study and may accommodate much of the expansion due to the magma body. In terms of focal mechanisms, normal mechanisms should be predominant in the data set due to Rio Grande Rift extension and magma body inflation.

It is also of interest to determine the temporal and spatial relationship between seismicity and uplift within the Socorro Seismic Anomaly. Recent campaign GPS studies (Newman et al., 2004) have interpreted that on short time scales of less than a year, uplift and subsidence on the centimeter scale take place above the Socorro Magma Body. How these affect seismicity could be determined by comparing the campaign GPS data with previously existing catalogues of seismicity. It could also be determined using continuous GPS whether specific incidents of uplift and subsidence were directly related to seismicity. If seismicity is temporally related to uplift, higher rates of uplift would correlate well with higher rates of seismicity, and sudden changes would be related to events or event clusters.

Due to campaign GPS observations of uplift and subsidence, it has been suggested that a shallow source of magma exists within the center of the seismic anomaly

(Newman et al., 2004). Evidence for this shallower source of magma includes increased uplift and potential cyclic up-down movement of the shallow magma body over short time and spatial scales specifically. Additionally, a seismic gap at depth may exist in the area due to highly elevated geothermal gradient, depending on the age of the feature. Anomalous arrivals from a shallow reflector would also be an interesting observation, though no evidence yet suggests these. Independent from observations of seismicity and deformation, other observations could be used to argue for the existence of shallow sources of magma such as a marked increase in heat flow. Alternatively, an equally valid explanation for this anomalous uplift and subsidence could be migration of hydrothermal fluids, which would also increase heat flow. Independent observations that would corroborate this hypothesis include changes in gravity and geochemistry associated with uplift.

1.3 Geological Setting

The Rio Grande Rift is a well-known extensional regime extending from Chihuahua, Mexico into central Colorado (Fig. 1.2). It is characterized by a sequence of north-south striking asymmetric sediment filled half-grabens (Chapin and Cather, 1994). Seismic experiments (Wilson et al., 2005) have suggested a symmetric region of thinning due to pure shear. The Rio Grande Rift began due to a reversal of Laramide compressional stresses which prevailed as late as the Eocene. This reversal of stresses is thought to have occurred due to subduction and foundering of the Farallon plate, which caused a marked change in asthenospheric flow (Humphreys, 1995). Initiation of rifting closely followed interbedded volcanic andesites and silica-rich ash flows of the Datil-Mogollon volcanic field. During the Oligocene, tensional stresses began to prevail,

producing such features as the Basin and Range Province in addition to the Rio Grande Rift. A possible lull in during the Miocene from 20 to 13 Ma was followed by a surge in volcanic activity, with basalt and rhyolite being the main constituents (Chapin, 1979).

Running through the Socorro area along a northeast trend lies the Morenci lineament (Chapin et al., 1978), an aligned series of late Oligocene calderas and other volcanic features that Chamberlin et al. (2004) interpret as a surface expression of a shear zone of Laramide ancestry. Sanford and Lin (1998) correlate this with other aligned features and seismic signature and refer to it as the Socorro Fracture Zone. This ~85 km wide, ~1400 km long ENE striking lineament has been suggested to be a crustal flaw of probable Precambrian age. This zone is very similar to the Jemez lineament to the north, a well-documented zone of weakness running through northern New Mexico. The Socorro Fracture Zone has been suggested to run from southern Arizona to the panhandle of Oklahoma. Evidence for its existence includes increased seismicity in the region, the existence of accommodation zones which switch the symmetry of half-grabens in the Rio Grande Rift (Chapin and Cather, 1994) and northeast trending faults mapped in parts of New Mexico and as far as the Arizona border (Woodward et al., 1978; Baldridge and Olsen, 1989).

The Socorro Accommodation Zone (Fig. 1.3), a prominent transverse structure cutting through the rift, is a major change in tilt block geometry, and has been suggested to define the southern boundary of the Socorro Fracture Zone (Sanford and Lin, 1998). Chamberlin et al. (2004) suggest that the Socorro Accomodation Zone is evidence of reactivation of the Morenci Lineament shear zone by Rio Grande Rift extension. The

Socorro Accomodation Zone is correlated to a group of caldera eruptions from 24-32 Ma and continued to exude magma every 1-3 million years until ~4 Ma (Chapin, 1989).

North of Socorro, the Albuquerque-Belen basin transitions into the Socorro basin, Jornada del Muerto to the east, and La Jencia Basin to the west (Figure 1.4), representing a major change in rift geometry (Chapin, 1989; Chapin and Cather, 1994). To the north of this zone, the Rio Grande Rift is a narrow series of en echelon basins. South of this zone, the Rift is a series of basins and ranges more than twice as wide as its northern component and eventually transitioning into the Basin and Range province proper. Additionally, the active portion of the rift steps abruptly to the west into the Socorro Basin.

1.4 Local Seismicity

Sitting at the intersection of the Rio Grande Rift and the Socorro Fracture Zone is an unusual area of elevated seismicity commonly referred to as the Socorro Seismic Anomaly (Sanford et al., 1973). This 5000 km^2 area, representing only 2% of the state of New Mexico is responsible for 45% of earthquakes above magnitude 2.5 as determined by duration between 1962 and 1994, and additionally, it is responsible for ~50% of earthquakes in the state with Mercalli intensity of V or greater between 1862 and 1962 (Sanford et al., 1995) (Fig. 1.1). According to Sanford et al. (1995), outside of the Socorro Seismic Anomaly is an aseismic halo in which no significant earthquake activity occurs.

Seismicity in this area usually occurs in clusters and swarms. In this paper, clusters are groups of events occurring within a confined area and include foreshock-mainshock-aftershock sequences, recurring seismicity in an area, and earthquake swarms.

Earthquake swarms are defined as a group of several microearthquakes in a confined area without the presence of a definite mainshock. These swarms may contain several hundred micro-earthquakes. One of the first known of these swarms is also the most severe. From 1906-1907, earthquakes devastated the Socorro area, with some events as great as M 6 (Reid, 1911; Sanford et al., 1977). From 1989 to 1990, swarms ~40 km north of Socorro resulted in four events greater than m_d 4.3 (Sanford et al., 1995) (Fig. 1.5A). A swarm in 1990 also occurred ~30 km ESE of Socorro near Socorro (SC) network seismic station CAR (Fig. 1.5C). Both of these areas continue to be seismically active today. Recent swarm activity during 2005-2007 has occurred ~7 km immediately west of Socorro near seismic station WTX (SC network) (Fig. 1.5B). Recently, this area has been responsible for two major events: a m_d 2.3 event in late October of 2005 (Stankova-Pursley and Bilek, 2005) and a m_d 2.9 event in late May of 2007. Both of these events showed a foreshock-mainshock-aftershock sequence, with hundreds of associated micro-earthquakes occurring before and after the main event.

1.5 Socorro Magma Body

Within the region of the Socorro Seismic Anomaly, there is a strong seismic reflector at 19 km depth interpreted to be indicative of melt contained within a buoyancy-controlled sill (Brown et al., 1987; Glazner and Ussler, 1988). This reflector was originally noticed and mapped using numerous microearthquake arrivals (Sanford et al., 1977) and further verified using seismic reflection tomography (Brown et al., 1980). This feature is ~3400 km^2 and has a maximum slope of less than 1° (Hartse et al., 1992; Balch et al., 1997). The thickness of this feature has been estimated to be ~100 m (Ake and Sanford, 1988; Brocher, 1981). If correct, these dimensions would make the Socorro

Magma Body one of the largest known magmatic intrusions extant within the contintental crust (Fialko and Simons, 2001). Schlue et al. (1996) used finite element modeling of P-to-SV converted phases to determine a likely root for the magma body in the Albuquerque-Belen basin and steeply dipping to the east. The boundaries of the Socorro Magma Body were originally determined using magma body reflections by Sanford et al. (1977) (Fig. 1.6), but more recent studies using a much larger dataset have reevaluated this original boundary (Balch et al., 1997). While it is generally accepted that this change in geometry is due to a better dataset and station coverage, it has also been suggested that this change might be due to short term (decade scale) evolution of the magma body (Fialko and Simons, 2001). Additionally, it has been suggested that based on conductive models of cooling over the course of tens of thousands of years, a consistent source of magma would be required, which may mean that the magma body may be the active portion of a lopolith, a relatively flat topped igneous intrusion, and that due to constraints on its uplift from terrace deposits, it is subsiding isostatically (Fialko and Simons, 2001).

1.6 Uplift

An interesting observation within this region is the anomalous uplift that is occurring in the area above the Socorro Magma Body region. This phenomenon was originally noticed due to leveling surveys conducted in 1911, 1951, and 1980-81 (Larsen et al., 1986). Annual uplift rate estimates were on the order of ~2 millimeters. Additionally, geologic evidence derived from Quaternary terrace deposits has often been interpreted to show a similar trend and uplift rate throughout the Holocene and into the Pleistocene epoch (Bachman and Mehnert, 1978; Ouchi, 1983). Based on the determination that the ~2 mm/year rate is an average over the Holocene and the 100 m

thickness of the magma body as determined by Ake and Sanford (1988) and Brocher (1981), Schlue et al. (1996) estimate that the magma body began forming around 50 ka ago. Another interesting observation by Larsen et al. (1986) is anomalous subsidence of similar amplitude to uplift occurring directly to the north and south of areas of uplift near Belen and south of Socorro. A study of relative horizontal displacement via trilateration between 1972 and 1984 determined that no consistent strain accumulation occurred (Savage et al., 1985), though no measurements of vertical displacement were attempted during this period. Recent studies using InSAR interferometry (Fialko and Simons, 2001), and campaign GPS measurements (Newman et al., 2004) have also shown a great deal of uplift on very short time scales in the area.

1.8 Shallow magma sources, magma injection, and hydrothermal migration

While few research projects have directly addressed the issue of upper crustal extension and magmatic injection above the Socorro Magma Body within the Socorro Seismic Anomaly, a small body of research suggests that such features might exist. An increased Poisson's ratio determined by differences in the velocity of P and S waves in the area suggests the possibility of small, shallow magma bodies in the upper crust (Toppozada and Sanford, 1976). Sanford and Einarson (1982) suggest that the predominance of swarm activity may be due to movements within shallow magma bodies. One of these areas 15 km southwest of Socorro also contains low P wave velocity (Ward, 1980) as well as high attenuation (Carpenter and Sanford, 1985). Recent campaign GPS observations (Newman et al., 2004) have suggested a great deal of uplift and subsidence located near seismic stations PETR and SNKE, between Lemitar and San Acacia possibly due to a shallow source of magma in the area (Fig. 1.7). This

mechanism has been suggested in other areas such as Yellowstone (Dzurisin et al., 1990), where the process of magmatic injection would produce uplift and crystallization and resulting loss of volatiles would produce subsidence. The predominance of one process over the other could determine the resulting vertical displacement.

An alternative to the hypothesis of a shallow magma source is that hydrothermal fluids have some part to play in the uplift and subsidence observed in the area. Hydrothermal potential in the Socorro area has been investigated by other researchers (e.g., Tobin et al., 2005, Barroll and Reiter, 1990), though the migration of hydrothermal fluids within the upper crust has not previously been considered as a major component in uplift and subsidence. However, the contribution of fluid migration to similar geodetic observations in Campi Flegrei near Naples and in Yellowstone National Park has been investigated thoroughly (e.g., Todesco and Berrino, 2005; Dzurisin et al., 1990, Wicks et al., 2006). Todesco and Berrino (2005) conclude that hydrothermal fluid migration in Campi Flegrei is the main contributor to uplift and subsidence based on correlations between geodetic datasets and geochemical and gravity signals. Wicks et al. (2006) conclude that uplift and subsidence in Yellowstone is related to magmatic processes based on lack of a geochemical correlation to uplift.

1.7 Analogous Features

Clear observation and imaging of magma bodies is rare in extensional regimes similar to the Rio Grande Rift (Schlue et al., 1996), though analogs do exist. The Long Valley Caldera in California is one example. It is much smaller in size, with an estimate of its present magma body of 3.2×10^{-2} km^3 (Fialko et al., 2001) versus the Socorro Magma Body, which is ~3400 km^2 and 100 m thick, which is a total volume of ~340

km^3. Uplift rates are much more significant within the caldera, with InSAR interferometry measuring an uplift of 11 cm in the two year period between June 1996 – July 1997 (Fialko et al., 2001). Estimates for a Long Valley magma body depth are on the order of 8-12 km based on uplift modeling (Fialko et al., 2001), though the influence of hydrothermal contributions to uplift is unknown. An additional sill-like feature in the U.S. exists in Death Valley, California. An estimate for its depth based on COCORP profiling is ~15 km (de Voogd et al., 1988), though this feature has not been the subject of a great deal of study. A similar but much more active analogue to the Socorro Magma Body is the Altiplano-Puna magma body in the central Andes, which resides at a similar depth of ~19 km (Chiemlowski et al., 1999). The Altiplano-Puna magma body is ~1 km thick. This body of magma underlies much of and is responsible for the Altiplano-Puna Volcanic Complex, making it the largest active continental magma body in the world. However, unlike the Socorro Magma Body, the Altiplano-Puna Magma Body is related to slab subduction. Magmatic emplacement in rift settings is also a widely observed phenomenon. The East African Rift is an excellent example of a very active modern rift system with incidence of magmatism similar to the early Rio Grande rift (Wright et al., 2006).

Hydrothermal migration in areas of active bradyseism (magmatic or hydrothermal uplift and subsidence) has been thoroughly researched in areas like Campi Flegrei near Naples, Italy and Yellowstone National Park in Wyoming. In both of these areas, significant uplift and subsequent subsidence have been observed (Todesco and Berrino, 2005; Dzurisin et al., 1990). To varying degrees, researchers have debated the

contribution of hydrothermal migration versus magmatic inflation and crystallization as processes responsible for bradyseism.

Campi Flegrei is an active volcanic complex located very near the urban center of Naples, Italy. Due to extensive observations of uplift and subsidence and its potential human impact, it is an area that has undergone extensive study. Due to its position at sea level, historic observations of ground deformation have existed for the last two millenia (Caputo, 1979). The most recent eruption in this area is the Monte Nuovo eruption in 1538 (Di Vito et al., 1987). Recent bradyseismic activity in the area took place in two main pulses: a major uplift of 1.7 m from 1969 through 1972 followed by minor subsidence, and another major event from 1982 through 1984 resulting in a total of 1.8 m of total uplift (Todesco and Berrino, 2005). Todesco and Berrino (2005) state that during the 1982-1984 episode, >15,000 earthquakes were recorded. These earthquakes occurred at depths of less than 4 km and only occurred during phases of uplift.

Determination of a hydrothermal source versus magmatic inflation and crystallization has been approached by two methods: geochemistry (Chiodino et al., 2003), and gravity (Todesco and Berrino, 2005). Both studies have suggested that bradyseism is the result of hydrothermal fluid migration. Chiodino et al. (2003) used chemical variations observed at hydrothermal vents. Specifically they used N_2/H_2O, CO_2/H_2S, and CO_2/H_2O ratios since the beginning of the 1982-1984 uplift episode. These ratios are precisely correlated with periods of uplift and subsidence, with major surges in CO_2 and N_2 after episodes of uplift. Todesco and Berrino (2005) observed significant gravity changes of hundreds of μGal during the same period of observation as Chiodino et al. (2003). Density changes resulting in a higher gravity anomaly are

attributed to displacement of groundwater to a point closer to the surface and pressurization of water vapor and other volatiles to a condensation point. After this process is complete, liquid water vaporizes, returning the area to a pre-crisis density. Major surges in gravity anomaly occur after episodes of uplift, providing evidence for the validity of this model. Of interest to the Socorro area is the fact that Todesco and Berrino (2005) state that a model relying solely on magmatic inflation would require a magma body in the top 6 km of the crust, which has not been observed geophysically in the area.

The Yellowstone Caldera in Wyoming is the largest in North America with the largest distribution of hydrothermal features in the world (Chang et al., 2007). It has extremely high heat flow measurements of ~2000 mW/m^2 (Chang et al., 2007). The most recent eruption in this region occurred at about 70 ka though many researchers still classify the caldera as active (Christiansen, 1984). Geodetic observation of vertical displacement has existed since the first leveling surveys of the area in 1923 (Pelton and Smith, 1979). Pelton and Smith (1979) concluded that between 1923 and 1975, Yellowstone experienced uplift of ~14 mm/year, and Chang et al. (2007) state that based on InSAR and GPS data, Yellowstone experiences maximum average rates of uplift and subsidence on the order of 1-2 cm/year with some stations recording as much as 7 cm of uplift in a year. The most recent period of accelerated bradyseism occurred from 2004-2006 (Chang et al., 2007). This uplift is associated with very high seismicity with several events estimated above moment magnitude 6 in recorded history (Dzurisin et al., 1990)

Despite the relationship between hydrothermal activity and uplift as determined seismically (Waite and Smith, 2002), the influence of hydrothermal migration has been doubted some researchers. One study in particular (Ingebritsen et al., 2001) used a

similar method to Chiodino et al. (2003) of comparing geochemistry of hydrothermal features, in this case chloride flux, and found no evidence of a relationship to uplift. However, Ingebritsen et al. (2001) did not look into N_2/H_2O, CO_2/H_2S, and CO_2/H_2O ratios, which Chiodino et al. (2003) have shown to be effective. Dzurisin et al. (1990) suggest two models for bradyseism in Yellowstone. One is the model of input of basaltic magma into crystallizing rhyolitic magma resulting in uplift and crystallization of the rhyolitic magma resulting in subsidence. The other involves trapping of magmatic fluids at lithostatic pressure beneath an impermeable layer to cause uplift. Once this layer ruptures, fluids escape causing subsidence, and the layer is sealed again by mineral exsolution from these hydrothermal fluids. Dzurisin et al. (1990) suggest that this model would result in decreased gravity anomaly due to displacement of groundwater by water vapor. It should be noted that while this second model is still cited (Chang et al., 2007), Chiodino et al. (2003) and Todesco and Berrino (2005) were able to model bradyseism as well as gravity anomaly increase and hydrothermal geochemistry changes without the presence of an impermeable layer.

Chapter 2: State of Research

2.1 Mapping the extent of the Socorro Magma Body

Three seismic studies in the area have been devoted to mapping the areal extent of the Socorro Magma Body. This has been accomplished in previous studies by determination of reflected phases from the top of the magma body (e.g. Sanford et al., 1977; Rinehart et al., 1979; Balch et al., 1997). The reflected phases used in these studies include (in order of importance and resolvability) SzS (an S wave reflected off of the magma body as an S), SzP (an S wave reflected off of the magma body as a P) and PzP (a P wave reflected off of the magma body as a P) (Fig. 2.1). The first study to use this method was Sanford et al. (1977), which involved 142 SzS arrivals. This study was followed by Rinehart et al. (1979), which used 220 SzS arrivals and COCORP profiles through Socorro (Brown et al., 1987).

The resulting magma body shape was small compared to the most recent outlines (Fig. 1.5). The main chamber of the magma body was an irregular ellipse extending from ~10 km south of Belen to ~10 km northeast of Magdalena. The most striking feature of this early outline was a tail that extended from the southern end of the ellipsoid and underlay the mountains west of Socorro. However, according to Balch et al. (1997), limitations existed in the data from these studies. Most importantly, the original studies were based on a relatively small number of SzS reflections. Station coverage was a

major issue, with little coverage in the south and southeast. Also, the original northern boundary was not constrained by any events.

Balch et al. (1997) used a catalogue of 1181 events with 5455 reflections, including 679 PzP, 2169 SzP, and 2589 SzS reflections. Based on this catalogue, reflection points were determined and a new outline of the Socorro Magma Body was determined. The outline is much larger and much less irregular than those of Sanford et al. (1973, 1977) and Rinehart et al. (1979). The main features of this new outline are a large increase in area to the south and southeast, establishment of the northern boundary to a position further south, and a shape that more closely corresponds to the shape of the Socorro Seismic Anomaly (Fig. 1.5). This correspondence in shape is a very important observation because it suggests a direct link between elevated seismicity in the area and the presence of the Socorro Magma Body. Furthermore, the study also showed that the magma body was very flat, with little evidence for lateral variation in depth.

2.2 Magma Body Uplift

A study by Fialko and Simons (2001) was undertaken to produce a more accurate image of this uplift. Fialko and Simons used Interferometric Synthetic Aperture Radar (InSAR) for seven years between 1992-1999. InSAR is a technique in which two satellite radar images are compared over time. Line of sight changes are determined by changes in phase. Based on line of sight displacements within this period, an average uplift rate of 2-3 mm/yr was observed with greatest uplift near the center of the seismic anomaly around the area of the Rio Salado (Fig. 2.2). Furthermore, subsidence was observed to the northeast and south of the Magma Body, which had also been observed by previous studies (Larsen et al., 1986). Based on modeling of this uplift, Fialko and

Simons found that the superposition of two flat-lying circular cracks of similar size and depth to the Socorro Magma Body produce inflation similar to what is occurring in the area. Circular cracks are used for computational simplicity. This observation is very important in determining that uplift in this area is indeed directly related to the Socorro Magma Body. It has been suggested that this uplift is due to either emplacement of magma or crustal anatexis (Fialko et al., 2001). Additionally, Fialko et al. (2001) suggest that variability in uplift as determined by previous geodetic studies (Larsen et al., 1986) may correspond to variations in the outline of the magma body itself as determined by the seismic studies of Sanford et al. (1973, 1977) and Balch et al. (1997). However, this conclusion may be invalid due to the increase in data points and station coverage of Balch et al. (1997).

Another important consideration addressed by Fialko and Simons (2001) is that based on conductive cooling, a thin sill such as the Socorro Magma Body would not be capable of remaining in liquid state since the late Pleistocene. Two hypotheses they make to explain the existence of this feature are presented. The first hypothesis is that the Socorro Magma Body is more on the order of a few hundred years in age as opposed to tens of thousands. This would allow for the existence of a liquid layer of its current thickness, though it disagrees the model proposed by Ouchi (1983) suggesting similar uplift since the late Pleistocene. The other hypothesis is that dense mafic magma is actively being injected, solidifying and subsiding isostatically. The combination of these factors would result in the current uplift rate.

2.3 Campaign GPS Measurements

Recently, campaign GPS measurements were taken for the years 2002, 2003, and 2004 (Newman et al., 2004) (Fig. 2.3). Vertical movement within this two year period was anomalous, with as much as ~2 cm of uplift in the one year period between 2002 and 2003 and ~1 cm of subsidence between 2003 and 2004. Most of this movement occurred on the center line of the survey, with greatest movement near the center of this line. This corresponds to the area of greatest uplift as seen by Fialko and Simons (2001). The magnitude of uplift in this area is surprising, as is the subsequent subsidence. This trend of movement is of great importance as this phenomenon of "breathing" is often observed in volcanic areas (e.g. Wicks et al., 2006). Newman et al. (2004) hypothesize a shallow source of magma, which would be located around the area of Lemitar and San Acacia near stations PETR and SNKE at a depth of 5-10 km.

Heat flow measurements do not seem to corroborate with this idea however. Barroll and Reiter (1990) published several heat flow measurements for the Socorro Area including the La Jencia Basin, the Socorro Peak area, and a few points stretching into Lemitar and San Acacia (Fig 2.4). In general, The La Jencia and Socorro Basins have low heat flow (~30-70 mW/m^2) while the Socorro and Lemitar Mountains have much higher heat flow (>90 mW/ m^2) with the largest (490 mW/m^2) around station WTX. For a basic comparison, the average continental heat flow is ~65 mW/m^2 (Turcotte and Schubert, 2002). Barroll and Reiter attribute this elevated value to upwelling of deeper groundwater, though they don't rule out the possibility of upper crustal magma. They do not support the idea of deeper-seated hydrothermal sources due to the wide variation of values in a relatively small area. Two points exist within the shallow source region. The first, which sits slightly northeast of station LEM, has a value of 91 mW/ m^2, and the

second, which sits within the Socorro Basin has a value of only 35 mW/ m^2, however this is a fairly shallow well measurement that probably does not reflect deeper hydrothermal processes.

Chapter 3: Methods

3.1 Earthquake location

Initial locations and relocations were performed using the New Mexico Tech in house location program SEISMOS originally developed by Hartse (1991). This program was originally developed to solve the joint hypocentral-velocity model problem in which earthquake locations, a one-dimensional velocity model, and station corrections are determined. The program uses a generalized least squares algorithm to invert for model parameters. The program was also developed to perform this inversion while including reflected phases PzP, SzP, PzS, and SzS from a mid-crustal reflector similar to the Socorro Magma Body as well as Moho reflections and critically refracted head waves. For the purposes of this research, the velocity model and station corrections are held constant. The velocity model used is based on Hartse (1991) (Fig. 3.1). Based upon his work, he showed a ~2.5% decrease in P wave velocity and a decrease in Poisson's ratio at 10 km. The magma body in this model is at a depth of 18.75 km.

Magnitude is determined by using the New Mexico duration magnitude scale (Newton et al., 1976; Ake et al., 1983). The magnitude is based on the equation:

$$M_d = 2.79 \log \tau_d - 3.63, \qquad (1)$$

where M_d is the magnitude and τ_d is the duration from initial P onset until shaking is indiscernible from background noise. Based on this scale, a 10 second event would have a duration magnitude of -0.84, and a 100 second event would have a duration magnitude

of 1.95. This magnitude scale is originally based on and calibrated to the response of Wood-Anderson seismograph recordings. Moment magnitude has been found to be approximately equivalent to duration magnitude and linearly related to $\log\tau_d$ (Hanks and Kanamori, 1979; Richter, 1958).

The process of earthquake location begins with determining arrival times from an event. This is done using software such as Seismic Analysis Code (SAC) or PASSCAL Quick Look (PQL). Along with the pick, a weight of 0 (best) to 9 (worst) is assigned based on possible error associated with the pick. For this project, a weight of 0 had an associated error of 0.1 seconds, with each consecutive weight increasing this error by 0.1 seconds. A data file (picfil.dat) is produced from these picks and weights either through manual entry using the program seisin or through scripts designed to read SAC headers or PQL pick files. Once this file is made, it can be read into SEISMOS along with velocity model (velmod.dat), station coordinates (stacrd.dat), and parameter file (jparam.dat). The station coordinate file stacrd.dat is in km east and north of a point centered at station WTX. The parameter file jparam.dat contains information about what parameters to invert for, number of iterations, maximum error, weighting, and focal depth constraints. Running SEISMOS produces a location file (refloc.dat), which contains location, focal depth (if resolvable), magnitude, origin time, and uncertainty associated with these parameters.

3.2 Waveform Cross-correlation

For many volcanic and tectonic datasets, there are numerous clusters of events containing similar waveforms (e.g. Waite and Smith, 2002; Fehler et al., 2000). To understand why this is the case, one must understand what factors determine the shape of

a seismic waveform. A seismogram is the result of several convolutions. There are, of course contributions due to the instrument and seismometer site properties, but these properties are time invariant. Various sources of noise are also included in this convolution. The signals most important for seismic analysis are those due to the motion that produced the seismic event and the effect of the path along which the seismic wave traveled. During an event cluster, the forces that produce rupture along fault lines will tend to produce earthquakes with similar motion along the fault. Additionally, within a cluster of events, all events occur in a small area relative to the distance of the seismometer recording the events. Therefore, these events will be traveling along similar paths, and their resultant waveforms will be affected by similar structures. This will produce similarity in the waveform itself (Fig. 3.2).

This fact results in methods by which the seismogram dataset can be manipulated. By means of waveform cross-correlation, events can be separated into similar clusters, the phase picks associated with those clusters can be modified such that they agree among each other, and new events can even be identified in a time series. In order to understand how these processes work, it is necessary to understand the underlying concept of waveform cross-correlation.

Waveform Cross-Correlation in the time domain

Waveform cross-correlation is a time-reversed form of convolution. While convolution in discrete time is defined as

$$f * g = \int_{-\infty}^{\infty} f(\tau)g(t-\tau)d\tau = \sum_{j} f_j g_{i-j}, \quad (2)$$

cross-correlation is defined as

$$f \# g = \int_{-\infty}^{\infty} f(\tau) g(t+\tau) d\tau = \sum_j f_j g_{i+j} \,. \quad (3)$$

where f and g are two discrete time signals, τ represents time, and t is a time step. In order to normalize this for every calculation to produce a meaningful basis for comparison, the equation contains additional terms:

$$f @ g = \frac{\sum_j f_j g_{i+j}}{\sqrt{\sum_j f_j^2 \sum_j g_j^2}} \,. \quad (4)$$

The scaled cross-correlation produces a resultant vector h_i containing the correlation of f and g bounded between +1 and -1.

If the two functions f and g contain a similar signal at some point along their length, there will be a maximum along h_i corresponding to the point at which the two functions have the greatest correlation and the signals are best aligned. In the case that these two waveforms are within a cluster, the maximum of this cross-correlation is the lag between the correlated signals in f and g. The amplitude of this maximum, which will vary between 0 and 1, is also the major determinant of the cutoff between clusters of events. This cutoff is the point at which an event is dropped from the dataset.

The basic technique for automatic clustering of events begins by constructing a matrix $M_{i,j}$, for which the entry (i,j) in the matrix is the maximum correlation of events i and j (Rowe et al., 2002). The matrix K is produced by the equation

$$K_{i,j} = 1.001 - M_{i,j} \quad (5)$$

where a value from 1.001 to 1.00001 is used to prevent divide by zero errors. Next, an iterative process begins in which the events i and j where $i \neq j$ with the smallest K value are combined, the ith and jth column and row are removed and a new vector representing the correlation of the cluster is formed and added as a new row and column producing a matrix K^g of dimension N-1 where g is the present iteration and N is the original dimension. There are two means by which this process is terminated. The first involves

the cophenetic correlation. The cophenetic correlation is a measure of the similarity between the original K matrix and a matrix K^c similar to K^g but maintaining the same dimension as the original matrix K. In this matrix, instead of removing any columns or rows, they are replaced. This change in correlation will be greatest when two unrelated events are combined. The more common method is to set a threshold value of this cophenetic correlation and cluster anything greater than that value. While both have been used, the second method may be the most reliable for seismogram clustering (e.g. Rowe et al. 2002). MATLAB's linkage function in its statistics toolbox performs this same process by using the nearest distance between two events. The events can then be divided into clusters by either means. The result of this is a hierarchical structure with main clusters of events and some orphaned events. For the purposes of this research, a first-pass threshold of 0.9 is used. If no events at a station cluster at 0.9, the threshold is reduced to 0.75. Of the 12 clusters on which cross-correlation was used, six clusters used a threshold of 0.9 for at least one station.

Lag adjustments can be made on clusters once they are identified. Two types of lag adjustments are commonly made: a coarse lag adjustment that estimates lag to the nearest sample, and a fine lag adjustment that uses data interpolation to attain sub-sample accuracy. This research uses solely the first type of lag adjustment. Coarse lag adjustment is a simple calculation. The coarse lag between any two events is the lag at which the maximum value of the cross-correlation takes place. Once this lag has been determined, the original seismic wave picks can be shifted to best accomodate these lags through least squares minimization (Fig. 3.3). This method has at least one drawback. Seismic arrivals often do not begin abruptly, so many picks may be systematically too

late. As this method assumes that the picks will be distributed evenly around the arrival time, it may pick an event too late (Rowe, 2000). However, this can be fixed easily if it is noticed by examining higher signal-to-noise event stacks. Such stacks have been created for this data (Fig 3.4), and late picks do not seem to be a problem.

Though this technique has many advantages, some problems do arise in its use. If a clustering threshold is too low, unrelated events may be included in the cross-correlation solution, which not only negatively affects the event in question, but the entire cluster. Additionally, cross correlation based relocation, like all location methods, requires an accurate velocity model. If the velocity model is inaccurate, artifacts that can potentially be misinterpreted as linear features may appear in the relocations.

Waveform Cross-Correlation Scripts

The most important codes used in this cross-correlation research are MATLAB codes originally developed by Rick Aster [NMT]. The first of these codes (prep.m) imports SAC waveforms surrounding picks of interest into MATLAB and bandpass filters them. It also saves arrival times of each pick. The second code (correlate.m) takes the waveforms and picks and performs clustering and cross-correlation. It then solves for coarse lag adjustment using a conjugate gradient least squares solution algorithm. The coarse lag adjustments are added to the arrival times and assigned to an unused SAC header variable. This SAC header variable can be read and pick files made with these new picks, which ideally results in a more accurate earthquake location.

In order to run these codes, it was necessary to create a script designed to cut clusters from my earthquake catalogue based on events falling within a defined area. This script accepts Latitude and Longitude boundaries and checks the location files for

each event. Any events that fall within these boundary conditions are copied into a cluster directory. They are separated into directories for each station, subdirectories for each event at that station, and a copy of the file is provided for each pick on that event (e.g. BAR.P). In this main cluster directory, several additional files are created: a GMT plotting package (Wessel and Smith, 2007) compatible list of locations, a list of event times, station-specific cross-correlation codes copied into each station directories, a script that converts cross-correlated files to alphanumeric and then reads through these to determine lag adjustments and output picfiles based on these, an automated SEISMOS script, a script to output GMT locations of relocated events, and a script to produce a catalogue including all pertinent information about the relocated events including location, origin time, magnitude, and uncertainty.

3.3 Addition of New Station Data

In addition to cross-correlation, an additional facet of this research is the addition of data from two temporary seismic stations. Many studies have been performed on addition of station data to improve earthquake location accuracy, but this is notoriously difficult to quantify. Statistical approaches have been performed by Rabinowitz and Steinberg (1990) and Bai et al. (2006). Hardt and Scherbaum (1994) model ideal networks using simulated annealing, a technique based on the metallurgical process, that moves stations from a starting point in a iterative process to a more useful position. Based on the work of Bai et al. (2006), location error decreases as a power law with increasing picks in up to a 15 station network. At this threshold, location error ceases to decrease.

A commonly used figure for estimating accuracy of an earthquake location based on station coverage is azimuthal gap, or the largest angle between any two stations and an event of interest. If an event is located outside of a seismic network, this value will be greater than 180°, which is considered unacceptable in most seismic networks. The program SEISMOS does not allow for location well outside of the boundaries of the SC network based on marked increase in azimuthal gap. A method by which a single station does not affect the results of a location is the second azimuthal gap, or the largest angle produced between a station and the second station separated from it with respect to an event of interest. Within the SC network (Fig. 3.5), azimuthal gap is smallest in the Socorro area and near Lemitar (60.9°) (Fig. 3.6). Azimuthal gap is worst north of MLM (>324°), but is generally poor outside the boundaries of the network (>180°) and within the network north-northeast of Lemitar approaching Belen (120-180°).

Two temporary, three-component broadband seismic stations SNKE and PETR were installed on either side of Interstate 25 near San Acacia (Fig. 3.5. Refer back to figure 1.3 for reference to towns and roads). These stations are situated over the locus of maximum uplift according to InSAR measurements of Fialko and Simons (2001) as well as campaign GPS measurements by Newman et al. (2004). PETR was installed near Puertocito de Bowling Green in October 2005. SNKE was installed west of San Acacia and began recording in mid-November 2005. The YN network resulted in better azimuthal coverage north and northeast of LEM, with minimum azimuthal gap of 53.9 degrees (Fig. 3.7). Figure 3.8 shows waveforms from PETR and nearby SC network station LEM, which both show similar arrivals of P, S, SzP, and SzS. In addition to using

initial picks from this temporary network of seismic stations, the process of waveform cross-correlation can be performed on the new station data as well.

Due to problems setting up telemetry at these stations, it was determined that it would be easier to pick up the data on a regular basis during maintenance runs. Using Antelope, a database software provided by IRIS PASSCAL, the data were collected and added to the database, then codes provided by IRIS were used to pack the information into archived files and send the archived data to the IRIS Data Management Center for storage.

3.4 Focal Mechanisms

The double couple mechanism of idealized earthquakes produces a distinct radiation pattern that can be utilized to determine the forces responsible for seismic radiation. The first motion of P waves will radiate out from a fault with a compressive nature in areas where the fault block moves toward the receiver and with dilational nature in areas where the fault block moves away from the receiver (Stein and Wysession, 2001). On a vertical component seismogram, compression will appear as up and dilation will appear as down. Based on the up or down motion of these picks, inferences about fault geometry and fault motion can be made.

To determine focal mechanisms, first motion polarities are determined at each station in the network. The azimuth from the source to the receiver is determined based on the location determined by SEISMOS. The takeoff angle, which is the angle between a line pointing straight down from the source and a line pointing to the receiver, is also determined based on the location and depth determined by SEISMOS and the velocity model. SEISMOS outputs both the azimuth and takeoff angle from the source to each

station as part of its inversion. These values as well as polarity are then plotted on a stereonet (Fig. 3.9). Based on visual inspection, the most likely focal mechanisms are determined.

The program FOCMEC is used to determine acceptable focal mechanisms based on input data (Snoke, 2003). This program requires an input file consisting of station name, azimuth, takeoff angle and polarity. The first line of this input file is a header line containing any pertinent information about the event. The script focconvert included with this thesis can be used to read in SEISMOS refloc.dat files and output a *foc.dat file containing azimuth and takeoff angle.

The script focproc is used to determine polarity for a *foc.dat file, run FOCMEC with set options, and plot a focal mechanism. This script opens the associated event folder and brings up a sac window for visual inspection of first motion polarity. After inspection, it allows the user to input either up, down, or uncertain/emergent. An example of the *foc.dat input file and a *focmec.dat output file produced by focproc is illustrated in Table 3.1. Once a focmec.dat file is produced, focmec can be run on the data. Focproc sets nearly all of the options automatically, using the default values for focmec, though with minor changes in the script, changes to these can easily be made. One possible modification that would be useful is to change the number of acceptable solutions focmec will output. The default value is 100. Focproc does prompt for the allowed P polarity errors. For the first iteration, it is advisable to use 0 errors. If no acceptable solutions are determined, this number can be increased as needed in successive runs. Once an event has been run in focproc, the script prompts whether to use the previously existing *focmec.dat file and skip the sac picker process. Focmec

outputs two files: a basic *focmec.out file containing all solutions determined by focmec and a more verbose *focmec.lst file containing detailed information about each solution. Output solutions from focmec contain a strike and dip of one plane and a rake to determine the orientation of the auxiliary plane.

Once focmec has been run by focproc, the script proceeds to plot the focal mechanism using the program FOCPLT. FOCPLT plots the azimuth, takeoff angle, and polarity for each station using the *focmec.dat file as input, and allows the user to input focal mechanism solutions to overlay on this plot. Focproc runs this script automatically, using an average of all acceptable solutions as the focal mechanism plotted. If no acceptable solutions are found, focplt simply plots the polarities without any solutions. If two or more dissimilar focal mechanisms are possible, the average of these will be somewhere in the middle meaning the solution plotted will not make sense. In this case, the script focplotter can be used to manually input strike, dip, and rake data for more than one acceptable solution and run focplt. This script plots the first solution as a solid line and additional solutions (up to 3) as dashed lines. FOCPLT outputs a temp.sgf file which is converted to postscript image using sgf2ps. Focproc and focplotter run these scripts automatically.

Chapter 4: Data Catalogue and Results

4.1 Socorro Seismic Network

The SC Network is a group of seismic stations run by New Mexico Tech including ten stations in the Socorro area and eight stations near the WIPP site in southeastern New Mexico. All of these sites are short period vertical component sites (EHZ) with the exception of LEM, which has north-south and east-west components. Telemetry is set up for all of these stations. Included in the data catalogue used for this research are temporary stations PETR and SNKE. These two stations comprise the temporary network YN. For more information on stations PETR and SNKE, refer to the Methods section and Figure 3.5. Table 4.1 is a list of latitude, longitude, and elevations for all SC network stations in the Socorro area as well as stations PETR and SNKE and United States (US) network station ANMO.

Recording for events in the SC network is all digitally handled by EARTHWORM software (Johnson et al., 1995), a seismic database software that is used to archive data at the Integrated Research Institutions for Seismology Data Management Center in Seattle, allow access to waveforms for recent events, identify possible events, and display near-real time pseudo-helicorder displays online (www.ees.nmt.edu/Geop/eworm-heli//). Three stations at a time in the Socorro area are also backed up by paper records. Data is acquired by way of the program earth2ah, which cuts a time interval specified by the user for all SC network stations as well as

certain US network stations in the southwest. Data can also be requested through the DMC via breq_fast. Earth2ah must be used within five days of an event while breq_fast can only be used after about five days.

4.2 Catalogue

The data used in this research is a catalogue of 346 earthquakes occurring between September 1, 2004 and June 1, 2007 (Appendix A and Fig. 4.1). Basic criteria for inclusion in the catalogue are a minimum of four discernible picks. The largest event in the dataset is a M_d 2.9 occurring on May 23rd, 2007. The smallest event is M_d -0.91. The average magnitude of earthquakes in the catalogue is 0.5. All earthquakes were located using SEISMOS, a hypocentral inversion program capable of using reflected arrivals from the magma body (Hartse, 1991). In addition to the earthquakes from this catalogue, the Sanford catalogues of seismicity above magnitude 1.3 for the years 1962-1998 as well as an additional 80 events from 1999 to 2004 are used to aid in interpretation of seismic features (Sanford et al., 2002).

This catalogue includes a total of 3043 arrival picks including 199 magma body reflections. The median number of picks per event is 8 picks at 6 stations. Based on the 203 events with depth determined, the average depth of earthquakes in the region is 5.7 km with an average first standard deviation of 1 km. The average first standard deviation for lat/long epicentral position is 0.55 minutes, which is approximately equal to .8 km. The average root mean square error for these events is 0.18. For more information, refer to the catalogue of earthquakes included as Appendix A.

4.3 Waveform Cross-Correlation of Catalogue

The process of cross-correlation was performed on 139 events representing all events which fell into a cluster. These events were divided into 14 separate clusters with a minimum of 4 events and a maximum of 29 (Fig. 4.2). Many of the earthquakes occur in the Socorro Basin south of station PETR. Of these, four clusters (cluster # 2, 3, 4, and 5) occur directly around Socorro itself and represent a disproportionately large amount of seismicity. Of the remainder of the clusters, most occur in the north near stations LAZ and SNKE (cluster # 7, 8, 9, 10). One cluster (# 14) occurs ~15 km east of station CAR in an area which has also seen some historic seismicity. Unfortunately, this cluster has a maximum azimuthal gap of well over 180°.

Waveform cross-correlation can have a positive effect in reducing error, however this is dependent on the cluster. In cases of several events occurring in a small geographic region, this process is able to resolve features, but if events are more widely distributed, the process often has a detrimental effect on both resolution and error. This detrimental effect dominates the data, with first standard deviation in location increasing from ~0.55 minutes to ~0.75 minutes. An increase in the standard deviation of this location error after cross-correlation shows that this increase is based on significant outliers in the data. The data before and after cross-correlation are included in Appendix B. Figure 4.3 shows all events after cross correlation.

For the effect of cross-correlation of a single cluster, a good example of the advantages of waveform CC occurs near station CAR (Fig. 4.4 Cluster # 14). For this particular cluster, a qualitative increase in accuracy can be noted on the map. A structure seems to be resolved through this process. This assumes that the structure visible is not an artifact of the location process, however local geology suggests a similar strike for

features near the locus of activity. Unfortunately, the locus of activity sits in the middle of an area of Quaternary basin fill, covering up any salient features. From a quantitative standpoint, first standard deviation in north-south decreases from 0.63 minutes to 0.47 minutes. First standard deviation in east-west decreases from 0.84 to 0.58. First standard deviation in depth decreases from 2.21 to 1.94. This is an example where cross-correlation is clearly advantageous.

4.4 YN Data Addition

Of the events in the waveform catalogue, 97 events were identified which contained discernible arrivals at YN stations PETR or SNKE. These 97 events contain a total of ~1600 picks including both SC and YN stations, which averages out to about 16 phase picks per event. In order to locate these events, the stacrd.dat file was modified to include lines for PETR and SNKE. Picks for YN locations were added to the dataset via concatenation of the original pick file and the formatted YN picks and modification of the header. All YN events (those containing YN picks) were located using SEISMOS in addition to their original locations (Fig. 4.5). In general, the revised locations have significantly reduced error. On average, the reduction in vertical and horizontal 1σ error was from ~.55 minutes to ~.45 minutes.

After the relocation process using YN picks was performed, all YN picks that could be included in clusters were added to the cluster directories. Of the 97 YN events, 62 events were part of a cluster. Five of the 14 clusters (Cluster # 1, 3, 4, 12, 13) in the local network contained YN events. Four of these clusters (Cluster # 1, 3, 4, 13) contained a minimum of four events necessary for waveform cross-correlation. These 62 events contain 151 P and S picks at stations PETR and/or SNKE. Cross-correlation was

performed on the four clusters. Of the four clusters on which cross-correlation could be performed, two of the clusters cross-correlated (Cluster # 1 and 3). Revised YN picks were added to the original pick files and relocated in this case. In the other cases, the original YN picks were added to cross-correlated picks from the other stations (Fig. 4.6). Maps showing original locations, relocations, and relocations using YN picks are included in Appendix B. Tables showing location and associated error are included after each figure.

As with the original attempts at cross-correlation, RMS error and horizontal/vertical error are not reduced by cross-correlation. The original horizontal/vertical 1σ error prior to cross-correlation was 0.55 minutes. After initial cross-correlation, error became 0.75 minutes. After cross-correlation with YN data, error became 0.65 minutes. These numbers clearly show the benefit of additional data for decreasing error in both initial locations and cross-correlated locations.

4.5 Focal Mechanisms

From the waveform catalogue, all 66 events with at least eight discernible P arrivals at SC and YN stations were analyzed to determine focal mechanisms. All events that maintained at least seven arrivals discernible as either up or down were kept in the dataset. A total of 27 events were above this quality threshold (Appendix C). Of these events, 23 had at least one fitting focal mechanism solution assuming a single error was possible in picking event polarity. Seven events possess at least one other significantly different focal mechanism solution.

Of these 23 events, a total of 17 possess predominantly normal fault mechanisms (Figure 4.7). This is consistent with the tectonic regime and actively inflating magma

chambers like the SMB. Eight events had a significant component of strike-slip. All but one of these strike slip events possessed interpreted dextral motion. A dextral component of strike-slip seemed to exist in several events near station WTX, which may suggest the possibility that shear forces still exist in the Socorro Accomodation Zone. Thrust events were only seen in three instances. Eight of the 27 events are in some way associated with an event cluster, and discussion of these events is included in the section on the analysis of individual clusters.

Chapter 5: Discussion

5.1 Relocation techniques

Relocation of earthquakes within the Socorro Seismic Anomaly is an excellent way to determine structures responsible for seismicity in the area. However, it is not by any means perfect and can only provide general information to compare with focal mechanisms and geologic data.

To its credit, the process of earthquake relocation using waveform cross-correlation can produce detailed images of earthquake clusters. Such images can then be used for interpretation. Waveform cross-correlation will sometimes lower error in earthquake location based on 1σ values and RMS error as output by SEISMOS. The difficult task of determination of depth can be performed using waveform cross-correlation. From a qualitative perspective, the precision of earthquake locations is generally increased. Events are more closely located relative to each other, and events generally collapse down onto discernible structures. Moreover, the process is fairly simple and can be performed with pre-existing data sets. From a practical perspective, the process requires negligible resources and very little money.

However, WCC contains its share of limits and drawbacks. In many cases, RMS error and location error increased slightly, and in a several cases, significantly (See individual clusters). Waveform cross-correlation often only ran properly for already tightly constrained clusters. WCC is most effective mainly for stations near a cluster due to low signal to noise ratio as distance from a cluster increases. Threshold values could

not often be found which would include similar events and exclude dissimilar events, which makes the process of automated WCC ineffective. This results in clusters that are constrained with respect to one or two stations, possibly producing a false image of seismic structures. The inclusion of dissimilar events in the cross-correlation process produces outliers in the data which can sit far outside of the locus of a cluster. While clusters that occur in this area can often contain hundreds of events, it is rare that more than a few events are identifiable at enough stations for location, let alone reliable location.

Additionally, secondary phases are unable to be cross-correlated due to low signal to noise ratio. The signals from S, SzS, and SzP are clear on a seismogram, however, removing the signal of preceding waves proves to be difficult, and cannot be done to the extent necessary to use waveform cross-correlation. Attempts to cross-correlate using secondary phases were made, but no meaningful results were produced.

The use of additional station data is the best choice for independent verification of structures. This process often resulted in decreased location error. Quantitatively, it was able to decrease scatter in earthquake clusters. Depth could very accurately be determined as both stations possessed SzP and SzS arrivals. As depth is very valuable, this is one of the major benefits of adding new station data over other forms of earthquake location. Another major benefit is the ability to relocate events outside of earthquake clusters.

Unfortunately, the process of expanding the network is expensive and requires a great deal of field work. Among the necessary costs are sensor, recording equipment, power, site preparation materials, and transportation. Work involves setting up and

testing equipment, planning and building telemetry equipment if it is used, site setup, frequent upkeep of the site, retrieval of data if telemetry is not used, and breakdown of the site and site remediation. The formatting, preparation, and sending to the IRIS data management center of seismic data from these sites is a time-consuming process requiring a large amount of disk space. Recent updates by IRIS have decreased the enigmatic aspects of this process, however, allowing for quicker processing of data.

5.2 Seismic structures

The Socorro area is seismically active in several regions, with nearly half of the earthquakes in the area occurring in swarms. These swarms are often produced along structures that can be inferred by plotting events on a map (Fig. 5.1). Comparison of this data set with previous datasets and determining the relationship to mapped faults aids in interpretation of these structures. Additionally, analysis of focal mechanisms can help to verify observations on maps.

North of station SNKE and east of station LAZ is a group of four small clusters. The orientation of fault associated with these clusters is unclear from the cluster geometry. However, geologic maps suggest that the faults in this region are primarily north-south (Fig. 5.2). Both historic and modern seismic activity is greatest in this area near the Rio Grande, and between the two datasets, a general north-south trend can be seen.

At the far north of the Socorro Seismic Anomaly is a very active small area near Bernardo. The clusters occurring in this area have stayed in the same place for the 45 years that the dataset covers (Fig. 5.3). No structural trends exist directly within this region (Fig. 5.4), however it is responsible for some of the largest earthquakes occurring

in this area in recent history with four events about magnitude 4.3 between 1989 and 1990. To the north of this locus of activity sit a series of north-south en echelon faults including the West Ceja and Sabinal faults (McCraw et al., 2006). To the south is the Cliff Fault (Connell and McCraw, 2007).

To the east-southeast of station CAR is a recurring cluster (14) at odds with the general trend of Socorro earthquakes. The trend of events in this area suggests a northwest-southeast structure. No focal mechanisms could be determined based on these events due to their inability to be constrained on all sides. These events lie outside of the Socorro Seismic Network and have an azimuthal gap of ~225°.

Individual Clusters

Maps of each individual cluster before and after cross-correlation and with addition of YN data are included in Appendix B along with indexed catalogues of the events themselves. Cluster interpretations are aided by Figure 5.2, which shows the fully relocated catalogue with superimposed faults from the New Mexico State Geologic Map (NMBGMR, 2003), Figure 5.3, which shows the fully relocated catalogue with the Sanford catalogues, and Figure 5.4, which shows the fully relocated catalogues, the Sanford catalogues, and superimposed faults.

Cluster 1 is a group of 12 events occurring between stations LEM and PETR. Cross-correlation at station SNKE required a threshold of 0.75. Most events in the cluster occurred on March 29th, 2006. The largest events in the cluster are M_d 0.89 and M_d 0.96, both occurring on March 29th, 2006. Before and after cross-correlation, the events within this cluster appear to be related to a north-south structure. Cross correlation with YN data suggests that depths are $\leq$5 km. Apart from one event

(ind#73), all locations decreased in error after cross-correlation and YN data addition. This is of considerable interest because this area is the region of the suggested shallow source of magma. Focal mechanisms from the March 29th, 2006 events agree with the lineation as seen on the map with clear north-south oriented normal fault motion. The trend of this particular cluster fits well with the Cliff Fault to the north and may suggest that the Cliff Fault extends further south than previously mapped.

Cluster 2 is a group of 9 events occurring east of station WTX directly beneath the New Mexico Tech golf course. At station SMC, the threshold value used was 0.9. Most events occurred from mid-January to early February of 2005. However, the largest of these events (M_d 0.92) occurred on December 12th, 2005 as an isolated event resulting in several felt reports. The cluster occurs near the southern terminus of a mapped north-south oriented fault which ends near Lemitar to the north. The single depth determined for this cluster was 0.41 km for the December 12th event, however a great deal of error (+/- 11.12 km) is associated with this depth. After cross correlation, error in location increases by approximately .2 minutes

Cluster 3 is a group of 21 events occurring in the immediate area of station WTX. At station WTX, the threshold value used was 0.9. Most events are related to the foreshock/aftershock sequence of the October 30th, 2005 M_d 2.3 event (Stankova-Pursley and Bilek, 2005), which resulted in numerous felt reports. This event is not included in the dataset due to clipping of the seismic waveform, which occurred to some degree at all stations. After inclusion of YN data, four more events were above minimum four pick threshold for location in SEISMOS. After cross-correlation and YN data addition, a north-north west striking structure is resolved, which matches the orientation of faults in

the area. Error is well constrained in all cases and does not change significantly after WCC. Focal mechanisms from the main shock agree with this fault orientation and suggest normal fault movement.

Cluster 4 is a group of 12 events occurring to the west of station WTX. At station BAR, a threshold of 0.75 was used. Most events are related to a swarm in early April, 2005. The largest of these events was M_d 1.36. After cross-correlation and YN data addition, little exists to suggest any structures. However, taken into account with events taking place after waveform cross-correlation was performed in late 2006 and early 2007, two structures become visible: a northwest striking feature agreeing well with mapped faults and a transverse east-west striking feature which is unmapped. Error in locations increases after WCC, but decreases again after inclusion of YN data. Location error along the transverse feature suggests that this is probably not a real structure. Additionally, focal mechanisms for two events from early April suggest normal fault motion on a northwest-southeast striking fault plane. The first event (200504021653, ind#82) clearly shows a northwest striking structure, while the second (200504022248, ind#85) has two possible focal mechanisms, one of which strikes north-northwest (Appendix C).

Cluster 5 is a group of 12 events occurring directly southwest of station WTX. At station WTX, a threshold of 0.75 was used. Many of these events are related to a swarm in early January of 2006. The largest of these events (M_d 0.85) occurred on January 2nd, 2006. This area contains a variety of depths from 4 to 10 km that are well constrained by magma body reflections. Error after WCC increases significantly, with 1st standard deviation above 1 arc-minute for most events. The features present in the maps seem to

be consistent with the general northwest-southeast strike of events in the area. A focal mechanism for the January 2nd, 2006 event suggests dextral strike-slip along a southwest dipping fault plane.

Cluster 6 is a group of 6 events occurring south of station WTX. At station CAR, the threshold used was 0.9. Most of these events occur from mid-April to early May of 2005. All of these events are above M_d 0.50, with the largest event being an M_d 1.27 event on May 11, 2005. No clear structure can be seen from maps of these events before or after cross correlation, and they are located in an area with complex fault structures at the surface. Error increases to more than double its initial value after WCC.

Cluster 7 is a group of 6 events occurring northwest of station SNKE and southeast of Ladron Peak. At station LEM, the threshold used was 0.75. Half of these events occurred on June 1st and 2nd, 2005. The largest event occurred on February 23rd, 2005, with M_d 1.82. Error is largely unaffected by WCC, and no features are resolved. However this cluster lies east of the Silver Creek fault, and a focal mechanism suggests normal movement on a north-south oriented structure. While the Sliver Creek Fault cannot be responsible as it is a west-dipping structure, the fault orientation and focal mechanism suggest other faults at depth with similar strike.

Cluster 8 is a group of 6 events occurring north-northeast of station SNKE and directly north of the Rio Salado. At station LEM, a threshold of 0.9 was used. Most events occur in late November to December of 2004, with the largest event (M_d 1.33) occurring November 25, 2004. No features are resolved, however cross-correlation does collapse the six events into a tight cluster. Error is decreased after WCC in all cases. These events lie on the Loma Blanca fault north of Rio Salado.

Cluster 9 is a group of 7 events occurring between PETR and SNKE directly beneath Rio Salado. At station LEM, the threshold value used was 0.75. These events are not temporally closely related, though most occur in the first half of 2005. The largest event (M_d 0.67) occurred on January 9th, 2005. Most events seem to occur at ~7-8 km. Error is not significantly affected by WCC in early 2005, but events in June and September of 2005 correlate poorly with earlier events and error is increased in these cases. In these later events, error of initial locations is 0.49 arc-minutes or more. These events occur along a portion of the Cliff Fault not mapped on the 1:24000 scale San Acacia quadrangle (Machette, 1978). This along with Cluster 8 suggests an active graben between the Cliff Fault and the Loma Blanca fault.

Cluster 10 is a group of 7 events occurring directly to the southeast of cluster 9. No discernible swarms exist in the area. Additionally, no stations were capable of cross-correlation above a threshold of 0.6. The largest event is an M_d 1.05 event on December 31st, 2006. In all of these events, the error is very large (0.43 – 1.77 arc-minutes), and WCC increases this error in all cases. These events lie further south along the Cliff Fault to the north of San Acacia proper. This event, along with clusters 1 and 9, provides further evidence for present day activity of the Cliff Fault.

Cluster 11 is a group of 4 events occurring east of station LEM near Lemitar. At LEM, the threshold used was 0.75. The events exhibit no swarm activity. The largest event is an M_d 0.63 event on January 11, 2006. Events are generally oriented in a northwest-southeast manner. After WCC, error increases from an initial value of 0.34-0.78 arc-minutes to 0.73-1.57 arc-minutes. This cluster is situated near the northern terminus of the same fault as cluster 2. According to the Socorro 1:24000 quadrangle

(Chamberlin, 1999), this fault dips to the west, suggesting a full graben between it and the Socorro Canyon Fault.

Cluster 12 is a group of 4 events occurring south of station PETR and northeast of Socorro. At station BAR, a threshold of 0.9 was used. All events are related to a swarm on April 25th, 2006. The largest event in this group has a duration magnitude of 0.22. After WCC, error increases, but once YN data is added, error drops below its initial value. This cluster of events lies directly beneath the Veranito Fault at a depth of 6 to 9 km. This cluster may be located along the Veranito Fault or possibly along a northern extension of the Coyote Fault.

Cluster 13 is a group of 11 events occurring near station LPM at the northeastern corner of the Socorro Seismic Anomaly. Four events are related to a swarm in late June of 2006. The largest event (M_d 0.88) occurred in October of 2004. No station was capable of cross correlation above a threshold of 0.5, possibly due to the larger area taken up by this cluster. Error is above 1 arc-minute in nearly all initial locations, and is negatively affected by WCC, but the addition of YN data decreased the error to below 1 in all but 3 events. Cross-correlation does not resolve any features in this case, but mapped faults suggest normal movement along northeast-southwest oriented faults as the Socorro basin opens into the Albuquerque-Belen basin.

Cluster 14 is the aforementioned cluster near CAR. At station CAR, the threshold used was 0.9. This cluster consists of 28 events. All but one event are related to a swarm on June 4th-8th, 2005. The largest event (M_d 1.38) occurred on June 5th, 2005. After cross-correlation, these earthquakes collapse onto a very well defined northwest-southeast striking structure, and error in location is significantly reduced. This structure

is well-supported by previous earthquakes occurring in the Sanford catalogues, though this cluster sits in the middle of Quaternary basin fill with no mapped faults. Depth is very well-constrained for these events, and relocation clearly shows deeper events to the northeast. However, no migration of these events with time is apparent in the data.

5.3 Forces driving seismicity

Based upon all of the information presented concerning fault geometry derived from relocated earthquake clusters and earthquake focal mechanisms, it is possible to make inferences about the current state of stress and forces driving present seismicity. Data that will be brought into consideration include orientation of faults, present knowledge about the region and interpretation of focal mechanism solutions, and cluster data.

A clear trend in the data can be seen when comparing the uplift rates of Fialko and Simons (2001) and the earthquake catalogues. Uplift and seismicity correlate well. This trend does not migrate or change with time in any of the catalogues: the Sanford et al. (2002) catalogue (Fig. 5.5), the Sanford et al. (2006) catalogue (Fig. 5.6), or the waveform catalogue from this study (Fig. 5.7). The combination of these three catalogues is displayed in Figure 5.8.

To more quantitatively compare events on a spatial scale, a count was performed for 1 arc-minute bins within an area including highest uplift. Boundaries of this area were 33° 53" N and 34° 30" N, and 107° 7" W and 106° 35" W. The result of this was a group of 1221 bins containing a total of 312 events from the waveform catalogue and a further 290 from the Sanford et al. catalogues (Fig. 5.9). Of these bins, 14 occur within

the suspect shallow source region, and 824 occur within the region of active inflation as defined by the circular crack model of Fialko and Simons (2001).

Seismicity is well correlated with uplift on a spatial scale. While the area of uplift as defined by Fialko and Simons takes up 67.5% of the bin area, 87% of events (270 events) from the waveform catalogue occur within this region (Figure 5.10), and 87.2% of events (525 events) from all catalogues occur within this region (Figure 5.11). If the bins of active seismicity near CAR are removed (26 events, 3 bins in waveform catalogue; 50 events, 11 bins in all catalogues) then 94.4% of events in the waveform catalogue occur within the region, and 95.1% of events from all catalogues occur within the region. On a temporal scale, the relationship is not as clear-cut. The Sanford et al. catalogues were used to compare seismicity above 1.3 between the two GPS campaigns (Figure 5.12). During the first campaign, only 8 events above M_d 1.3 occurred. During the second campaign, 14 events above M_d 1.3 occurred. This is insufficient information to compare the two years, and the catalogue should contain all locatable events. Continuous GPS would also be helpful, but it is not necessary to successfully analyze the temporal correlation between uplift and seismicity.

The case for further elevated seismicity within the proposed shallow source region is less convincing. The shallow source region represents 1.15% of the total map and lies completely within the area of modeled uplift of Fialko and Simons (2001). This region is responsible for 1.28% (4 events) of waveform catalogue events and 1.33% (8 events) of events from all catalogues, however, this elevated seismicity is characteristic of the region of active uplift. The shallow source represents 1.7% of the region of active uplift and contains 1.48% of waveform catalogue events and 1.52% of all catalogue

events within the region of modeled uplift. These lines of evidence, in addition with the possible heat flow data of Barroll and Reiter (1990) argue against the existence of a shallow magma body or active hydrothermal migration in the area. However, a lack of events below 6 km exists within the region and needs to be explained (Figure 5.13). Another study of heat flow inside and outside the area of the proposed shallow source may be necessary to verify the heat flow measurements of Barroll and Reiter (1990). Future studies should also search for anomalous arrivals in the area consistent with a shallow source to provide solid evidence of its presence.

Seismicity is seemingly related to two processes as determined by focal mechanisms and cluster locations: Rio Grande Rift extension as evidenced by the large percentage of normal motion earthquakes occurring on North-South oriented faults and expansion of the Socorro Magma Body. Socorro Magma Body expansion is inferred to be a driving force in the area as evinced by the spatial relationship between uplift and seismicity. Rio Grande Rift extension is clear in the north-south trend of seismic structures and large majority of normal focal mechanisms. Complex fault geometry resulting in events with a significant oblique component is also possible. Focal mechanisms are predominantly normal and north-south to northwest-southeast striking. The effect of the Socorro Accomodation Zone is a possible candidate to explain the presence of oblique strike-slip near WTX interpreted to be dextral in nature, though it cannot be said whether there is a clear-cut connection between these oblique strike-slip events and accommodation.

The seismically active area near Bernardo may be an area of future interest. Relatively large earthquakes for the area have occurred in this region, though this area

seems to have little relationship with any mapped faults. No stations were able to correlate clustered events in this area, suggesting a possible variety of mechanisms. However, no focal mechanisms could be determined due to lack of sufficient phase picks and large azimuthal gap. Additionally, depth could not be determined for any of these events. This may require processes like hydrothermal migration or even magmatic injection.

Chapter 6: Conclusions

Earthquakes within the Socorro Seismic Anomaly occur along roughly north-south structures related to the Rio Grande Rift. Active seismicity has been verified on the Socorro Canyon Fault, the Loma Blanca Fault, the Loma Pelada Fault, the Ladron Fault, the Veranito Fault, and the Cliff Fault. Active graben formation exists between the Cliff Fault and the Loma Blanca Fault. A smaller graben exists between the Socorro Canyon Fault and a fault that runs between the NMT golf course and Lemitar. Sense of motion on all of these faults is generally normal with a component of strike-slip near WTX, either due to structural complexity in the area or due to the Socorro Accommodation Zone.

Uplift and seismicity have been compared using earthquake locations and the InSAR data of Fialko and Simons (2001). A very convincing spatial relationship between uplift and seismicity occurs within the Socorro Seismic Anomaly. This suggests that seismicity itself is driven by uplift. No temporal relationship could be accurately determined based on the limited dataset.

The case for a shallow source of magma or hydrothermal migration has been weakened by lack of elevated seismicity relative to the region of uplift within the Socorro Seismic Anomaly. Heat flow measurements may suggest that the geothermal gradient in the area may not be elevated significantly, though only shallow wells exist within the

proposed shallow source. However, a lack of earthquakes below six kilometers still allows for the possibility that such a feature exists.

Future work should be devoted to processing the continuous GPS data currently being collected at the permanent GPS stations near the former locations of PETR and SNKE. Comparison with seismicity will aid in determining the temporal relationship between uplift and seismicity. Modern heat flow data from the San Acacia area should help to verify the presence or absence of shallow magma or hydrothermal fluids, while definitive verification could be achieved by observation of reflected phases from a shallow magma body.

References

Ake, J. P., and Sanford, A. R., 1988, New evidence for the existence and internal structure of a thin layer of magma at mid-crustal depths near Socorro, New Mexico: Bulletin of the Seismological Society of America, v. 78, no. 3, p. 1335-1359.

Ake, J. P., Sanford, A. R., and Jarpe, S. J., 1983, A magnitude scale for central New Mexico based on signal duration: New Mexico Institute of Mining and Technology: Geophysics Open-file Report, v. 45, p. 26.

Bachman, G. O., and Mehnert, H. H., 1978, New K-Ar dates and the late Pliocene to Holocene geomorphic history of the central Rio Grande region: New Mexico: Geological Society of America Bulletin, v. 89, no. 2, p. 283–292.

Bai, L., Wu, Z., Zhang, T., and Kawasaki, I., 2006, The effect of distribution of stations upon location error: Statistical tests based on the double-difference earthquake location algorithm and the bootstrap method: Earth Planets Space, v. 58, no. 2, p. e9-e12.

Balch, R. S., Hartse, H. E., Sanford, A. R., and Lin, K., 1997, A new map of the geographic extent of the Socorro mid-crustal magma body: Bulletin of the Seismological Society of America, v. 87, no. 1, p. 174-182.

Baldridge, W. S., and Olsen, K. H., 1989, The Rio Grande Rift: American Scientist, v. 77, no. 3, p. 240-247.

Barroll, M. W., and Reiter, M., 1990, Analysis of the Socorro hydrogeothermal system, central New Mexico: Journal of Geophysical Research, v. 95, p. 21949-21964.

Brocher, T. M., 1981, Shallow velocity structure of the Rio Grande rift north of Socorro, New Mexico: A reinterpretation: Journal of Geophysical Research, v. 86, no. B6, p. 4960-4970.

Brown, L., Wille, D., Zheng, L., DeVoogd, B., Mayer, J., Hearn, T., Sanford, W., Caruso, C., Zhu, T. F., and Nelson, D., 1987, COCORP: New perspectives on the deep crust: Geophysical Journal International, v. 89, p. 47-54.

Brown, L. D., Chapin, C. E., Sanford, A. R., Kaufman, S., and Oliver, J., 1980, Deep

structure of the Rio Grande Rift from seismic reflection profiling: Journal of Geophysical Research, v. 85, no. B9, p. 4773-4800.

Caputo, M., 1979, Two thousand years of geodetic and geophysical observation in the Phlegrean Fields near Naples: Geophysical Journal International, v. 56, no. 2, p. 319-328.

Carpenter, P. J., and Sanford, A. R., 1985, Apparent Q for upper crustal rocks of the Central Rio Grande Rift: J. Geophys. Res, v. 90, no. B10, p. 8661-8674.

Cather, S. M., 2002, Preliminary geologic map of the San Antonio 7.5 minute quadrangle, Socorro County, New Mexico: New Mexico Bureau of Geology and Mineral Resources, scale 1:24000.

-, 2007, Preliminary geologic map of the Cañon Agua Buena quadrangle, Socorro County, New Mexico: New Mexico Bureau of Geology and Mineral Resources, scale 1:24000.

Cather, S. M., and Colpitts, J., R. M., 2005, Preliminary geologic map of the Loma de las Cañas 7.5 minute quadrangle, Socorro County, New Mexico: New Mexico Bureau of Geology and Mineral Resources, scale 1:24000.

Cather, S. M., Colpitts, J., R. M., and Hook, S. C., 2005, Preliminary geologic map of the Mesa del Yeso 7.5 minute quadrangle, Socorro County, New Mexico: New Mexico Bureau of Geology and Mineral Resources, scale 1:24000.

Cather, S. M., and Read, A. S., 2003, Preliminary geologic map of the Silver Creek 7.5 minute quadrangle: New Mexico Bureau of Geology and Mineral Resources, scale 1:24000.

Chamberlin, R. M., 1999, Preliminary geologic map of the Socorro 7.5 minute quadrangle, Socorro County, New Mexico: New Mexico Bureau of Geology and Mineral Resources, scale 1:24000.

-, 2004, Preliminary geologic map of the San Lorenzo Spring 7.5 minute quadrangle, Socorro County, New Mexico: New Mexico Bureau of Geology and Mineral Resources, scale 1:24000.

Chamberlin, R. M., Cather, S. M., Nyman, M., and McLemore, V., 2001, Preliminary geologic map of the Lemitar 7.5 minute quadrangle, Socorro County, New Mexico: New Mexico Bureau of Mines and Mineral Resources, scale 1:24000.

Chamberlin, R. M., Eggleston, T. L., and McIntosh, W. C., 2002, Preliminary geologic map of the Luis Lopez 7.5 minute quadrangle, Socorro County, New Mexico: New Mexico Bureau of Geology and Mineral Resources, scale 1:24000.

Chamberlin, R. M., McIntosh, W. C., and Eggleston, T. L., 2004, 40Ar/39Ar geochronology and eruptive history of the eastern sector of the Oligocene Socorro caldera, central Rio Grande rift, New Mexico, *in* Cather, S. M., McIntosh, W. C., and Kelley, S. A., eds., Tectonics, geochronology, and volcanism in the Southern Rocky Mountains and Rio Grande rift, Bulletin 160: Socorro, New Mexico Bureau of Geology and Mineral Resources, p. 251-279.

Chamberlin, R. M., and Osburn, G. R., 2006, Preliminary geologic map of the Water Canyon quadrangle, Socorro County, New Mexico: New Mexico Bureau of Geology and Mineral Resources, scale 1:24000.

Chang, W. L., Smith, R. B., Wicks, C., Farrell, J. M., and Puskas, C. M., 2007, Accelerated Uplift and Magmatic Intrusion of the Yellowstone Caldera, 2004 to 2006: Science, v. 318, no. 5852, p. 952-956.

Chapin, C. E., 1979, Evolution of the Rio Grande Rift: A summary, *in* Rieker, R. E., ed., Rio Grande Rift--Tectonics and Magmatism, American Geophysical Union, p. 1-5.

-, 1989, Volcanism along the Socorro accommodation zone, Rio Grande rift, New Mexico, *in* Chapin, C. E., and Zideck, J., eds., Field Excursions to Volcanic Terranes in Western United States, Volume 1: Southern Rocky Mountains, N. M. Bur. Mines Miner. Resour., Memoir 46, p. 46-57.

Chapin, C. E., and Cather, S. M., 1994, Tectonic setting of the axial basins of the northern and central Rio Grande rift: Basins of the Rio Grande rift: Structure, stratigraphy, and tectonic setting: Geological Society of America Special Paper, v. 291, p. 5–25.

Chapin, C. E., Chamberlin, R. M., Osburn, G. R., White, D. W., and Sanford, A. R., 1978, Exploration framework of the Socorro geothermal area, New Mexico, *in* Chapin, C. E., and Elston, W. E., eds., Field Guide to Selected Cauldrons and Mining Districts of the Datil-Mogollon Volcanic Field, New Mexico, New Mex. Geol. Soc., Special Publication 7, p. 114-129.

Chiodini, G., Todesco, M., Caliro, S., Del Gaudio, C., Macedonio, G., and Russo, M., 2003, Magma degassing as a trigger of bradyseismic events: The case of Phlegrean Fields (Italy): Geophysical Research Letters, v. 30, no. 8, doi:10.1029/2002GL016790.

Chmielowski, J., Zandt, G., and Haberland, C., 1999, The Central Andean Altiplano-Puna Magma Body: Geophysical Research Letters, v. 26, no. 6, p. 783-786.

Christiansen, R. L., 1984, Yellowstone magmatic evolution: Its bearing on understanding large-volume explosive volcanism, Explosive Volcanism, Its Inception, Evolution and Hazards: Washington D.C., National Academy of Sciences, p. 84-95.

Connell, S. D., and McCraw, D. J., 2007, Preliminary geologic map of the La Joya NW quadrangle, Socorro, New Mexico: New Mexico Bureau of Geology and Mineral Resources, scale 1:24000.

de Moor, M., Zinsser, A., Karlstrom, K. E., Chamberlin, R. M., Connell, S. D., and Read, A. S., 2005, Preliminary geologic map of the La Joya 7.5 minute quadrangle, Socorro County, New Mexico: New Mexico Bureau of Geology and Mineral Resources, scale 1:24000.

de Voogd, B., Serpa, L., and Brown, L., 1988, Crustal extension and magmatic processes; COCORP profiles from Death Valley and the Rio Grande Rift: Bulletin of the Geological Society of America, v. 100, no. 10, p. 1550-1567.

Di Vito, M., Lirer, L., Mastrolorenzo, G., and Rolandi, G., 1987, The 1538 Monte Nuovo eruption (Campi Flegrei, Italy): Bulletin of Volcanology, v. 49, no. 4, p. 608-615.

Dzurisin, D., Savage, J. C., and Fournier, R. O., 1990, Recent crustal subsidence at Yellowstone Caldera, Wyoming: Bulletin of Volcanology, v. 52, p. 247-270.

Fehler, M. C., Phillips, W. S., House, L., Jones, R. H., Aster, R., and Rowe, C. A., 2000, Improved Relative Locations of Clustered Earthquakes Using Constrained Multiple Event Location: Bulletin of the Seismological Society of America, v. 90, no. 3, p. 775-780.

Fialko, Y., and Simons, M., 2001, Evidence for on-going inflation of the Socorro magma body, New Mexico, from Interferometric Synthetic Aperture Radar imaging: Geophysical Research Letters, v. 28, no. 18, p. 3549-3552.

Fialko, Y., Simons, M., and Khazan, Y., 2001, Finite source modelling of magmatic unrest in Socorro, New Mexico, and Long Valley, California: Geophysical Journal International, v. 146, no. 1, p. 191-200.

Glazner, A. F., and Ussler Iii, W., 1988, Trapping of magma at midcrustal density discontinuities: Geophysical Research Letters, v. 15, no. 7, p. 673-675.

Hanks, T. C., and Kanamori, H., 1979, A moment magnitude scale: J. Geophys. Res, v. 84, no. 2, p. 348–350.

Hardt, M., and Scherbaum, F., 1994, The design of optimum networks for aftershock recordings: Geophys. J. Int, v. 117, p. 716–726.

Hartse, H. E., 1991, Simultaneous Hypocenter and Velocity Model Estimation Using Direct and Reflected Phases from Microearthquakes Recorded Within the Central Rio Grande Rift, New Mexico: Ph.D. Dissertation, New Mexico Institute of Mining and Technology, 251 pp.

Hartse, H. E., Sanford, A. R., and Knapp, J. S., 1992, Incorporating Socorro magma body reflections into the earthquake location process: Bulletin of the Seismological Society of America, v. 82, no. 6, p. 2511-2532.

Humphreys, E. D., 1995, Post-Laramide removal of the Farallon Slab, Western United States: Geology, v. 23, no. 11, p. 987-990.

Ingebritsen, S. E., Galloway, D. L., Colvard, E. M., Sorey, M. L., and Mariner, R. H., 2001, Time-variation of hydrothermal discharge at selected sites in the western United States: implications for monitoring: Journal of Volcanology and Geothermal Research, v. 111, no. 1, p. 1-23.

Johnson, C. E., Bittenbinder, A., Bogaert, B., Dietz, L., and Kohler, W., 1995, Earthworm: A Flexible Approach to Seismic Network Processing: Incorporated Research Institutions for Seismology (IRIS) Newsletter, v. 14, no. 2, p. 1-4.

Larsen, S., Brown, L., and Reilinger, R., 1986, Evidence of ongoing crustal deformation related to magmatic activity near Socorro, New Mexico: Journal of Geophysical Research, v. 91, p. 6283-6292.

McCraw, D. J., Love, D. W., and Connell, S. D., 2006, Preliminary geologic map of the Abeytas quadrangle, Socorro County, New Mexico: New Mexico Bureau of Geology and Mineral Resources, scale 1:24000.

Machette, M. N., 1978, Geologic Map of the San Acacia quadrangle, Socorro County, New Mexico: United States Geological Survey Geologic Quadrangle Map GQ-1415, scale 1:24000.

Newman, A., Chamberlin, R. M., Love, D. W., Dixon, T. H., and La Femina, P., 2004, Rapid Transient Deformation From a Shallow Magmatic Source at the Socorro Magma Body, NM, USA, *in* American Geophysical Union, Fall Meeting, San Francisco.

Newton, C. A., Cash, D. J., Olsen, K. H., and Homuth, E. F., 1976, LASL seismic programs in the vicinity of Los Alamos, New Mexico: Los Alamos Scientific Laboratory: Informal Report LA–6406–MS, 42 pp.

NMBGMR, 2003, Geologic Map of New Mexico: New Mexico Bureau of Geology and Mineral Resources.

Ouchi, S., 1983, Effects of Uplift on the Rio Grande over the Socorro Magma Body, New Mexico: New Mexico Geological Society, Guidebook to the, v. 34.

Pelton, J. R., and Smith, R. B., 1979, Recent Crustal Uplift in Yellowstone National Park: Science, v. 206, no. 4423, p. 1179-1182.

Rabinowitz, N., and Steinberg, D. M., 1990, Optimal configuration of a seismographic network: A statistical approach: Bulletin of the Seismological Society of America, v. 80, no. 1, p. 187-196.

Read, A. S., Cather, S. M., Chamberlin, R. M., Connell, S. D., and Karlstrom, K. E., 2007, Preliminary geologic map of the Ladron Peak quadrangle, Socorro County, New Mexico: New Mexico Bureau of Geology and Mineral Resources, scale 1:24000.

Reid, H. F., 1911, Remarkable earthquakes in Central New Mexico in 1906 and 1907: Bulletin of the Seismological Society of America, v. 1, no. 1, p. 10-16.

Richter, C. F., 1958, Elementary Seismology: San Francisco, 768 pp.

Rinehart, E. J., Sanford, A. R., and Ward, R. M., 1979, Geographic extent and shape of an extensive magma body at mid-crustal depths in the Rio Grande rift near Socorro, New Mexico: Rio Grande rift: Tectonics and magmatism: American Geophysical Union, p. 237–251.

Rowe, C. A., 2000, Correlation-based Phase Pick Correction and Similar Earthquake Family Identification in Large Seismic Waveform Catalogues: Ph.D. Dissertation, New Mexico Institute of Mining and Technology, Department of Earth and Environmental Science, 172 pp.

Rowe, C. A., Aster, R. C., Phillips, W. S., Jones, R. H., Borchers, B., and Fehler, M. C., 2002, Using Automated, High-precision Repicking to Improve Delineation of Microseismic Structures at the Soultz Geothermal Reservoir: Pure and Applied Geophysics, v. 159, no. 1, p. 563-596.

Sanford, A. R., Alptekin, O., and Toppozada, T. R., 1973, Use of reflection phases on microearthquake seismograms to map an unusual discontinuity beneath the Rio Grande rift: Bulletin of the Seismological Society of America, v. 63, no. 6-1, p. 2021-2034.

Sanford, A. R., Balch, R., and Lin, K., 1995, A seismic anomaly in the Rio Grande rift near Socorro: New Mexico: Seismological Research Letters (abstract), v. 66, no. 2, p. 44.

Sanford, A. R., and Einarsson, P., 1982, Magma chambers in rifts: Continental and Oceanic Rifts, American Geophysical Union, Washington, DC, p. 147–168.

Sanford, A. R., Lin, K., Tsai, I., and Jaksha, L. H., 2002, Earthquake catalogs for New Mexico and bordering areas: 1869–1998, Circular 210, New Mexico Bureau of Geology and Mineral Resources.

Sanford, A. R., and Lin, K. W., 1998, Evidence for a 1,400 km long Socorro Fracture Zone: New Mexico Institute of Mining and Technology: Geophysics Open-file Report, v. 89, p. 18.

Sanford, A. R., Mayeau, T. M., Schlue, J. W., Aster, R., and Jaksha, L. H., 2006, Earthquake catalogs for New Mexico and bordering areas II: 1999 - 2004: New Mexico Geology, v. 28, no. 4, p. 99-109.

Sanford, A. R., Mott, R. P., Shuleski, P. J., Rinehart, E. J., Caravella, F. J., Ward, R. M., and Wallace, T. C., 1977, Geophysical evidence for a magma body in the vicinity of Socorro: New Mexico: in Heacock, JG, ed., The earth's crust, its nature and physical properties: American Geophysical Union Monograph, v. 20, p. 385-404.

Savage, J. C., Lisowski, M., and Prescott, W. H., 1985, Strain accumulation in the Rocky Mountain states: Journal of Geophysical Research, v. 90, no. B12, p. 10310-10320.

Schlue, J. W., Aster, R. C., and Meyer, R. P., 1996, A lower crustal extension to a midcrustal magma body in the Rio Grande Rift, New Mexico: J. Geophys. Res, v. 101, p. 25,283–25,291.

Snoke, J. A., 2003, FOCMEC: FOcal MEChanism determinations, *in* Lee, W. H. K., Kanamori, H., Jennings, P. C., and Kisslinger, C., eds., International Handbook of Earthquake and Engineering Seismology: San Diego, Academic Press, Chapter 85.12.

Stankova-Pursley, J., Bilek, S. L., Rowe, C. A., and Aster, R. C., 2008, Characteristics of the October 2005 microearthquake swarm and the reactivation of seismic swarms over decade-scale time periods near Socorro, New Mexico: Bulletin of the Seismological Society of America, v. 98, p. 93-105.

Stankova-Pursley, J., and Bilek, S., 2006, Characterization of the October 2005 microearthquake swarm in the Socorro region, *in* NMGS Annual Spring Meeting, Socorro, NM.

Stein, S., and Wysession, M., 2002, Introduction to Seismology, Earthquakes, and Earth Structure, Blackwell Publishing, 498 pp.

Tobin, H. J., Baars, R. M., Norman, D., Owens, L., and Cumming, W., 2005, Geophysical Investigations to Assess Geothermal Energy Potential, Socorro Peak, New Mexico, *in* American Geophysical Union, Fall Meeting 2005, San Francisco.

Todesco, M., and Berrino, G., 2005, Modeling hydrothermal fluid circulation and gravity signals at the Phlegraean Fields caldera: Earth and Planetary Science Letters, v. 240, p. 328-338.

Toppozada, T. R., and Sanford, A. R., 1976, Crustal structure in central New Mexico interpreted from the gasbuggy explosion* Present address: California Division of Mines and Geology, Sacramento, California: Bulletin of the Seismological Society of America, v. 66, no. 3, p. 877-886.

Turcotte, D. L., and Schubert, G., 2002, Geodynamics: New York, Cambridge University Press, 528 p.

Waite, G. R., and Smith, R. B., 2002, Seismic evidence for fluid migration accompanying subsidence of the Yellowstone Caldera: Journal of Geophysical Research, v. 107, no. B9, 2177.

Ward, R. M., 1980, Determination of three-dimensional velocity anomalies within the upper crust in the vicinity of Socorro, New Mexico, using P arrival times from local microearthquakes: Ph. D. Dissertation, New Mexico Institute of Mining and Technology, Socorro, New Mexico, 239 pp.

Wessel, P., and Smith, W. H. F., 1991, Free Software Helps Map and Display Data: EOS Trans. AGU, v. 72, p. 441, 445-446.

Wicks, C., Thatcher, W., Dzurisin, D., and Svarc, J., 2006, Uplift, Thermal Unrest, and Magma Intrusion at Yellowstone Caldera: Nature, v. 440, p. 72-75.

Wilson, D., Aster, R., Ni, J., Grand, S., West, M., Gao, W., Baldridge, W. S., and Semken, S., 2005, Imaging the seismic structure of the crust and upper mantle beneath the Great Plains, Rio Grande Rift, and Colorado Plateau using receiver functions: J Geophys Res, v. 110, doi:10.1029/2004JB003430.

Woodward, L. A., Callender, J. F., Seager, W. R., Chapin, C. E., Gries, J. C., Shaffer, W. L., and Zilinski, R. E., 1978, Tectonic map of the Rio Grande rift region in New Mexico, Chihuahua, and Texas: New Mexico Bureau of Mines and Mineral Resources.

Wright, T. J., Ebinger, C., Biggs, J., Ayele, A., Yirgu, G., Keir, D., and Stork, A., 2006, Magma-maintained rift segmentation at continental rupture in the 2005 Afar dyking episode: Nature, v. 442, p. 291-294.

Figures & Tables

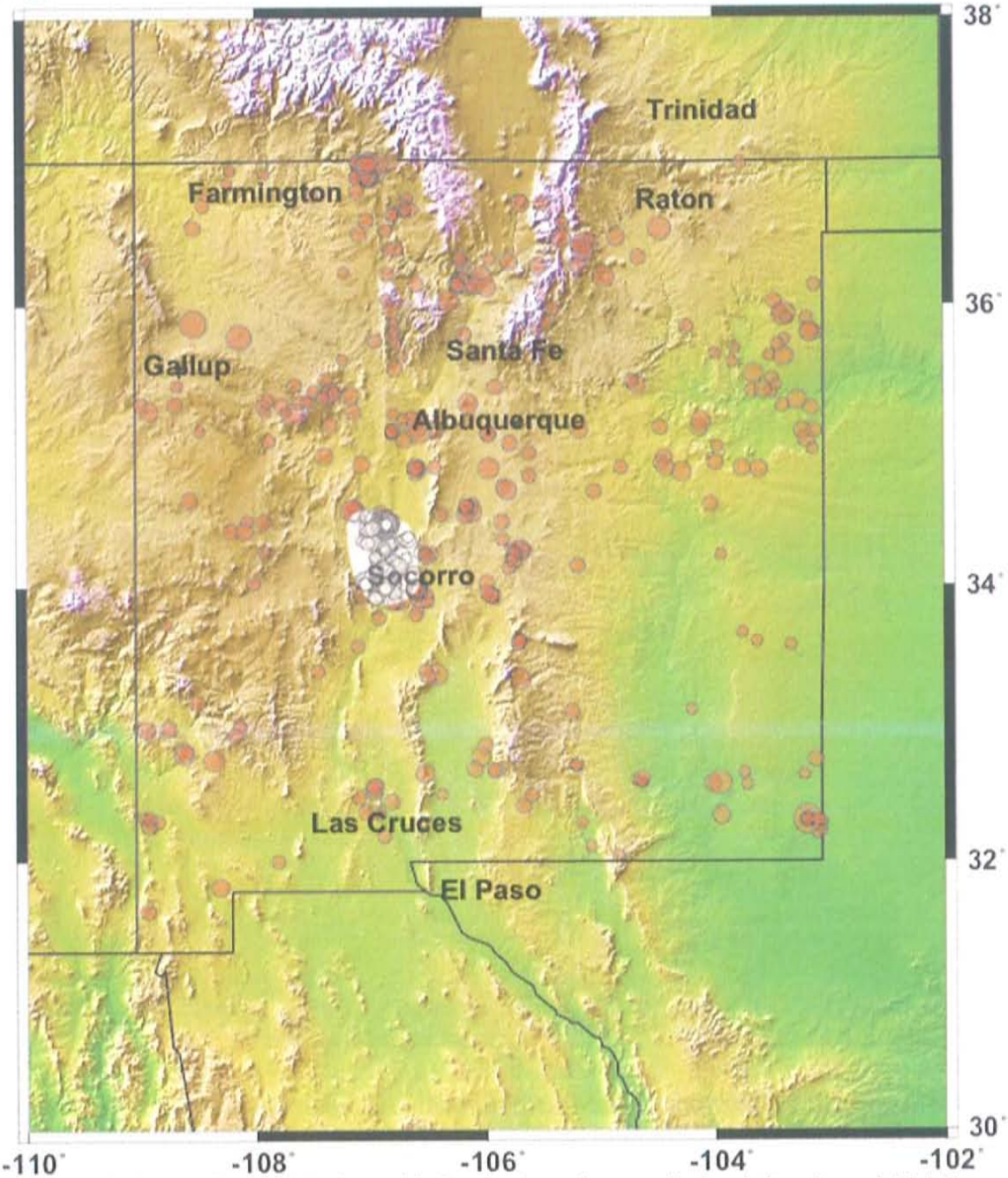

Figure 1.1: Map of New Mexico with Sanford catalogue of seismicity above Md 1.3 between the years 1962 and 2004 (Sanford et al., 2002; Sanford et al., 2006). The Socorro Magma Body of Balch et al. (1997) is illustrated in the center of the figure (shaded). The Socorro Seismic Anomaly is clear from accentuated seismicity above the Magma Body. Earthquake locations are red dots.

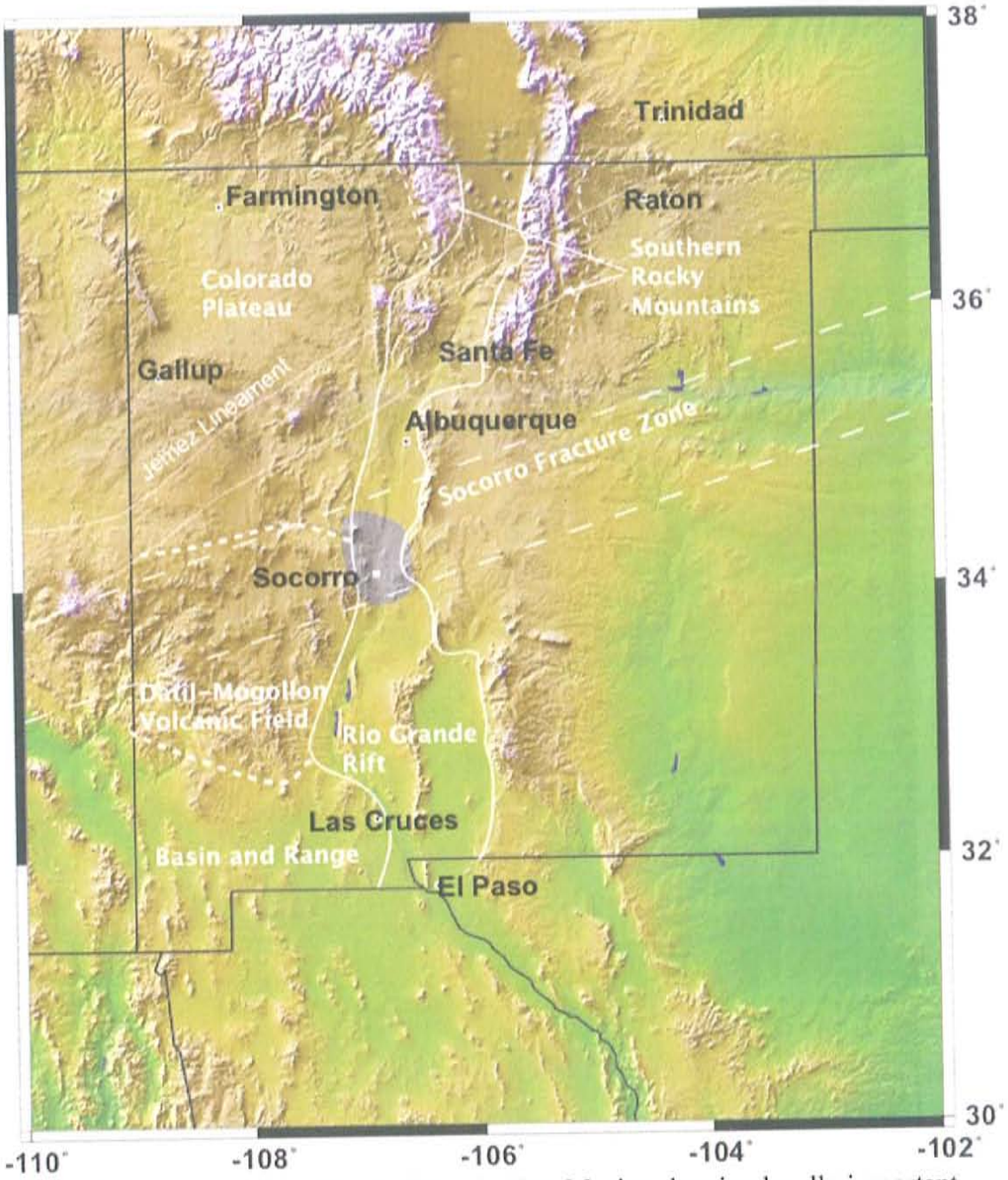

Figure 1.2: General geographic provinces in New Mexico showing locally important features such as the Socorro Fracture Zone, Datil-Mogollon Volcanic Field, and Rio Grande Rift. Lines separate geographic provinces. Shaded area is Socorro Magma Body of Balch et al. (1997).

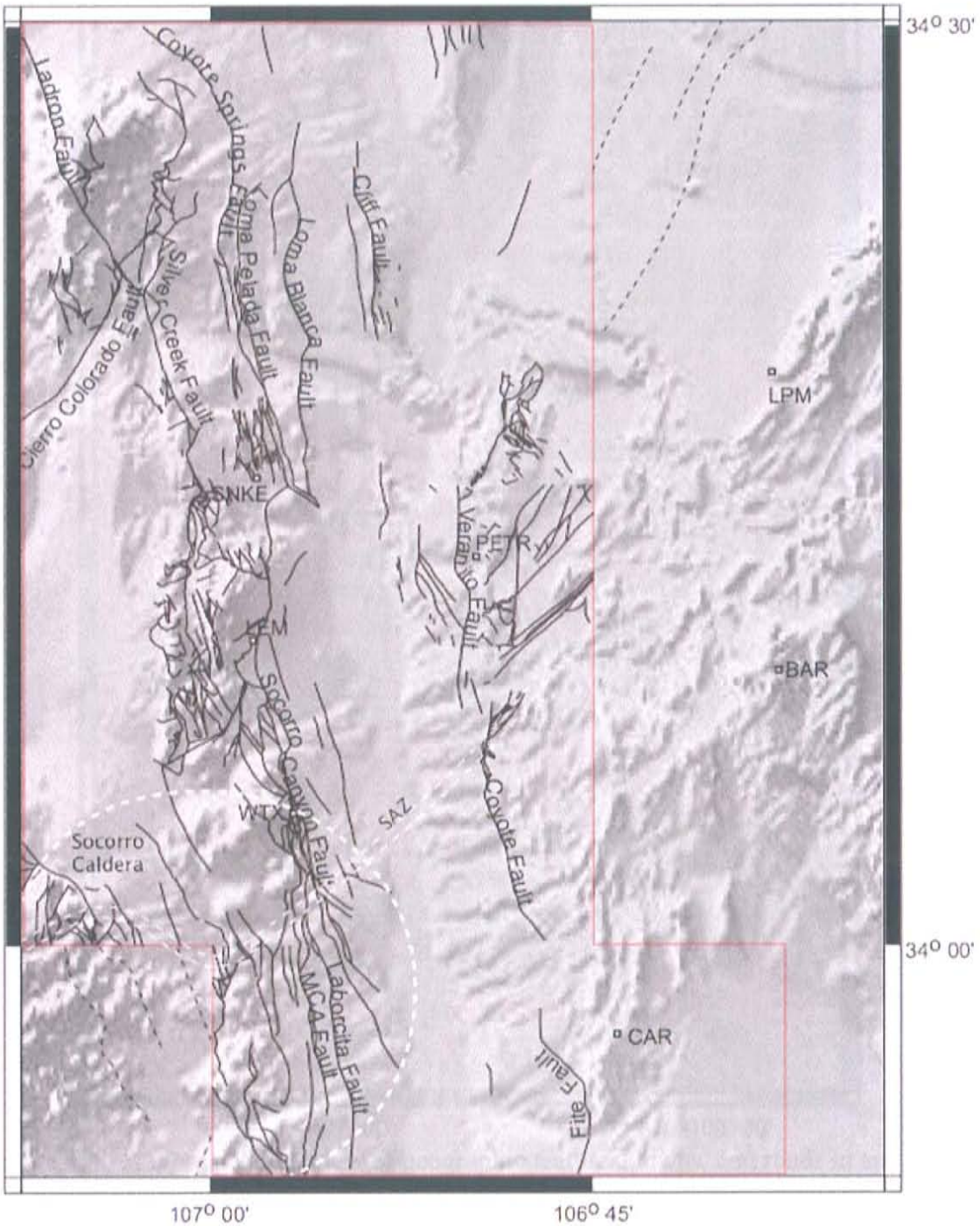

Figure 1.3: Fault map of the Socorro Area with major faults labeled. Red line shows boundaries of available 1:24000 quadrangles (See references for citations). Outside of this area, dashed lines are faults from New Mexico State Geologic Map (NMBGMR, 2003). Socorro Accommodation Zone (SAZ) and boundaries of Socorro Caldera from Chamberlin et al. (2004) are displayed in white.

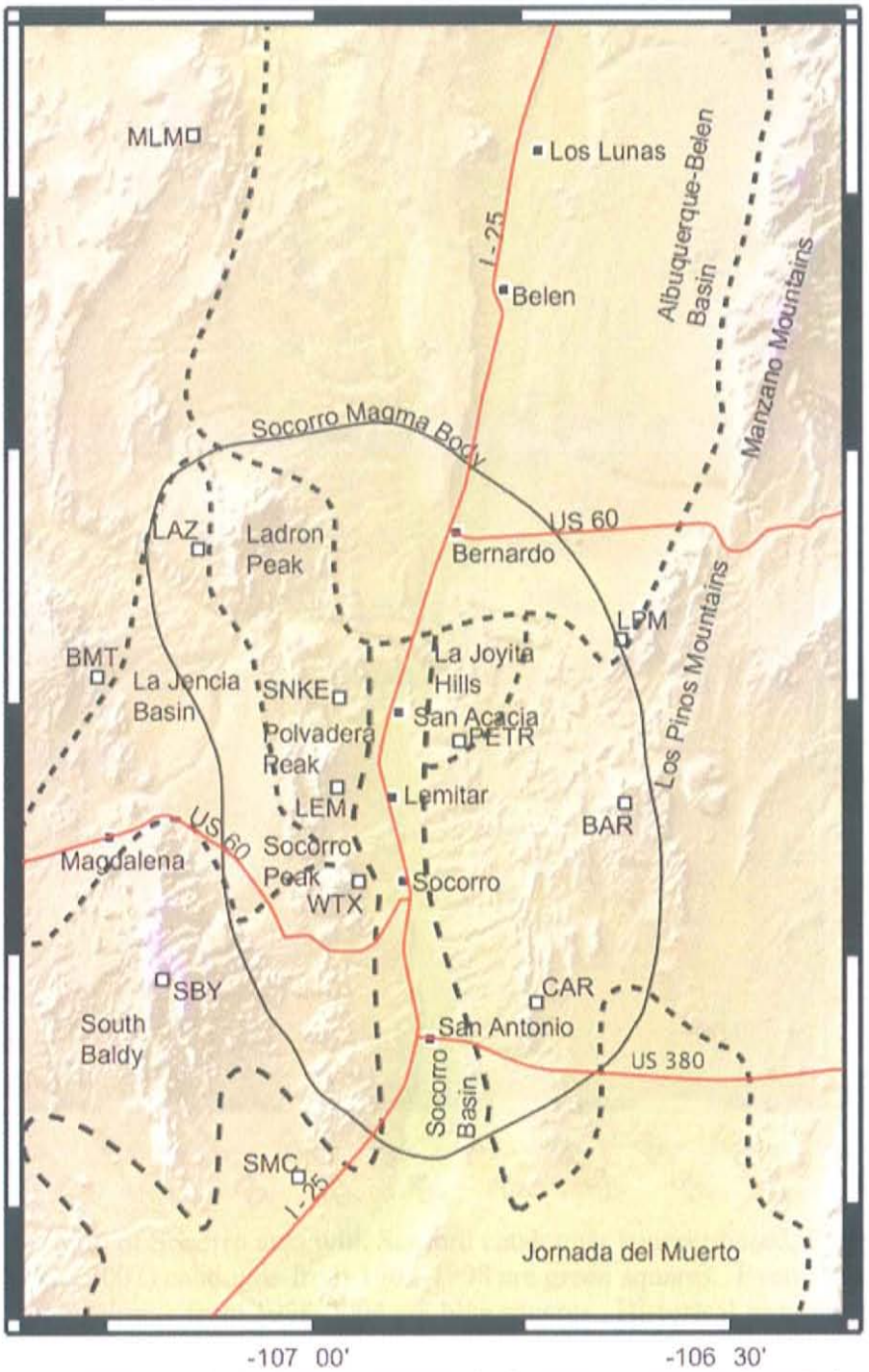

Figure 1.4: A more detailed view of geographic features, towns, and roads in and around the Socorro Seismic Anomaly. Dashed lines separate physiographic provinces. A solid black line delineates the Socorro Magma Body of Balch et al. (1997). Red lines are main roads. White boxes are seismic stations.

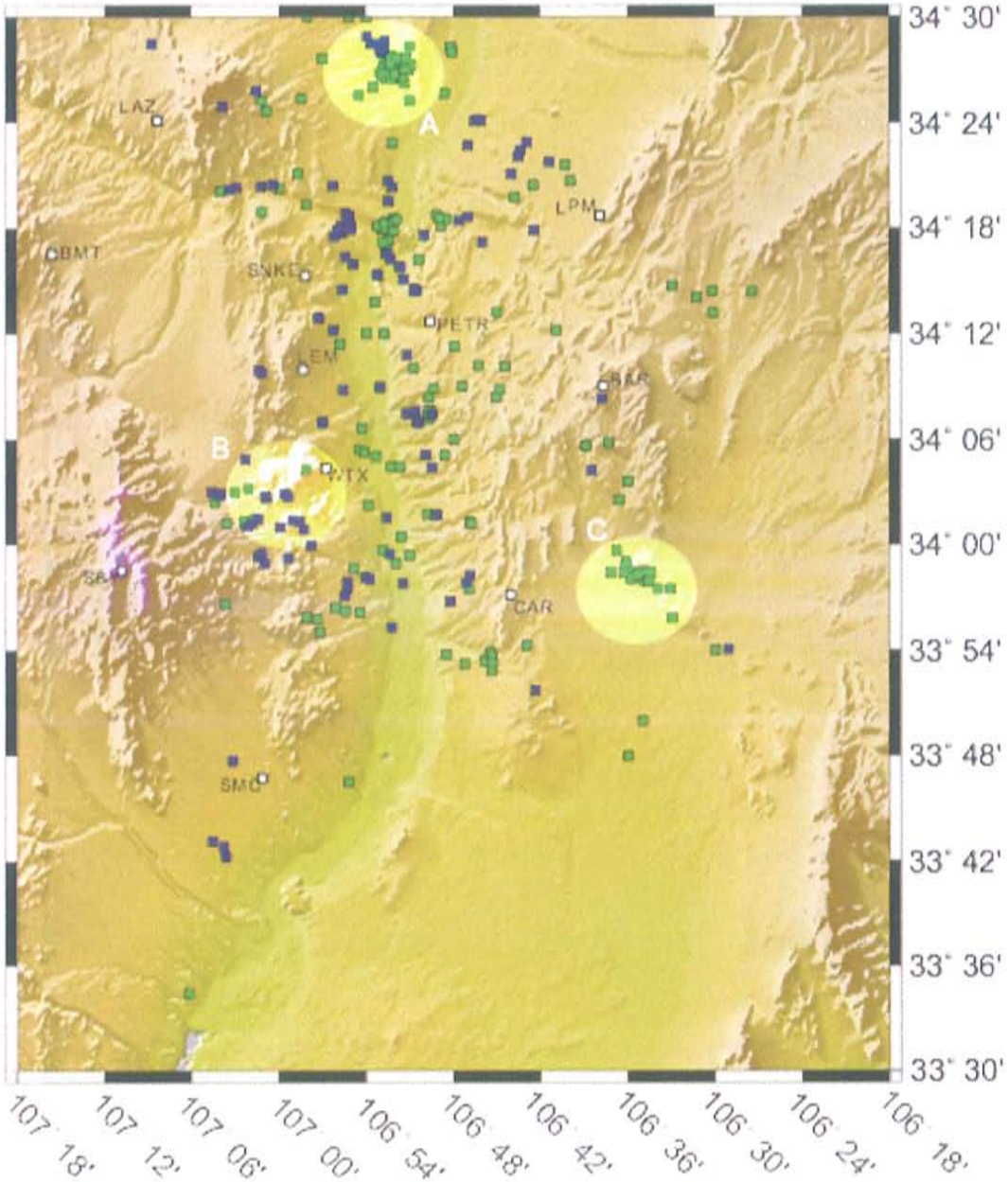

Figure 1.5: Map of Socorro area with Sanford catalogues superimposed. Events from Sanford et al. (2002) catalogue from 1962-1998 are green squares. Events from Sanford et al. (2006) catalogue from 1998-2004 are blue squares. Historical swarms are highlighted. A is a 1989-90 swarm resulting in four events about 4.3. B is proposed historical source for the large events of 1906. C is an early 1990 swarm resulting in 6 events above M_d 3.2, the largest of which was an M_d 3.9 event. All of these areas are present locations of continued seismicity.

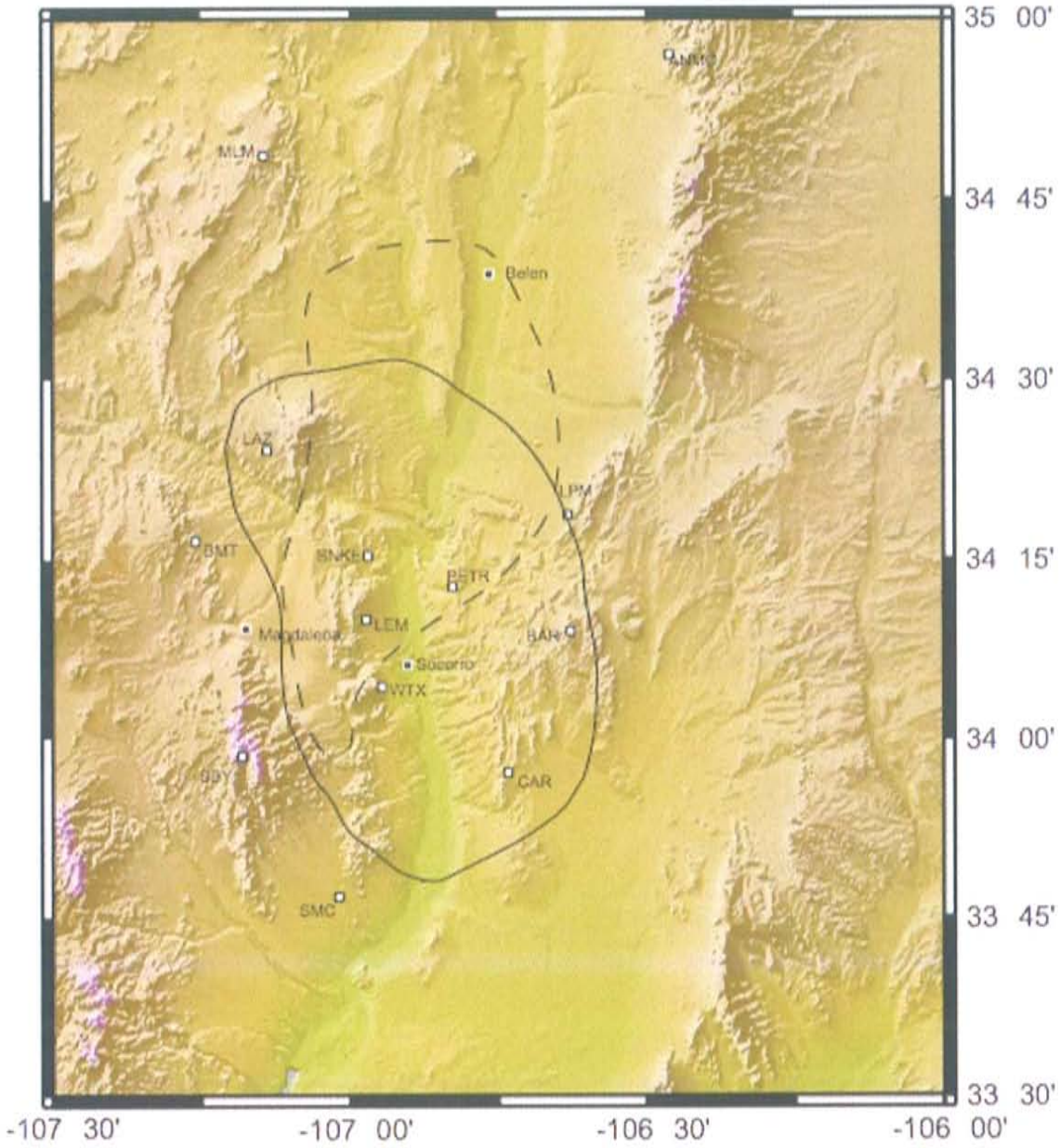

Figure 1.6: Boundary of the Socorro Magma Body from previous studies. Dashed outline is developed from Sanford et al. (1977) and Rinehart et al. (1979). Solid outline is from Balch et al., 1997. SC (Socorro) network stations and YN (temporary) network stations are white squares.

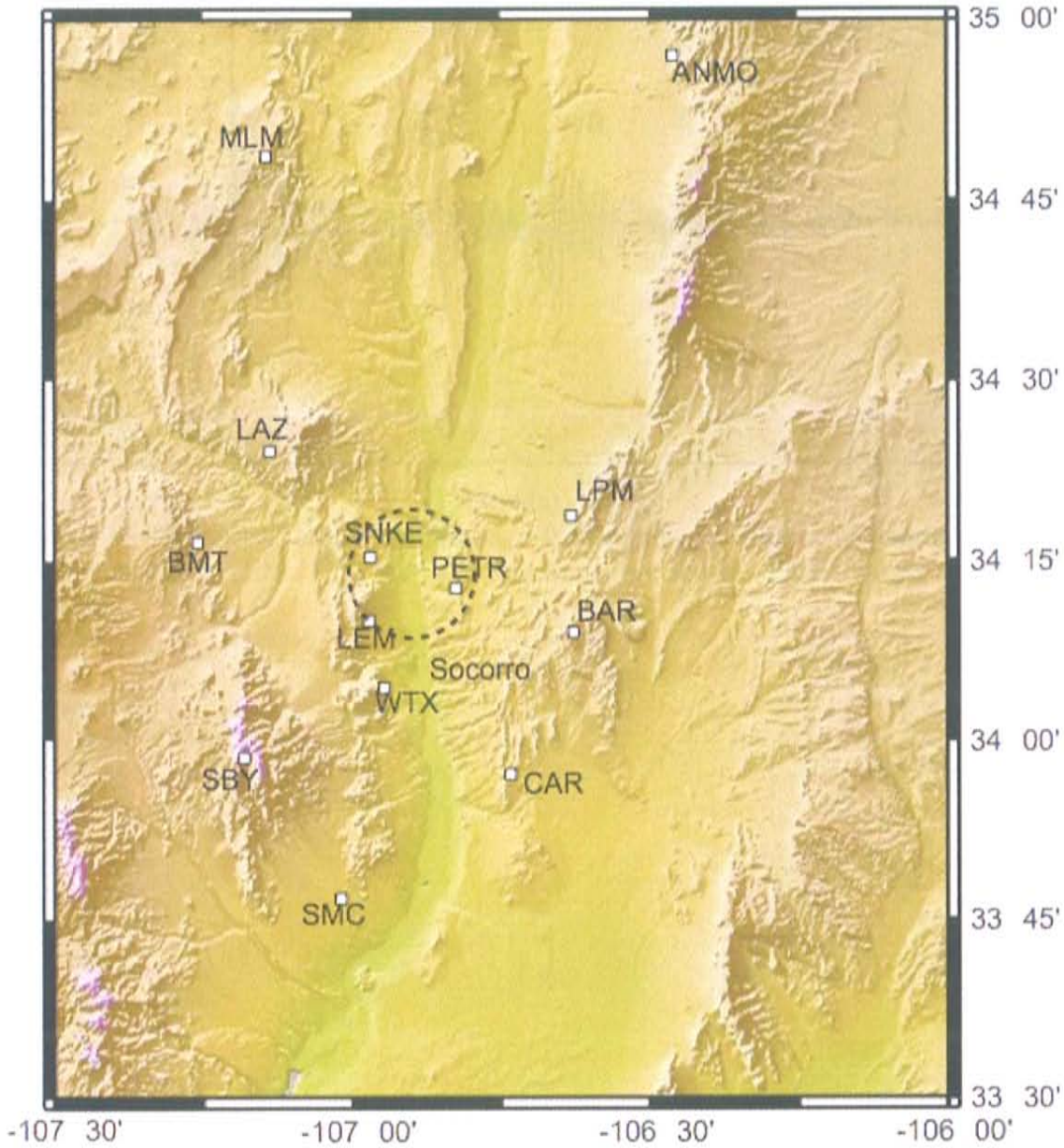

Figure 1.7: Map showing suspected area for a shallow source of magma within the Socorro Seismic Anomaly. The suspect area is the dashed outline. Seismic stations are white squares.

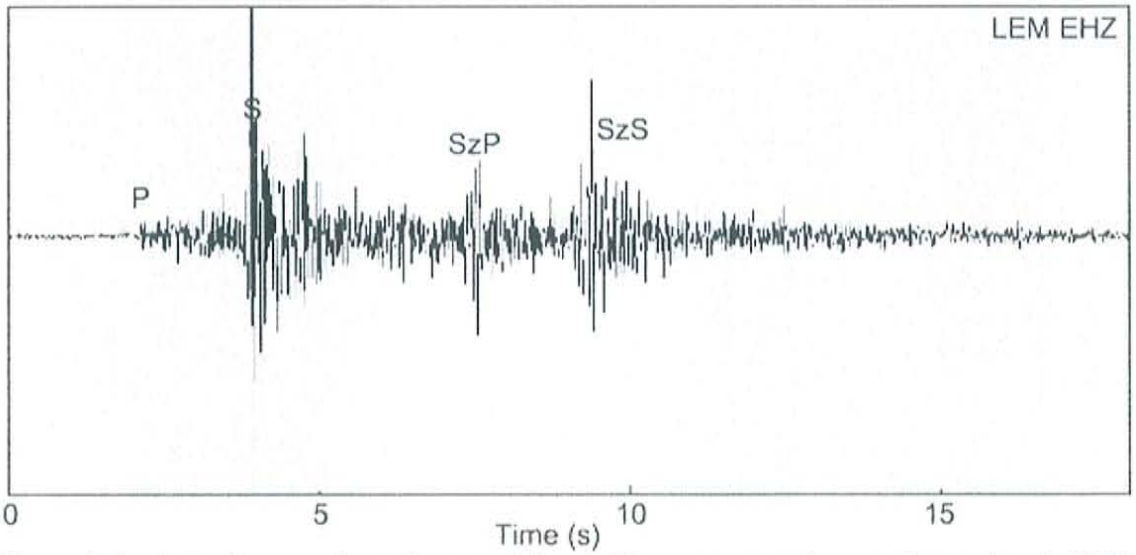

Figure 2.1: Seismic waveform from an $M_d = 0.62$ event occurring on November 1, 2005 recorded at station LEM. P, S, SzP, and SzS waves are shown. PzP is not seen in the waveform.

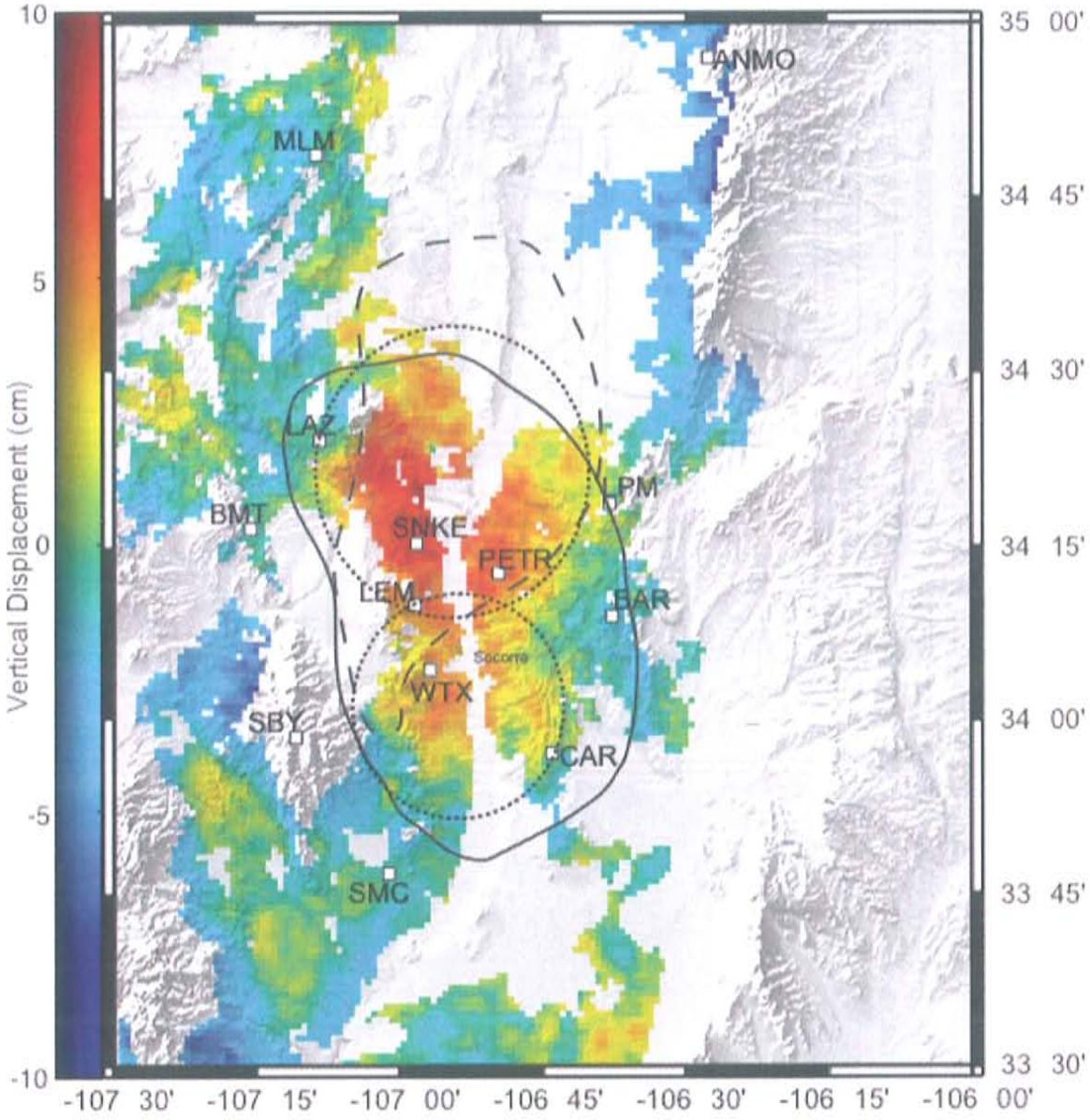

Figure 2.2: Stack of interferograms modified from Fialko and Simons (2001) for period from 1992-1999. Redundancy of data results in a cumulative time span of 29.3 years. Scale bar on the left is in cm for 29.3 year stack. Solid line is magma body outline from Balch et al. (1997). Dashed line is from Rinehart et al. (1979). Dashed circles are best fitting model of inflating cracks at ~19km depth. SC and YN stations are white squares.

Figure 2.3: Campaign GPS measurements in the Socorro area between 2002 and 2004. A) Map showing GPS stations and horizontal movement from 2002-2003. B) Vertical movement from November, 2002 through November 2003. Uplift of ~2 cm occurs at stations VVRS and BOWL, with all stations in middle transect except SLVR showing uplift. C) Vertical movement from November, 2003 through November, 2004. Subsidence of ~1 cm occurs at stations VVRS and BOWL, with all stations in middle transect except SLVR showing subsidence. Notice anomalously high values near center of second transect in both B and C.

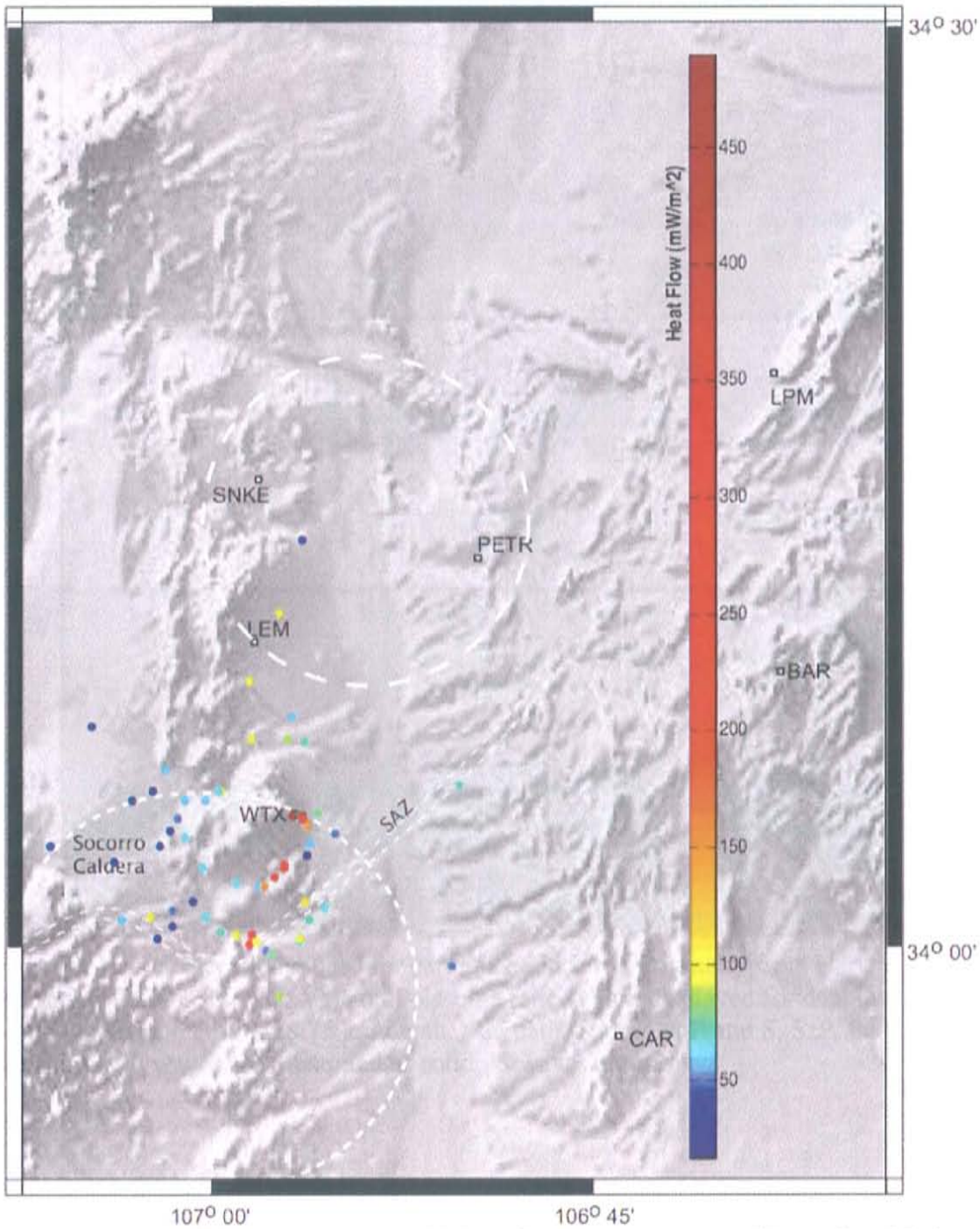

Figure 2.4: Map of the Socorro area with heat flow measurements of Barroll and Reiter, (1990) color coded by value in mW/ m^2. Socorro Caldera and Socorro Accomodation Zone are labeled. Coarsely dashed line is area of proposed shallow source.

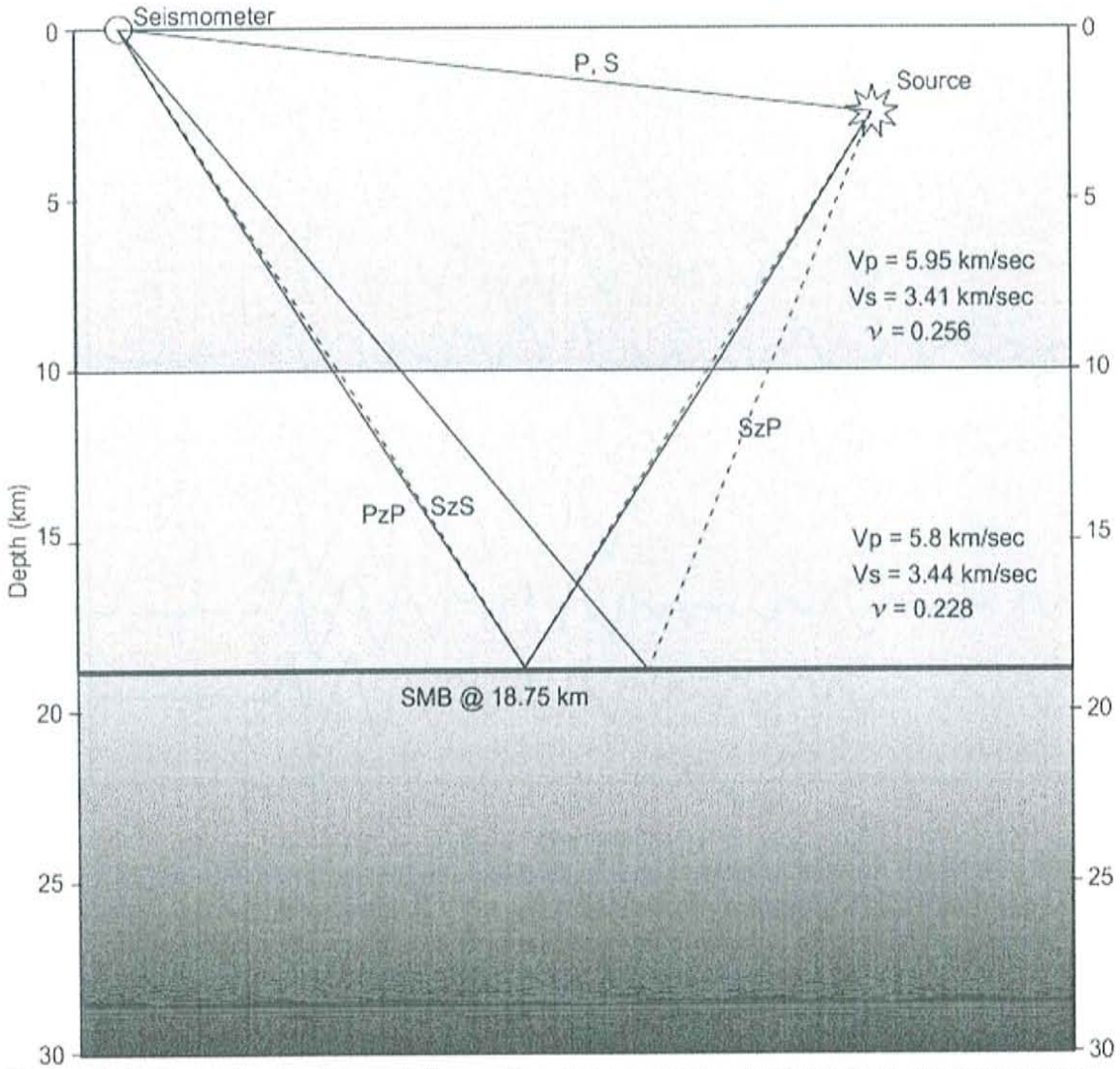

Figure 3.1: Velocity model used for earthquake location originally from Hartse (1991). P and S velocities (Vp and Vs) and Poisson's ratio (v) are displayed for dual layer model. Notice SMB reflector at 18.75 km depth. Raypaths for direct P and S, SzP, PzP, and SzS are shown. P waves are illustrated as solid. S waves are dashed.

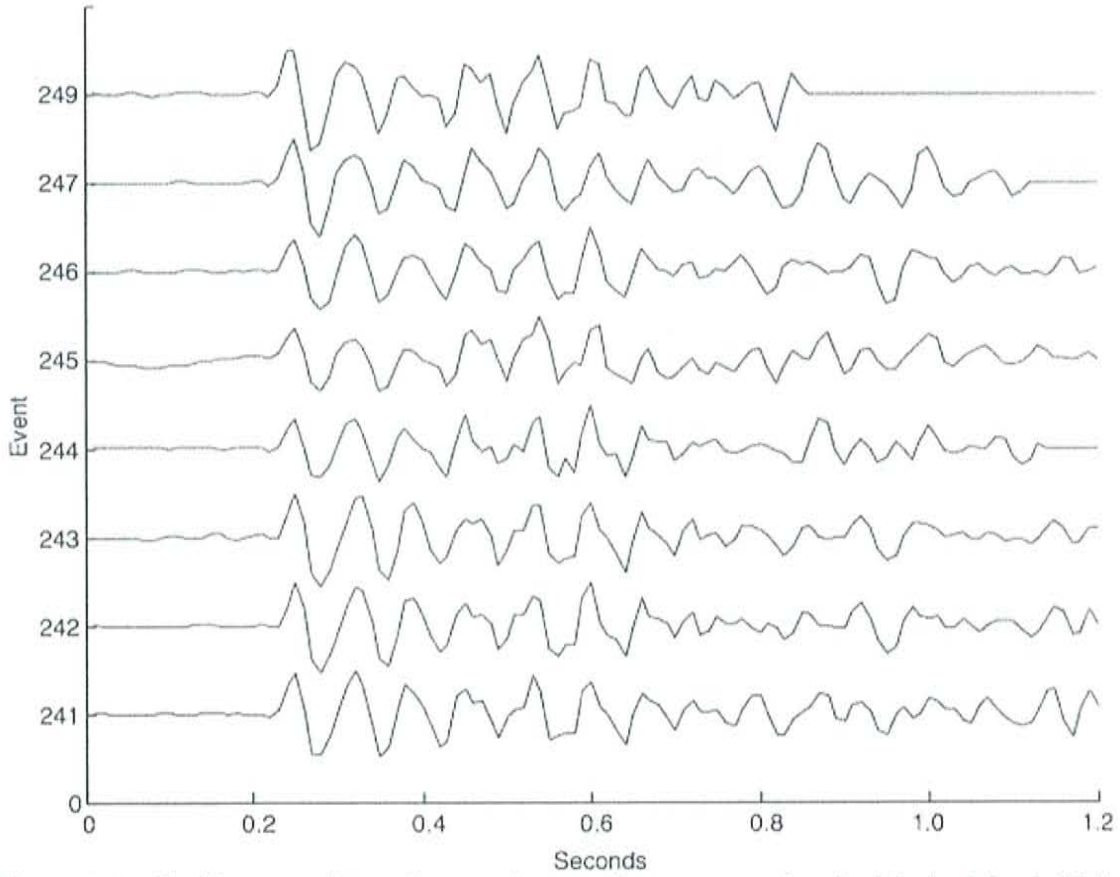

Figure 3.2: Similar waveforms from a cluster of events associated with the March 29th, 2007 earthquake swarm (cluster 1). Waveforms are from station SNKE. Flat lines near the end of the waveforms are due to zero padding which occurs after shifting a waveform. Event numbers correspond to event numbers in Appendices A and D.

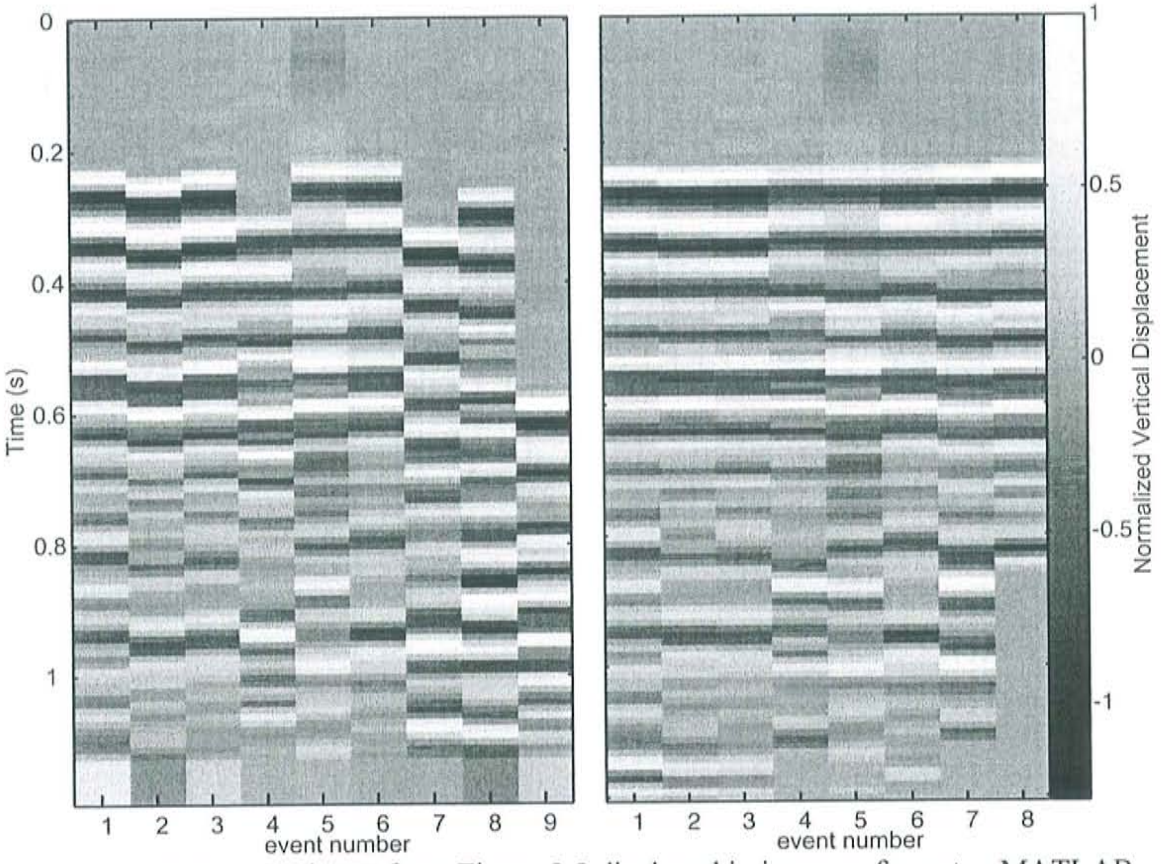

Figure 3.3: The same cluster from Figure 3.2 displayed in imagesc format, a MATLAB plotting format that represents values as colors. In this format, positive values corresponding to upward movement are displayed as light colors while negative values corresponding to downward movement are displayed as dark colors. Events are displayed prior to (left) and post (right) waveform cross-correlation. Each seismogram is displayed vertically down with time on the y-axis. Of the nine events in the cluster, eight events correlated while one was thrown out of the dataset.

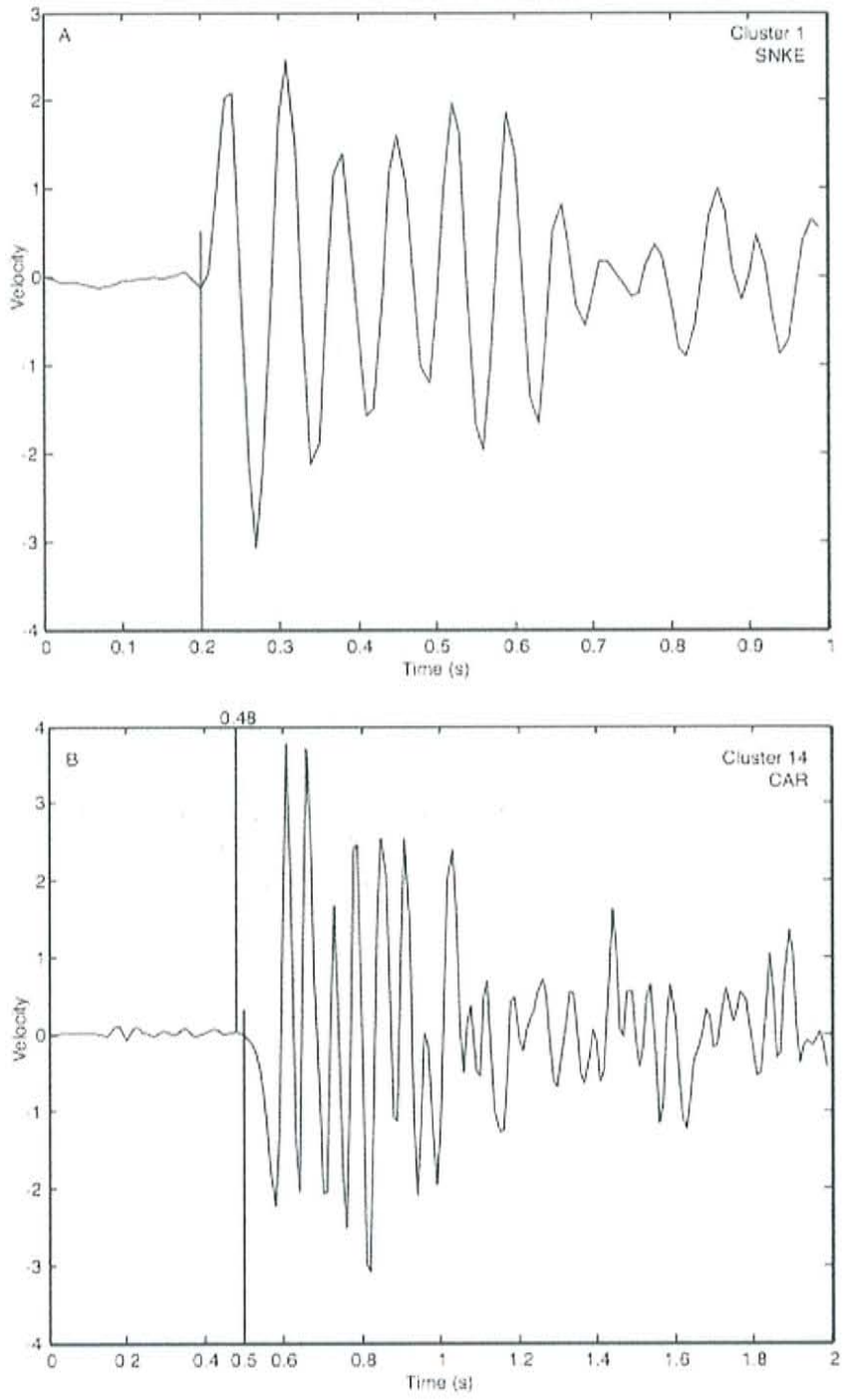

Figure 3.4: Waveform stacks after cross-correlation. A) Stacked seismograms of 8 events from Cluster 1 at station SNKE. No discernible lag exists. B) Stacked seismograms of 21 events from Cluster 14 at station CAR. A 0.02 second lag seems to exist, however inclusion of somewhat dissimilar waveforms in stack may be a contributor.

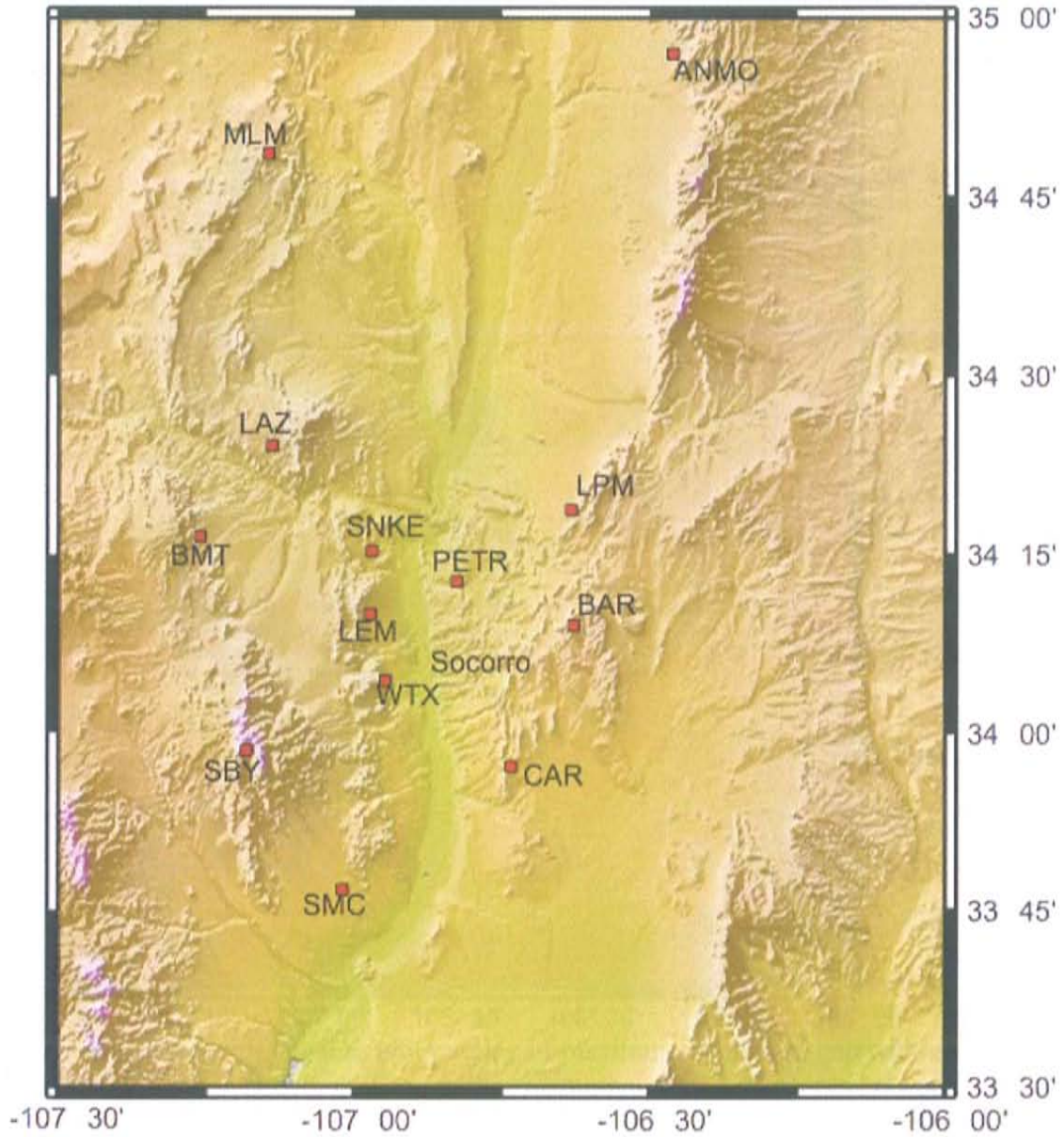

Figure 3.5: Figure clearly showing Socorro (SC) network and temporary (YN) network stations PETR and SNKE. Azimuthal gaps above 180° can be noted for stations CAR, BAR, SMC, SBY, BMT, and LPM (excluding ANMO).

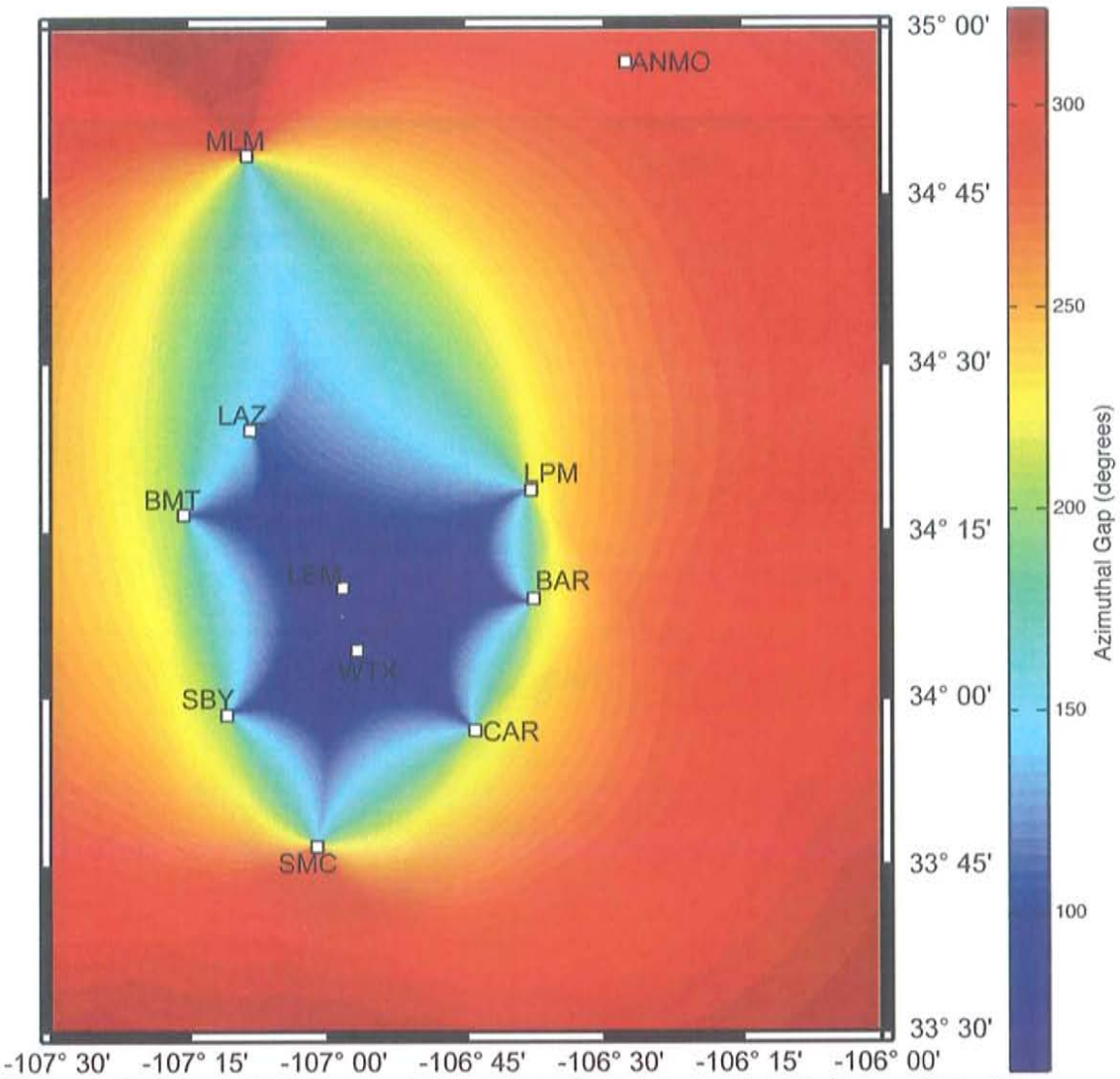

Figure 3.6: Map with imagesc plot overlay of maximum azimuthal gap within the Socorro SC seismic network. The smallest azimuthal gap (61°) occurs between LEM and WTX.

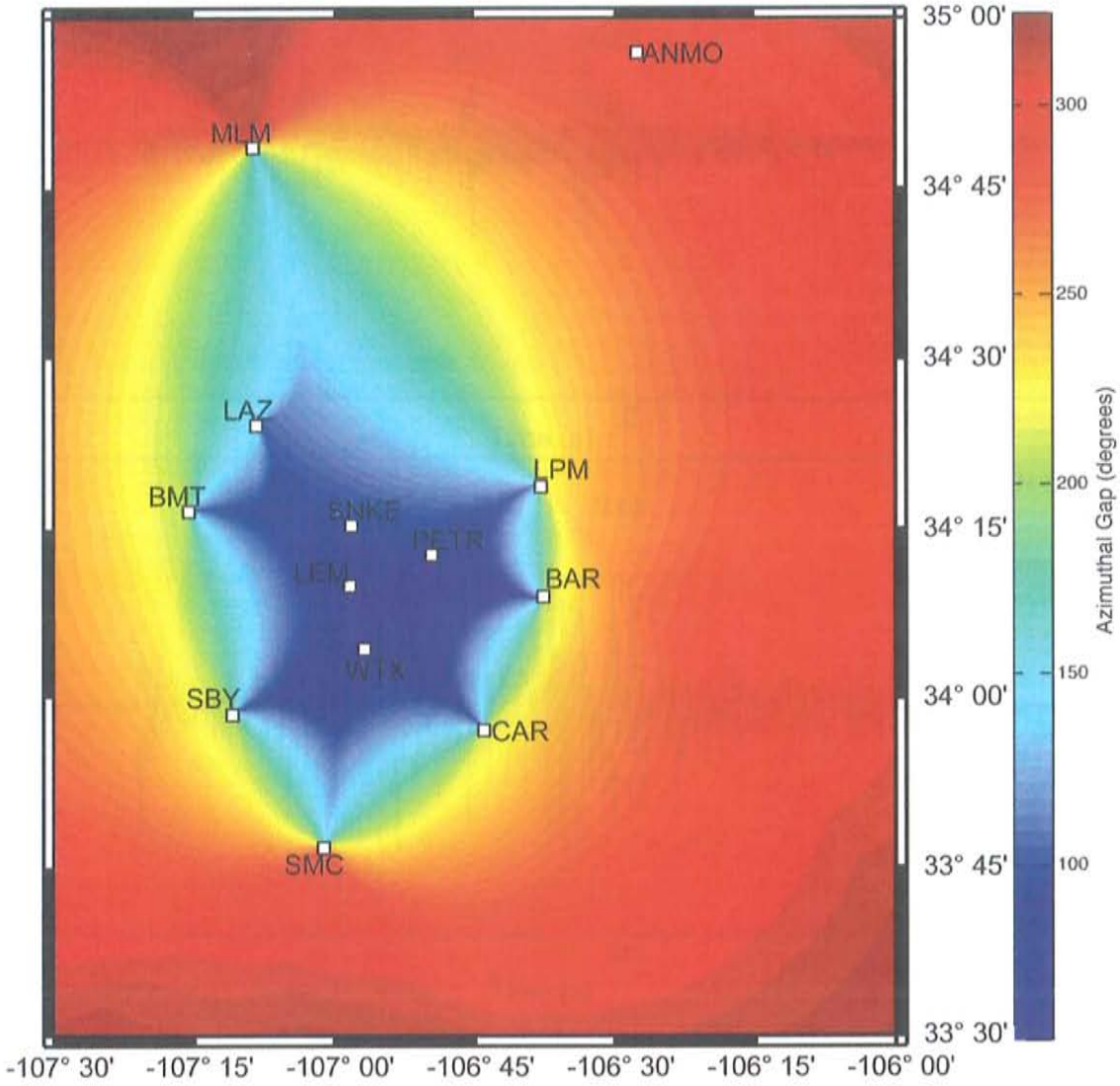

Figure 3.7: Same as Figure 3.6 with addition of YN seismic network stations PETR and SNKE. Minimum azimuthal gap (54°) is now immediately southwest of PETR.

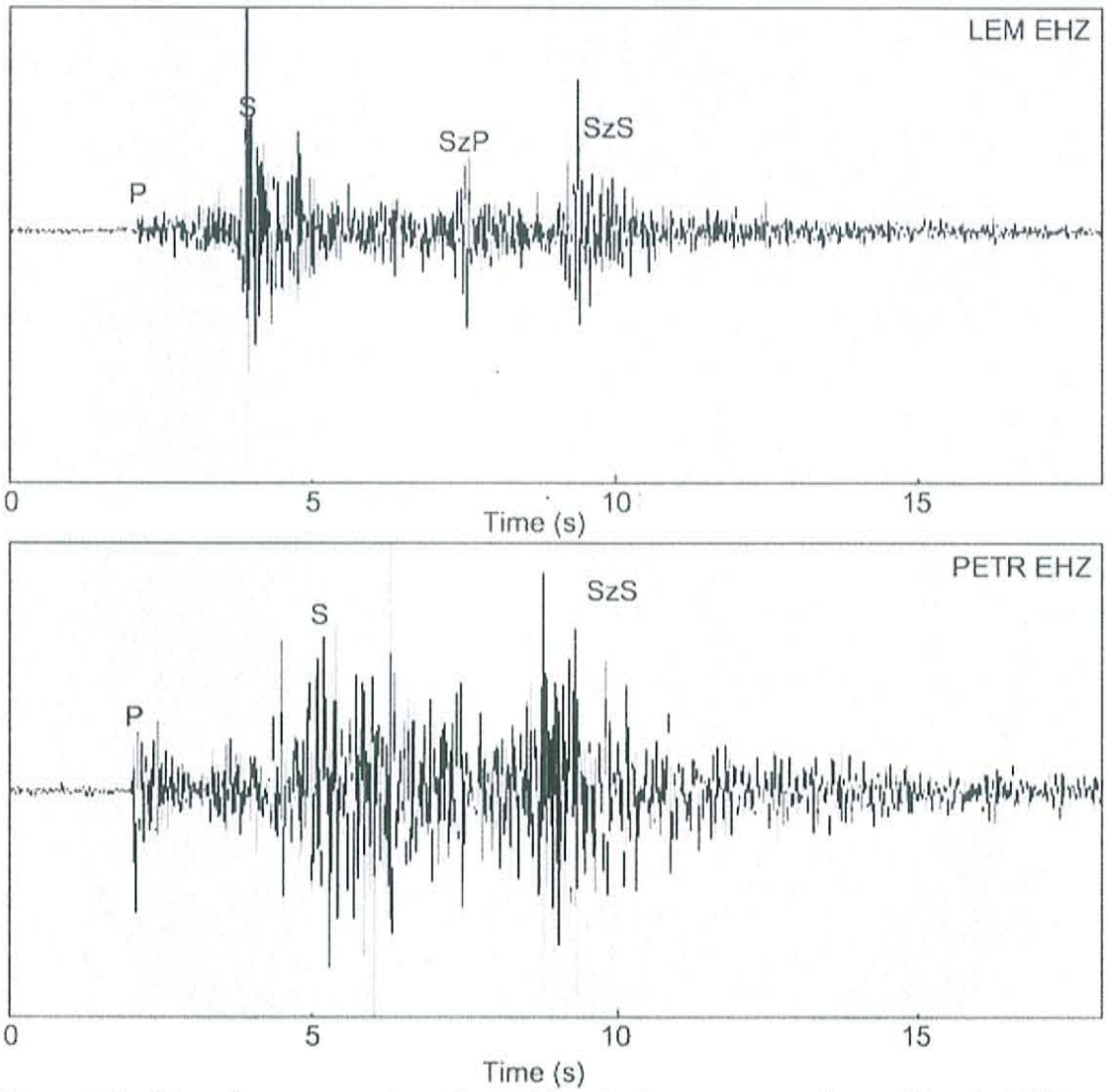

Figure 3.8: Waveform comparison for an $M_d = 0.62$ event occurring on Nov 1, 2005 at 09:27 GMT. Labelled are P, S, and identifiable reflections. Note clear presence of magma body reflection SzS in both waveforms.

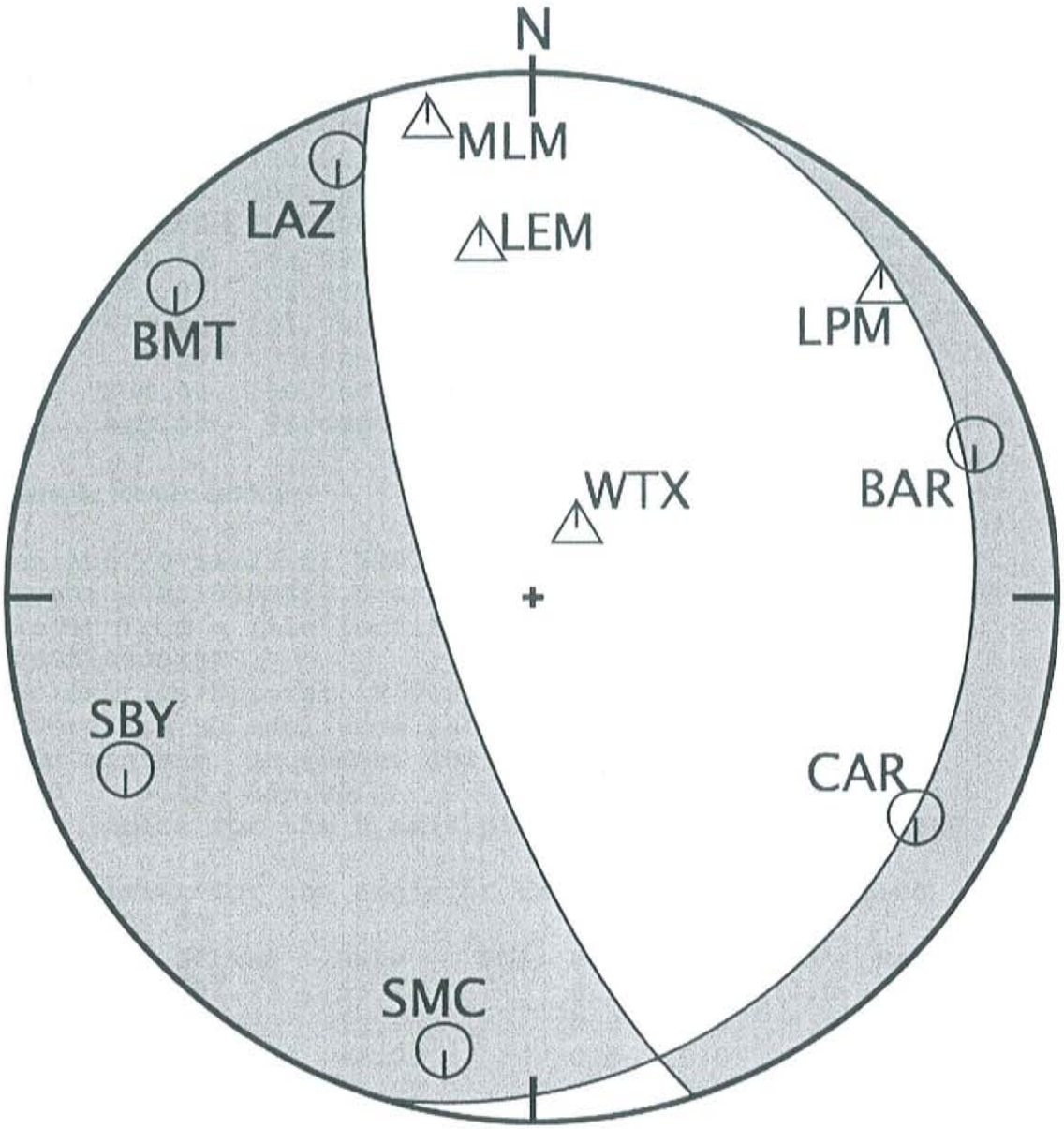

Figure 3.9: Basic focal mechanism showing compression (circles) and dilation (triangles). Stations in SC network are labeled. This event is the M 2.3 Oct. 29th 2005 event (Appendix C event 200510300257)

Example focmec.dat file:

```
200510300257
WTX     27.00   165.00D
LEM    352.00   120.00D
SB     247.00   107.00U
CAR    120.00   107.00U
SMC    191.00   103.00U
BAR     71.00   102.00U
BMT    311.00   101.00U
LPM     47.00   100.00D
LAZ    336.00   100.00U
MLM    348.00    95.00D
```

Example focmec.out file:

```
Mon Aug 20 11:29:41 2007 for program FOCMEC
 Event 200510300257 0 errors
 Input from a file locfiles/200510300257focmec.dat
 200510300257
 Polarities/Errors:  P 010/00  SV 000/00  SH 000/00
 There are no amplitude ratio data
 The minimum, increment and maximum B axis trend are
0.00    5.00  355.00
 The limits for the B axis plunge are     0.00    5.00
90.00
 The limits for the angle of the A axis are     0.00
5.00   85.00
    Dip   Strike   Rake     Pol: P     SV    SH   Rat Err
   17.96  197.73  -55.73          0.0   0.0   0.0
   17.96  202.80  -55.73          0.0   0.0   0.0
   21.09  208.58  -44.01          0.0   0.0   0.0
   24.81  205.13  -51.92          0.0   0.0   0.0
   21.09  213.72  -44.01          0.0   0.0   0.0
   24.81  210.27  -51.92          0.0   0.0   0.0
   24.81  216.04  -35.42          0.0   0.0   0.0
   27.99  212.63  -43.22          0.0   0.0   0.0
   31.61  210.96  -49.26          0.0   0.0   0.0
   71.94  233.05  -63.61          0.0   0.0   0.0
   72.77  236.77  -58.43          0.0   0.0   0.0
   81.35  248.91  -59.62          0.0   0.0   0.0
```

Table 3.1: Example focmec.dat and focmec.out files. The focmec.dat file includes an arbitrary header line and then lines with station name, azimuth, takeoff angle, and polarity of an event at each station. The focmec.out file contains a number of different parameters used in the solution, then a list of possible solutions.

Station	Latitude (N)	Longitude (W)	Elevation (m)
BAR	34° 8.52′	106° 37.68′	2120
BMT	34° 16.50′	107° 15.61′	1972
CAR	33° 57.15′	106° 44.07′	1662
LAZ	34° 24.12′	107° 08.36′	1853
LEM	34° 9.93′	106° 58.45′	1689
LPM	34° 18.77′	106° 38.03′	1707
MLM	34° 48.85′	107° 8.70′	2088
SBY	33° 58.51′	107° 10.84′	3230
SMC	33° 46.72′	107° 1.16′	1560
WTX	34° 4.33′	106° 56.75′	1555
PETR	34° 15.264′	106° 58.17′	1577
SNKE	34° 12.66′	106° 49.56′	1510

Table 4.1: Latitude, longitude, and elevation of seismic stations from SC and YN networks.

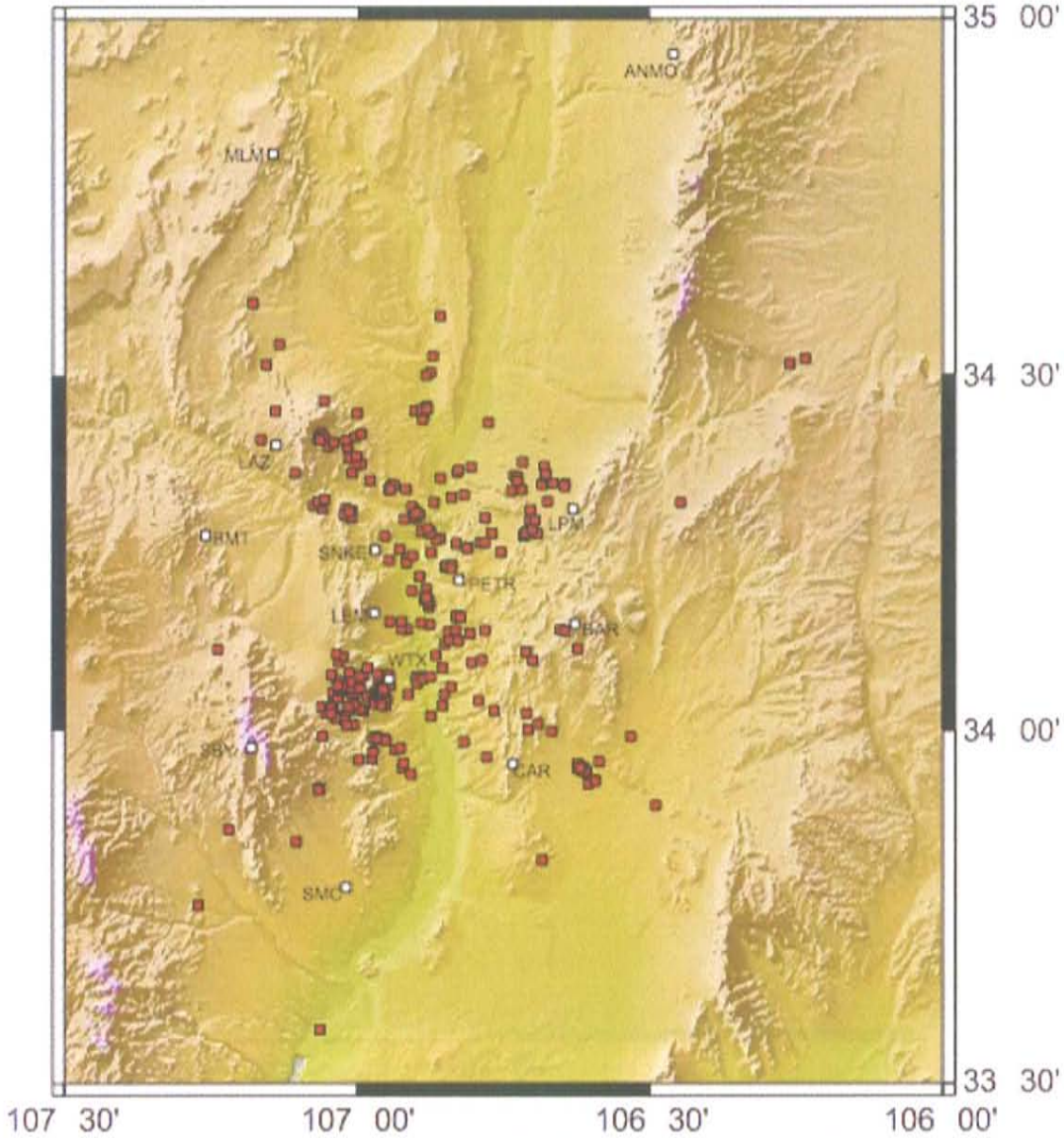

Figure 4.1: Map of original locations of all 346 events in catalogue from September, 2004 through May, 2007. SC and YN stations are white squares. Events are red squares.

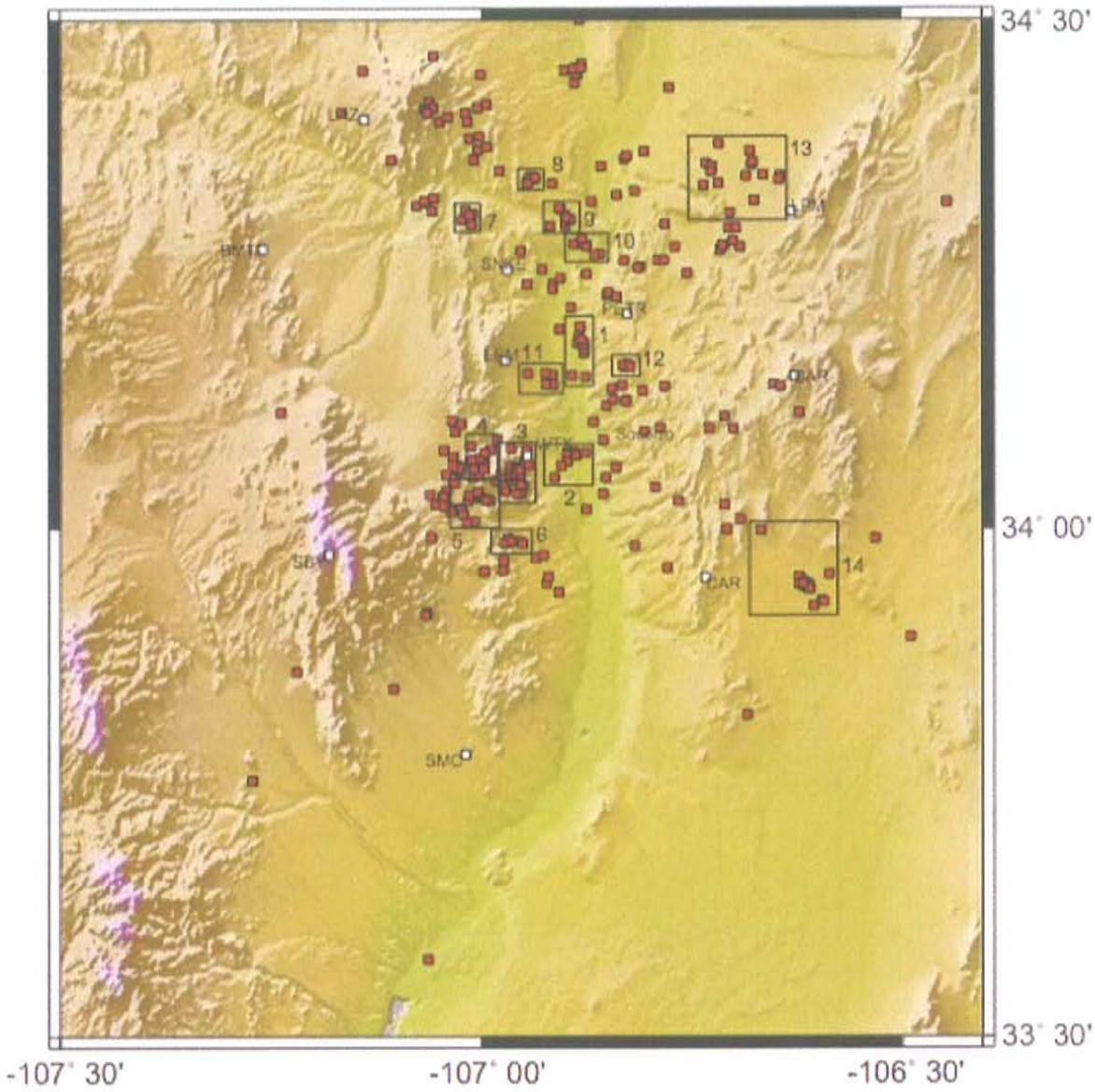

Figure 4.2: Map illustrating clusters used in this study as black rectangles. Catalogue events prior to relocation are red squares. Stations are white squares.

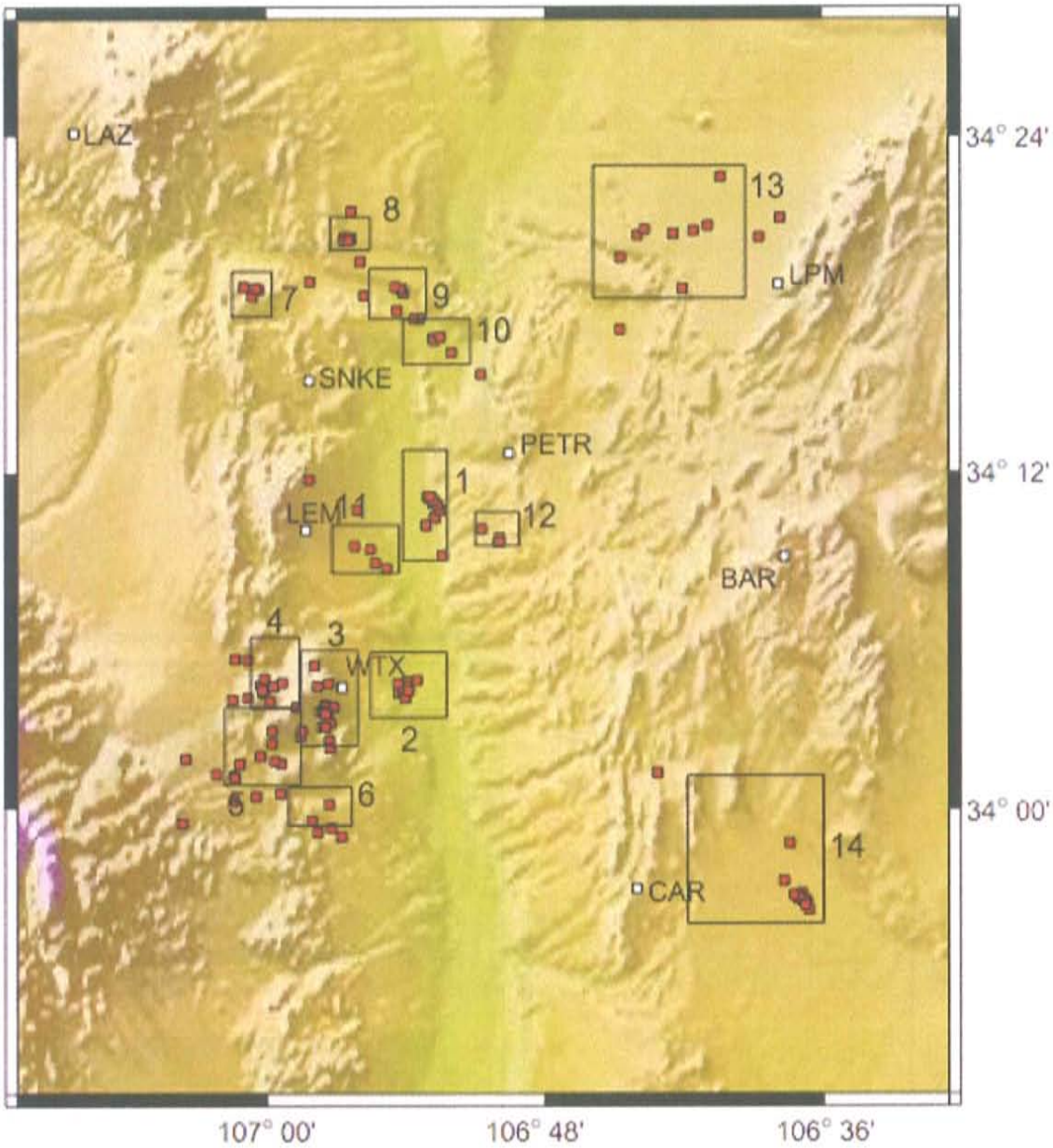

Figure 4.3: Relocated earthquakes from clusters displayed as red squares. Seismic stations are white squares.

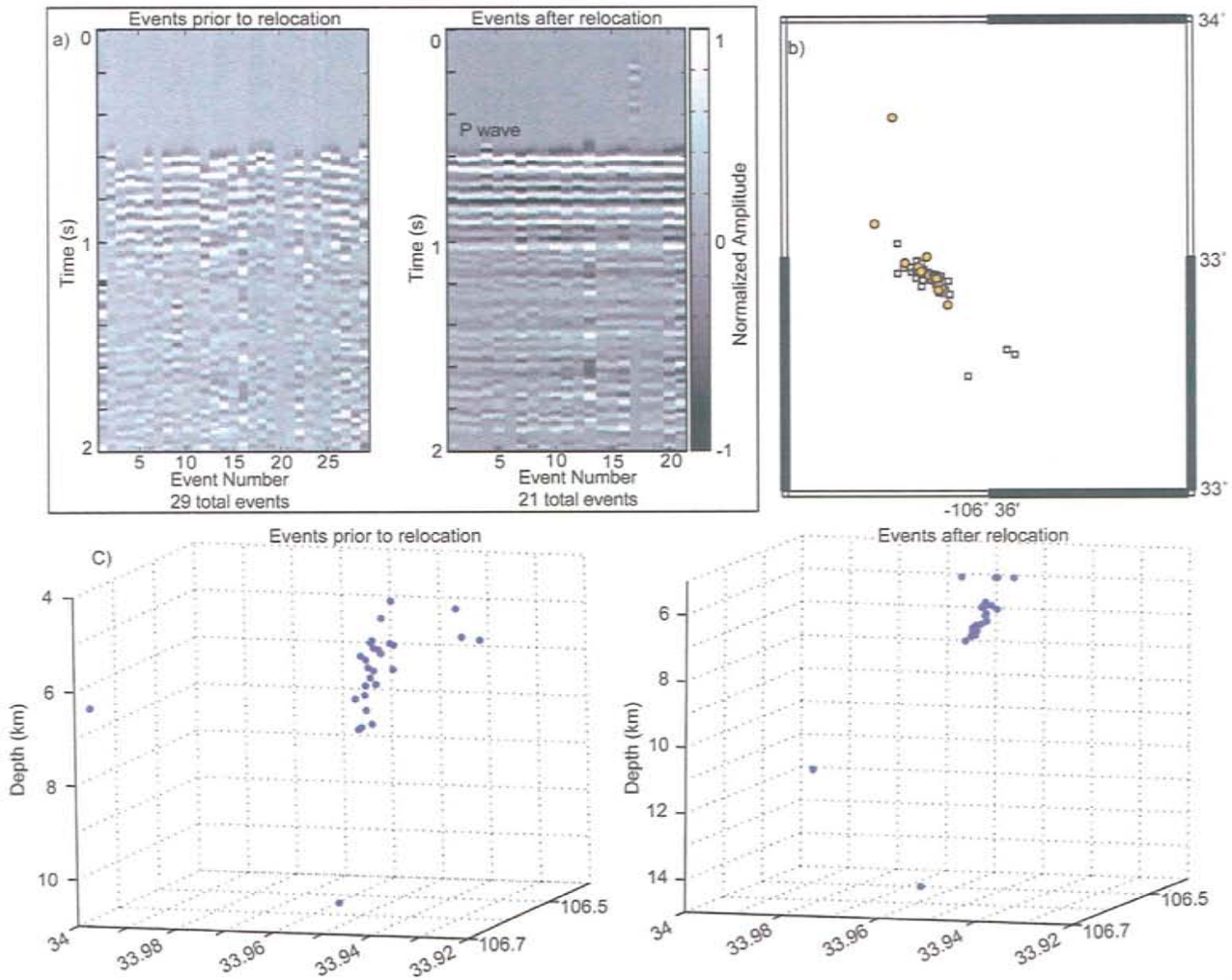

Figure 4.4: a) Waveform comparison aligned on P pick before and after cross-correlation at SC Network station CAR for a cluster of events east of that station. b) Comparison of cluster before and after WCC relocation. White squares are prior to WCC. Orange circles are after WCC. c) Comparison of hypocentral location on 3-d plots before WCC and after WCC.

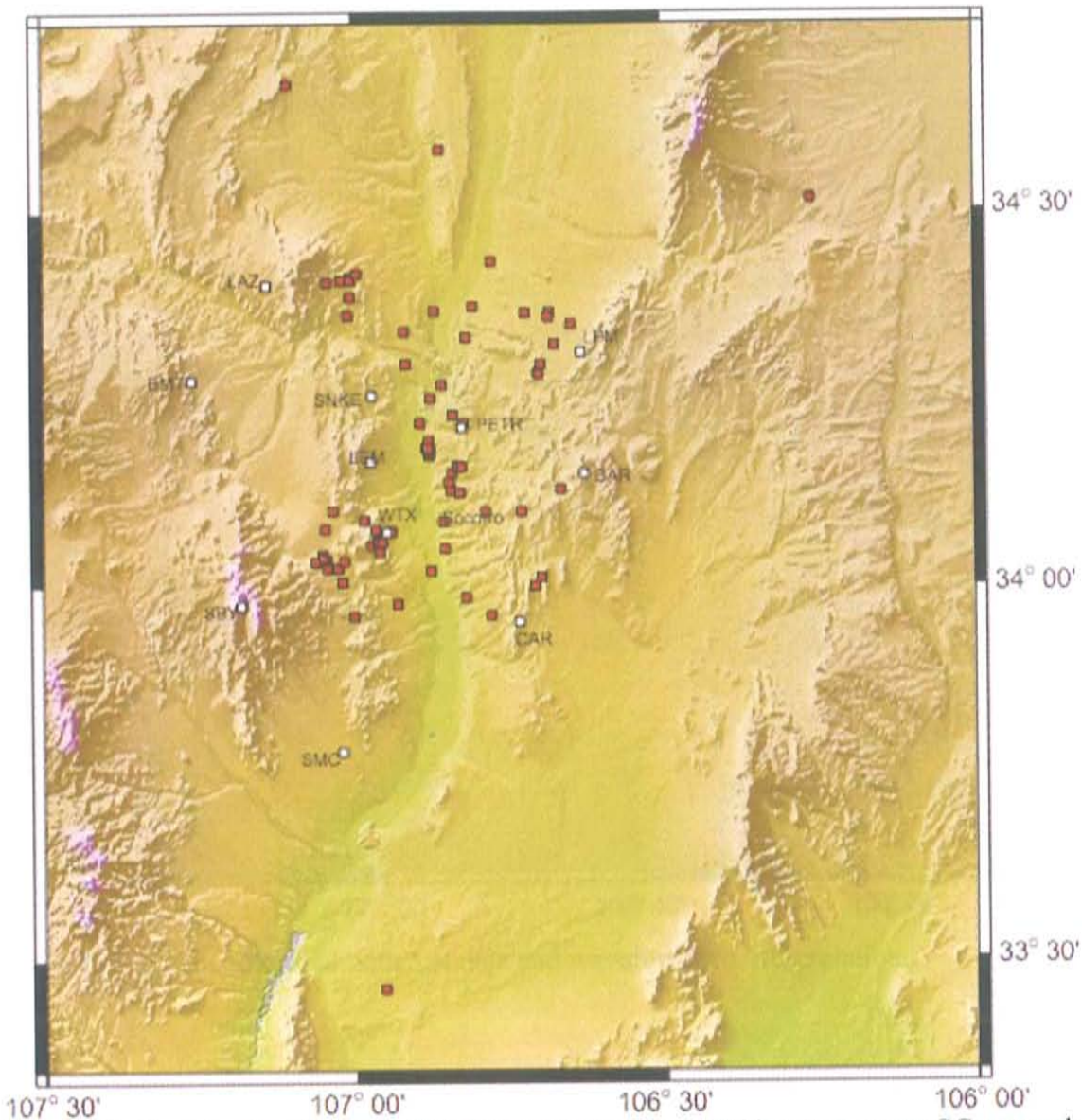

Figure 4.5: Events relocated with YN data as red squares. White squares are SC network stations.

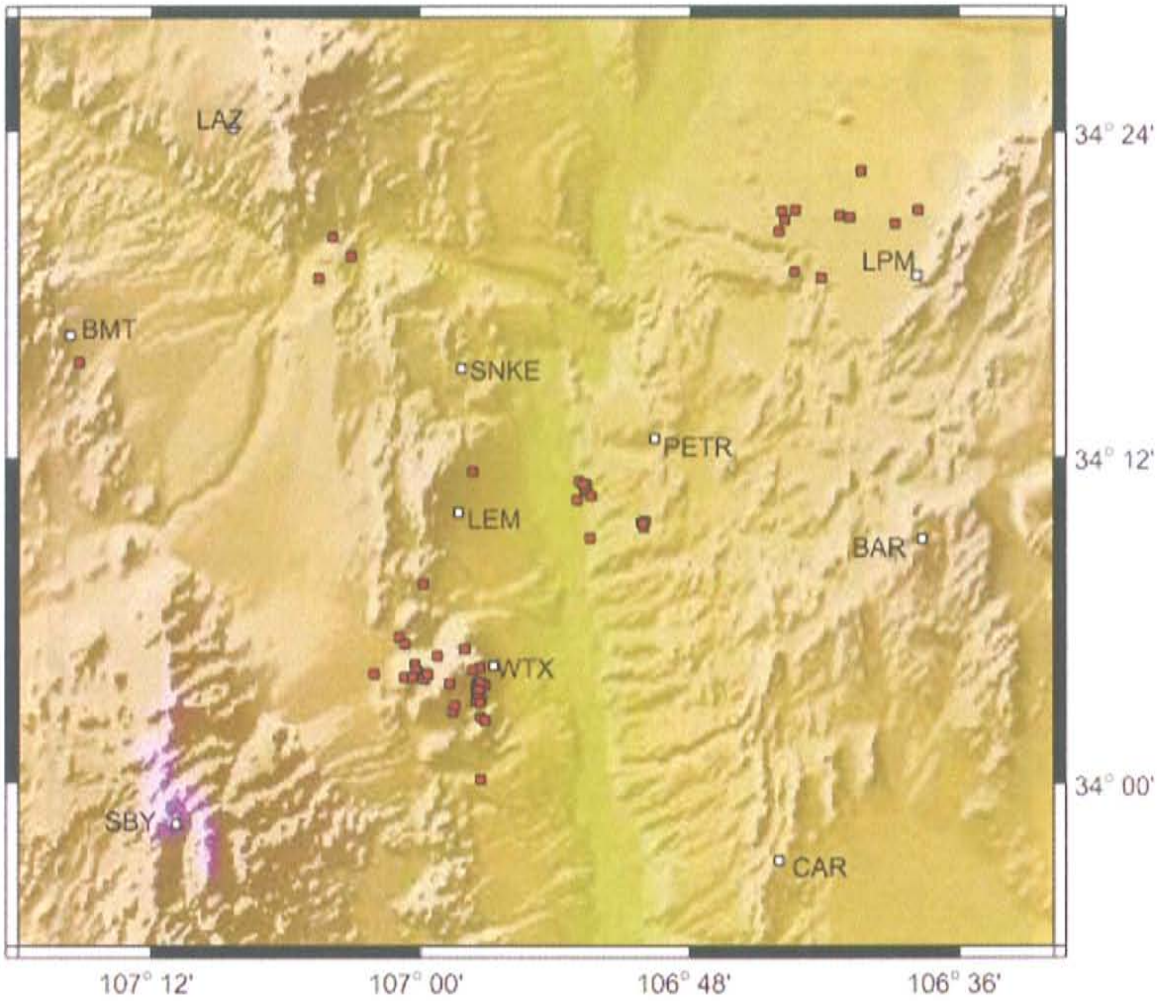

Figure 4.6: Events relocated with YN data and waveform cross-correlation.

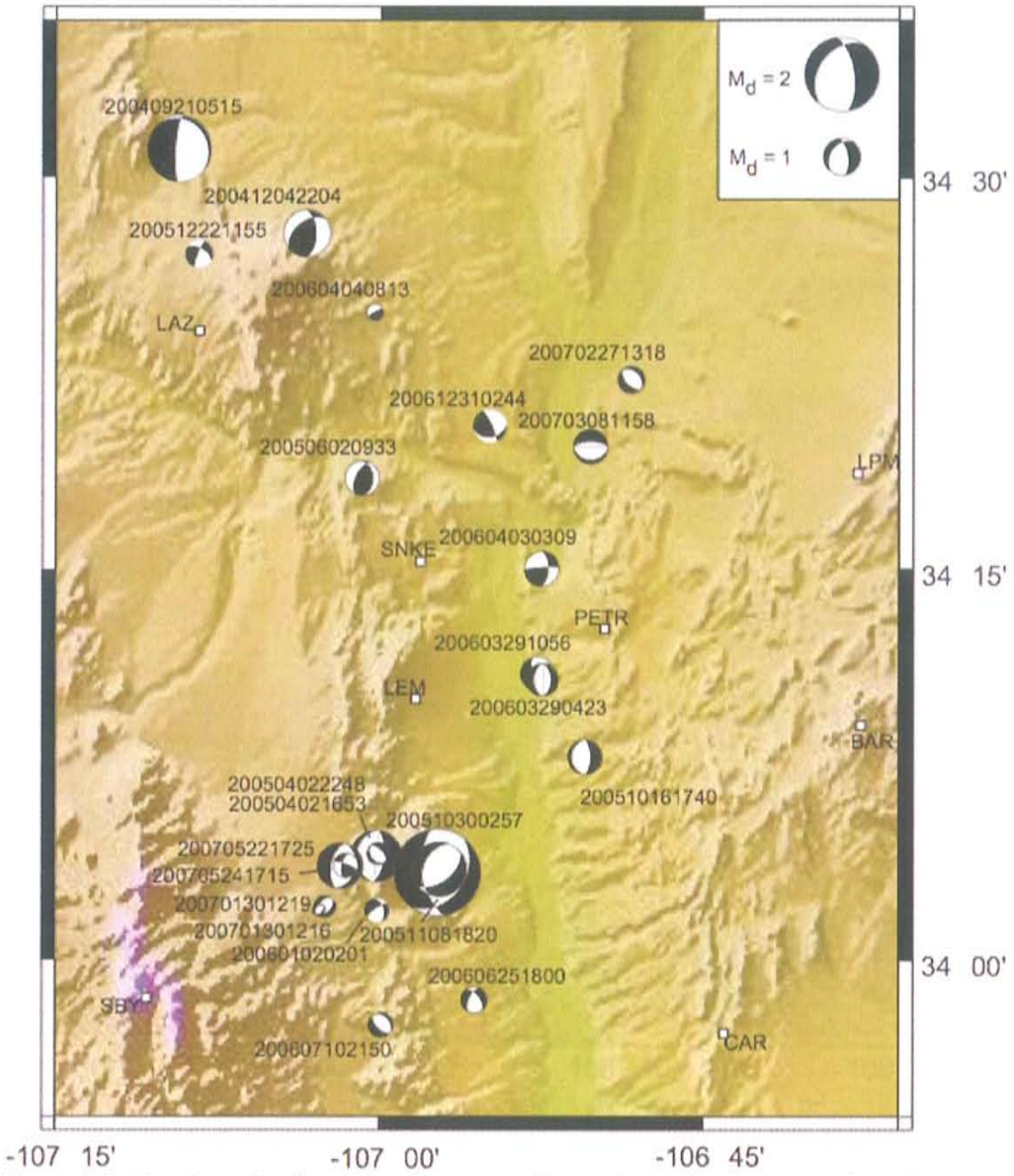

Figure 4.7: Focal mechanisms for all events without alternative interpretations. Date stamp is given in year-month-day-hour-minute. Notice predominance of normal events and presence of dextral strike-slip and oblique strike-slip events.

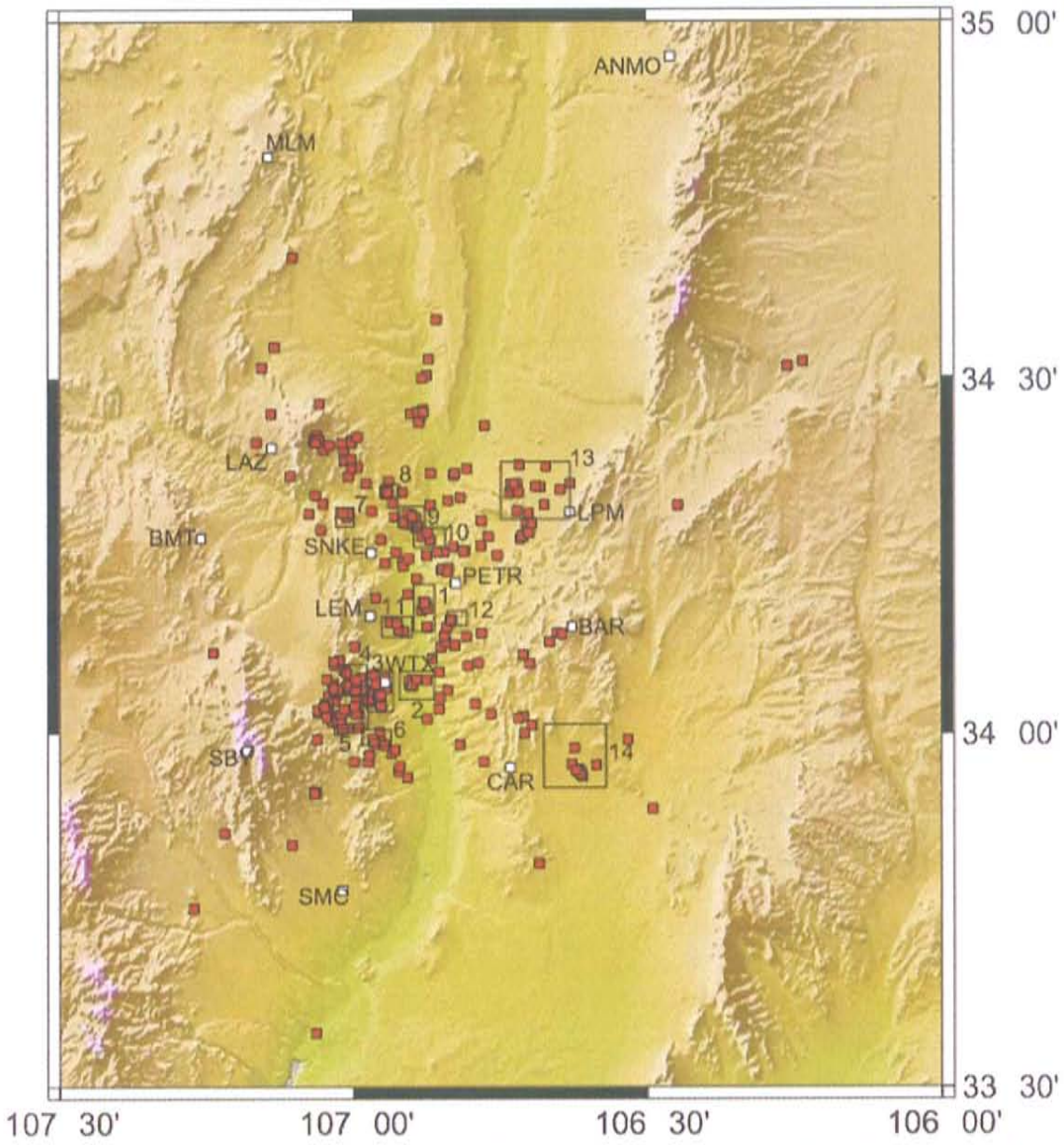

Fig 5.1: Fully relocated catalogue. YN relocations and waveform CC relocations replace original locations where appropriate. If no CC relocation with YN data exists, original location with YN data is used. If no original location with YN data exists, CC relocation without YN data is used. If no YN data or CC relocation exists, original location is used.

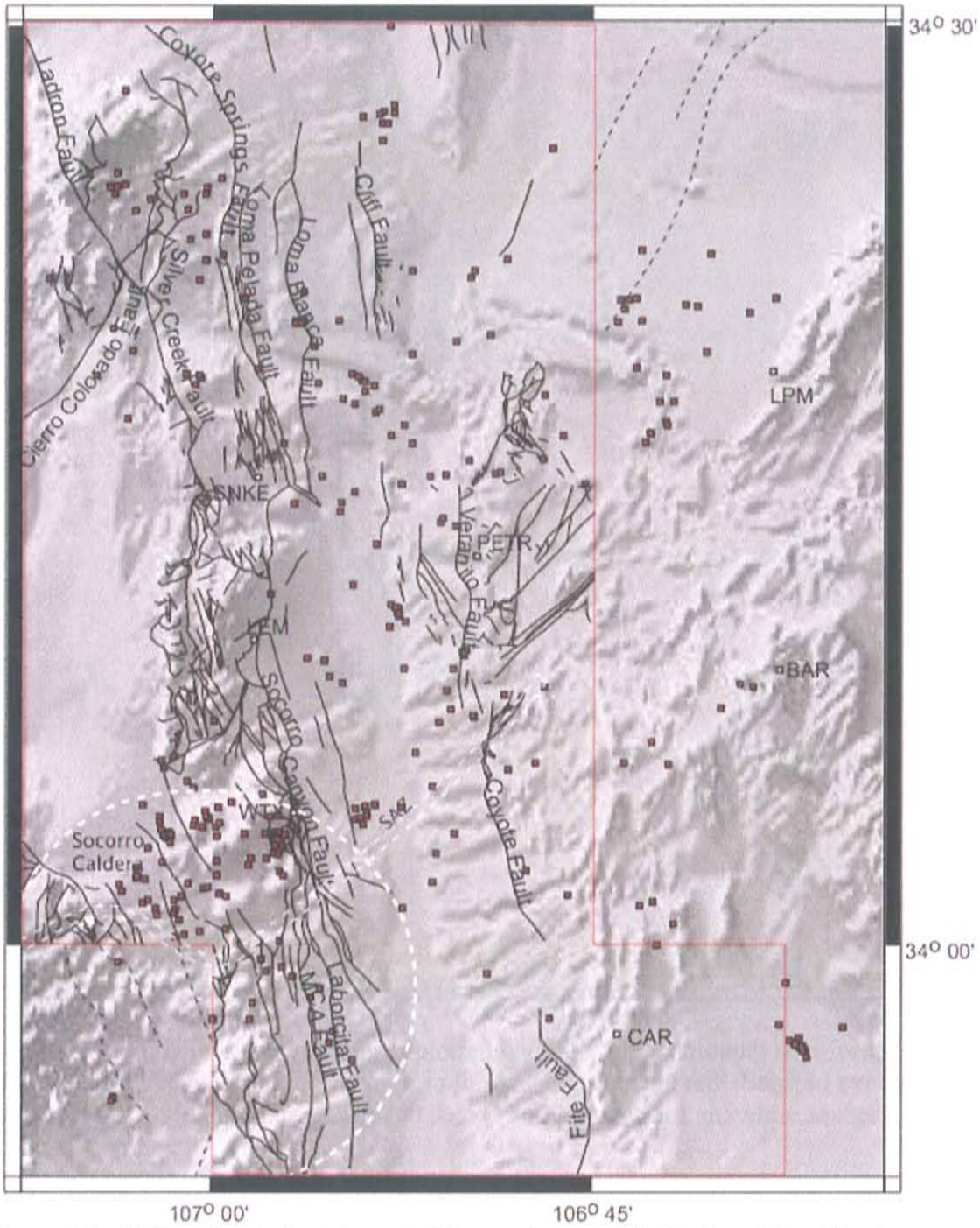

Figure 5.2: Fully relocated catalogue with superimposed faults from New Mexico 1:24000 quadrangle maps and New Mexico state map. Red line is the boundary of mapped quadrangles. Outline of Socorro Caldera and Socorro Accomodation Zone are labeled.

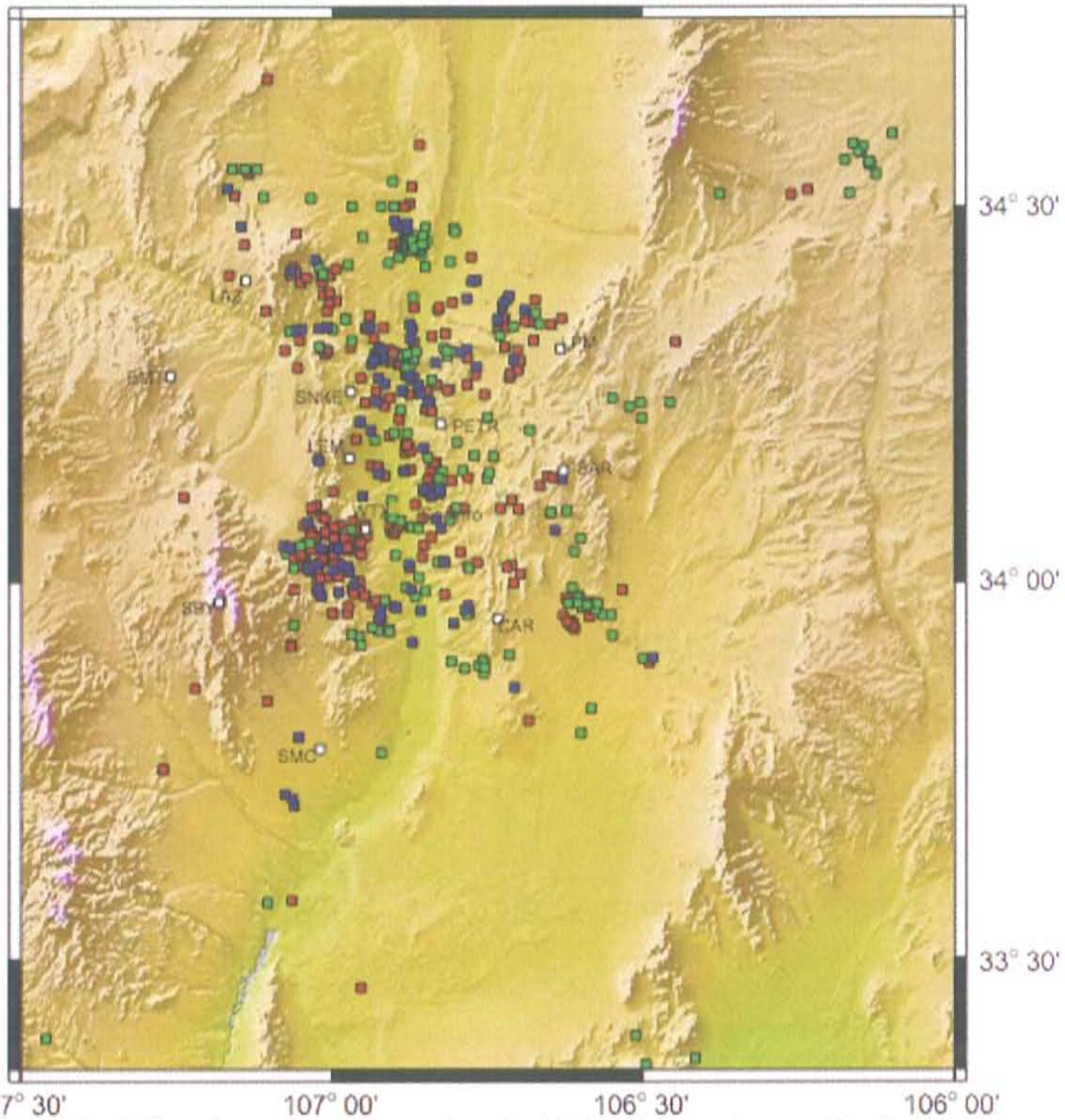

Figure 5.3: Fully relocated catalogue plotted with Sanford catalogues (Sanford et al., 2002; Sanford et al., 2006). Events from this catalogue are in red. Sanford events are in green (1962-1999) and blue (2000-2004). SC and YN stations are white squares.

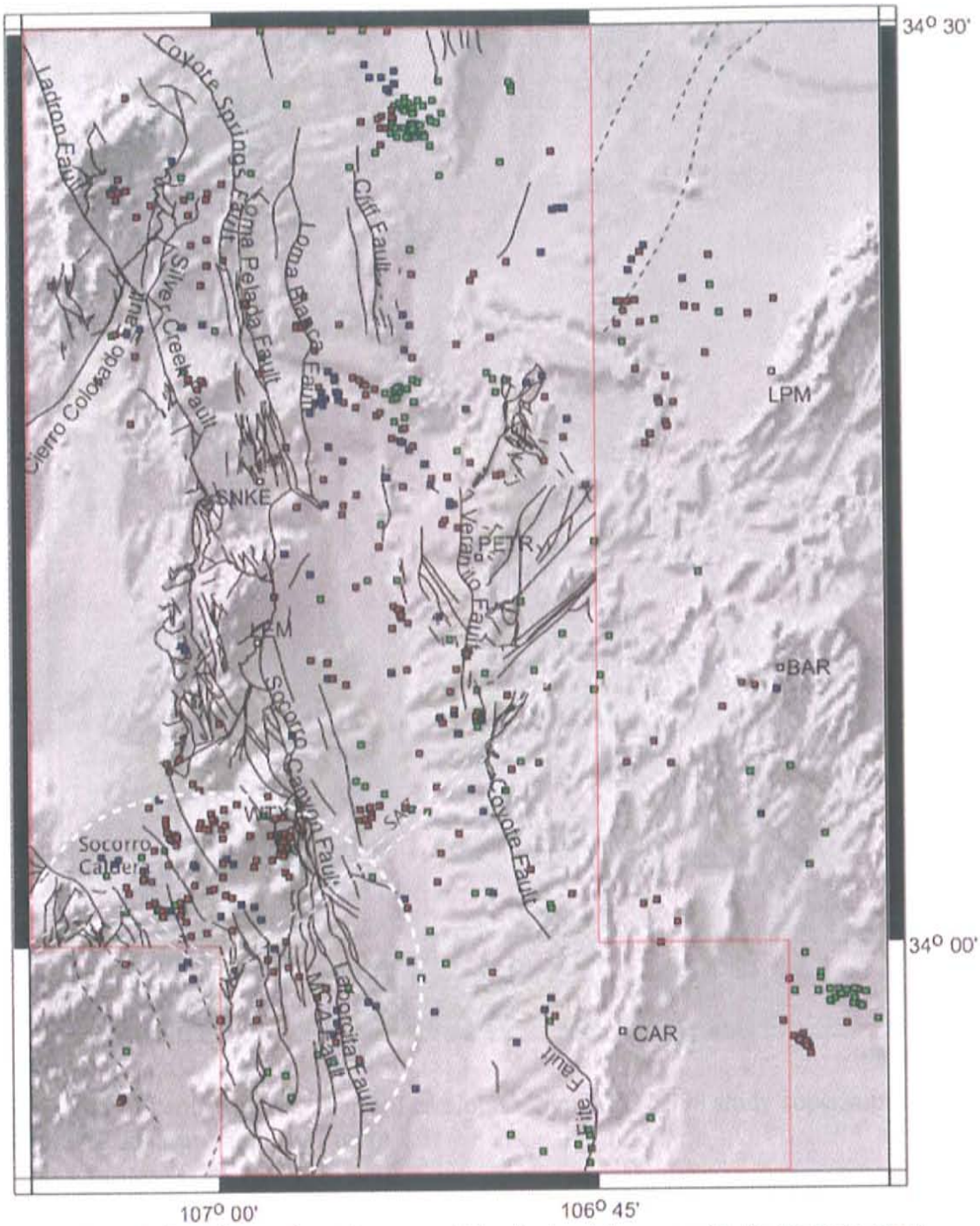

Figure 5.4: Fully relocated catalogue and Sanford catalogues with faults from New Mexico 1:24000 quadrangle maps and New Mexico state map superimposed. Colors are same as Figure 5.3. Red line is the boundary of mapped quadrangles.

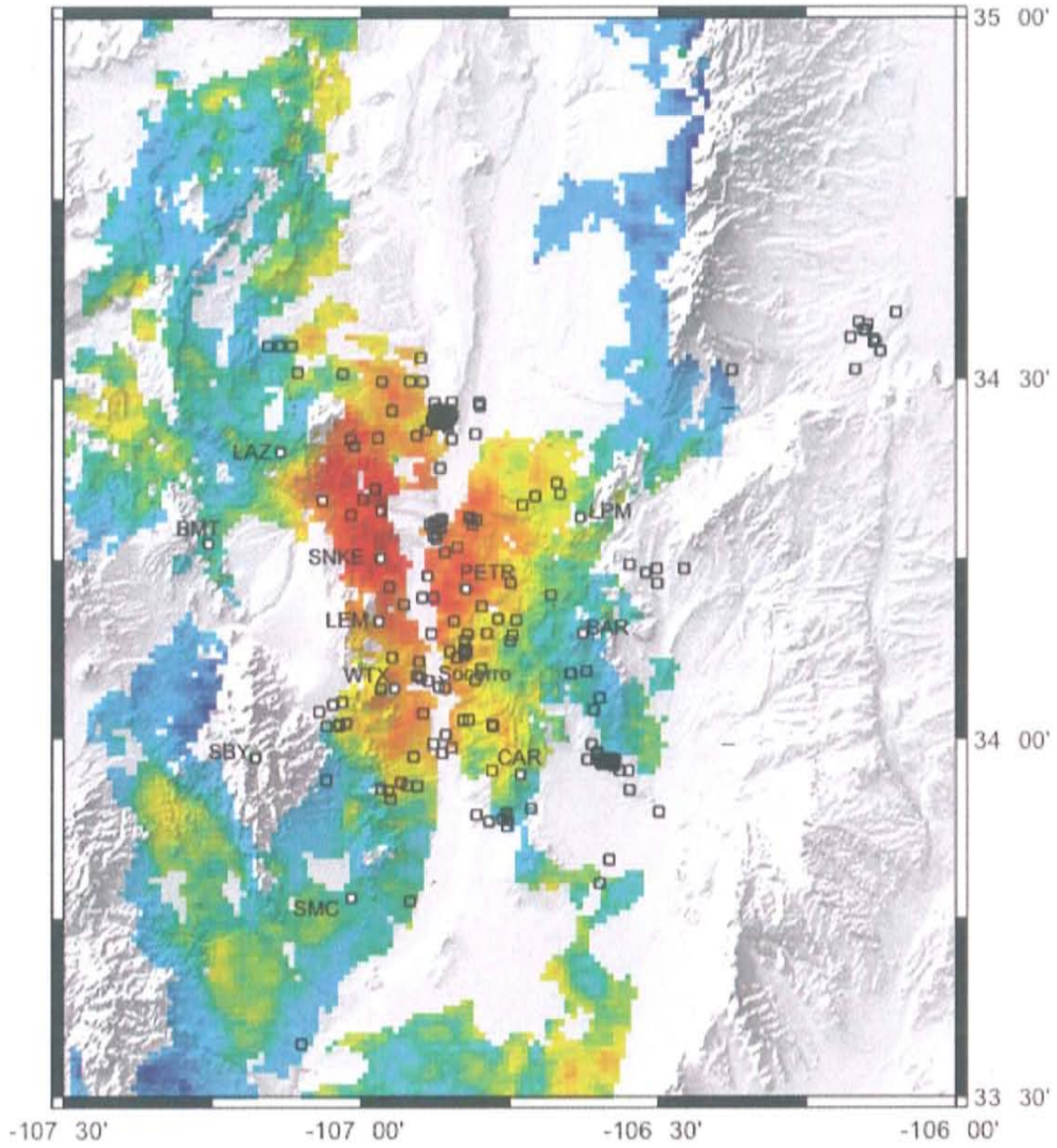

Figure 5.5: Events from the Sanford catalogue from 1962-1998 study superimposed on the InSAR measurements of Figure 2.3.

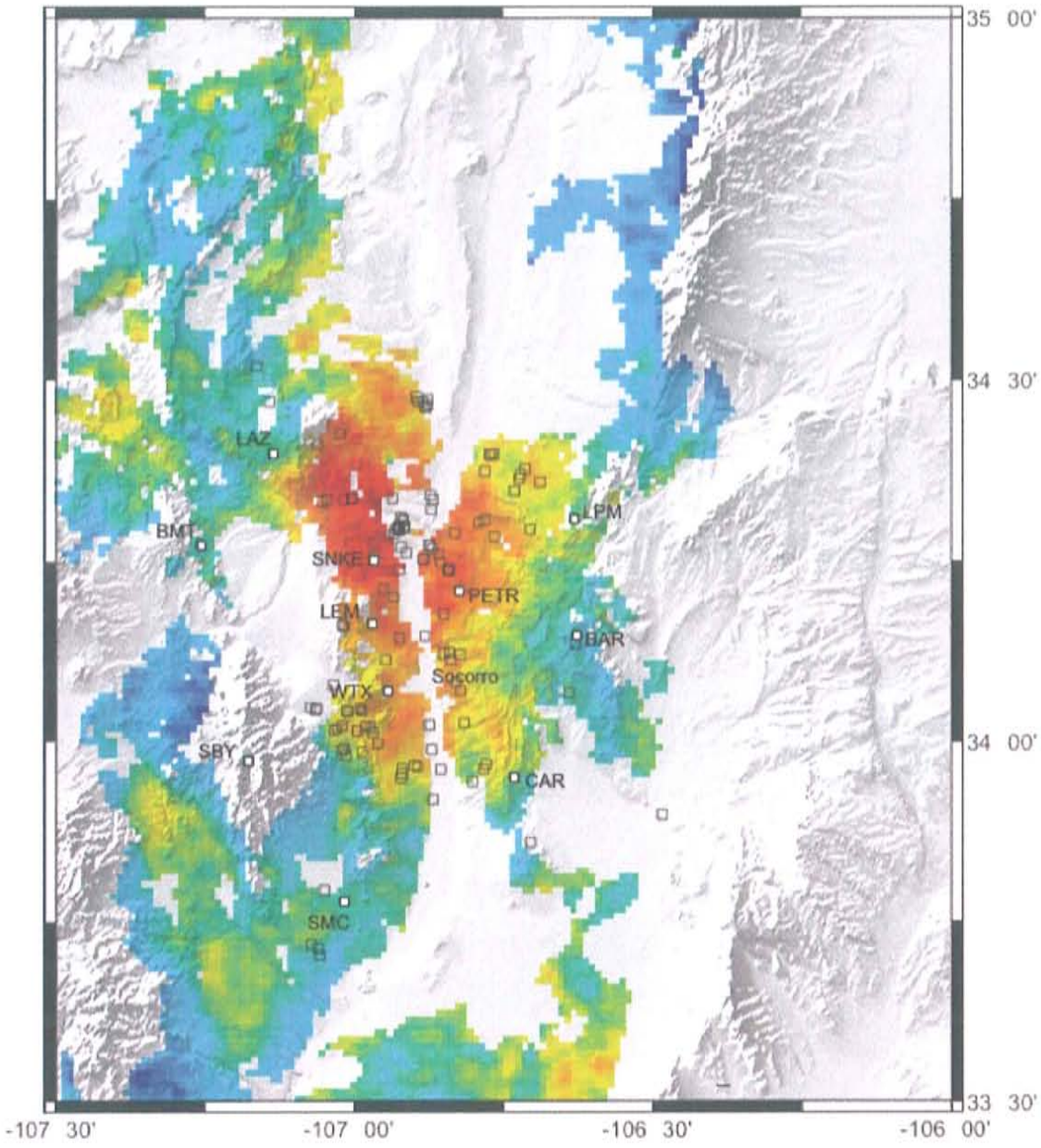

Figure 5.6: Events from the Sanford catalogue from 1999-2004 superimposed on the InSAR measurements of Figure 2.3.

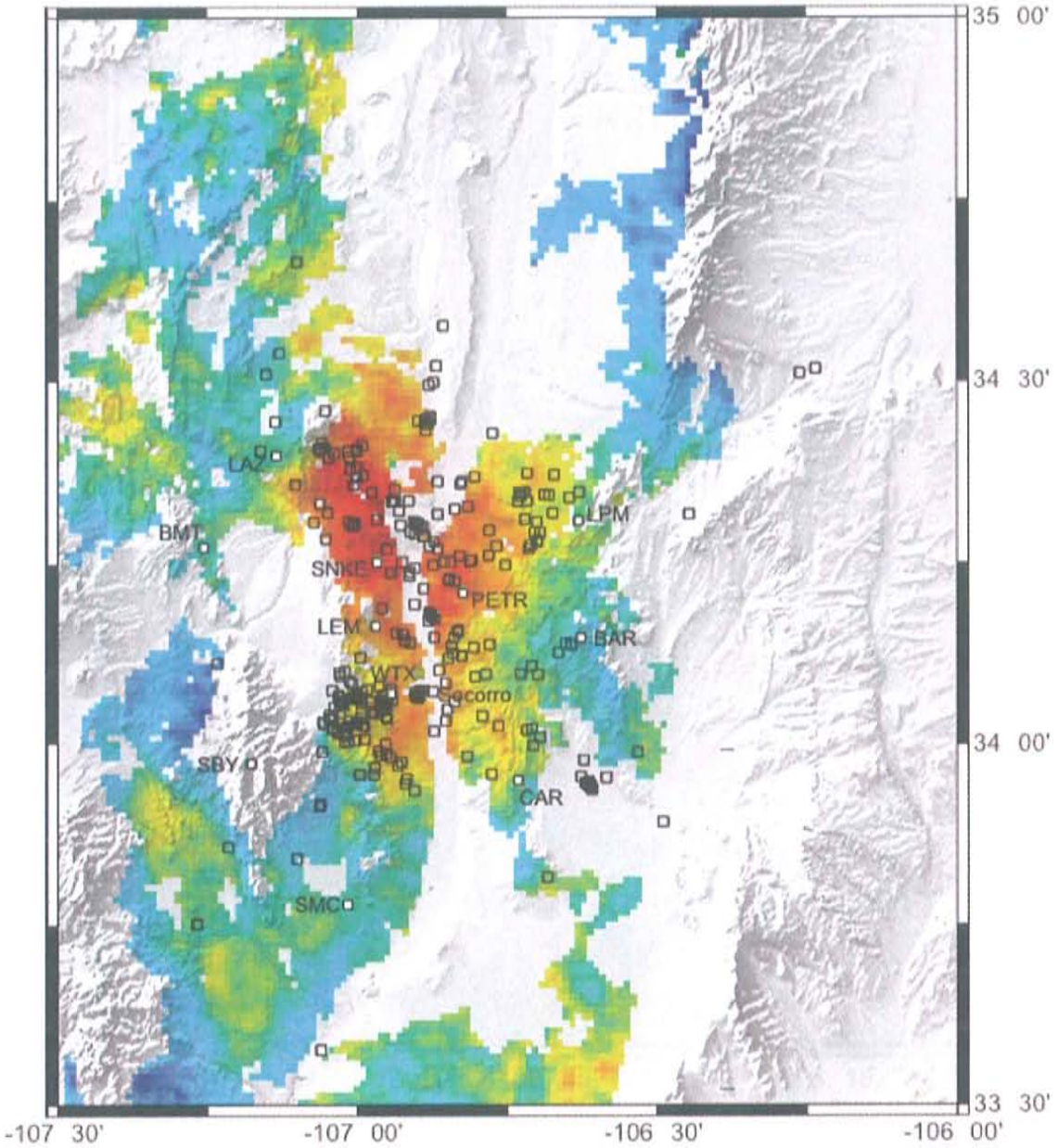

Figure 5.7: Events from the catalogue of earthquakes from this study superimposed on the InSAR measurements of Figure 2.3.

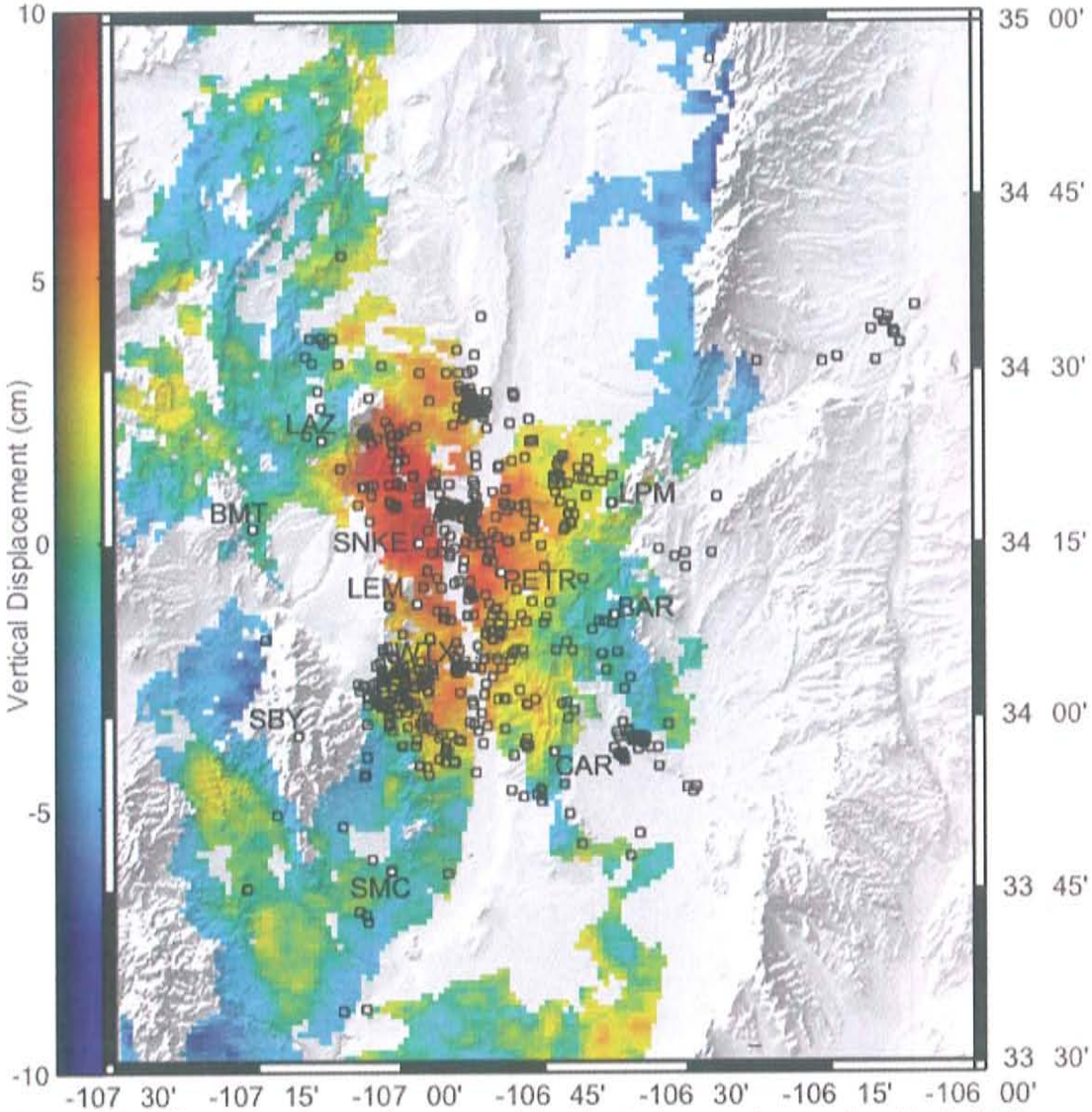

Figure 5.8: All earthquake catalogues used in this study superimposed on the InSAR measurements of Figure 2.3.

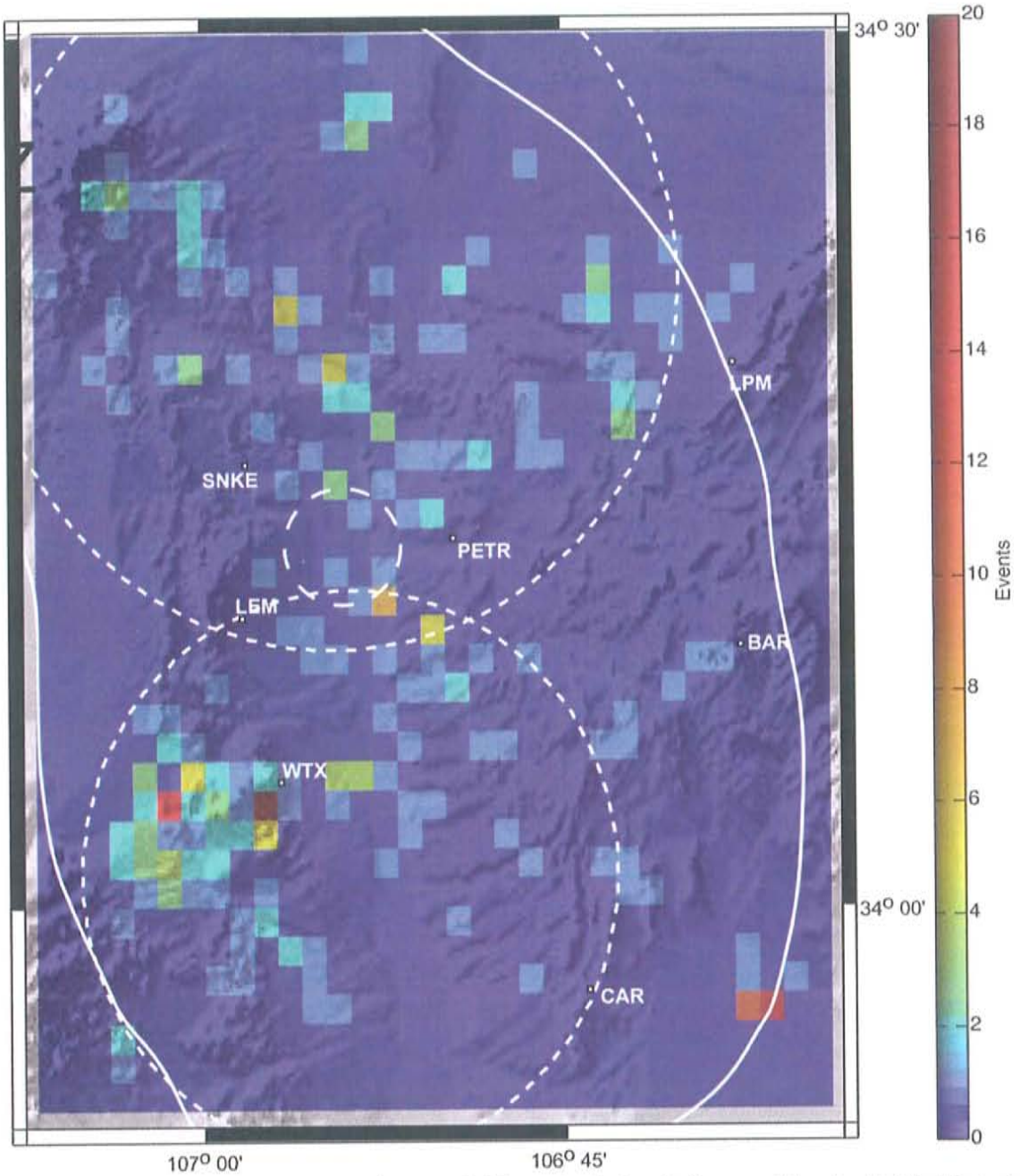

Figure 5.9: Imagesc histogram plot overlaid on shaded relief map. Map is divided into 1 minute bins, and events occurring within each bin are represented by color bar on the right. This map shows events occurring within waveform catalogue. Solid line is outline of Socorro Magma Body. Finely dashed circles are regions of maximum uplift as modeled by Fialko and Simons (2001). Coarsely dashed circle is proposed shallow source.

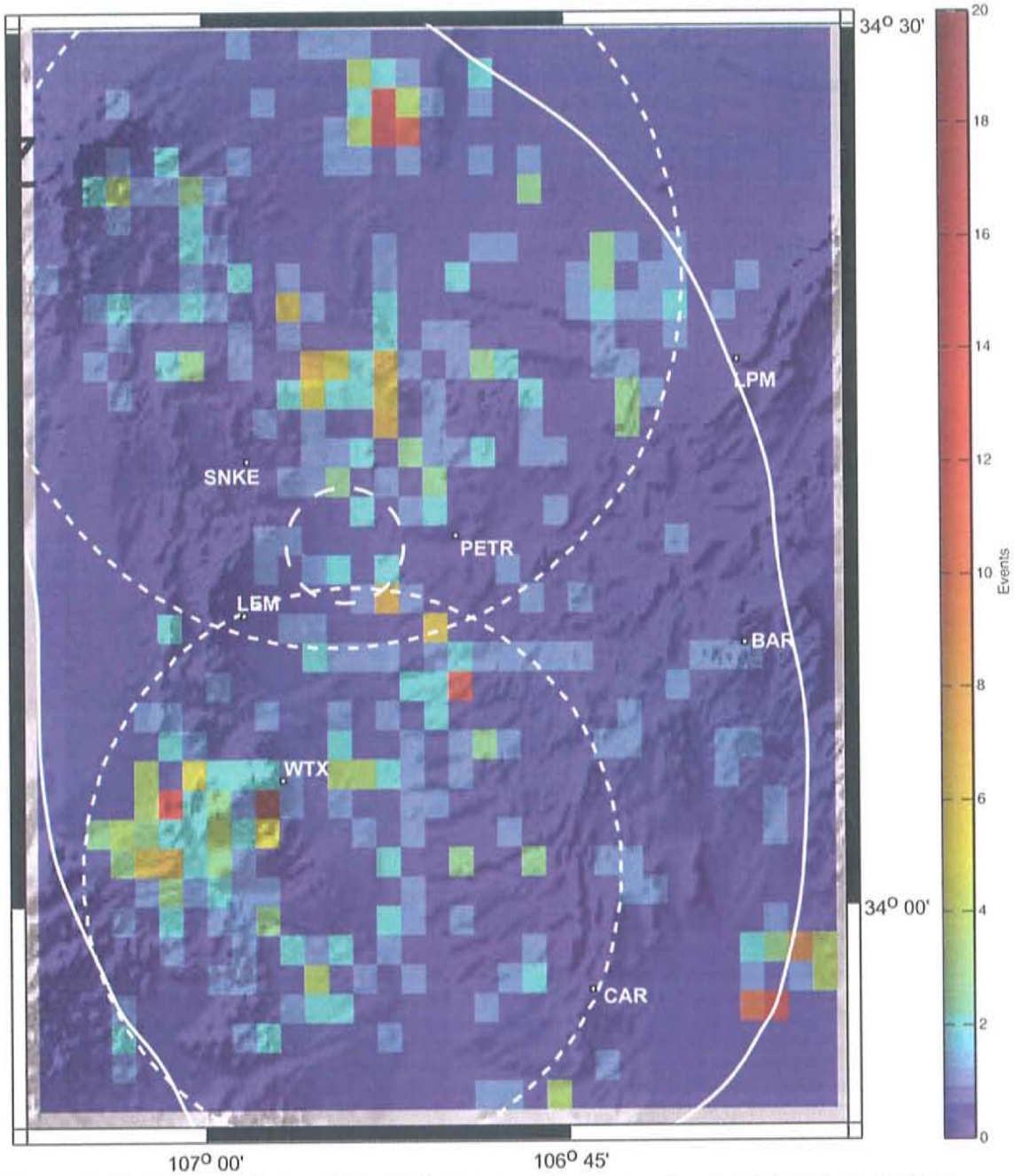

Figure 5.10: Same as figure 5.9 with histogram from waveform catalogue as well as Sanford et al. catalogues.

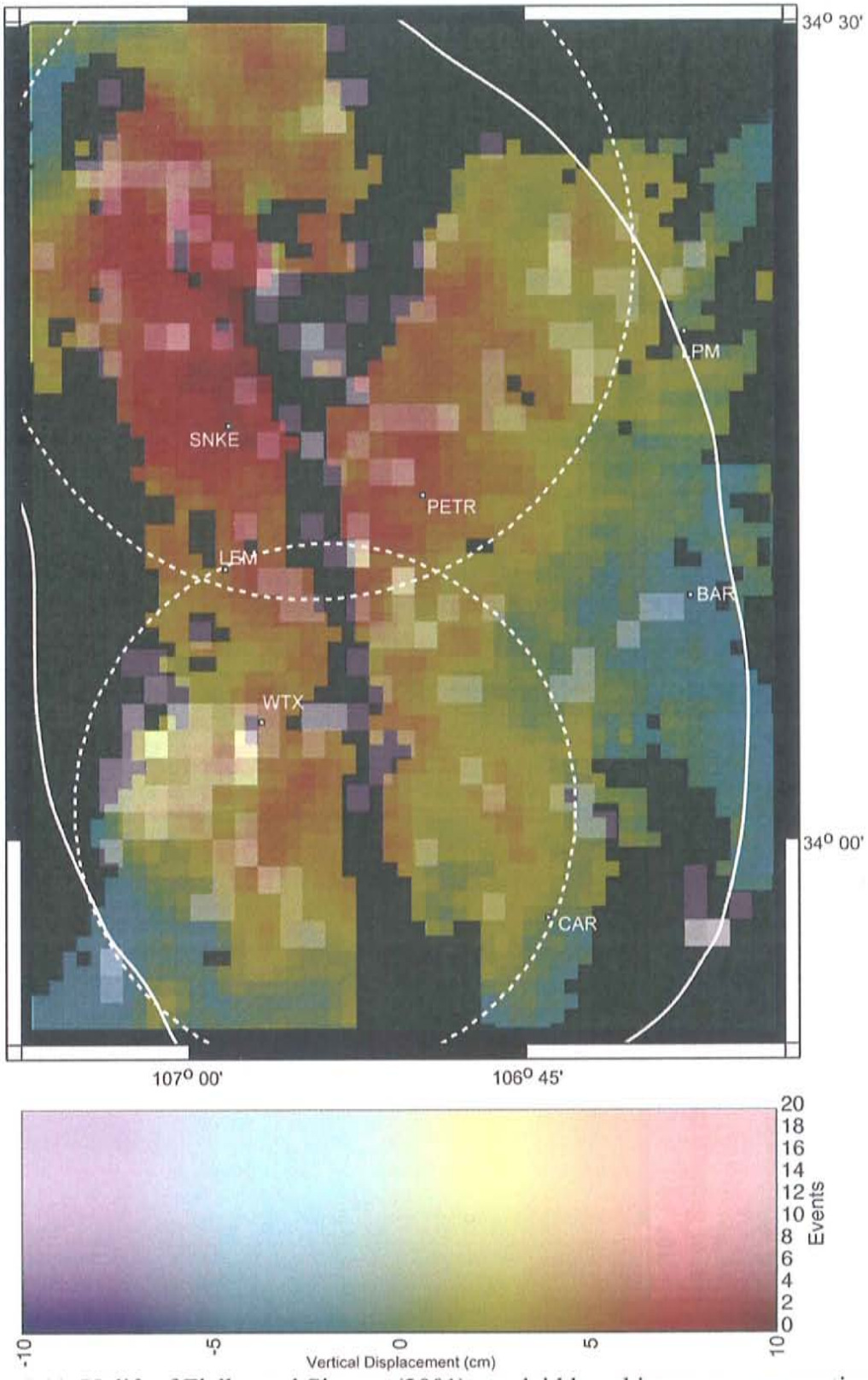

Figure 5.11: Uplift of Fialko and Simons (2001) overlaid by a histogram representing number of events from waveform catalogue occurring within 1 minute bins. Notice the clear relationship between the modeled uplift (dashed lines) and elevated seismicity.

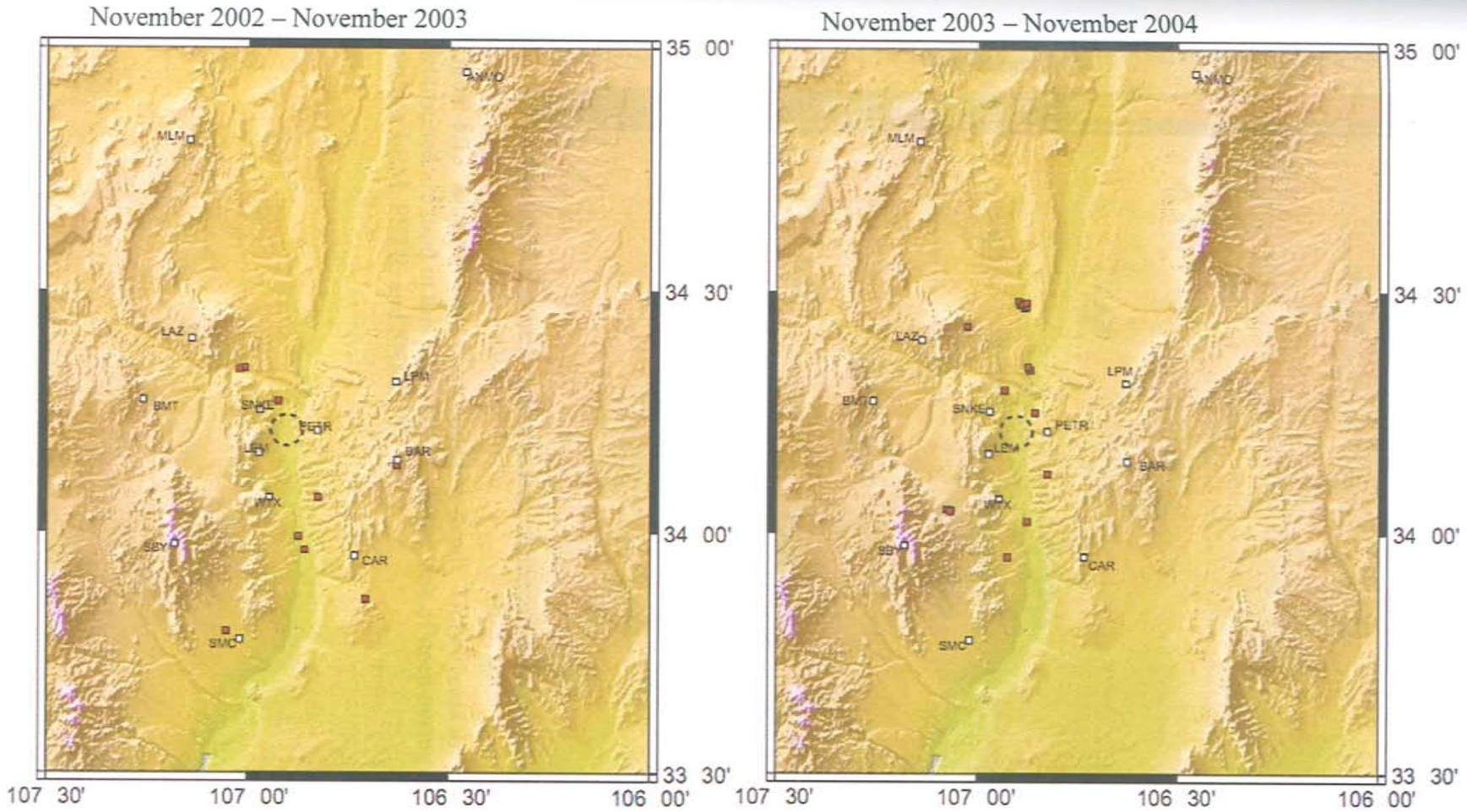

Figure 5.12: Maps of Sanford catalogue events for the periods between GPS campaigns led by Newman (Newman et al., 2004).

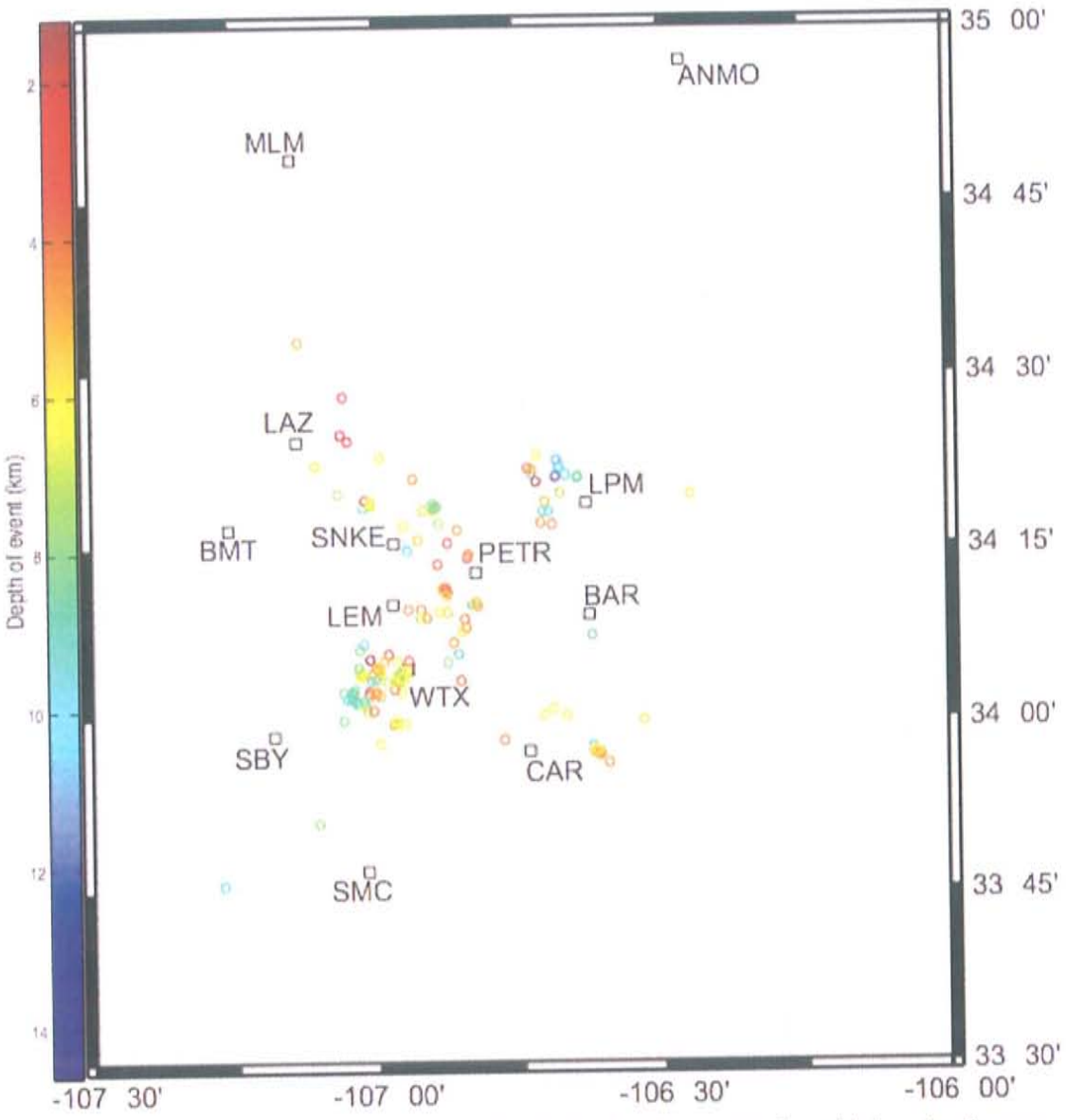

Figure 5.13: Map of events color coded by depth. Only events for which a depth was determined are used in this plot. Of note is the lack of deep events (>6 km) between stations LEM, PETR, and SNKE.

Appendix A: Earthquake Catalogue – Initial Locations

ind = index | lat = latitude | 1std = 1st standard deviation | dep = depth | yyyy = year

m = month | d = day | h = hour | mi = minute | orig = origin time

mag = magnitude | rms = root mean square error | sta = initial stations | pic = initial picks | ref = reflections

ind	lat	1std	long	1std	dep	1std	yyyy	m	d	h	m	orig	1std	mag	rms	sta	pic	ref
1	34.03483	0.40	-106.85517	0.38	5.00	0.00	2004	9	3	22	41	2.34	0.07	0.96	0.25	6	9	0
2	33.94717	0.31	-106.92300	0.34	5.00	0.00	2004	9	7	10	58	48.87	0.05	1.11	0.23	7	13	0
3	34.24583	1.48	-105.82583	1.03	5.00	0.00	2004	9	10	0	8	52.45	0.20	1.30	0.31	5	9	0
4	34.06117	0.36	-106.84050	0.35	5.00	0.00	2004	9	20	15	12	4.74	0.05	0.94	0.17	5	9	0
5	34.51417	0.31	-107.15633	0.44	5.00	0.00	2004	9	21	5	15	51.39	0.05	1.73	0.13	9	12	0
6	34.04133	0.29	-106.79333	0.37	5.00	0.00	2004	9	22	1	29	6.66	0.04	0.85	0.15	5	8	0
7	33.95600	0.97	-106.58633	0.97	5.00	0.00	2004	9	25	10	5	46.75	0.18	0.51	0.02	4	4	0
8	34.29567	0.65	-106.70633	0.52	8.93	1.04	2004	9	27	7	44	40.31	0.12	0.33	0.45	4	7	1
9	34.27700	0.50	-106.77000	0.37	5.00	0.00	2004	9	28	12	40	39.20	0.07	-0.03	0.13	4	8	0
10	34.11083	0.35	-106.71133	0.44	5.00	0.00	2004	10	5	7	16	58.70	0.05	0.41	0.26	4	7	0
11	34.07050	2.18	-107.03383	0.68	8.07	2.39	2004	10	5	12	30	0.44	0.21	1.58	0.02	4	5	0
12	33.97217	0.65	-106.93467	0.62	5.00	0.00	2004	10	9	7	2	34.43	0.13	0.62	0.23	4	8	0
13	34.44650	1.45	-106.88533	0.39	5.00	0.00	2004	10	14	13	55	0.58	0.17	0.35	0.02	5	5	0
14	34.45250	1.18	-106.88767	0.39	5.00	0.00	2004	10	14	19	24	57.56	0.13	0.36	0.12	4	6	0
15	34.45633	0.38	-106.88100	0.37	5.00	0.00	2004	10	16	0	52	5.72	0.05	0.57	0.04	7	8	0
16	34.14067	0.36	-106.78183	0.27	5.00	0.00	2004	10	21	4	50	27.74	0.05	0.32	0.19	4	7	0
17	33.75283	0.68	-107.27133	0.75	9.71	1.72	2004	10	22	1	11	18.86	0.16	0.58	0.14	5	10	0
18	34.33750	0.36	-106.73617	0.33	5.00	0.00	2004	10	24	10	41	8.41	0.05	0.88	0.33	6	10	0
19	34.09633	0.25	-107.03133	0.27	8.05	1.30	2004	10	24	13	43	26.64	0.08	0.84	0.24	8	15	0
20	34.52250	0.49	-106.23433	1.12	5.00	0.00	2004	10	25	9	19	11.31	0.18	1.10	0.29	5	9	0

21	34.10333	0.75	-107.02400	0.95	9.76	0.83	2004	10	31	9	1	14.87	0.15	0.10	0.22	3	7	1
22	34.08183	0.51	-107.01250	0.60	1.35	8.04	2004	10	31	15	28	22.93	0.16	0.21	0.33	4	8	0
23	34.11433	0.34	-107.23817	0.49	5.00	0.00	2004	11	1	1	24	19.01	0.07	0.13	0.15	5	8	0
24	34.05933	0.30	-107.02883	0.49	5.00	0.00	2004	11	11	19	30	7.94	0.06	0.42	0.31	7	11	0
25	34.34633	0.30	-106.94033	0.23	5.00	0.00	2004	11	16	21	12	28.57	0.04	1.08	0.23	8	13	0
26	34.34367	0.61	-106.93867	0.43	5.00	0.00	2004	11	16	22	6	8.77	0.07	0.38	0.20	5	7	0
27	33.95367	0.31	-106.92050	0.31	5.00	0.00	2004	11	20	1	27	0.25	0.04	1.31	0.30	8	11	0
28	34.34300	0.31	-106.94367	0.28	5.00	0.00	2004	11	25	21	9	44.45	0.04	1.33	0.15	8	11	0
29	34.46400	0.31	-107.05667	0.43	2.96	3.42	2004	12	4	22	4	53.28	0.07	1.26	0.15	9	12	0
30	34.14967	0.36	-106.87617	0.31	5.21	0.80	2004	12	5	0	14	33.51	0.06	0.50	0.14	5	10	1
31	34.37500	0.88	-106.99300	0.72	6.49	1.39	2004	12	5	2	31	4.65	0.17	0.49	0.13	4	9	1
32	34.02750	0.44	-106.98950	0.36	5.00	0.00	2004	12	14	6	59	27.55	0.05	0.36	0.04	4	6	0
33	34.33883	0.29	-106.94567	0.32	5.00	0.00	2004	12	18	17	37	20.38	0.04	0.79	0.22	8	11	0
34	34.28017	1.21	-106.88283	0.78	5.00	0.00	2004	12	21	0	50	14.07	0.15	0.47	0.07	4	6	0
35	34.41950	0.59	-107.06183	0.37	5.00	0.00	2004	12	21	12	2	8.99	0.08	0.58	0.17	5	8	0
36	34.41250	0.31	-107.06733	0.32	5.00	0.00	2004	12	21	12	6	39.40	0.04	0.76	0.12	8	12	0
37	34.41200	0.31	-107.06600	0.33	5.00	0.00	2004	12	21	21	31	52.64	0.04	1.17	0.11	8	11	0
38	34.41283	0.68	-107.06167	0.45	5.00	0.00	2004	12	22	20	48	56.13	0.11	1.63	0.07	6	8	0
39	34.41317	1.51	-107.05717	0.53	5.00	0.00	2004	12	22	21	15	17.38	0.21	0.71	0.06	4	5	0
40	34.39967	0.64	-107.01600	0.32	5.00	0.00	2004	12	29	8	43	27.29	0.07	0.62	0.18	6	8	0
41	34.30817	0.39	-106.90000	0.30	8.23	0.63	2005	1	6	12	7	3.55	0.06	0.28	0.25	6	12	2
42	34.29783	0.26	-106.91867	0.27	5.78	0.89	2005	1	9	14	0	53.58	0.04	0.67	0.29	8	15	1
43	34.27950	0.43	-106.89017	0.33	7.30	0.67	2005	1	11	7	51	55.52	0.07	-0.14	0.32	5	12	2
44	34.27317	0.25	-106.95283	0.35	6.53	0.79	2005	1	14	21	7	18.20	0.05	0.51	0.15	8	13	1
45	34.06550	0.27	-107.01283	0.48	5.00	0.00	2005	1	15	9	54	58.66	0.05	0.55	0.24	5	9	0
46	34.10550	0.30	-106.86667	0.36	4.52	0.87	2005	1	15	14	28	22.80	0.05	0.31	0.22	4	9	1
47	34.09567	0.34	-106.80550	0.41	5.00	0.00	2005	1	17	23	31	36.27	0.05	0.70	0.07	4	6	0
48	34.07333	0.36	-106.88933	0.38	5.00	0.00	2005	1	18	19	33	25.61	0.04	0.47	0.11	5	6	0
49	34.07550	0.32	-106.89750	0.41	5.00	0.00	2005	1	18	20	56	54.28	0.05	0.48	0.35	4	7	0
50	34.07633	0.34	-106.88917	0.45	5.00	0.00	2005	1	19	1	13	52.02	0.04	0.36	0.27	5	7	0
51	34.07367	0.27	-106.88833	0.37	5.00	0.00	2005	1	19	2	52	29.21	0.04	0.90	0.42	7	10	0

52	34.07017	0.29	-106.89733	0.40	5.00	0.00	2005	1	19	6	19	10.78	0.05	0.58	0.22	4	8	0
53	34.07333	0.33	-106.89833	0.36	5.00	0.00	2005	1	19	12	1	0.34	0.04	0.38	0.33	5	7	0
54	34.03533	0.30	-106.95267	0.39	5.00	0.00	2005	1	19	21	46	56.45	0.05	0.05	0.11	4	8	0
55	34.04283	0.38	-106.94983	0.35	5.00	0.00	2005	1	19	23	56	5.13	0.05	0.26	0.07	4	7	0
56	34.04317	0.39	-106.95233	0.30	5.00	0.00	2005	1	20	3	16	33.08	0.05	0.45	0.03	5	8	0
57	34.06667	0.30	-106.89767	0.44	5.00	0.00	2005	1	21	3	26	7.61	0.04	0.34	0.07	4	7	0
58	34.04750	0.34	-106.98233	0.42	6.95	0.85	2005	1	22	0	53	41.18	0.07	0.55	0.15	4	8	1
59	34.30400	0.41	-106.89867	0.39	7.61	0.90	2005	1	25	1	51	16.80	0.07	0.26	0.19	4	8	1
60	34.15317	0.53	-106.94450	0.78	4.30	0.59	2005	1	27	1	3	49.69	0.06	0.55	0.40	4	8	1
61	34.07250	0.32	-106.88717	0.41	5.00	0.00	2005	2	1	8	23	20.29	0.05	0.10	0.27	4	7	0
62	34.39933	0.37	-107.04983	0.62	2.73	1.24	2005	2	4	0	35	28.37	0.06	0.29	0.17	4	8	1
63	34.40850	0.33	-107.06350	0.29	1.99	1.17	2005	2	4	1	20	30.41	0.05	0.47	0.12	6	12	1
64	34.44667	0.38	-106.88817	0.32	5.00	0.00	2005	2	9	4	53	27.78	0.05	0.39	0.13	5	9	0
65	34.45000	0.34	-106.90117	0.35	5.00	0.00	2005	2	9	10	40	21.50	0.05	0.86	0.46	6	10	0
66	34.34667	1.29	-106.68517	1.29	14.60	2.66	2005	2	11	9	25	42.58	0.40	0.58	0.05	4	5	0
67	34.43750	0.42	-106.88883	0.41	5.00	0.00	2005	2	16	6	12	46.78	0.05	0.85	0.06	5	6	0
68	34.34500	0.40	-106.93633	0.29	4.48	0.73	2005	2	21	16	49	24.56	0.06	0.31	0.37	5	12	2
69	34.30600	0.31	-107.01133	0.39	6.68	2.08	2005	2	23	18	18	5.90	0.09	1.82	0.03	8	8	0
70	33.81733	0.47	-106.68400	0.75	5.00	0.00	2005	2	28	9	57	28.49	0.09	0.47	4.15	3	6	0
71	34.14200	0.42	-106.65317	0.60	5.00	0.00	2005	3	4	3	7	3.13	0.07	0.53	0.39	4	7	0
72	34.30317	0.38	-106.89850	0.38	7.83	0.88	2005	3	5	0	48	13.68	0.07	-0.11	0.17	5	9	1
73	34.15133	0.43	-106.89167	0.58	6.51	1.60	2005	3	5	16	17	2.30	0.12	0.73	0.15	5	7	0
74	34.14050	0.42	-106.64467	0.69	5.00	0.00	2005	3	7	18	52	13.19	0.08	0.24	0.12	3	5	0
75	34.50383	0.30	-106.87533	0.34	5.00	0.00	2005	3	20	12	59	13.88	0.05	1.13	0.20	8	15	1
76	34.33950	0.26	-106.94433	0.32	5.00	0.00	2005	3	20	14	4	8.96	0.04	1.06	0.23	9	15	1
77	34.05100	0.27	-106.97167	0.26	6.14	0.64	2005	3	29	14	6	33.45	0.04	0.53	0.17	7	14	2
78	34.49950	0.39	-106.88317	0.37	5.00	0.00	2005	3	31	17	31	42.31	0.06	0.37	0.13	5	8	0
79	34.52650	0.96	-106.87167	0.42	5.00	0.00	2005	3	31	20	30	26.22	0.15	0.46	0.70	4	8	1
80	33.99183	0.32	-107.05900	0.34	7.96	0.48	2005	4	1	4	45	6.60	0.05	0.05	0.15	5	14	3
81	34.06883	0.27	-107.00050	0.27	5.64	0.67	2005	4	2	11	3	4.01	0.05	0.81	0.06	8	14	1
82	34.06800	0.24	-107.00117	0.26	4.47	0.45	2005	4	2	16	53	14.83	0.03	0.60	0.34	9	18	4

83	34.06500	0.35	-106.99617	0.37	5.74	0.58	2005	4	2	17	22	53.18	0.05	0.26	0.13	6	12	1
84	34.07800	0.35	-106.98867	0.68	5.04	0.61	2005	4	2	21	44	12.11	0.07	0.22	0.23	4	8	1
85	34.06817	0.26	-107.00017	0.31	4.18	1.16	2005	4	2	22	48	6.13	0.05	1.36	0.13	10	11	0
86	34.06933	0.27	-107.00167	0.28	4.84	0.86	2005	4	2	23	41	15.53	0.05	0.81	0.15	8	13	0
87	34.02117	0.36	-107.03717	0.34	8.69	0.52	2005	4	11	14	1	33.85	0.05	0.35	0.08	7	14	2
88	33.98800	0.32	-106.95400	0.29	6.50	1.25	2005	4	15	10	44	18.40	0.08	0.64	0.11	7	13	0
89	34.23000	0.26	-106.85033	0.31	5.00	0.00	2005	4	17	8	55	22.55	0.04	0.69	0.14	7	11	0
90	34.23217	0.37	-106.84867	0.34	5.00	0.00	2005	4	17	9	11	57.84	0.05	0.63	0.06	6	8	0
91	34.30950	0.42	-107.00983	0.42	6.60	2.11	2005	4	22	21	44	20.15	0.11	0.24	0.02	6	8	0
92	34.27917	0.68	-106.87550	0.50	5.00	0.00	2005	4	23	12	24	32.48	0.10	0.68	0.23	5	8	0
93	34.05117	0.88	-107.00917	1.41	8.25	1.38	2005	4	23	19	15	25.61	0.25	0.14	0.05	4	6	0
94	34.05367	0.35	-107.00300	0.36	9.28	0.93	2005	4	24	4	53	59.02	0.08	0.93	0.11	7	10	0
95	34.31017	0.49	-106.70433	0.56	5.06	2.23	2005	4	29	18	46	19.89	0.14	0.76	0.16	7	10	0
96	34.02400	0.39	-106.71100	0.62	5.00	0.00	2005	4	30	3	16	7.61	0.05	1.00	0.13	5	6	0
97	33.91800	0.33	-107.06483	0.72	5.00	0.00	2005	5	1	6	3	9.96	0.08	0.36	0.05	4	7	0
98	33.91750	0.37	-107.06367	1.19	5.00	0.00	2005	5	1	7	26	8.61	0.12	0.49	0.10	3	6	0
99	33.91617	0.31	-107.06567	0.64	5.00	0.00	2005	5	1	7	37	46.58	0.08	0.50	0.11	5	9	0
100	34.35883	0.82	-106.73333	0.54	3.76	3.07	2005	5	2	6	23	10.40	0.17	0.39	0.17	5	9	0
101	33.85967	0.64	-107.21933	1.19	5.00	0.00	2005	5	3	11	59	39.71	0.19	0.13	0.73	4	6	1
102	34.27383	0.30	-106.71583	0.28	5.00	0.00	2005	5	4	7	3	31.19	0.04	1.28	0.19	9	13	0
103	34.27867	0.34	-106.71217	0.62	4.51	2.46	2005	5	4	7	6	24.95	0.12	0.49	0.09	8	9	0
104	34.27817	0.29	-106.71283	0.30	5.00	0.00	2005	5	4	7	8	30.06	0.04	1.02	0.29	8	12	0
105	34.27817	0.30	-106.71267	0.32	5.00	0.00	2005	5	4	12	3	59.21	0.04	1.13	0.20	9	11	0
106	34.31250	0.32	-107.05867	0.44	5.00	0.00	2005	5	8	11	13	42.47	0.04	0.53	0.31	7	10	1
107	33.98783	0.53	-106.96783	0.38	5.00	0.00	2005	5	11	16	48	18.93	0.08	1.27	0.42	8	13	0
108	33.99150	1.03	-106.96800	1.09	6.44	1.54	2005	5	11	16	50	32.29	0.19	0.73	0.03	4	7	0
109	33.98700	0.79	-106.97267	0.74	4.61	2.11	2005	5	11	19	48	8.25	0.14	0.58	0.05	4	8	0
110	34.29850	0.29	-107.01100	0.31	5.00	0.00	2005	5	12	13	31	24.94	0.03	0.76	0.22	8	12	0
111	33.93817	0.34	-106.90767	0.39	5.00	0.00	2005	5	15	5	48	38.89	0.05	0.85	0.08	6	8	0
112	34.02750	0.49	-106.76600	0.39	5.00	0.00	2005	5	24	5	52	48.88	0.05	0.34	0.05	4	6	0
113	34.31267	1.14	-107.01917	0.60	3.20	6.25	2005	6	1	11	27	18.28	0.10	0.15	0.15	5	8	0

114	34.30317	0.44	-107.02267	0.48	8.64	0.77	2005	6	1	14	5	44.88	0.07	0.39	0.30	7	11	1
115	34.09883	0.60	-106.70050	0.58	5.00	0.00	2005	6	2	3	38	51.78	0.06	0.61	0.02	4	4	0
116	34.30800	0.28	-107.01383	0.33	6.97	1.58	2005	6	2	9	33	0.38	0.07	0.93	0.05	10	12	0
117	34.24083	0.85	-106.91483	0.52	5.00	0.00	2005	6	3	5	20	41.52	0.14	0.75	0.23	4	7	0
118	34.25500	0.42	-106.92750	0.45	5.36	1.69	2005	6	4	0	34	13.58	0.07	0.64	0.06	7	9	0
119	33.94633	0.64	-106.61367	0.87	5.85	2.31	2005	6	4	2	15	0.24	0.16	0.50	0.01	4	6	0
120	33.94550	0.52	-106.61783	0.69	5.03	2.23	2005	6	4	13	13	58.10	0.14	0.65	0.04	5	8	0
121	33.94533	0.52	-106.61650	0.70	5.20	2.20	2005	6	4	21	5	11.27	0.14	0.64	0.04	5	8	0
122	33.94217	0.60	-106.61100	0.84	4.21	2.76	2005	6	4	21	7	6.75	0.15	0.51	0.02	5	7	0
123	33.94500	0.63	-106.61617	0.84	5.97	2.24	2005	6	4	21	26	30.81	0.16	0.69	0.10	4	7	0
124	33.94233	0.64	-106.61217	0.85	5.10	2.63	2005	6	4	22	53	16.30	0.16	0.63	0.11	4	7	0
125	33.94733	0.52	-106.61600	0.70	6.21	1.94	2005	6	4	23	7	3.11	0.14	0.66	0.05	5	8	0
126	33.94483	0.70	-106.60983	0.88	5.26	2.66	2005	6	5	1	32	28.50	0.16	0.47	0.05	4	5	0
127	33.94617	0.96	-106.61283	0.94	5.10	2.57	2005	6	5	2	0	33.73	0.24	0.74	0.01	4	6	0
128	33.94583	0.52	-106.61167	0.71	5.70	2.13	2005	6	5	3	8	30.23	0.14	0.65	0.05	5	8	0
129	33.94367	0.52	-106.61650	0.70	4.56	2.44	2005	6	5	4	6	23.60	0.14	0.85	0.05	5	8	0
130	33.94600	0.52	-106.61483	0.70	6.83	1.84	2005	6	5	4	38	39.17	0.14	1.01	0.06	5	8	0
131	33.94917	0.57	-106.61767	0.80	6.29	1.89	2005	6	5	7	0	28.70	0.15	0.99	0.03	5	8	0
132	33.94683	0.56	-106.61900	0.70	6.52	1.93	2005	6	5	8	8	24.39	0.14	0.79	0.02	5	7	0
133	33.94767	0.49	-106.62100	0.61	5.36	1.92	2005	6	5	10	19	28.64	0.13	1.38	0.11	6	11	0
134	33.94183	0.64	-106.60950	0.86	5.15	2.67	2005	6	5	10	42	9.97	0.16	0.75	0.05	4	7	0
135	33.94417	0.68	-106.61300	0.85	5.32	2.57	2005	6	5	11	11	14.29	0.16	0.50	0.03	4	6	0
136	33.89417	0.81	-106.49017	2.12	5.00	0.00	2005	6	5	12	36	37.64	0.35	0.39	1.51	4	6	0
137	33.94783	0.57	-106.61917	0.80	6.89	1.77	2005	6	5	13	26	14.13	0.16	0.73	0.02	5	8	0
138	33.95283	0.61	-106.62250	0.75	10.65	1.06	2005	6	5	13	29	54.37	0.15	0.43	0.50	5	9	0
139	33.93017	1.08	-106.59533	1.53	4.40	3.74	2005	6	5	15	26	44.79	0.23	0.70	0.00	4	4	0
140	33.94667	0.59	-106.61483	0.83	5.63	2.10	2005	6	5	15	51	27.74	0.15	0.98	0.05	5	7	0
141	33.92450	0.86	-106.60500	1.36	5.00	0.00	2005	6	5	17	28	14.17	0.21	0.63	0.17	4	5	0
142	33.92917	0.60	-106.59333	0.86	5.00	0.00	2005	6	5	21	14	11.89	0.15	0.73	0.40	5	8	0
143	33.94200	0.64	-106.60950	0.86	5.67	2.47	2005	6	5	22	16	20.05	0.16	0.34	0.03	4	7	0
144	33.94867	0.52	-106.61650	0.70	6.95	1.79	2005	6	6	0	27	58.92	0.14	0.57	0.09	5	8	0

145	33.94650	0.57	-106.62250	0.69	5.43	1.91	2005	6	6	0	48	17.81	0.14	0.82	0.09	6	9	0
146	34.23600	0.98	-106.91567	0.51	5.00	0.00	2005	6	8	6	31	32.23	0.15	0.56	0.20	4	6	0
147	33.94700	0.62	-106.61800	0.88	6.00	2.13	2005	6	8	9	23	23.71	0.16	0.42	0.03	4	5	0
148	34.00767	0.39	-107.00733	0.55	3.77	2.18	2005	6	11	10	18	55.58	0.10	0.27	0.05	5	8	0
149	34.05333	0.38	-107.04150	0.39	5.00	0.00	2005	6	11	15	57	1.90	0.05	0.39	0.10	6	8	0
150	34.29817	0.49	-106.90000	0.54	6.72	2.24	2005	6	13	20	22	49.87	0.10	0.42	0.04	6	8	0
151	34.06467	0.70	-106.94767	0.83	5.79	0.66	2005	6	14	3	51	55.62	0.11	0.13	0.10	4	7	1
152	34.14167	0.40	-106.91417	0.34	4.62	1.16	2005	6	14	5	38	41.66	0.07	0.52	0.05	6	8	0
153	34.14283	0.53	-106.92317	0.41	7.12	0.50	2005	6	14	5	47	52.49	0.07	0.08	0.20	4	9	2
154	34.45167	0.35	-106.89033	0.37	5.00	0.00	2005	6	19	3	49	20.27	0.05	0.78	0.25	7	11	0
155	34.37217	0.51	-107.00367	0.42	5.00	0.00	2005	6	23	6	42	12.96	0.07	0.62	0.12	8	12	0
156	34.24633	1.00	-106.90633	0.52	5.00	0.00	2005	6	30	14	46	50.88	0.15	0.39	0.19	4	6	0
157	34.35150	1.29	-106.97850	1.19	5.00	0.00	2005	7	4	3	28	14.24	0.24	0.55	0.07	4	6	0
158	33.95983	0.31	-106.97450	0.31	5.00	0.00	2005	7	12	8	34	49.97	0.04	0.76	0.25	7	10	0
159	34.19633	0.89	-106.90717	0.60	5.00	0.00	2005	7	12	11	49	39.62	0.15	0.79	0.48	4	7	0
160	34.34717	1.29	-106.64483	1.19	8.65	1.82	2005	7	23	0	33	45.36	0.31	0.72	0.06	6	7	0
161	34.05950	0.26	-107.00883	0.25	4.34	0.57	2005	8	5	12	44	58.49	0.04	0.69	0.19	10	17	2
162	34.26333	0.73	-106.83083	0.46	5.00	0.00	2005	8	6	6	44	30.84	0.08	0.37	0.02	5	7	0
163	34.02050	0.41	-107.02367	0.41	10.08	1.61	2005	8	7	17	11	21.51	0.15	0.71	0.05	7	9	0
164	34.12167	0.44	-106.85100	0.34	5.62	2.05	2005	8	10	2	4	1.82	0.10	0.63	0.07	6	8	0
165	33.99950	0.61	-106.66817	0.97	6.47	1.55	2005	8	14	13	49	15.36	0.15	0.46	0.20	5	7	0
166	34.38367	0.32	-107.01433	0.31	5.00	0.00	2005	8	16	20	58	48.00	0.04	0.51	0.11	7	10	0
167	33.98850	0.36	-106.96483	0.53	6.40	1.44	2005	8	22	14	49	14.36	0.10	0.65	0.09	6	9	0
168	34.37133	1.62	-106.68067	1.26	11.20	3.13	2005	8	25	5	21	45.04	0.47	0.16	0.05	4	5	0
169	34.34783	1.28	-106.66533	1.24	9.39	2.06	2005	8	27	21	2	48.41	0.31	0.06	0.03	4	5	0
170	34.24017	0.82	-106.94550	0.84	9.68	1.47	2005	8	27	23	9	29.50	0.19	0.67	0.15	4	6	0
171	34.45233	0.41	-106.88100	0.44	5.00	0.00	2005	9	1	9	38	1.68	0.05	0.64	0.04	7	7	0
172	34.31367	0.91	-106.90517	0.62	5.00	0.00	2005	9	1	16	50	55.08	0.14	0.44	0.16	5	7	0
173	34.31517	0.91	-106.90683	0.63	5.00	0.00	2005	9	4	11	25	15.69	0.15	0.28	0.14	5	7	0
174	34.00950	1.25	-106.69167	2.32	6.09	1.54	2005	9	18	10	59	35.73	0.19	0.28	0.11	4	7	0
175	34.12667	0.41	-106.82833	0.31	5.00	0.00	2005	9	20	9	59	39.89	0.04	0.58	0.06	7	8	0

176	34.12583	0.41	-106.82867	0.35	5.00	0.00	2005	9	20	17	40	54.05	0.04	0.57	0.03	6	6	0
177	34.27000	1.04	-106.85850	0.91	4.47	5.70	2005	9	20	18	22	32.32	0.31	0.50	0.00	4	5	0
178	34.07783	0.55	-107.04400	0.56	5.00	0.00	2005	9	25	13	8	14.51	0.06	-0.01	0.06	4	5	0
179	33.99150	0.49	-106.53267	1.20	5.65	0.73	2005	10	2	18	23	5.82	0.17	0.51	0.09	4	8	1
180	34.32083	0.81	-106.44767	1.67	5.99	5.08	2005	10	5	23	37	56.61	0.23	0.42	0.13	4	7	0
181	34.43300	0.26	-106.77667	0.24	5.00	0.00	2005	10	7	18	37	33.60	0.04	0.95	0.17	8	12	0
182	34.17300	0.42	-106.87767	0.30	5.74	0.58	2005	10	12	18	54	46.30	0.05	0.57	0.12	5	11	2
183	34.05083	0.38	-106.85267	0.35	3.66	0.65	2005	10	15	19	23	11.71	0.05	0.00	0.10	5	8	1
184	34.12683	0.34	-106.84350	0.22	4.24	0.45	2005	10	16	17	40	46.50	0.03	0.90	0.15	8	13	2
185	34.01983	0.28	-106.87467	0.23	5.00	0.00	2005	10	17	7	47	53.38	0.04	0.67	0.25	8	13	0
186	34.13883	0.56	-106.84517	0.31	4.03	0.47	2005	10	18	5	17	27.73	0.05	0.62	0.07	5	9	2
187	34.05683	0.36	-106.95583	0.34	6.46	0.34	2005	10	21	8	11	36.44	0.05	-0.21	0.18	5	9	2
188	34.05917	0.77	-106.95833	0.46	7.66	0.72	2005	10	21	8	29	55.91	0.11	-0.91	0.12	4	6	0
189	34.03767	0.38	-106.97100	0.38	3.54	0.45	2005	10	24	18	14	11.83	0.05	-0.34	0.47	4	9	2
190	34.05817	0.35	-106.95850	0.38	6.31	0.35	2005	10	24	18	16	27.44	0.05	-0.88	0.19	4	8	2
191	34.06000	0.40	-106.95900	0.27	7.71	0.60	2005	10	24	18	27	53.67	0.09	-0.41	0.04	4	7	0
192	33.84283	0.44	-107.10417	0.44	7.84	1.30	2005	10	25	18	6	53.49	0.14	0.05	0.06	6	8	0
193	34.05583	0.39	-106.95467	0.35	6.39	0.35	2005	10	26	23	28	18.01	0.05	0.16	0.15	6	11	2
194	34.04733	0.73	-106.96350	0.75	6.98	0.47	2005	10	27	4	29	51.25	0.09	-0.94	0.24	4	6	1
195	34.01750	0.74	-107.02433	0.56	5.96	0.59	2005	10	29	0	31	12.73	0.10	-0.93	0.26	4	7	1
196	34.05517	0.28	-106.95800	0.34	7.08	0.34	2005	10	30	1	56	49.98	0.04	1.15	0.19	7	14	3
197	34.05550	0.60	-106.95467	0.50	7.00	0.33	2005	10	30	2	5	25.22	0.07	0.06	0.20	6	12	2
198	34.29933	0.85	-106.78150	0.40	5.00	0.00	2005	10	30	2	5	0.13	0.13	0.05	0.11	4	8	0
199	34.05633	0.42	-106.95633	0.36	6.47	0.33	2005	10	30	2	9	18.76	0.04	0.56	0.19	6	14	3
200	34.05650	0.31	-106.95533	0.32	7.07	0.79	2005	10	30	2	57	35.18	0.06	2.33	0.07	10	10	0
201	34.05817	0.54	-106.95983	0.48	7.42	0.29	2005	10	30	2	59	24.50	0.05	0.00	0.37	4	7	3
202	34.05717	0.33	-106.95867	0.33	6.37	0.34	2005	10	30	3	3	38.00	0.04	0.00	0.28	7	17	3
203	34.05733	0.39	-106.95700	0.33	5.90	0.24	2005	10	30	3	6	50.79	0.04	0.40	0.18	5	12	3
204	34.05517	0.49	-106.95600	0.38	5.71	0.27	2005	10	30	3	7	25.96	0.04	0.29	0.16	5	8	3
205	34.05133	0.57	-106.96600	0.48	6.93	0.85	2005	10	30	3	14	32.46	0.08	-0.51	0.16	4	5	1
206	34.05517	1.60	-106.96467	2.46	7.85	1.82	2005	10	30	3	15	52.70	0.36	0.11	0.00	4	4	0

207	34.05800	0.50	-106.95767	0.39	6.84	0.28	2005	10	30	3	19	55.73	0.04	-0.21	0.18	5	8	3
208	34.05817	0.53	-106.95850	0.40	6.16	0.59	2005	10	30	3	26	37.41	0.06	0.21	0.20	5	7	2
209	34.05667	0.52	-106.95767	0.38	6.11	0.40	2005	10	30	4	43	6.69	0.05	0.11	0.18	5	8	3
210	34.06100	0.54	-106.95700	0.39	7.23	0.48	2005	10	30	4	45	20.86	0.05	-0.01	0.15	5	7	2
211	34.05917	0.54	-106.95783	0.39	6.59	0.54	2005	10	30	4	50	47.47	0.05	0.22	0.19	5	8	3
212	34.06583	2.12	-106.94767	2.88	6.93	1.03	2005	10	30	5	1	24.00	0.23	-0.63	0.00	3	4	1
213	34.01917	0.65	-107.02317	0.46	7.68	1.31	2005	10	30	5	26	15.79	0.10	-0.26	0.07	4	5	1
214	34.05167	0.47	-106.95717	0.45	6.07	0.40	2005	11	1	9	28	12.91	0.05	0.62	0.19	6	9	3
215	34.05500	0.48	-106.95783	0.36	6.30	0.34	2005	11	3	14	58	57.27	0.05	0.28	0.16	4	10	3
216	34.05267	0.55	-106.95683	0.47	5.81	0.43	2005	11	3	14	58	57.28	0.06	0.28	0.20	4	7	3
217	34.06333	0.26	-106.94383	0.27	5.00	0.00	2005	11	4	22	15	43.34	0.04	0.28	0.74	6	13	2
218	34.06083	0.50	-106.96467	0.52	6.06	0.40	2005	11	4	22	26	17.80	0.07	-0.27	0.16	4	10	2
219	34.05983	0.42	-106.95783	0.32	6.90	0.42	2005	11	4	23	26	41.00	0.05	0.24	0.09	5	11	2
220	34.07967	0.39	-106.96483	0.30	6.63	0.29	2005	11	5	2	9	33.89	0.04	0.30	0.34	5	13	3
221	34.05900	0.46	-106.95683	0.46	7.43	1.08	2005	11	6	12	33	43.35	0.10	1.25	0.03	7	7	0
222	34.05350	0.40	-106.95900	0.47	5.94	0.44	2005	11	6	12	45	19.67	0.05	0.47	0.14	5	7	2
223	34.03517	0.39	-106.95750	0.46	6.34	0.46	2005	11	6	13	16	28.76	0.05	0.44	0.33	5	7	2
224	34.05400	0.41	-106.95300	0.35	6.15	0.41	2005	11	6	14	33	23.75	0.05	0.50	0.14	6	12	2
225	34.05817	0.35	-106.95400	0.34	6.23	0.48	2005	11	8	18	20	52.62	0.04	1.47	0.16	9	13	3
226	34.05083	0.92	-106.91300	0.56	5.00	0.00	2005	12	12	4	36	58.28	0.08	1.02	0.28	5	5	0
227	34.44933	1.44	-107.14067	0.71	5.00	0.00	2005	12	22	11	55	42.82	0.22	0.75	0.13	9	9	0
228	34.07550	0.97	-106.87583	0.86	7.98	2.40	2005	12	29	2	31	27.55	0.25	-0.61	0.10	4	8	0
229	34.03183	0.27	-107.00183	0.28	4.17	1.00	2006	1	2	2	1	57.51	0.05	0.64	0.17	9	18	1
230	34.02917	0.35	-106.99483	0.50	5.16	0.77	2006	1	2	15	27	37.60	0.07	-0.02	0.04	4	9	1
231	34.02817	0.31	-107.01567	0.51	4.01	0.84	2006	1	3	6	8	24.35	0.07	0.43	0.19	5	11	1
232	34.03633	0.47	-107.00400	0.41	4.92	0.74	2006	1	5	11	17	10.38	0.07	0.41	0.10	5	9	1
233	34.15333	0.35	-106.92367	0.45	4.23	1.30	2006	1	11	17	20	51.91	0.10	0.63	0.23	6	12	0
234	34.02467	0.51	-107.05367	0.39	9.45	0.55	2006	1	20	22	14	19.21	0.07	-0.69	0.30	4	10	2
235	34.25100	0.43	-106.75550	0.34	5.00	0.00	2006	1	21	7	57	40.80	0.05	0.43	1.29	5	12	2
236	34.01433	0.81	-107.02067	0.70	8.43	0.56	2006	1	24	12	2	52.61	0.10	-0.87	0.09	4	8	1
237	34.31717	0.60	-107.07667	0.90	5.00	0.00	2006	2	9	21	0	34.53	0.05	0.07	0.19	4	7	0

238	34.27700	0.44	-106.69233	0.40	4.06	0.81	2006	3	10	3	51	26.29	0.07	0.17	0.24	5	9	1
239	33.98383	0.34	-106.81817	0.35	5.00	0.00	2006	3	10	8	10	17.67	0.04	1.23	0.14	6	9	0
240	34.38533	1.15	-107.00183	1.11	5.00	0.00	2006	3	28	4	14	8.71	0.15	-0.22	0.05	4	5	0
241	34.18267	0.65	-106.87933	0.66	3.67	4.09	2006	3	29	3	33	13.31	0.18	0.70	0.01	6	6	0
242	34.19000	0.45	-106.88283	0.35	5.00	0.00	2006	3	29	3	53	22.61	0.06	0.60	0.14	6	9	0
243	34.17717	0.34	-106.87667	0.30	3.25	2.68	2006	3	29	4	23	0.32	0.08	0.88	0.13	8	10	0
244	34.18317	0.58	-106.88583	0.59	4.85	2.63	2006	3	29	6	27	48.33	0.17	0.19	0.17	5	7	0
245	34.19917	0.59	-106.88250	0.35	5.00	0.00	2006	3	29	8	56	5.33	0.06	-0.17	0.12	5	7	0
246	34.18350	0.32	-106.87850	0.26	4.79	0.94	2006	3	29	10	56	14.85	0.05	0.89	0.20	8	13	1
247	34.18150	0.39	-106.87767	0.28	3.93	1.94	2006	3	29	11	27	41.42	0.08	0.96	0.08	6	10	0
248	34.18933	0.56	-106.88400	0.33	5.00	0.00	2006	3	29	11	29	31.32	0.06	0.27	0.14	5	7	0
249	34.18617	0.48	-106.88083	0.50	3.88	2.99	2006	3	29	12	30	8.73	0.15	0.35	0.14	6	9	0
250	34.25050	0.33	-106.87483	0.31	2.58	3.93	2006	4	3	3	9	29.55	0.08	0.95	0.16	8	11	0
251	34.44600	1.17	-107.00033	0.37	5.00	0.00	2006	4	3	21	36	0.45	0.13	0.26	0.21	4	5	0
252	34.41333	0.62	-107.00433	0.32	5.00	0.00	2006	4	4	8	13	35.24	0.08	0.46	0.12	7	9	0
253	34.36250	0.71	-107.00867	0.61	5.00	0.00	2006	4	4	16	47	44.00	0.08	0.54	0.12	4	6	0
254	34.26900	1.77	-106.86533	1.26	5.00	0.00	2006	4	18	1	8	40.10	0.16	0.54	0.27	4	5	0
255	34.27750	1.21	-106.87567	0.76	5.00	0.00	2006	4	18	1	32	0.31	0.14	0.30	0.13	4	4	0
256	34.16217	0.54	-106.82617	0.32	4.88	0.88	2006	4	25	4	31	10.38	0.07	0.22	0.23	4	8	1
257	34.14117	0.43	-106.83283	0.35	5.00	0.00	2006	4	25	4	33	44.33	0.04	0.79	0.11	6	6	0
258	34.16000	0.54	-106.83067	0.32	8.90	0.57	2006	4	25	4	45	41.77	0.07	-0.07	0.39	5	10	2
259	34.16133	0.53	-106.83150	0.50	6.31	3.23	2006	4	25	5	9	8.52	0.19	-0.25	0.13	4	6	0
260	34.15967	0.37	-106.82350	0.27	4.29	0.87	2006	4	25	7	33	37.50	0.05	-0.12	0.14	5	11	1
261	34.11450	0.47	-106.62267	0.99	8.15	1.49	2006	4	30	10	3	30.74	0.18	0.37	0.21	5	6	0
262	34.40433	0.36	-107.03967	0.35	5.00	0.00	2006	5	2	11	33	11.72	0.04	0.60	0.11	8	8	0
263	34.08800	0.28	-106.98150	0.36	2.20	0.59	2006	5	6	10	59	0.56	0.04	0.81	0.14	7	13	2
264	34.35617	1.17	-106.72667	0.84	5.01	3.08	2006	6	23	20	58	39.64	0.24	0.58	0.21	4	6	0
265	34.35583	0.99	-106.85767	0.59	5.00	0.00	2006	6	24	12	25	28.94	0.16	0.36	0.08	4	6	0
266	34.35733	1.31	-106.67900	1.17	9.50	2.22	2006	6	25	14	30	19.82	0.31	0.25	0.01	4	5	0
267	33.97467	0.29	-106.92667	0.29	5.00	0.00	2006	6	25	18	0	24.42	0.04	0.71	0.13	7	12	0
268	34.34300	1.34	-106.64617	1.36	8.05	1.87	2006	6	27	23	35	5.38	0.32	0.66	0.05	4	5	0

269	34.36067	0.95	-106.67717	1.01	10.58	1.53	2006	6	28	17	41	37.66	0.25	0.59	0.12	4	7	0
270	33.96233	0.44	-106.77900	0.42	3.79	1.63	2006	7	1	14	28	51.59	0.09	0.68	0.11	6	9	0
271	33.95850	0.35	-106.99650	0.44	6.13	2.54	2006	7	10	21	50	42.42	0.13	0.59	0.04	7	9	0
272	34.10683	0.42	-107.03500	0.85	5.00	0.00	2006	7	11	20	52	32.25	0.10	0.72	0.16	5	6	0
273	34.09917	0.32	-106.78733	0.35	5.00	0.00	2006	7	12	19	1	46.16	0.04	0.53	0.07	5	8	0
274	34.32000	0.48	-107.06383	0.57	5.00	0.00	2006	7	24	12	38	6.59	0.05	0.59	0.31	5	9	1
275	34.32167	0.51	-107.06733	0.65	7.46	0.93	2006	7	24	14	14	11.85	0.08	0.28	0.16	5	8	1
276	34.32500	0.51	-107.05633	0.60	5.00	0.00	2006	7	25	17	21	8.77	0.05	0.14	0.12	4	6	0
277	34.26383	0.37	-106.79017	0.44	5.00	0.00	2006	7	26	20	6	58.94	0.09	-1.71	3.00	4	7	0
278	34.23367	0.32	-106.83817	0.25	4.16	0.53	2006	7	31	8	19	50.18	0.04	0.46	0.24	9	15	2
279	34.22817	0.30	-106.83983	0.24	3.44	0.54	2006	7	31	8	20	59.42	0.04	0.63	0.33	9	16	2
280	34.00050	0.39	-106.70850	0.66	6.72	1.39	2006	8	6	10	58	31.64	0.13	0.64	0.14	7	9	0
281	34.32233	0.92	-106.67567	0.55	7.22	0.66	2006	8	8	8	31	52.78	0.11	-0.14	0.07	4	6	1
282	34.03350	0.33	-107.06067	0.43	8.08	0.70	2006	8	29	14	41	57.65	0.06	0.48	0.10	8	13	1
283	34.00667	0.29	-107.01750	0.37	7.16	0.49	2006	9	2	3	39	17.65	0.05	0.73	0.65	9	15	3
284	34.41700	0.49	-106.99350	0.32	5.00	0.00	2006	9	5	8	30	43.46	0.07	0.82	0.21	8	14	1
285	34.40850	0.54	-107.01867	0.34	5.00	0.00	2006	9	6	12	9	0.67	0.07	0.55	0.07	6	10	0
286	34.28283	0.50	-106.70117	0.32	5.00	0.00	2006	10	7	13	48	31.19	0.05	0.17	0.95	4	9	2
287	34.29567	0.55	-106.69717	0.45	10.17	0.89	2006	10	7	13	52	59.33	0.13	0.59	0.09	8	13	1
288	34.51583	1.25	-106.26083	1.17	5.00	0.00	2006	10	10	6	10	38.32	0.22	1.02	0.12	6	8	0
289	34.33200	0.72	-106.81783	0.43	5.00	0.00	2006	11	10	7	37	38.83	0.11	0.28	0.11	6	9	0
290	34.25750	0.51	-106.81067	0.36	5.00	0.00	2006	12	6	2	5	31.93	0.07	0.08	0.08	4	8	0
291	34.25667	0.31	-106.81383	0.25	5.00	0.00	2006	12	6	5	12	14.28	0.04	0.84	0.10	7	13	0
292	34.26417	0.48	-106.78283	0.36	5.00	0.00	2006	12	23	8	5	19.07	0.07	0.39	0.07	5	9	0
293	33.57650	1.64	-107.06333	0.69	7.25	3.16	2006	12	29	17	37	9.14	0.27	1.66	0.07	8	9	0
294	34.32800	0.38	-106.83933	0.28	5.00	0.00	2006	12	31	2	44	31.18	0.05	0.91	0.12	8	14	1
295	34.28517	0.40	-106.88017	0.30	5.00	0.00	2006	12	31	13	3	4.16	0.05	1.05	0.07	7	8	0
296	33.98600	0.32	-106.95067	0.30	5.00	0.00	2006	12	31	13	49	44.27	0.04	0.77	0.07	6	9	0
297	34.40900	0.91	-107.16517	1.12	5.00	0.00	2007	1	1	20	47	27.63	0.18	0.39	0.18	6	6	0
298	34.07833	0.45	-106.94600	0.63	3.13	0.63	2007	1	2	7	12	2.39	0.07	0.25	0.17	4	6	0
299	34.08767	0.24	-106.85517	0.28	8.99	0.77	2007	1	28	4	5	16.72	0.08	0.09	0.18	6	10	0

300	34.02383	0.60	-107.04267	0.52	8.83	1.29	2007	1	29	2	14	11.19	0.12	-0.53	0.03	5	7	0
301	34.01733	0.58	-107.03550	0.64	9.21	2.38	2007	1	29	2	15	19.67	0.20	-0.49	0.05	5	6	0
302	34.03417	0.37	-107.04183	0.39	8.48	0.38	2007	1	30	12	16	15.14	0.05	0.58	0.07	8	12	2
303	34.03767	0.56	-107.04067	0.98	8.25	1.31	2007	1	30	12	18	15.41	0.12	-0.13	0.01	4	5	0
304	34.03217	0.46	-107.04600	0.41	8.18	1.26	2007	1	30	12	19	50.21	0.10	0.33	0.07	7	10	0
305	34.03100	0.55	-107.04367	0.52	8.25	1.46	2007	1	30	12	22	3.71	0.13	0.35	0.04	6	8	0
306	34.03183	0.56	-107.04483	0.65	7.71	2.38	2007	1	30	13	10	21.29	0.18	0.65	0.05	6	8	0
307	34.60067	1.35	-107.17783	0.89	5.00	0.00	2007	1	30	21	23	22.94	0.24	1.47	0.43	8	9	0
308	34.07533	0.40	-106.99567	0.49	5.00	0.00	2007	1	30	22	1	1.42	0.06	1.69	0.09	6	6	0
309	34.06817	0.36	-107.01067	0.36	5.00	0.00	2007	1	30	22	40	40.90	0.04	1.30	0.17	7	7	0
310	34.05967	0.49	-106.99600	0.42	6.59	0.80	2007	2	12	18	51	20.06	0.07	0.92	0.21	7	10	1
311	34.21750	0.33	-106.89367	0.30	3.26	2.19	2007	2	26	0	0	50.44	0.06	0.69	0.06	8	10	0
312	34.37083	0.58	-106.80633	0.35	5.00	0.00	2007	2	27	13	18	29.30	0.08	0.72	0.15	8	9	0
313	34.03300	0.27	-107.01433	0.30	1.20	4.77	2007	3	4	7	47	34.88	0.06	0.97	0.23	10	11	0
314	34.58217	0.47	-106.85850	0.50	5.00	0.00	2007	3	5	7	55	55.66	0.07	1.41	0.10	9	9	0
315	34.33933	0.50	-106.91617	0.32	5.00	0.00	2007	3	8	11	58	57.34	0.06	0.95	0.09	7	8	0
316	34.33933	1.46	-106.71867	2.09	1.38	18.83	2007	3	9	2	0	59.54	0.33	0.95	0.13	4	6	0
317	34.02317	0.30	-107.04500	0.32	8.66	0.46	2007	3	12	17	5	11.78	0.05	0.79	0.08	8	13	3
318	34.36233	0.64	-107.10650	0.76	6.02	1.27	2007	3	27	16	34	7.04	0.13	0.76	0.63	4	7	1
319	33.96900	0.33	-106.97300	0.32	5.00	0.00	2007	4	2	23	42	41.63	0.04	0.84	0.22	7	10	0
320	34.54333	0.33	-107.13417	0.50	4.80	2.82	2007	4	22	10	21	40.12	0.09	0.84	0.07	6	11	0
321	34.35100	0.46	-106.72683	0.38	9.27	0.97	2007	5	9	1	41	8.07	0.10	1.15	0.18	8	15	1
322	34.32117	0.40	-106.86883	0.30	5.00	0.00	2007	5	11	17	42	20.93	0.05	1.10	0.04	8	10	0
323	34.30133	0.40	-106.89950	0.30	8.19	0.87	2007	5	14	22	52	19.59	0.06	0.53	0.13	7	11	1
324	34.04533	0.29	-107.03217	0.31	5.00	0.00	2007	5	15	2	16	48.24	0.04	0.72	0.46	7	11	1
325	34.30400	0.67	-106.89383	0.45	8.75	0.77	2007	5	15	19	45	37.72	0.10	0.37	0.22	5	10	2
326	34.30600	0.38	-106.89933	0.29	5.00	0.00	2007	5	15	21	5	56.33	0.05	0.46	0.09	7	10	0
327	34.36300	0.44	-106.83033	0.25	5.00	0.00	2007	5	19	0	48	11.27	0.06	1.05	0.17	8	14	0
328	34.36633	0.47	-106.82767	0.29	5.00	0.00	2007	5	19	4	17	33.55	0.06	0.58	0.16	6	12	1
329	34.37800	0.86	-106.71800	0.95	6.43	2.70	2007	5	22	2	38	17.60	0.21	0.30	0.97	5	8	0
330	34.06017	0.27	-107.02983	0.26	5.65	0.97	2007	5	22	17	25	49.67	0.05	1.22	0.06	10	13	0

331	34.05850	0.32	-107.02817	0.36	6.50	0.36	2007	5	23	3	0	53.24	0.04	0.20	0.29	8	17	5
332	34.06067	0.27	-107.03100	0.26	6.55	0.38	2007	5	23	3	5	38.15	0.04	0.48	0.07	8	16	4
333	34.06050	0.28	-107.02983	0.28	5.51	1.29	2007	5	23	3	20	51.47	0.07	1.28	0.06	10	11	0
334	34.06200	0.28	-107.02800	0.27	6.80	0.45	2007	5	23	3	41	43.91	0.04	0.24	0.08	8	14	3
335	34.06200	0.27	-107.02983	0.26	6.85	0.40	2007	5	23	3	42	6.61	0.04	0.36	0.06	8	15	3
336	34.05633	0.43	-107.02717	0.38	6.72	0.33	2007	5	23	3	57	27.47	0.05	0.02	0.06	4	10	3
337	34.06033	0.29	-107.02950	0.31	5.82	1.26	2007	5	23	5	16	54.91	0.06	2.91	0.06	10	10	0
338	34.06017	0.41	-107.03117	0.38	6.67	0.75	2007	5	23	6	55	17.93	0.07	0.29	0.07	6	10	1
339	34.06000	0.24	-107.02683	0.20	7.04	0.37	2007	5	23	7	38	2.49	0.04	0.54	0.07	10	18	3
340	34.06100	0.25	-107.03033	0.25	5.49	1.09	2007	5	23	10	46	43.46	0.06	1.15	0.09	11	16	0
341	34.05933	0.49	-107.02967	0.35	6.42	0.53	2007	5	23	11	45	41.68	0.06	0.10	0.08	6	13	2
342	34.05950	0.34	-107.03050	0.43	6.38	0.51	2007	5	23	21	35	51.46	0.06	0.59	0.09	7	13	3
343	34.06133	0.44	-107.02800	0.43	6.05	1.26	2007	5	23	22	21	43.32	0.09	0.61	0.05	8	8	0
344	34.06067	0.27	-107.02567	0.30	6.75	0.40	2007	5	24	17	15	55.26	0.04	0.65	0.12	10	20	4
345	34.06333	0.35	-107.03283	0.36	6.70	0.41	2007	5	28	11	24	3.05	0.05	0.24	0.12	6	13	3
346	34.13633	0.29	-106.80800	0.25	5.00	0.00	2007	5	31	6	4	59.50	0.04	0.58	0.25	7	13	1

Appendix B: Individual event clusters

For each of the 14 clusters used in this study, original locations are displayed on a shaded relief map with faults superimposed from Figure 5.2. Where available, focal mechanism solutions are displayed. Events are displayed as red squares. Additional maps show events after initial waveform cross-correlation and relocation and, where available, after waveform cross-correlation with YN data. Final locations are displayed with other events (small green squares) from the Sanford et al. catalogues. Example waveforms before and after cross-correlation are also displayed. Additional maps for each cluster show first standard deviation in location displayed as blue bars for each location.

Cluster 1

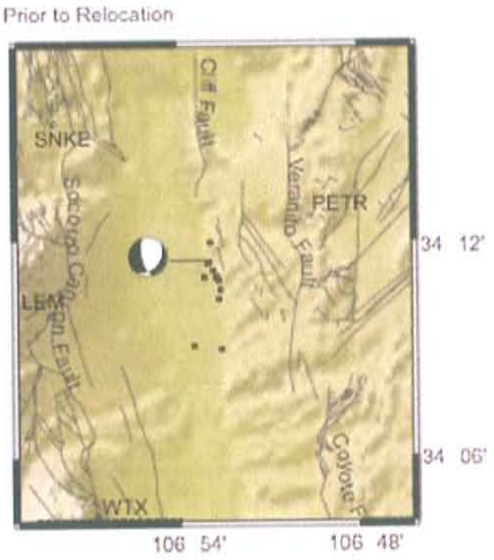
Prior to Relocation
SNKE
Cliff Fault
Vaca
PETR
LEM
WTX
34 12'
34 06'
106 54'
106 48'

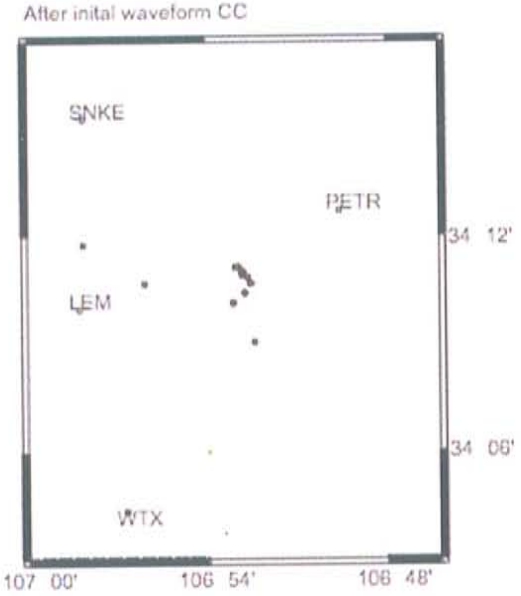
After inital waveform CC
SNKE
PETR
LEM
WTX
34 12'
34 06'
107 00'
106 54'
106 48'

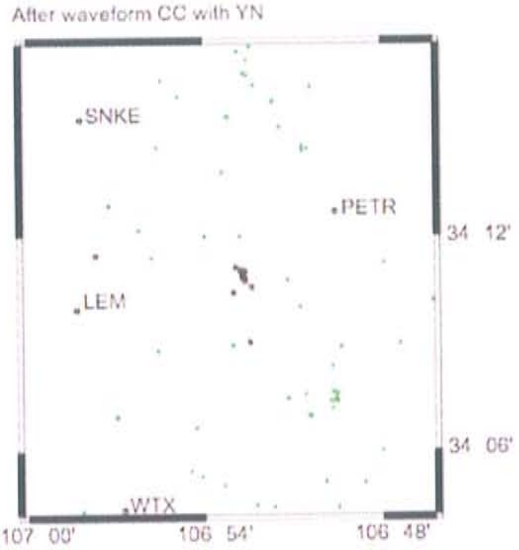
After waveform CC with YN
SNKE
PETR
LEM
WTX
34 12'
34 06'
107 00'
106 54'
106 48'

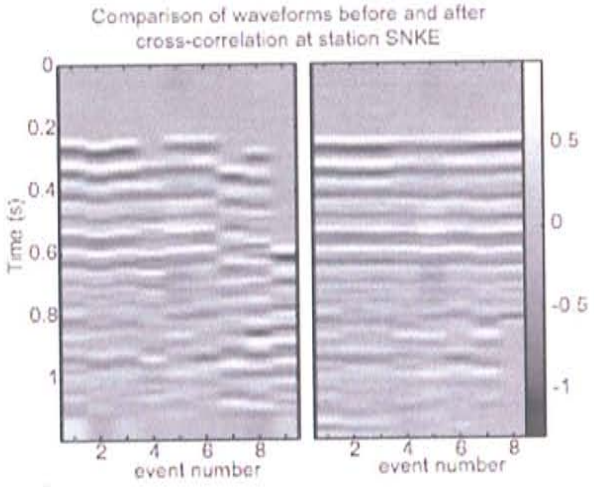
Comparison of waveforms before and after
cross-correlation at station SNKE
Time (s)
0
0.2
0.4
0.6
0.8
1
2
4
6
8
event number
event number
0.5
0
-0.5
-1

Cluster 1 Error Margins

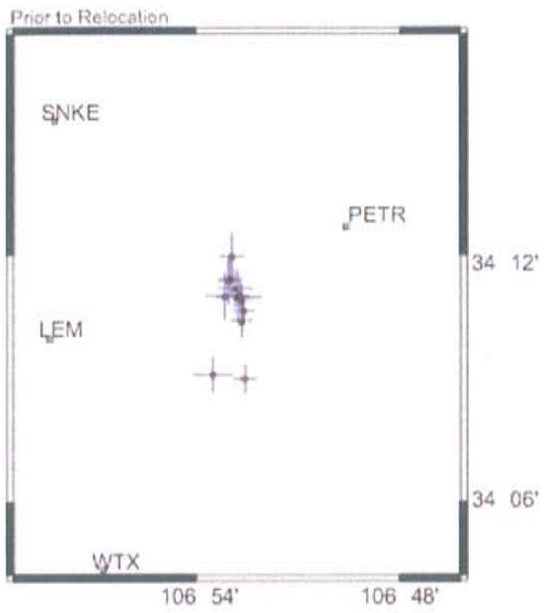

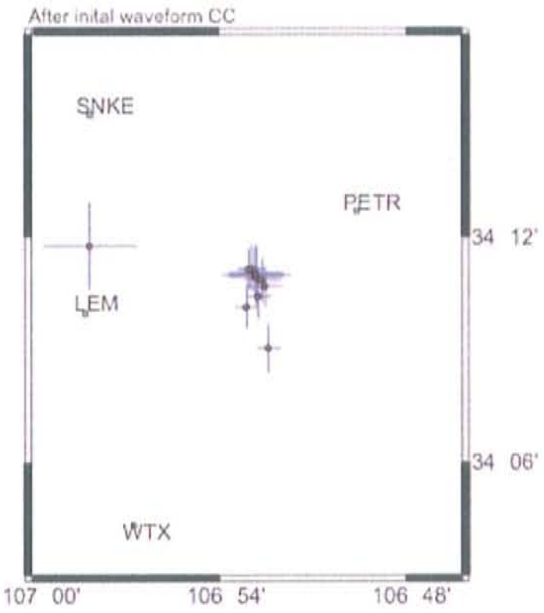

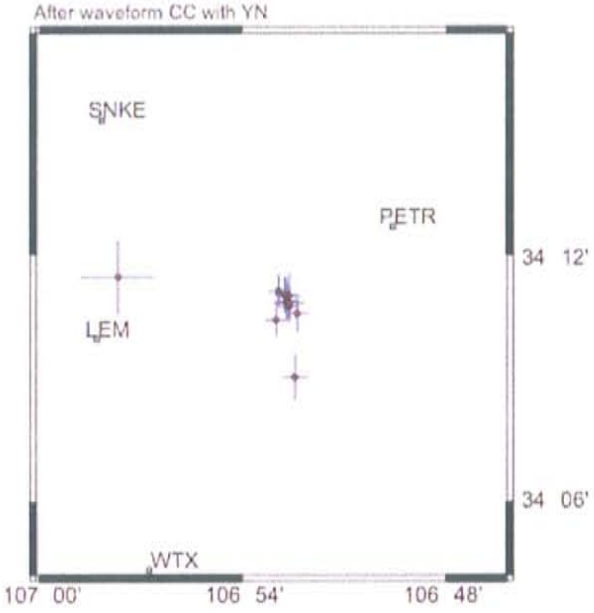

Cluster 1 prior to relocation

ind	lat	lstd	long	lstd	depth	lstd	yyyy	mm	dd	hh	mm	orig	lstd	mag	rms	stats	picks	refls
30	34.14967	0.36	-106.87617	0.31	5.21	0.80	2004	12	5	0	14	33.51	0.06	0.50	0.14	5	10	1
73	34.15133	0.43	-106.89167	0.58	6.51	1.60	2005	3	5	16	17	2.30	0.12	0.73	0.15	5	7	0
182	34.17300	0.42	-106.87767	0.30	5.74	0.58	2005	10	12	18	54	46.30	0.05	0.57	0.12	5	11	2
241	34.18267	0.65	-106.87933	0.66	3.67	4.09	2006	3	29	3	33	13.31	0.18	0.70	0.01	6	6	0
242	34.19000	0.45	-106.88283	0.35	5.00	0.00	2006	3	29	3	53	22.61	0.06	0.60	0.14	6	9	0
243	34.17717	0.34	-106.87667	0.30	3.25	2.68	2006	3	29	4	23	0.32	0.08	0.88	0.13	8	10	0
244	34.18317	0.58	-106.88583	0.59	4.85	2.63	2006	3	29	6	27	48.33	0.17	0.19	0.17	5	7	0
245	34.19917	0.59	-106.88250	0.35	5.00	0.00	2006	3	29	8	56	5.33	0.06	-0.17	0.12	5	7	0
246	34.18350	0.32	-106.87850	0.26	4.79	0.94	2006	3	29	10	56	14.85	0.05	0.89	0.20	8	13	1
247	34.18150	0.39	-106.87767	0.28	3.93	1.94	2006	3	29	11	27	41.42	0.08	0.96	0.08	6	10	0
248	34.18933	0.56	-106.88400	0.33	5.00	0.00	2006	3	29	11	29	31.32	0.06	0.27	0.14	5	7	0
249	34.18617	0.48	-106.88083	0.50	3.88	2.99	2006	3	29	12	30	8.73	0.15	0.35	0.14	6	9	0

Cluster 1 after waveform CC

ind	lat	lstd	long	lstd	depth	lstd	yyyy	mm	dd	hh	mm	orig	lstd	mag	rms	stats	picks	refls
30	34.15067	0.65	-106.87383	0.39	4.78	1.13	2004	12	5	0	14	33.53	0.08	0.00	0.13	5	10	1
73	34.19600	1.16	-106.96967	1.52	5.00	0.00	2005	3	5	16	17	1.64	0.17	0.00	0.22	5	5	0
182	34.17350	0.62	-106.87933	0.40	5.64	0.78	2005	10	12	18	54	46.28	0.06	0.00	0.12	5	11	2
241	34.18283	0.78	-106.88050	1.11	4.18	6.89	2006	3	29	3	33	13.29	0.33	0.00	0.01	6	6	0
242	34.16883	0.59	-106.88567	0.40	5.00	0.00	2006	3	29	3	53	22.51	0.05	0.00	0.30	6	9	0
243	34.17800	0.54	-106.87583	0.56	2.46	6.46	2006	3	29	4	23	0.35	0.18	0.00	0.13	8	10	0
244	34.18200	0.71	-106.88067	0.89	4.60	5.08	2006	3	29	6	27	48.26	0.28	0.00	0.07	5	7	0
245	34.18383	0.72	-106.88100	0.89	3.89	5.83	2006	3	29	8	56	5.35	0.27	0.00	0.17	5	7	0
246	34.18550	0.53	-106.88450	0.39	5.76	1.04	2006	3	29	10	56	14.74	0.08	0.00	0.24	8	13	1
247	34.18083	0.59	-106.87750	0.58	2.16	7.24	2006	3	29	11	27	41.48	0.19	0.00	0.15	6	10	0
248	34.18333	0.72	-106.88033	0.89	4.07	5.63	2006	3	29	11	29	31.33	0.27	0.00	0.14	5	7	0
249	34.18583	0.64	-106.88300	0.41	5.00	0.00	2006	3	29	12	30	8.67	0.06	0.00	0.16	6	9	0

Cluster 1 after waveform CC with YN

ind	lat	lstd	long	lstd	depth	lstd	yyyy	mm	dd	hh	mm	orig	lstd	mag	rms	stats	picks	refls
30	34.15050	0.57	-106.87433	0.39	4.85	1.10	2004	12	5	0	14	33.52	0.07	0.00	0.13	5	10	1
73	34.19117	0.91	-106.96150	1.10	5.00	0.00	2005	3	5	16	17	1.70	0.12	0.00	0.19	5	5	0
182	34.18350	0.55	-106.87733	0.38	3.98	0.75	2005	10	12	18	54	46.25	0.06	0.00	0.29	6	12	2
241	34.18100	0.44	-106.87817	0.33	3.14	2.08	2006	3	29	3	33	13.35	0.09	0.00	0.05	8	9	0
242	34.17367	0.40	-106.88367	0.32	5.00	0.00	2006	3	29	3	53	22.49	0.04	0.00	0.39	8	12	0
243	34.17917	0.40	-106.87717	0.30	3.04	1.97	2006	3	29	4	23	0.32	0.08	0.00	0.14	10	12	0
244	34.18133	0.45	-106.87817	0.31	3.05	1.89	2006	3	29	6	27	48.34	0.09	0.00	0.07	7	10	0
245	34.18383	0.45	-106.87950	0.32	2.70	2.27	2006	3	29	8	56	5.42	0.09	0.00	0.14	7	9	0
246	34.18550	0.39	-106.88233	0.30	5.16	0.84	2006	3	29	10	56	14.76	0.06	0.00	0.23	10	16	1
247	34.18050	0.42	-106.87733	0.45	2.21	5.87	2006	3	29	11	27	41.48	0.15	0.00	0.14	7	11	0
248	34.17633	0.44	-106.87333	0.32	5.00	0.00	2006	3	29	11	29	31.36	0.04	0.00	0.21	7	10	0
249	34.18383	0.42	-106.87867	0.31	2.49	2.34	2006	3	29	12	30	8.81	0.09	0.00	0.13	8	11	0

Cluster 2

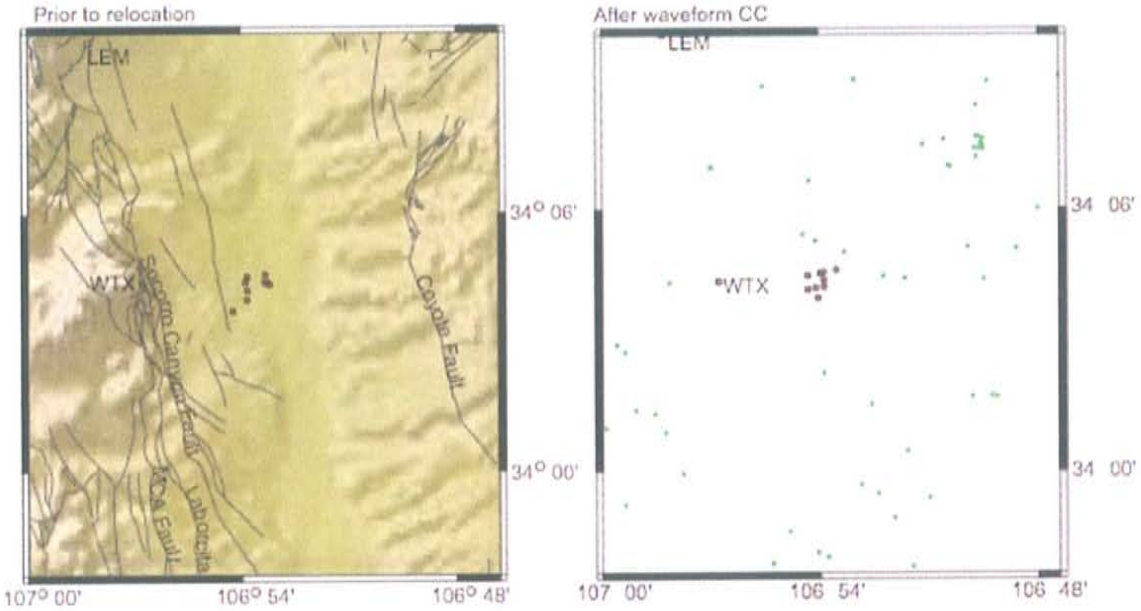
Prior to relocation
LEM
WTX
Socorro Canyon Fault
Lemitar
Rio Grande Fault
Loma de la Cruz
Coyote Fault
34° 06'
34° 00'
107° 00'
106° 54'
106° 48'
After waveform CC
LEM
WTX
34 06'
34 00'
107 00'
106 54'
106 48'

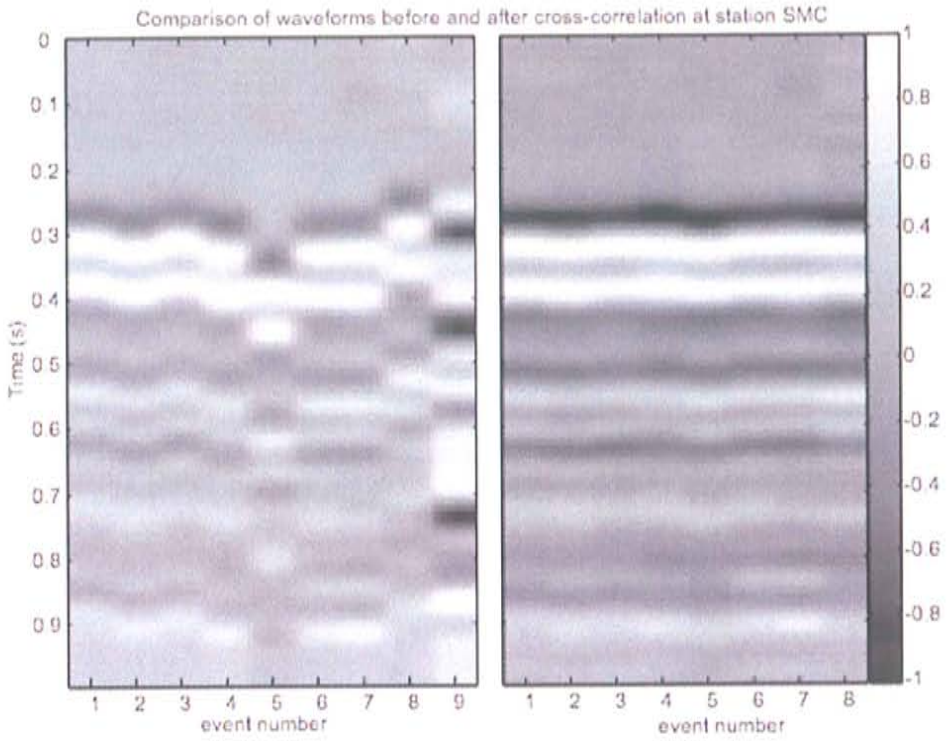
Comparison of waveforms before and after cross-correlation at station SMC
Time (s)
0
0.1
0.2
0.3
0.4
0.5
0.6
0.7
0.8
0.9
1 2 3 4 5 6 7 8 9
event number
1 2 3 4 5 6 7 8
event number
1
0.8
0.6
0.4
0.2
0
-0.2
-0.4
-0.6
-0.8
-1

Cluster 2 Error Margins

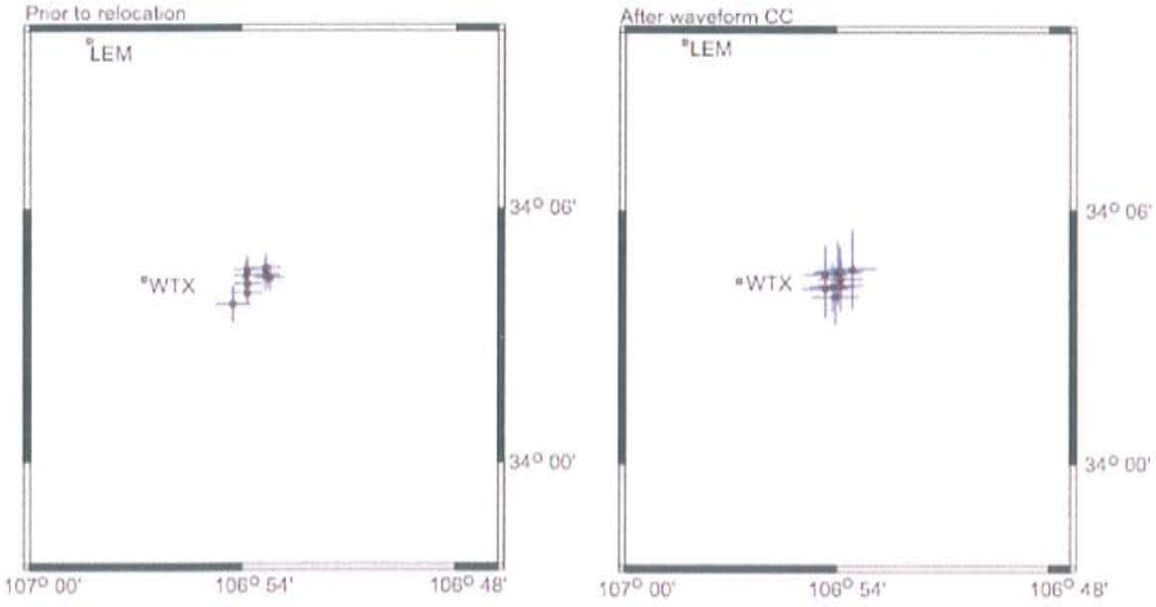

Cluster 2 prior to relocation

ind	lat	lstd	long	lstd	depth	lstd	yyyy	mm	dd	hh	mm	orig	lstd	mag	rms	stats	picks	refls
48	34.07333	0.36	-106.88933	0.38	5.00	0.00	2005	1	18	19	33	25.61	0.04	0.47	0.11	5	6	0
49	34.07550	0.32	-106.89750	0.41	5.00	0.00	2005	1	18	20	56	54.28	0.05	0.48	0.35	4	7	0
50	34.07633	0.34	-106.88917	0.45	5.00	0.00	2005	1	19	1	13	52.02	0.04	0.36	0.27	5	7	0
51	34.07367	0.27	-106.88833	0.37	5.00	0.00	2005	1	19	2	52	29.21	0.04	0.90	0.42	7	10	0
52	34.07017	0.29	-106.89733	0.40	5.00	0.00	2005	1	19	6	19	10.78	0.05	0.58	0.22	4	8	0
53	34.07333	0.33	-106.89833	0.36	5.00	0.00	2005	1	19	12	1	0.34	0.04	0.38	0.33	5	7	0
57	34.06667	0.30	-106.89767	0.44	5.00	0.00	2005	1	21	3	26	7.61	0.04	0.34	0.07	4	7	0
61	34.07250	0.32	-106.88717	0.41	5.00	0.00	2005	2	1	8	23	20.29	0.05	0.10	0.27	4	7	0
226	34.06233	0.42	-106.90433	0.49	0.41	11.12	2005	12	12	4	36	58.60	0.08	0.92	0.01	5	5	0

Cluster 2 after waveform CC

ind	lat	lstd	long	lstd	depth	lstd	yyyy	mm	dd	hh	mm	orig	lstd	mag	rms	stats	picks	refls
48	34.07533	0.72	-106.89967	0.68	5.00	0.00	2005	1	18	19	33	25.59	0.10	0.00	0.18	5	6	0
49	34.06917	0.67	-106.90533	0.67	5.00	0.00	2005	1	18	20	56	54.28	0.09	0.00	0.37	4	6	0
50	34.07583	0.56	-106.89833	0.68	5.00	0.00	2005	1	19	1	13	51.98	0.08	0.00	0.34	5	7	0
51	34.07283	0.48	-106.89817	0.64	5.00	0.00	2005	1	19	2	52	29.22	0.07	0.00	0.43	7	10	0
52	34.06983	0.58	-106.90183	0.64	5.00	0.00	2005	1	19	6	19	10.80	0.09	0.00	0.22	4	8	0
53	34.07450	0.67	-106.90550	0.63	5.00	0.00	2005	1	19	12	1	0.25	0.09	0.00	0.30	5	7	0
57	34.06600	0.65	-106.90067	0.69	5.00	0.00	2005	1	21	3	26	7.64	0.09	0.00	0.08	4	6	0
61	34.07033	0.60	-106.89817	0.65	5.00	0.00	2005	2	1	8	23	20.23	0.09	0.00	0.32	4	7	0
226	34.07667	0.91	-106.89250	0.69	5.00	0.00	2005	12	12	4	36	58.50	0.12	0.00	0.23	5	5	0

Cluster 3

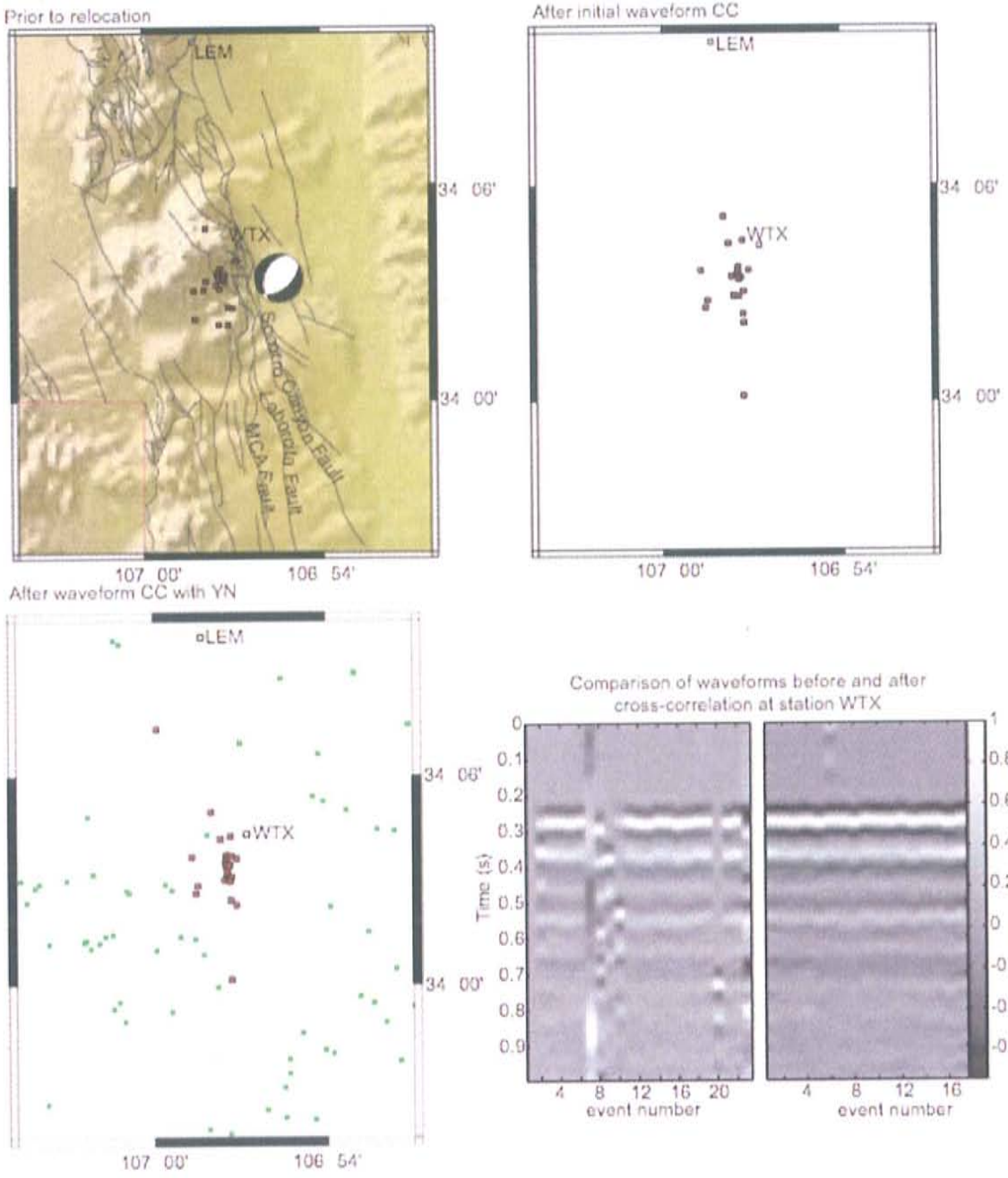
Prior to relocation
LEM
WTX
Sonora Canyon Fault
Laborcita Fault
McGinn Fault
34 06'
34 00'
107 00'
106 54'
After initial waveform CC
LEM
WTX
34 06'
34 00'
107 00'
106 54'
After waveform CC with YN
LEM
WTX
34 06'
34 00'
107 00'
106 54'
Comparison of waveforms before and after cross-correlation at station WTX
Time (s)
0
0.1
0.2
0.3
0.4
0.5
0.6
0.7
0.8
0.9
4 8 12 16 20
event number
4 8 12 16
event number
1
0.8
0.6
0.4
0.2
0
-0.2
-0.4
-0.6

Cluster 3 Error Margins

Prior to relocation

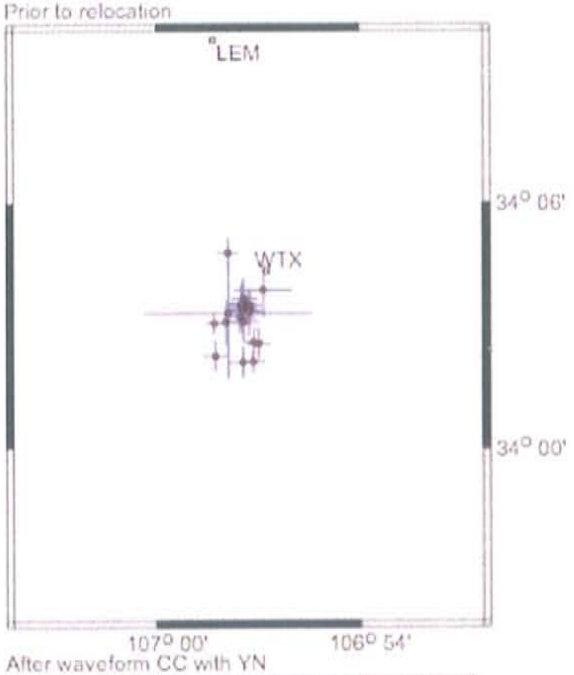

After initial waveform CC

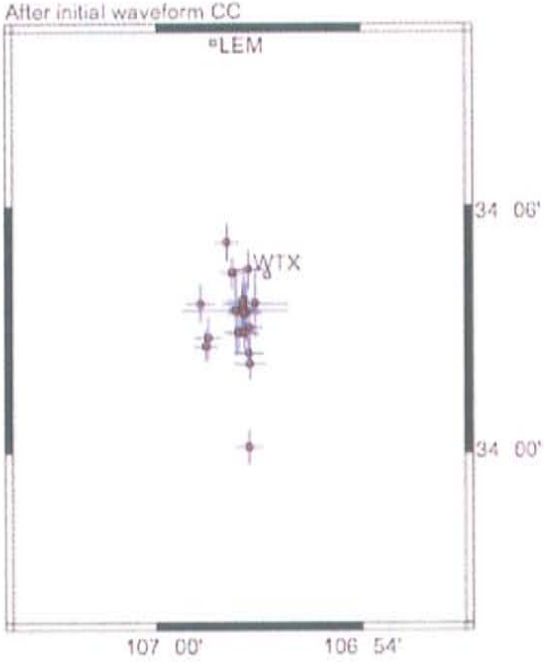

After waveform CC with YN

Cluster 3 prior to relocation

ind	lat	lstd	long	lstd	depth	lstd	yyyy	mm	dd	hh	mm	orig	lstd	mag	rms	stats	picks	refls
54	34.03533	0.30	-106.95267	0.39	5.00	0.00	2005	1	19	21	46	56.45	0.05	0.05	0.11	4	8	0
55	34.04283	0.38	-106.94983	0.35	5.00	0.00	2005	1	19	23	56	5.13	0.05	0.26	0.07	4	7	0
56	34.04317	0.39	-106.95233	0.30	5.00	0.00	2005	1	20	3	16	33.08	0.05	0.45	0.03	5	8	0
77	34.05100	0.27	-106.97167	0.26	6.14	0.64	2005	3	29	14	6	33.45	0.04	0.53	0.17	7	14	2
151	34.06467	0.70	-106.94767	0.83	5.79	0.66	2005	6	14	3	51	55.62	0.11	0.13	0.10	4	7	1
187	34.05683	0.36	-106.95583	0.34	6.46	0.34	2005	10	21	8	11	36.44	0.05	-0.21	0.18	5	9	2
189	34.03767	0.38	-106.97100	0.38	3.54	0.45	2005	10	24	18	14	11.83	0.05	-0.34	0.47	4	9	2
193	34.05583	0.39	-106.95467	0.35	6.39	0.35	2005	10	26	23	28	18.01	0.05	0.16	0.15	6	11	2
197	34.05550	0.60	-106.95467	0.50	7.00	0.33	2005	10	30	2	5	25.22	0.07	0.06	0.20	6	12	2
205	34.05133	0.57	-106.96600	0.48	6.93	0.85	2005	10	30	3	14	32.46	0.08	-0.51	0.16	4	5	1
206	34.05517	1.60	-106.96467	2.46	7.85	1.82	2005	10	30	3	15	52.70	0.36	0.11	0.00	4	4	0
207	34.05800	0.50	-106.95767	0.39	6.84	0.28	2005	10	30	3	19	55.73	0.04	-0.21	0.18	5	8	3
208	34.05817	0.53	-106.95850	0.40	6.16	0.59	2005	10	30	3	26	37.41	0.06	0.21	0.20	5	7	2
209	34.05667	0.52	-106.95767	0.38	6.11	0.40	2005	10	30	4	43	6.69	0.05	0.11	0.18	5	8	3
210	34.06100	0.54	-106.95700	0.39	7.23	0.48	2005	10	30	4	45	20.86	0.05	-0.01	0.15	5	7	2
211	34.05917	0.54	-106.95783	0.39	6.59	0.54	2005	10	30	4	50	47.47	0.05	0.22	0.19	5	8	3
214	34.05167	0.47	-106.95717	0.45	6.07	0.40	2005	11	1	9	28	12.91	0.05	0.62	0.19	6	9	3
220	34.07967	0.39	-106.96483	0.30	6.63	0.29	2005	11	5	2	9	33.89	0.04	0.30	0.34	5	13	3
222	34.05350	0.40	-106.95900	0.47	5.94	0.44	2005	11	6	12	45	19.67	0.05	0.47	0.14	5	7	2
223	34.03517	0.39	-106.95750	0.46	6.34	0.46	2005	11	6	13	16	28.76	0.05	0.44	0.33	5	7	2
225	34.05817	0.35	-106.95400	0.34	6.23	0.48	2005	11	8	18	20	52.62	0.04	1.47	0.16	9	13	3

Cluster 3 after waveform CC

ind	lat	lstd	long	lstd	depth	lstd	yyyy	mm	dd	hh	mm	orig	lstd	mag	rms	stats	picks	refls
54	34.04067	0.39	-106.95517	0.44	5.00	0.00	2005	1	19	21	46	56.41	0.05	0.00	0.16	4	7	0
55	34.00267	0.42	-106.95500	0.42	5.00	0.00	2005	1	19	23	56	5.46	0.05	0.00	0.29	4	6	0
56	34.07450	0.49	-106.95550	0.45	5.00	0.00	2005	1	20	3	16	32.83	0.05	0.00	0.48	5	7	0
77	34.04333	0.37	-106.97583	0.35	6.46	0.87	2005	3	29	14	6	33.53	0.06	0.00	0.26	7	14	2
151	34.06067	0.83	-106.95200	0.97	5.61	0.82	2005	6	14	3	51	55.56	0.14	0.00	0.10	4	7	1
187	34.05733	0.72	-106.95617	0.41	6.66	0.60	2005	10	21	8	11	36.51	0.07	0.00	0.18	5	9	2
189	34.04883	0.51	-106.96000	0.45	4.29	0.72	2005	10	24	18	14	11.78	0.06	0.00	0.56	4	9	2
193	34.06050	0.48	-106.97850	0.42	5.45	0.65	2005	10	26	23	28	18.05	0.06	0.00	0.36	6	11	2
197	34.05100	0.49	-106.95483	0.39	6.51	0.61	2005	10	30	2	5	25.19	0.06	0.00	0.18	6	12	2
205	34.06200	0.59	-106.95767	0.50	7.88	0.81	2005	10	30	3	14	32.58	0.08	0.00	0.04	4	5	1
206	34.05783	1.03	-106.96133	1.55	7.59	1.71	2005	10	30	3	15	52.76	0.28	0.00	0.00	4	4	0
207	34.05800	0.54	-106.95850	0.40	6.68	0.57	2005	10	30	3	19	55.74	0.06	0.00	0.16	5	8	3
208	34.05917	0.54	-106.95800	0.40	6.54	0.62	2005	10	30	3	26	37.41	0.06	0.00	0.21	5	7	2
209	34.04667	0.54	-106.97467	0.40	6.78	0.60	2005	10	30	4	43	6.45	0.06	0.00	0.24	5	8	3
210	34.06050	0.55	-106.95783	0.40	7.41	0.66	2005	10	30	4	45	20.85	0.06	0.00	0.15	5	7	2
211	34.05800	0.54	-106.95767	0.40	6.68	0.57	2005	10	30	4	50	47.47	0.06	0.00	0.19	5	8	3
214	34.04867	0.41	-106.95733	0.46	6.43	0.60	2005	11	1	9	28	12.93	0.06	0.00	0.19	6	9	3
220	34.08550	0.47	-106.96583	0.37	6.17	0.53	2005	11	5	2	9	33.80	0.06	0.00	0.38	5	13	3
222	34.05667	0.42	-106.95733	0.48	6.33	0.65	2005	11	6	12	45	19.65	0.06	0.00	0.15	5	7	2
223	34.03633	0.40	-106.95467	0.46	5.92	0.71	2005	11	6	13	16	28.78	0.06	0.00	0.35	5	7	2
225	34.07300	0.38	-106.96317	0.38	6.67	0.55	2005	11	8	18	20	52.50	0.05	0.00	0.28	9	13	3

Cluster 3 after waveform CC with YN

ind	lat	lstd	long	lstd	depth	lstd	yyyy	mm	dd	hh	mm	orig	lstd	mag	rms	stats	picks	refls
54	34.04067	0.39	-106.95517	0.44	5.00	0.00	2005	1	19	21	46	56.41	0.05	0.00	0.16	4	7	0
55	34.00267	0.42	-106.95500	0.42	5.00	0.00	2005	1	19	23	56	5.46	0.05	0.00	0.29	4	6	0
56	34.07117	0.47	-106.95567	0.43	5.00	0.00	2005	1	20	3	16	32.87	0.05	0.00	0.43	5	7	0
77	34.04400	0.36	-106.97567	0.35	6.53	0.87	2005	3	29	14	6	33.52	0.06	0.00	0.25	7	14	2
151	34.06067	0.83	-106.95200	0.97	5.61	0.82	2005	6	14	3	51	55.56	0.14	0.00	0.10	4	7	1
187	34.05733	0.61	-106.95617	0.41	6.66	0.59	2005	10	21	8	11	36.51	0.06	0.00	0.16	6	11	2
188	34.05333	0.89	-106.95733	0.46	6.60	1.23	2005	10	21	8	29	56.02	0.12	0.00	0.13	5	7	0
189	34.05050	0.47	-106.95883	0.43	4.46	0.68	2005	10	24	18	14	11.76	0.06	0.00	0.52	5	11	2
191	34.12250	0.56	-106.99783	0.59	5.00	0.00	2005	10	24	18	27	53.57	0.06	0.00	0.47	4	7	0
193	34.06133	0.46	-106.97800	0.42	5.50	0.64	2005	10	26	23	28	18.04	0.06	0.00	0.32	7	13	2
197	34.05200	0.46	-106.95483	0.39	6.56	0.60	2005	10	30	2	5	25.18	0.06	0.00	0.18	7	13	2
205	34.06200	0.59	-106.95767	0.50	7.88	0.81	2005	10	30	3	14	32.58	0.08	0.00	0.04	4	5	1
205	34.06200	0.59	-106.95767	0.50	7.88	0.81	2005	10	30	3	14	32.58	0.08	0.00	0.04	0	0	0
207	34.05817	0.52	-106.95850	0.39	6.69	0.57	2005	10	30	3	19	55.74	0.06	0.00	0.15	6	9	3
208	34.05900	0.51	-106.95817	0.40	6.54	0.62	2005	10	30	3	26	37.41	0.06	0.00	0.20	6	8	2
209	34.04767	0.53	-106.97433	0.40	6.82	0.59	2005	10	30	4	43	6.45	0.06	0.00	0.23	6	9	3
210	34.06000	0.53	-106.95783	0.40	7.39	0.66	2005	10	30	4	45	20.85	0.06	0.00	0.14	6	8	2
211	34.05800	0.54	-106.95767	0.40	6.68	0.57	2005	10	30	4	50	47.47	0.06	0.00	0.19	5	8	3
212	34.06200	1.21	-106.95517	1.75	7.04	0.89	2005	10	30	5	1	23.95	0.18	0.00	0.02	4	5	1
214	34.05000	0.39	-106.95583	0.45	6.54	0.59	2005	11	1	9	28	12.90	0.05	0.00	0.18	7	10	3
215	34.05467	0.66	-106.95750	0.43	6.33	0.57	2005	11	3	14	58	57.23	0.07	0.00	0.16	5	11	3
220	34.08267	0.45	-106.96667	0.37	6.12	0.53	2005	11	5	2	9	33.82	0.06	0.00	0.35	6	15	3
222	34.05750	0.40	-106.95633	0.46	6.37	0.64	2005	11	6	12	45	19.64	0.06	0.00	0.18	6	9	2
223	34.03867	0.39	-106.95217	0.46	6.12	0.69	2005	11	6	13	16	28.74	0.06	0.00	0.33	6	8	2
225	34.07000	0.35	-106.96117	0.36	6.55	0.54	2005	11	8	18	20	52.53	0.05	0.00	0.25	10	14	3

Cluster 4

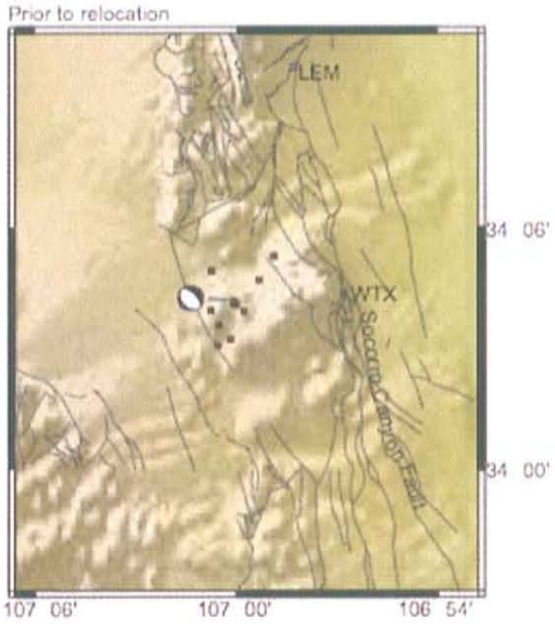
Prior to relocation
LEM
WTX
Soccorro Canyon Fault
34 06'
34 00'
107 06'
107 00'
106 54'

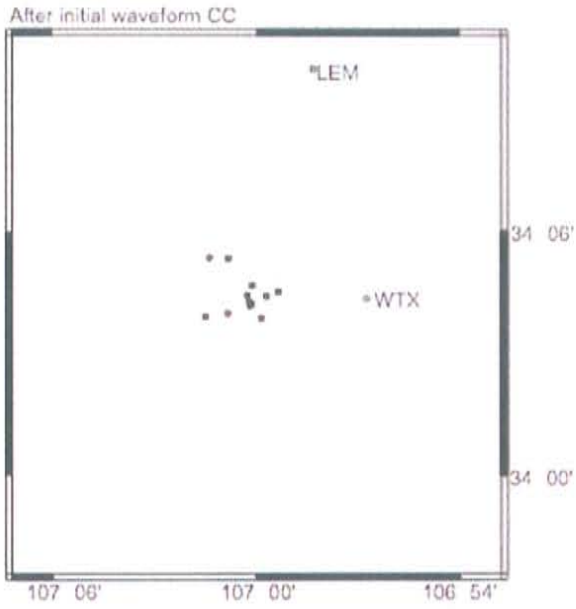
After initial waveform CC
LEM
WTX
34 06'
34 00'
107 06'
107 00'
106 54'

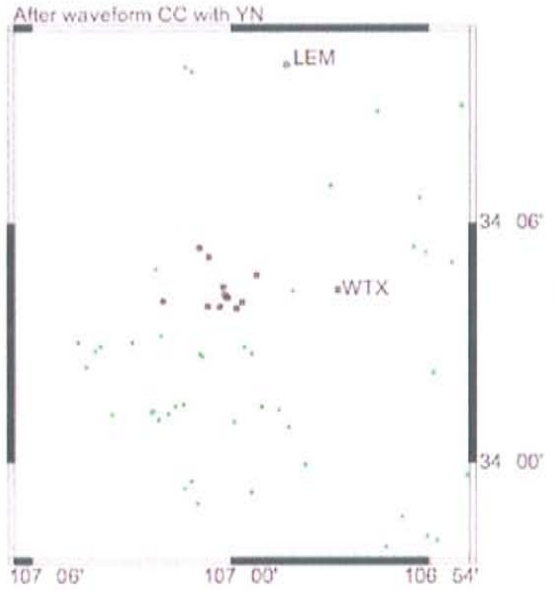
After waveform CC with YN
LEM
WTX
34 06'
34 00'
107 06'
107 00'
106 54'

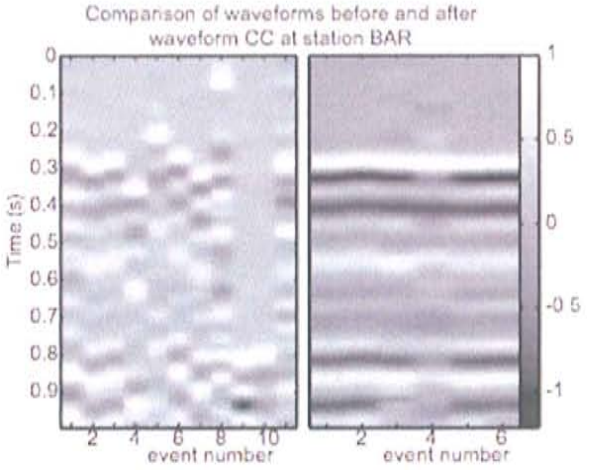
Comparison of waveforms before and after
waveform CC at station BAR
Time (s)
0
0.1
0.2
0.3
0.4
0.5
0.6
0.7
0.8
0.9
2
4
6
8
10
event number
2
4
6
event number
1
0.5
0
-0.5
-1

Cluster 4 Error Margins

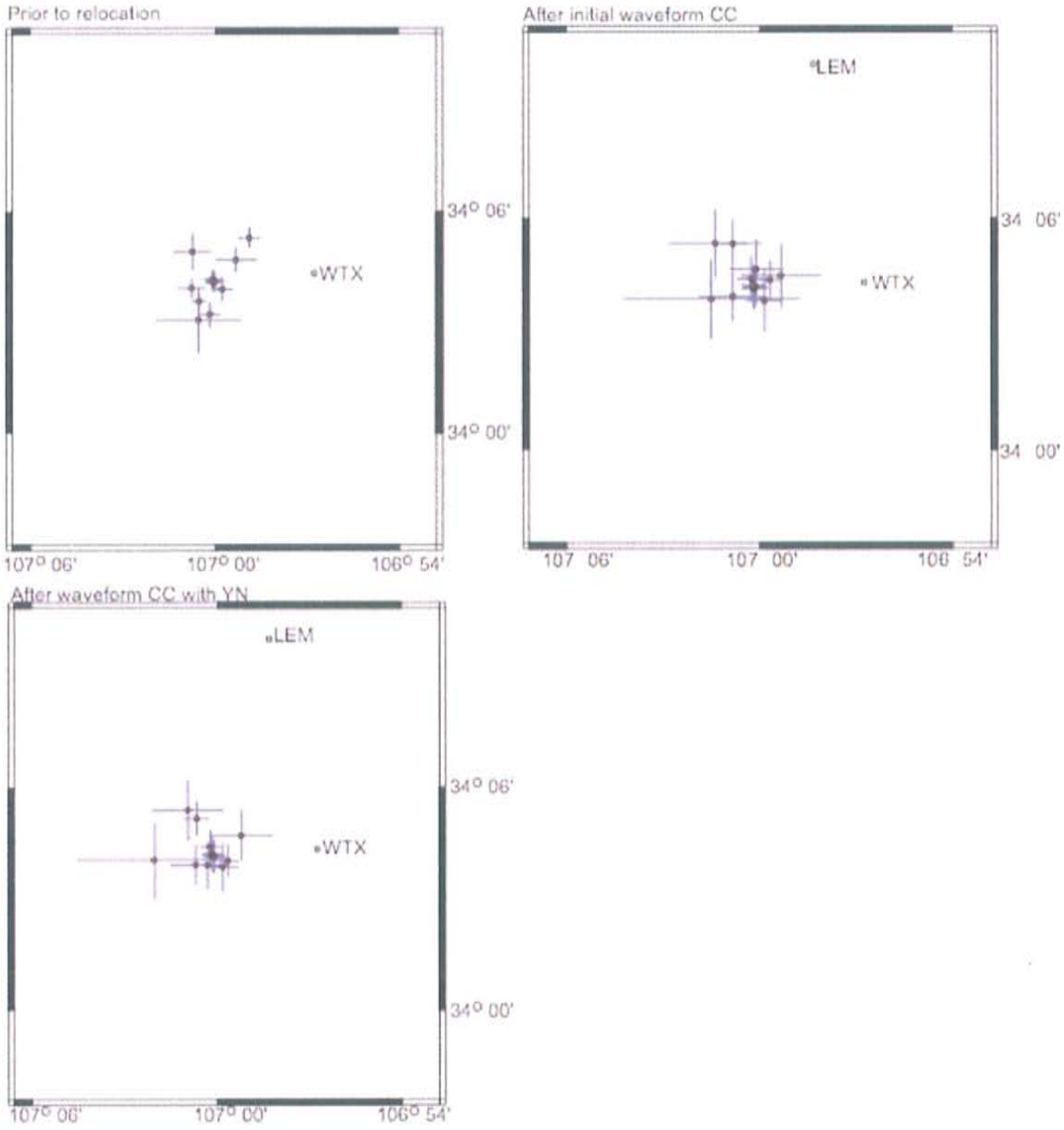

Cluster 4 prior to relocation

ind	lat	lstd	long	lstd	depth	lstd	yyyy	mm	dd	hh	mm	orig	lstd	mag	rms	stats	picks	refls
22	34.08183	0.51	-107.01250	0.60	1.35	8.04	2004	10	31	15	28	22.93	0.16	0.21	0.33	4	8	0
ind	34.06550	0.27	-107.01283	0.48	5.00	0.00	100	0	0	0	61	58.66	0.05	0.00	0.00	1	0	0
81	34.06883	0.27	-107.00050	0.27	5.64	0.67	2005	4	2	11	3	4.01	0.05	0.81	0.06	8	14	1
82	34.06800	0.24	-107.00117	0.26	4.47	0.45	2005	4	2	16	53	14.83	0.03	0.60	0.34	9	18	4
83	34.06500	0.35	-106.99617	0.37	5.74	0.58	2005	4	2	17	22	53.18	0.05	0.26	0.13	6	12	1
84	34.07800	0.35	-106.98867	0.68	5.04	0.61	2005	4	2	21	44	12.11	0.07	0.22	0.23	4	8	1
85	34.06817	0.26	-107.00017	0.31	4.18	1.16	2005	4	2	22	48	6.13	0.05	1.36	0.13	10	11	0
86	34.06933	0.27	-107.00167	0.28	4.84	0.86	2005	4	2	23	41	15.53	0.05	0.81	0.15	8	13	0
93	34.05117	0.88	-107.00917	1.41	8.25	1.38	2005	4	23	19	15	25.61	0.25	0.14	0.05	4	6	0
94	34.05367	0.35	-107.00300	0.36	9.28	0.93	2005	4	24	4	53	59.02	0.08	0.93	0.11	7	10	0
161	34.05950	0.26	-107.00883	0.25	4.34	0.57	2005	8	5	12	44	58.49	0.04	0.69	0.19	10	17	2
263	34.08800	0.28	-106.98150	0.36	2.20	0.59	2006	5	6	10	59	0.56	0.04	0.81	0.14	7	13	2

Cluster 4 after waveform CC

ind	lat	lstd	long	lstd	depth	lstd	yyyy	mm	dd	hh	mm	orig	lstd	mag	rms	stats	picks	refls
22	34.08900	0.88	-107.02300	1.44	6.18	3.21	2004	10	31	15	28	22.62	0.30	0.00	0.35	4	8	0
45	34.06617	0.65	-107.01400	1.06	5.00	0.00	2005	1	15	9	54	58.61	0.13	0.00	0.23	5	9	0
81	34.06933	0.55	-107.00300	0.39	5.78	1.11	2005	4	2	11	3	4.01	0.07	0.00	0.06	8	14	1
82	34.07000	0.49	-107.00233	0.37	4.35	0.65	2005	4	2	16	53	14.82	0.05	0.00	0.33	9	18	4
83	34.06417	0.82	-106.99767	0.56	4.74	1.03	2005	4	2	17	22	53.21	0.07	0.00	0.21	6	12	1
84	34.07500	0.84	-106.98933	1.23	5.59	0.97	2005	4	2	21	44	12.04	0.16	0.00	0.19	4	8	1
85	34.07367	0.58	-107.00450	0.43	6.02	2.78	2005	4	2	22	48	5.99	0.13	0.00	0.13	10	11	0
86	34.07083	0.56	-107.00350	0.38	4.40	1.90	2005	4	2	23	41	15.55	0.09	0.00	0.15	8	13	0
93	34.06483	1.03	-107.02500	2.72	7.08	2.90	2005	4	23	19	15	25.40	0.48	0.00	0.21	4	6	0
94	34.07767	0.79	-107.00200	0.83	15.14	2.08	2005	4	24	4	53	58.25	0.24	0.00	0.43	7	10	0
161	34.07317	0.50	-106.99500	0.36	4.62	0.81	2005	8	5	12	44	58.29	0.06	0.00	0.39	10	17	2
263	34.08867	0.64	-107.01383	0.45	1.44	0.96	2006	5	6	10	59	0.17	0.07	0.00	0.25	7	13	2

Cluster 4 after waveform CC with YN

ind	lat	lstd	long	lstd	depth	lstd	yyyy	mm	dd	hh	mm	orig	lstd	mag	rms	stats	picks	refls
22	34.08967	0.83	-107.01600	1.18	5.69	3.29	2004	10	31	15	28	22.74	0.27	0.00	0.38	4	8	0
45	34.06517	0.53	-107.01183	0.85	5.00	0.00	2005	1	15	9	54	58.66	0.10	0.00	0.24	5	9	0
81	34.06933	0.47	-107.00233	0.36	5.66	1.03	2005	4	2	11	3	4.01	0.07	0.00	0.06	8	14	1
82	34.06883	0.42	-107.00150	0.35	4.41	0.63	2005	4	2	16	53	14.83	0.05	0.00	0.34	9	18	4
83	34.06433	0.67	-106.99717	0.52	4.40	0.99	2005	4	2	17	22	53.21	0.07	0.00	0.21	6	12	1
84	34.07833	0.69	-106.98717	1.01	5.39	0.90	2005	4	2	21	44	12.08	0.13	0.00	0.22	4	8	1
85	34.07333	0.45	-107.00400	0.38	6.07	1.87	2005	4	2	22	48	5.98	0.09	0.00	0.13	10	11	0
86	34.07000	0.48	-107.00317	0.36	4.54	1.62	2005	4	2	23	41	15.55	0.08	0.00	0.15	8	13	0
93	34.06733	1.03	-107.03417	2.48	8.12	2.40	2005	4	23	19	15	25.22	0.44	0.00	0.23	4	6	0
94	34.06500	0.63	-107.00550	0.65	12.64	1.75	2005	4	24	4	53	58.43	0.18	0.00	0.33	7	10	0
161	34.06700	0.42	-106.99417	0.35	4.89	0.77	2005	8	5	12	44	58.34	0.05	0.00	0.35	10	17	2
263	34.08583	0.46	-107.01133	0.42	1.62	0.93	2006	5	6	10	59	0.22	0.06	0.00	0.22	9	15	2

Cluster 5

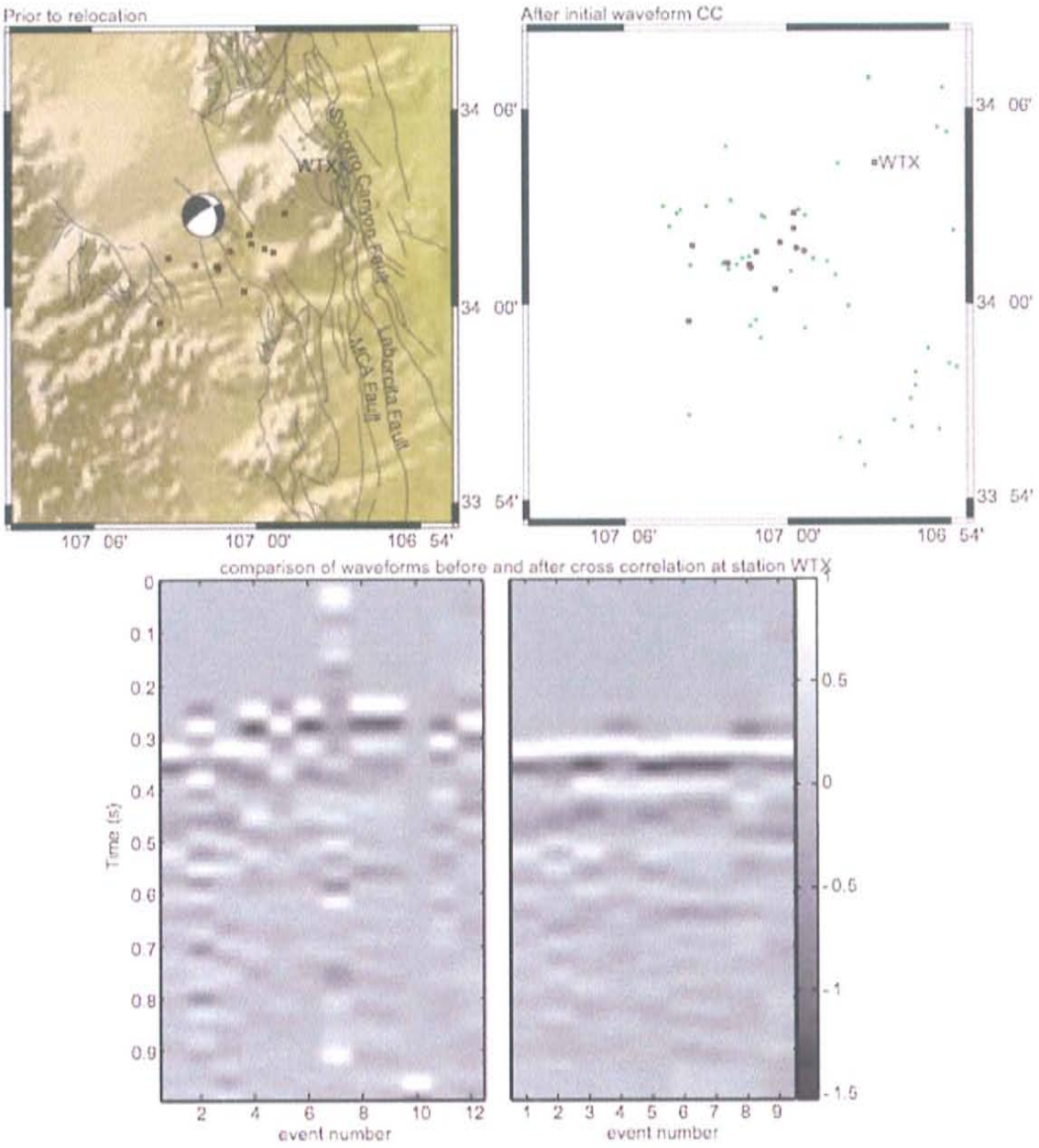
Prior to relocation
After initial waveform CC
WTX
34 06'
34 00'
33 54'
107 06'
107 00'
106 54'
Labarcita Fault
MCA Fault
comparison of waveforms before and after cross correlation at station WTX
Time (s)
event number
0
0.1
0.2
0.3
0.4
0.5
0.6
0.7
0.8
0.9
2
4
6
8
10
12
1
2
3
4
5
6
7
8
9
0.5
0
-0.5
-1
-1.5

Cluster 5 Error Margins

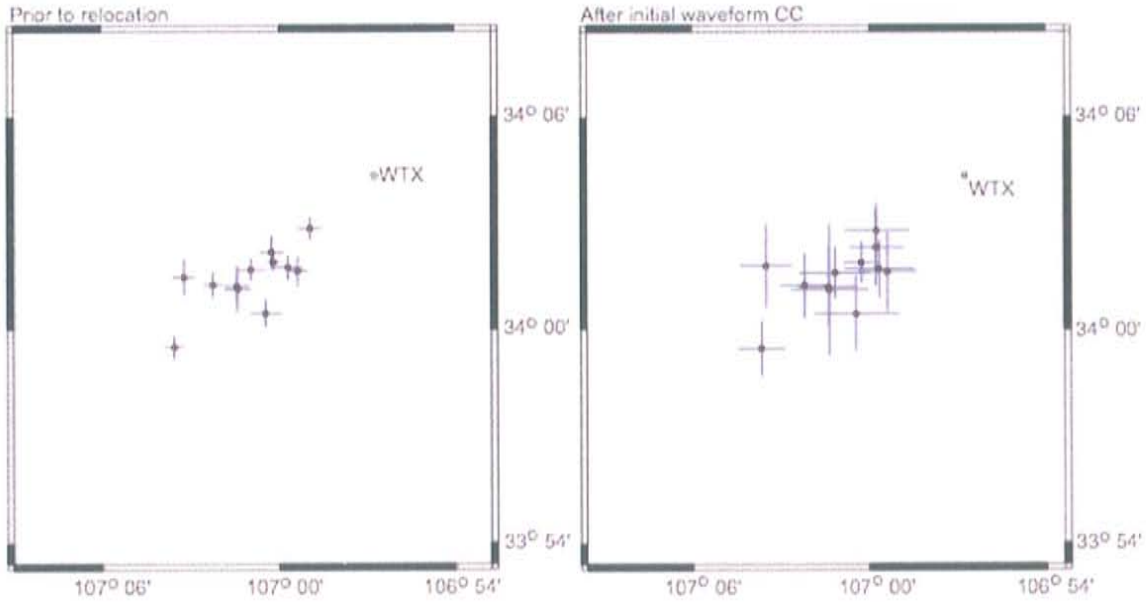

Cluster 5 prior to relocation

ind	lat	lstd	long	lstd	depth	lstd	yyyy	mm	dd	hh	mm	orig	lstd	mag	rms	stats	picks	refls
32	34.02750	0.44	-106.98950	0.36	5.00	0.00	2004	12	14	6	59	27.55	0.05	0.36	0.04	4	6	0
58	34.04750	0.34	-106.98233	0.42	6.95	0.85	2005	1	22	0	53	41.18	0.07	0.55	0.15	4	8	1
80	33.99183	0.32	-107.05900	0.34	7.96	0.48	2005	4	1	4	45	6.60	0.05	0.05	0.15	5	14	3
87	34.02117	0.36	-107.03717	0.34	8.69	0.52	2005	4	11	14	1	33.85	0.05	0.35	0.08	7	14	2
148	34.00767	0.39	-107.00733	0.55	3.77	2.18	2005	6	11	10	18	55.58	0.10	0.27	0.05	5	8	0
163	34.02050	0.41	-107.02367	0.41	10.08	1.61	2005	8	7	17	11	21.51	0.15	0.71	0.05	7	9	0
213	34.01917	0.65	-107.02317	0.46	7.68	1.31	2005	10	30	5	26	15.79	0.10	-0.26	0.07	4	5	1
229	34.03183	0.24	-107.00300	0.24	4.16	1.42	2006	1	2	2	1	57.51	0.06	0.85	0.16	9	16	0
230	34.02917	0.35	-106.99483	0.50	5.16	0.77	2006	1	2	15	27	37.60	0.07	-0.02	0.04	4	9	1
231	34.02817	0.31	-107.01567	0.51	4.01	0.84	2006	1	3	6	8	24.35	0.07	0.43	0.19	5	11	1
232	34.03633	0.47	-107.00400	0.41	4.92	0.74	2006	1	5	11	17	10.38	0.07	0.41	0.10	5	9	1
234	34.02467	0.51	-107.05367	0.39	9.45	0.55	2006	1	20	22	14	19.21	0.07	-0.69	0.30	4	10	2

Cluster 5 after waveform CC

ind	lat	lstd	long	lstd	depth	lstd	yyyy	mm	dd	hh	mm	orig	lstd	mag	rms	stats	picks	refls
32	34.02717	1.12	-106.99000	1.01	5.00	0.00	2004	12	14	6	59	27.55	0.16	0.00	0.03	4	6	0
58	34.04650	0.80	-106.99617	1.12	6.78	1.22	2005	1	22	0	53	41.15	0.13	0.00	0.15	4	8	1
80	33.99133	0.78	-107.06117	0.83	8.14	0.73	2005	4	1	4	45	6.57	0.11	0.00	0.14	5	13	3
87	34.02083	0.92	-107.03667	0.83	8.72	0.77	2005	4	11	14	1	33.84	0.11	0.00	0.08	7	14	2
148	34.00750	1.07	-107.00767	1.44	4.20	5.03	2005	6	11	10	18	55.56	0.26	0.00	0.04	5	8	0
163	34.02017	1.15	-107.02367	1.02	10.02	4.51	2005	8	7	17	11	21.51	0.42	0.00	0.05	7	9	0
213	34.01867	1.88	-107.02283	1.34	7.27	1.44	2005	10	30	5	26	15.82	0.15	0.00	0.03	4	5	1
229	34.03150	0.58	-107.00467	0.62	4.56	3.67	2006	1	2	2	1	57.50	0.17	0.00	0.16	9	16	0
230	34.02850	0.82	-106.99450	1.20	5.19	1.14	2006	1	2	15	27	37.60	0.13	0.00	0.04	4	9	1
231	34.02667	0.73	-107.01950	1.23	4.22	1.30	2006	1	3	6	8	24.27	0.17	0.00	0.16	5	11	1
232	34.03867	1.10	-106.99633	0.91	4.02	1.16	2006	1	5	11	17	10.29	0.13	0.00	0.30	5	9	1
234	34.03000	1.19	-107.05850	0.91	9.20	0.79	2006	1	20	22	14	19.22	0.13	0.00	0.28	4	10	2

Cluster 6

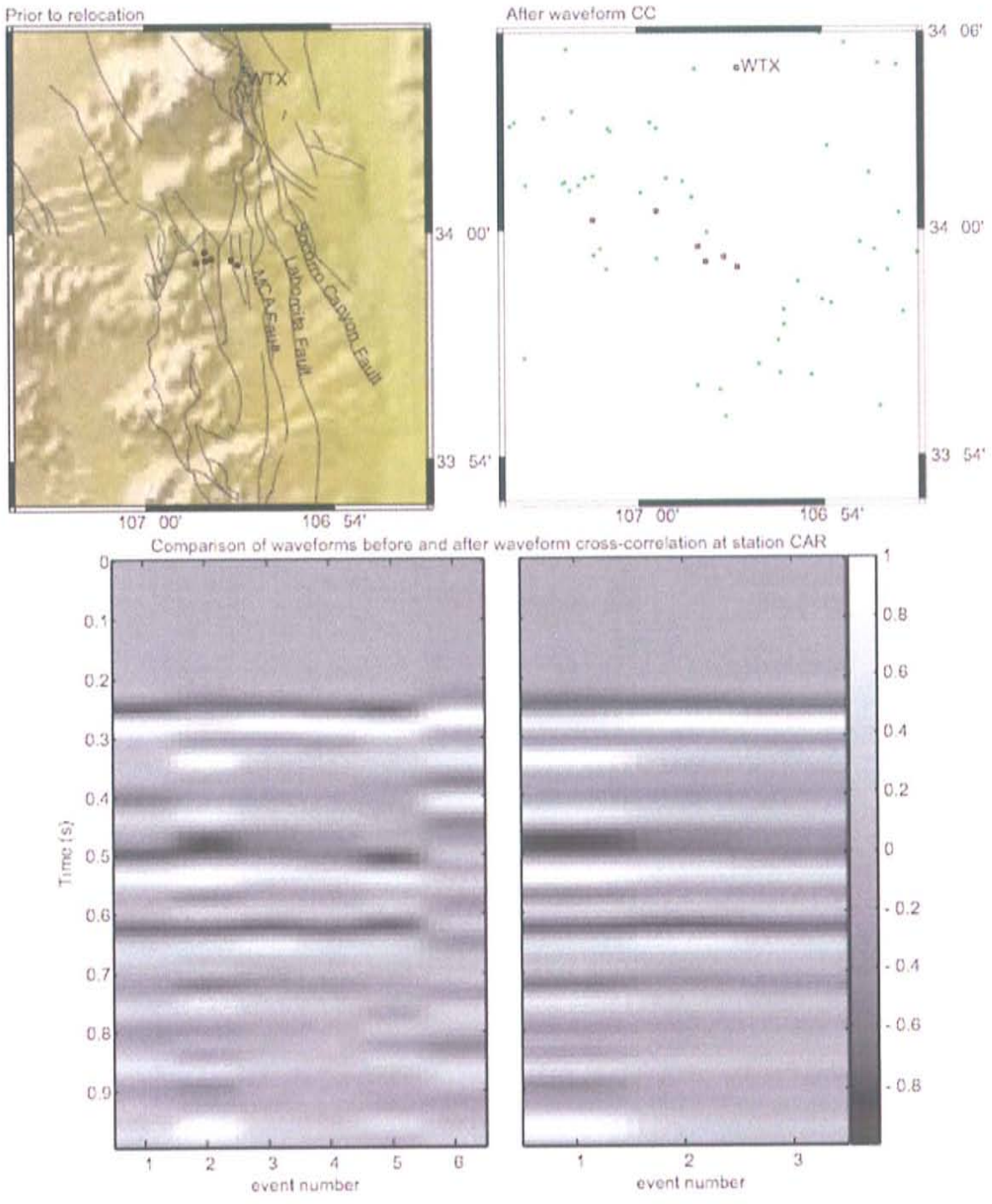
Prior to relocation
WTX
Socorro Canyon Fault
Lemitar Fault
34 00'
33 54'
107 00'
106 54'
After waveform CC
WTX
34 06'
34 00'
33 54'
107 00'
106 54'
Comparison of waveforms before and after waveform cross-correlation at station CAR
Time (s)
0
0.1
0.2
0.3
0.4
0.5
0.6
0.7
0.8
0.9
1
2
3
4
5
6
event number
1
2
3
event number
1
0.8
0.6
0.4
0.2
0
- 0.2
- 0.4
- 0.6
- 0.8

Cluster 6 Error Margins

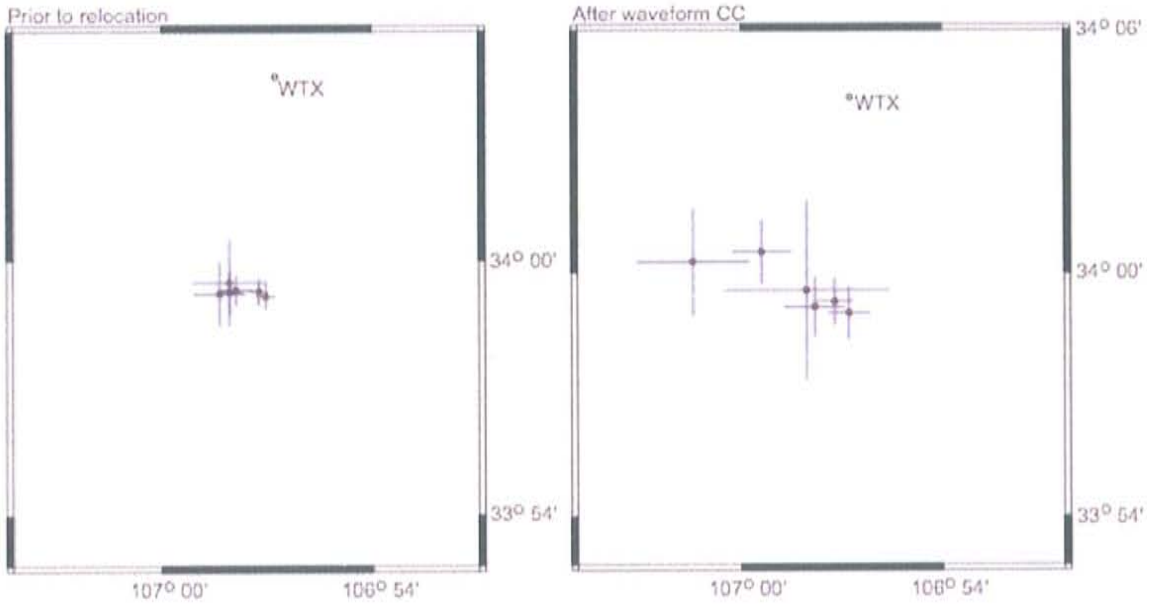

Cluster 6 prior to relocation

ind	lat	lstd	long	lstd	depth	lstd	yyyy	mm	dd	hh	mm	orig	lstd	mag	rms	stats	picks	refls
88	33.98800	0.32	-106.95400	0.29	6.50	1.25	2005	4	15	10	44	18.40	0.08	0.64	0.11	7	13	0
107	33.98783	0.53	-106.96783	0.38	5.00	0.00	2005	5	11	16	48	18.93	0.08	1.27	0.42	8	13	0
108	33.99150	1.03	-106.96800	1.09	6.44	1.54	2005	5	11	16	50	32.29	0.19	0.73	0.03	4	7	0
109	33.98700	0.79	-106.97267	0.74	4.61	2.11	2005	5	11	19	48	8.25	0.14	0.58	0.05	4	8	0
167	33.98850	0.36	-106.96483	0.53	6.40	1.44	2005	8	22	14	49	14.36	0.10	0.65	0.09	6	9	0
296	33.98600	0.32	-106.95067	0.30	5.00	0.00	2006	12	31	13	49	44.27	0.04	0.77	0.07	6	9	0

Cluster 6 after waveform CC

ind	lat	lstd	long	lstd	depth	lstd	yyyy	mm	dd	hh	mm	orig	lstd	mag	rms	stats	picks	refls
88	33.98833	0.59	-106.95367	0.56	6.73	2.69	2005	4	15	10	44	18.40	0.17	0.00	0.11	7	13	0
107	34.00883	0.81	-106.98983	0.92	5.00	0.00	2005	5	11	16	48	18.38	0.14	0.00	0.83	8	13	0
108	33.99300	2.23	-106.96750	2.48	6.67	3.57	2005	5	11	16	50	32.30	0.29	0.00	0.03	4	7	0
109	34.00483	1.35	-107.02383	1.68	11.00	3.02	2005	5	11	19	48	7.14	0.31	0.00	0.22	4	7	0
167	33.98617	0.75	-106.96350	0.90	5.82	3.34	2005	8	22	14	49	14.38	0.19	0.00	0.09	6	9	0
296	33.98367	0.66	-106.94650	0.65	5.00	0.00	2006	12	31	13	49	44.15	0.09	0.00	0.25	6	10	0

Cluster 7

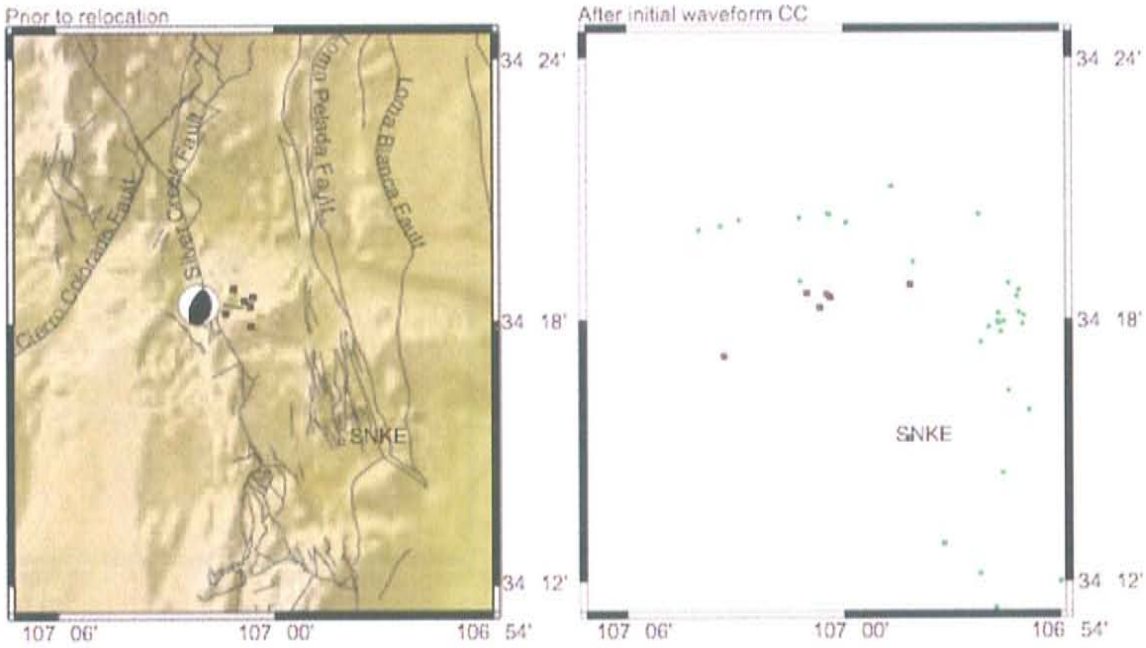
Prior to relocation
After initial waveform CC
Silver Creek Fault
Cerro Colorado Fault
Loma Blanca Fault
SNKE
34 24'
34 18'
34 12'
107 06'
107 00'
106 54'

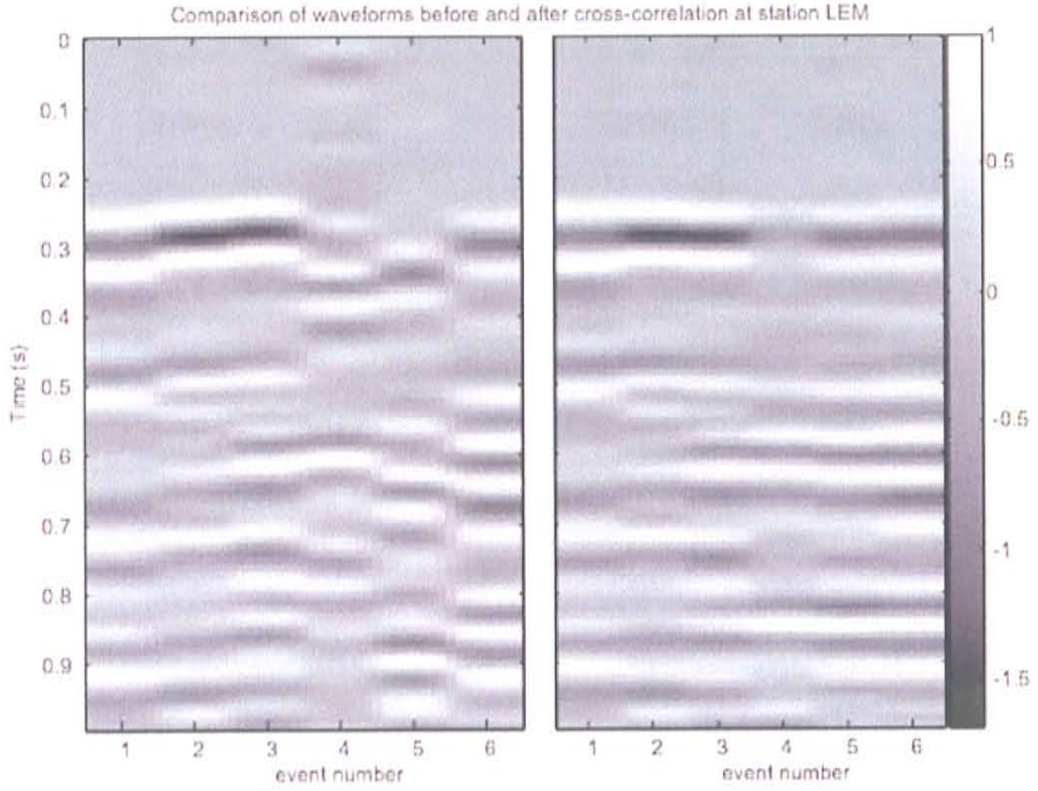
Comparison of waveforms before and after cross-correlation at station LEM
Time (s)
event number
event number

Cluster 7 Error Margins

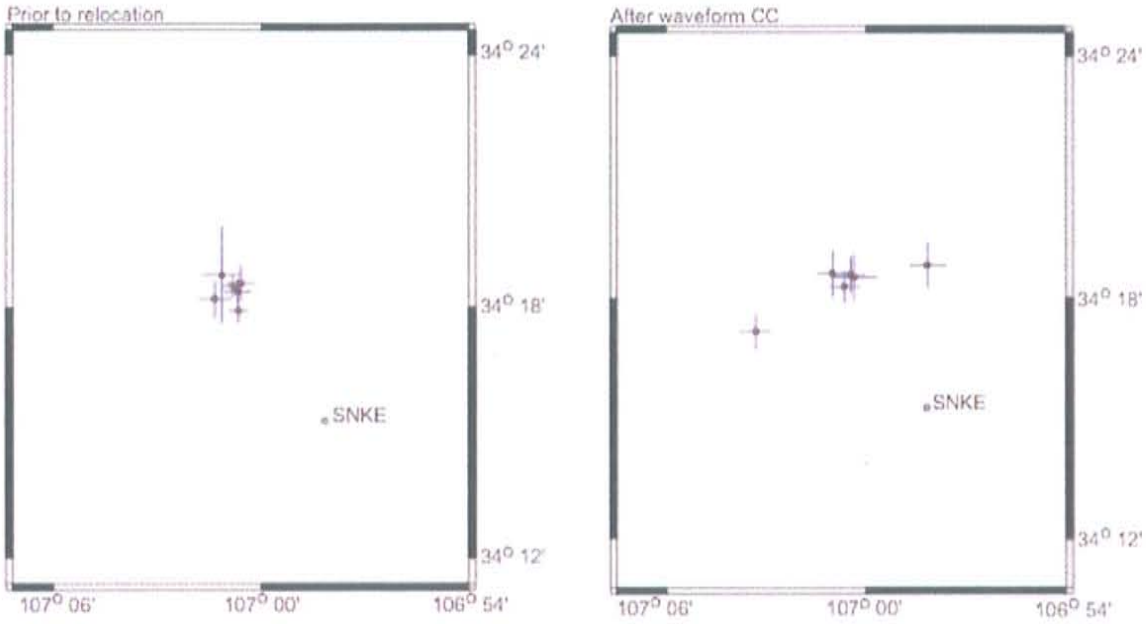

Cluster 7 prior to relocation

ind	lat	lstd	long	lstd	depth	lstd	yyyy	mm	dd	hh	mm	orig	lstd	mag	rms	stats	picks	refls
69	34.30600	0.31	-107.01133	0.39	6.68	2.08	2005	2	23	18	18	5.90	0.09	1.82	0.03	8	8	0
91	34.30950	0.42	-107.00983	0.42	6.60	2.11	2005	4	22	21	44	20.15	0.11	0.24	0.02	6	8	0
110	34.29850	0.29	-107.01100	0.31	5.00	0.00	2005	5	12	13	31	24.94	0.03	0.76	0.22	8	12	0
113	34.31267	1.14	-107.01917	0.60	3.20	6.25	2005	6	1	11	27	18.28	0.10	0.15	0.15	5	8	0
114	34.30317	0.44	-107.02267	0.48	8.64	0.77	2005	6	1	14	5	44.88	0.07	0.39	0.30	7	11	1
116	34.30800	0.28	-107.01383	0.33	6.97	1.58	2005	6	2	9	33	0.38	0.07	0.93	0.05	10	12	0

Cluster 7 after waveform CC

ind	lat	lstd	long	lstd	depth	lstd	yyyy	mm	dd	hh	mm	orig	lstd	mag	rms	stats	picks	refls
69	34.30850	0.60	-107.00600	0.71	6.38	3.70	2005	2	23	18	18	5.93	0.21	0.00	0.06	8	8	0
91	34.30467	0.41	-107.01083	0.45	5.00	0.00	2005	4	22	21	44	20.24	0.05	0.00	0.08	6	8	0
110	34.30967	0.45	-107.00783	0.46	4.59	2.43	2005	5	12	13	31	24.89	0.09	0.00	0.25	8	12	0
113	34.31017	0.59	-107.01683	0.46	5.00	0.00	2005	6	1	11	27	18.21	0.09	0.00	0.18	5	7	0
114	34.28617	0.45	-107.05517	0.48	5.00	0.00	2005	6	1	14	5	45.37	0.05	0.00	0.31	7	11	1
116	34.31350	0.58	-106.96933	0.55	12.99	1.39	2005	6	2	9	33	59.49	0.12	0.00	0.31	8	9	0

Cluster 8

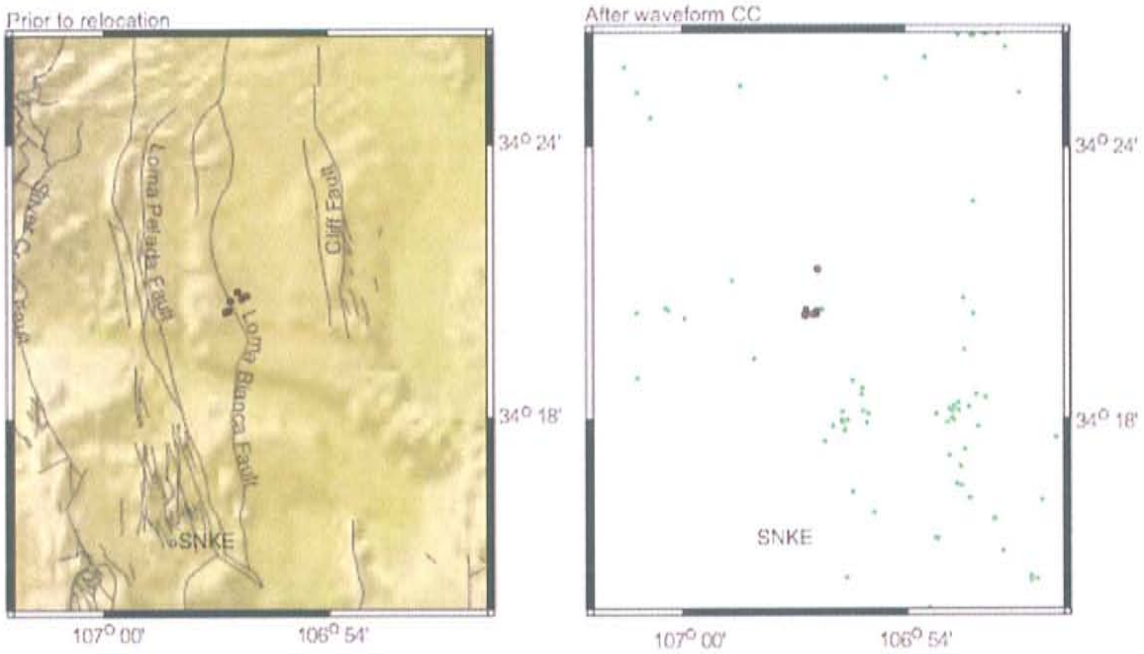
Prior to relocation
After waveform CC
Loma Pelada Fault
Cliff Fault
Loma Blanca Fault
SNKE
34° 24'
34° 18'
107° 00'
106° 54'

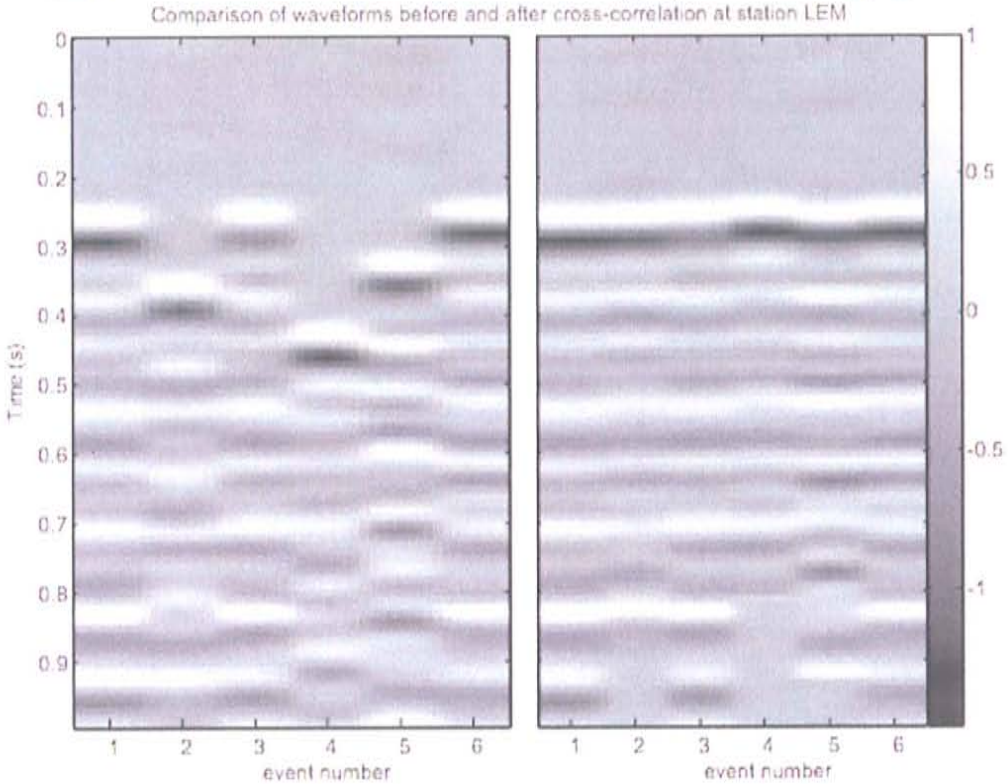
Comparison of waveforms before and after cross-correlation at station LEM
Time (s)
event number
event number

Cluster 8 Error Margins

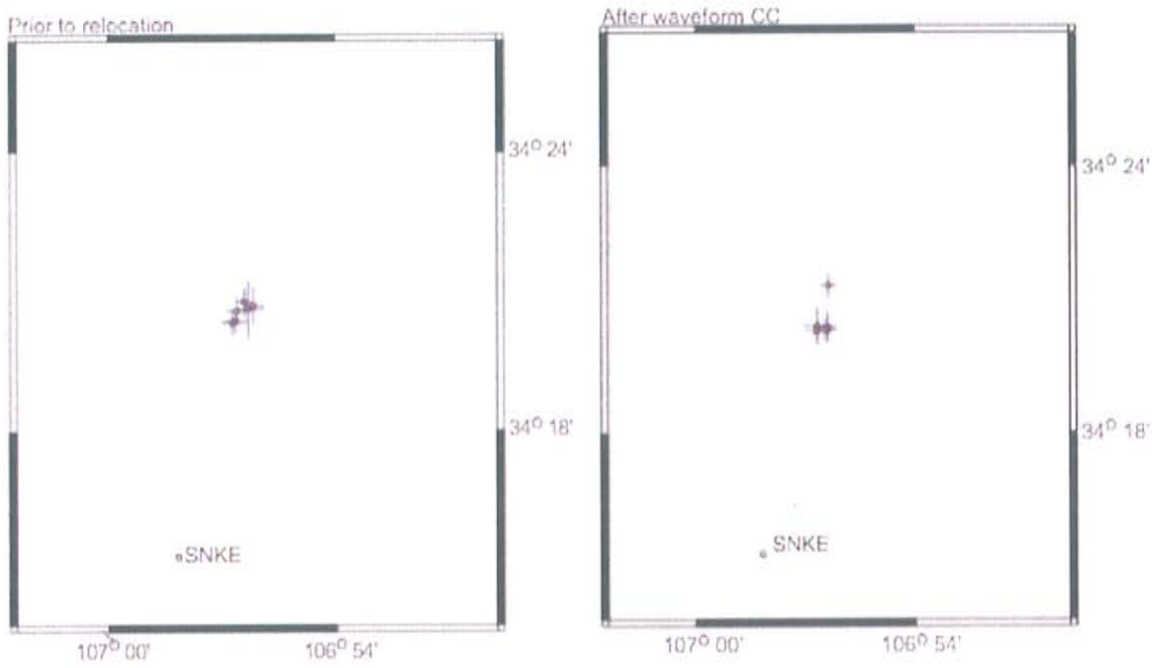

Cluster 8 prior to relocation

ind	lat	lstd	long	lstd	depth	lstd	yyyy	mm	dd	hh	mm	orig	lstd	mag	rms	stats	picks	refls
25	34.34633	0.30	-106.94033	0.23	5.00	0.00	2004	11	16	21	12	28.57	0.04	1.08	0.23	8	13	0
26	34.34367	0.61	-106.93867	0.43	5.00	0.00	2004	11	16	22	6	8.77	0.07	0.38	0.20	5	7	0
28	34.34300	0.31	-106.94367	0.28	5.00	0.00	2004	11	25	21	9	44.45	0.04	1.33	0.15	8	11	0
33	34.33883	0.29	-106.94567	0.32	5.00	0.00	2004	12	18	17	37	20.38	0.04	0.79	0.22	8	11	0
68	34.34500	0.40	-106.93633	0.29	4.48	0.73	2005	2	21	16	49	24.56	0.06	0.31	0.37	5	12	2
76	34.33950	0.26	-106.94433	0.32	5.00	0.00	2005	3	20	14	4	8.96	0.04	1.06	0.23	9	15	1

Cluster 8 after waveform CC

ind	lat	lstd	long	lstd	depth	lstd	yyyy	mm	dd	hh	mm	orig	lstd	mag	rms	stats	picks	refls
25	34.35500	0.28	-106.93950	0.24	5.00	0.00	2004	11	16	21	12	28.42	0.04	0.00	0.25	8	13	0
26	34.33983	0.43	-106.94467	0.41	5.00	0.00	2004	11	16	22	6	8.81	0.07	0.00	0.24	5	7	0
28	34.33850	0.27	-106.94000	0.25	5.00	0.00	2004	11	25	21	9	44.50	0.04	0.00	0.20	8	11	0
33	34.33800	0.27	-106.94500	0.32	5.00	0.00	2004	12	18	17	37	20.37	0.04	0.00	0.22	8	11	0
68	34.33950	0.35	-106.94000	0.28	5.00	0.00	2005	2	21	16	49	24.67	0.06	0.00	0.36	5	12	2
76	34.33833	0.27	-106.94133	0.27	5.00	0.00	2005	3	20	14	4	8.97	0.04	0.00	0.21	8	12	0

Cluster 9

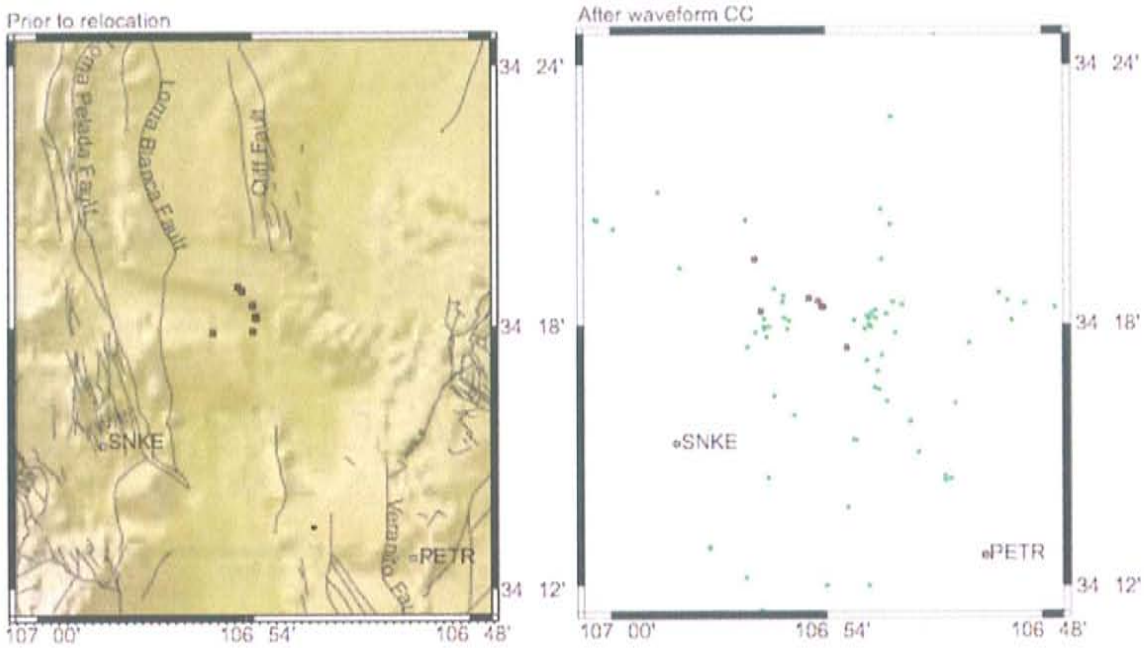
Prior to relocation
After waveform CC
Loma Pelada Fault
Loma Blanca Fault
Cliff Fault
Vernal Fault
SNKE
PETR
34 24'
34 18'
34 12'
107 00'
106 54'
106 48'

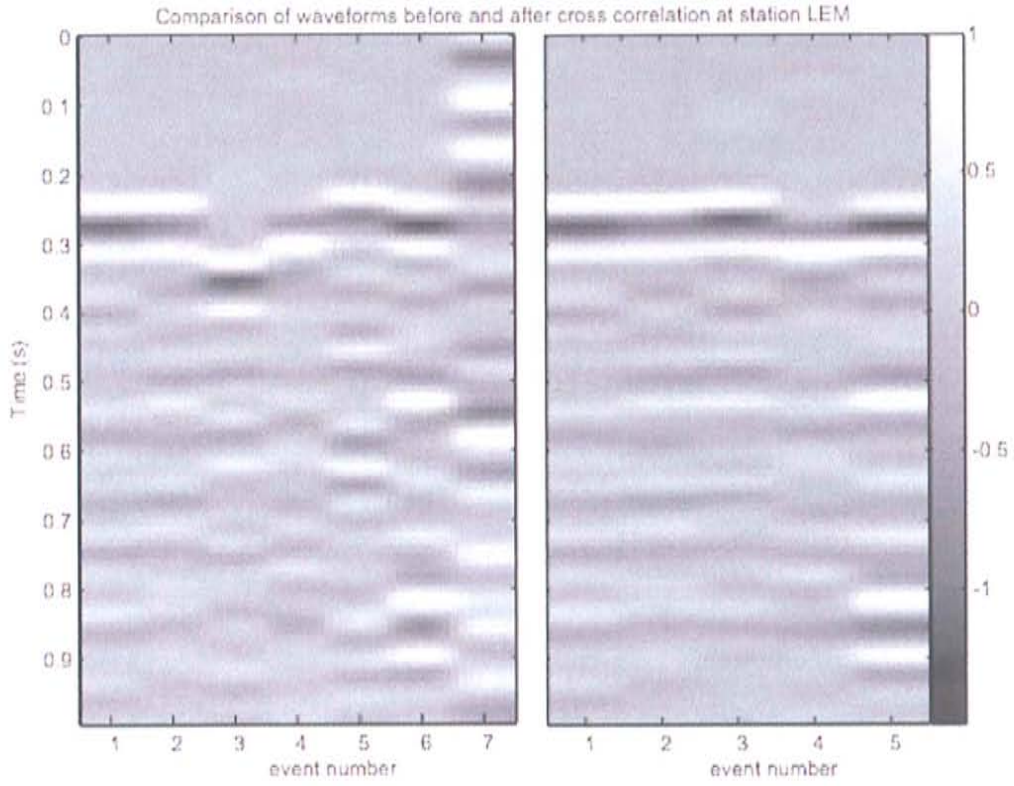
Comparison of waveforms before and after cross correlation at station LEM
Time (s)
0
0.1
0.2
0.3
0.4
0.5
0.6
0.7
0.8
0.9
1
0.5
0
-0.5
-1
1 2 3 4 5 6 7
event number
1 2 3 4 5
event number

Cluster 9 Error Margins

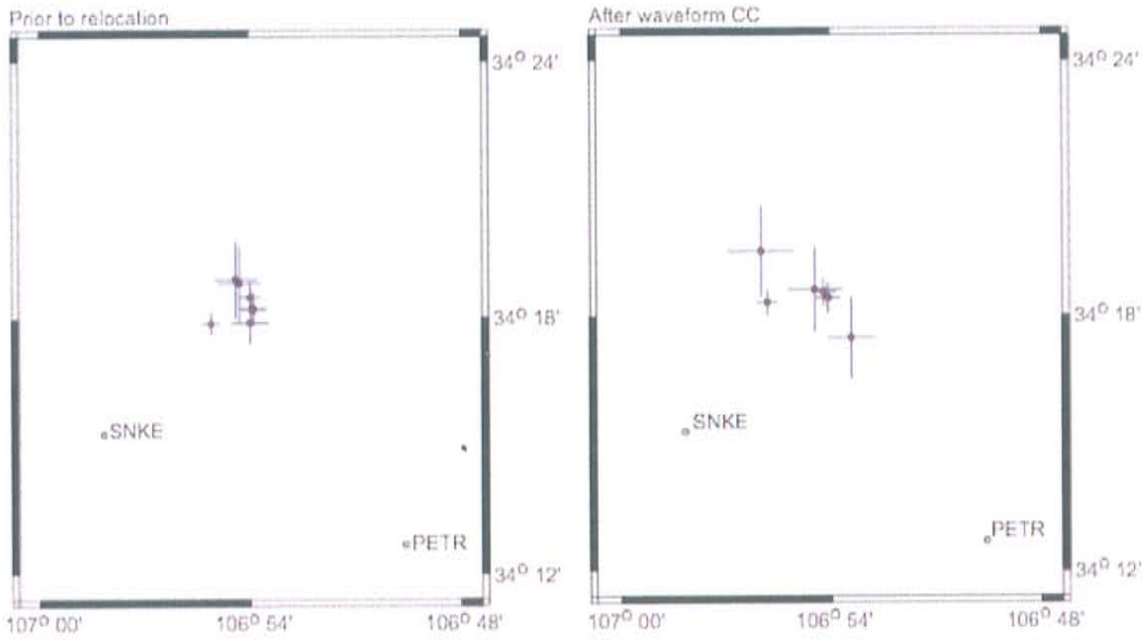

Cluster 9 prior to relocation

ind	lat	lstd	long	lstd	depth	lstd	yyyy	mm	dd	hh	mm	orig	lstd	mag	rms	stats	picks	refls
41	34.30817	0.39	-106.90000	0.30	8.23	0.63	2005	1	6	12	7	3.55	0.06	0.28	0.25	6	12	2
42	34.29783	0.26	-106.91867	0.27	5.78	0.89	2005	1	9	14	0	53.58	0.04	0.67	0.29	8	15	1
59	34.30400	0.41	-106.89867	0.39	7.61	0.90	2005	1	25	1	51	16.80	0.07	0.26	0.19	4	8	1
72	34.30317	0.38	-106.89850	0.38	7.83	0.88	2005	3	5	0	48	13.68	0.07	-0.11	0.17	5	9	1
150	34.29817	0.49	-106.90000	0.54	6.72	2.24	2005	6	13	20	22	49.87	0.10	0.42	0.04	6	8	0
172	34.31367	0.91	-106.90517	0.62	5.00	0.00	2005	9	1	16	50	55.08	0.14	0.44	0.16	5	7	0
173	34.31517	0.91	-106.90683	0.63	5.00	0.00	2005	9	4	11	25	15.69	0.15	0.28	0.14	5	7	0

Cluster 9 after waveform CC

ind	lat	lstd	long	lstd	depth	lstd	yyyy	mm	dd	hh	mm	orig	lstd	mag	rms	stats	picks	refls
41	34.30717	0.36	-106.90167	0.33	7.50	1.06	2005	1	6	12	7	3.57	0.07	0.00	0.19	6	9	1
42	34.30517	0.31	-106.93033	0.31	4.96	1.13	2005	1	9	14	0	53.46	0.06	0.00	0.53	8	15	1
59	34.30683	0.35	-106.90167	0.36	7.00	1.09	2005	1	25	1	51	16.76	0.08	0.00	0.21	4	8	1
72	34.30917	0.34	-106.90367	0.35	6.41	1.10	2005	3	5	0	48	13.69	0.07	0.00	0.32	5	9	1
150	34.29133	0.96	-106.89050	0.69	2.56	6.20	2005	6	13	20	22	50.18	0.15	0.00	0.18	6	8	0
172	34.31033	1.00	-106.90783	0.79	5.00	0.00	2005	9	1	16	50	55.11	0.17	0.00	0.15	5	7	0
173	34.32517	1.08	-106.93333	0.96	10.39	1.97	2005	9	4	11	25	14.59	0.23	0.00	0.59	5	7	0

Cluster 10

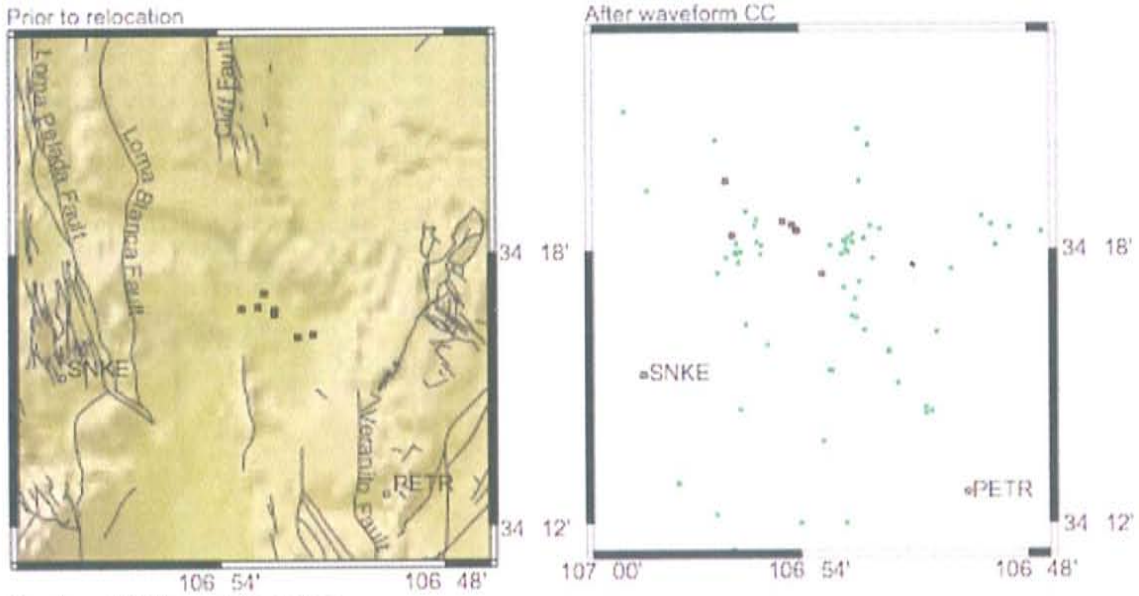

Cluster 10 Error Margins

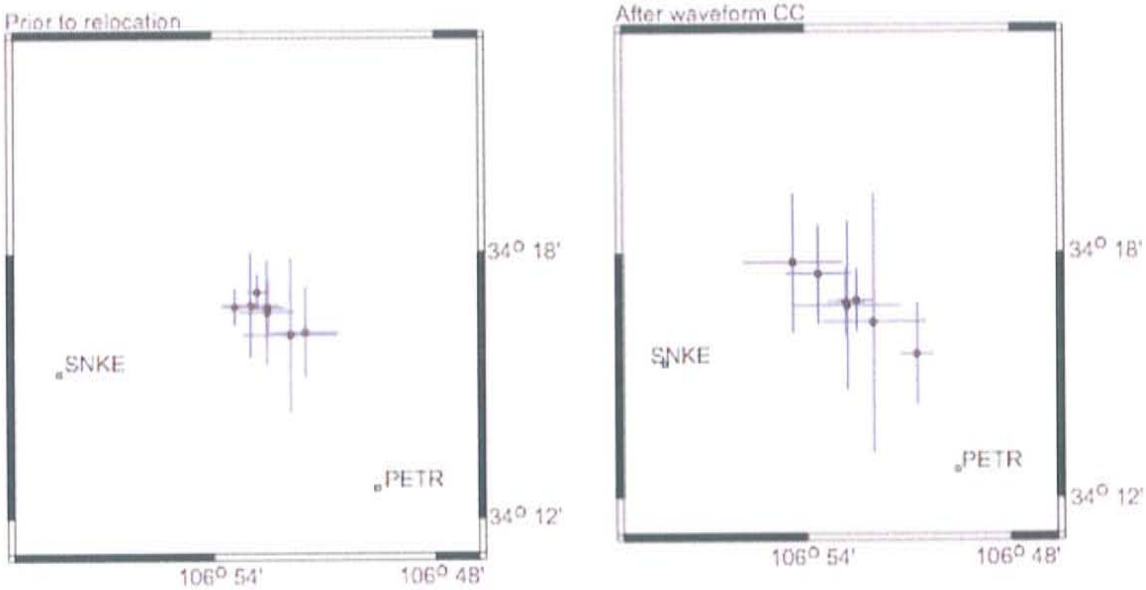

Cluster 10 prior to relocation

ind	lat	lstd	long	lstd	depth	lstd	yyyy	mm	dd	hh	mm	orig	lstd	mag	rms	stats	picks	refls
34	34.28017	1.21	-106.88283	0.78	5.00	0.00	2004	12	21	0	50	14.07	0.15	0.47	0.07	4	6	0
43	34.27950	0.43	-106.89017	0.33	7.30	0.67	2005	1	11	7	51	55.52	0.07	-0.14	0.32	5	12	2
92	34.27917	0.68	-106.87550	0.50	5.00	0.00	2005	4	23	12	24	32.48	0.10	0.68	0.23	5	8	0
177	34.27000	1.04	-106.85850	0.91	4.47	5.70	2005	9	20	18	22	32.32	0.31	0.50	0.00	4	5	0
254	34.26900	1.77	-106.86533	1.26	5.00	0.00	2006	4	18	1	8	40.10	0.16	0.54	0.27	4	5	0
255	34.27750	1.21	-106.87567	0.76	5.00	0.00	2006	4	18	1	32	0.31	0.14	0.30	0.13	4	4	0
295	34.28517	0.40	-106.88017	0.30	5.00	0.00	2006	12	31	13	3	4.16	0.05	1.05	0.07	7	8	0

Cluster 10 after waveform CC

ind	lat	lstd	long	lstd	depth	lstd	yyyy	mm	dd	hh	mm	orig	lstd	mag	rms	stats	picks	refls
34	34.29617	1.72	-106.90650	1.46	5.00	0.00	2004	12	21	0	50	13.62	0.25	0.00	0.17	4	6	0
43	34.27983	0.82	-106.88050	0.57	7.67	0.91	2005	1	11	7	51	55.44	0.12	0.00	0.32	5	10	2
92	34.29133	1.22	-106.89400	0.98	9.11	1.94	2005	4	23	12	24	31.85	0.23	0.00	0.29	5	8	0
177	34.25850	1.26	-106.84617	0.51	5.00	0.00	2005	9	20	18	22	32.26	0.17	0.00	0.16	4	5	0
254	34.27850	2.10	-106.88000	1.57	5.00	0.00	2006	4	18	1	8	40.10	0.24	0.00	0.15	4	5	0
255	34.27150	3.19	-106.86717	1.54	5.00	0.00	2006	4	18	1	32	0.44	0.30	0.00	0.15	4	4	0
295	34.28067	0.77	-106.87550	0.51	5.00	0.00	2006	12	31	13	3	4.08	0.12	0.00	0.28	7	9	0

Cluster 11

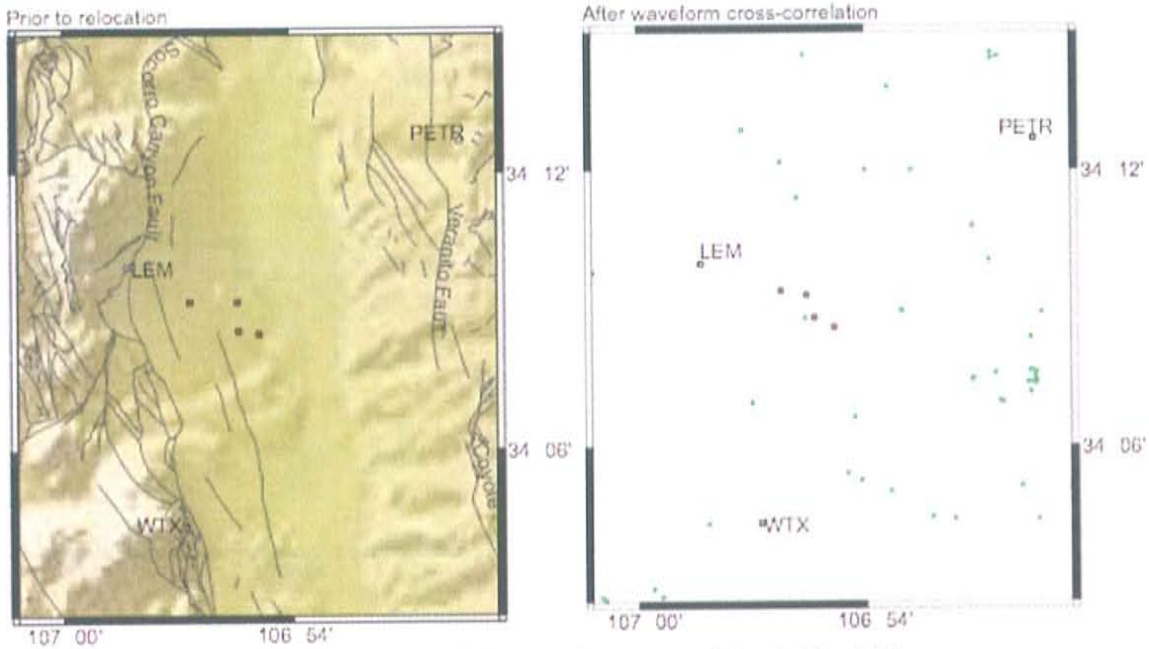
Prior to relocation
After waveform cross-correlation
Socorro Canyon Fault
Valverde Fault
Canyon
PETR
LEM
WTX
34 12'
34 06'
107 00'
106 54'

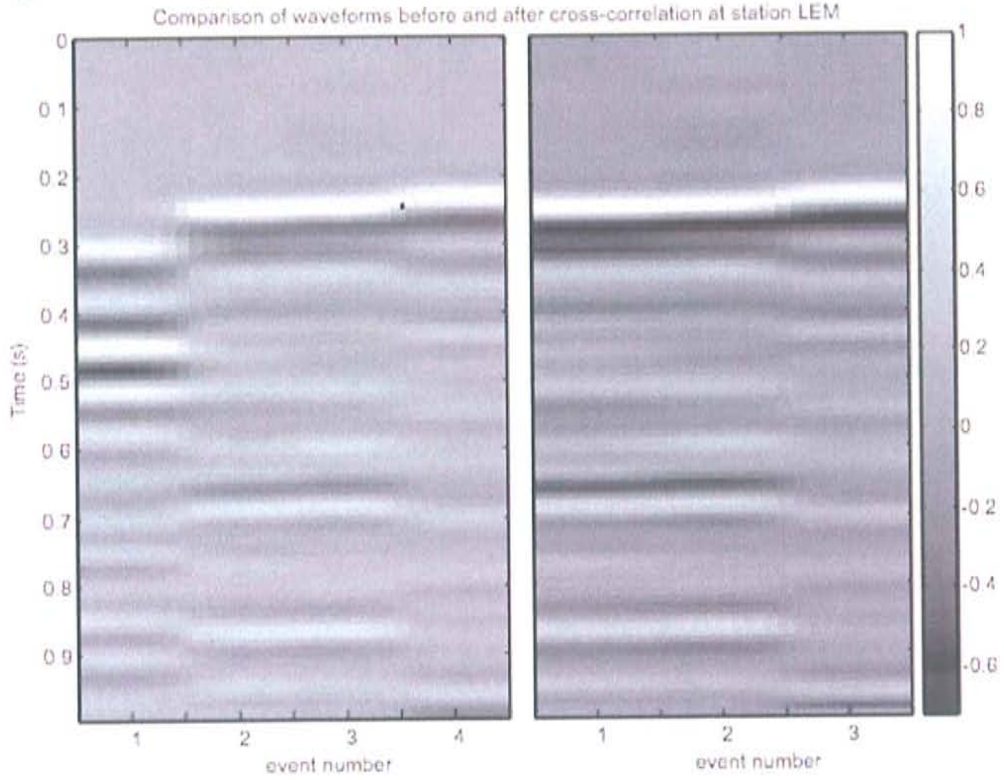
Comparison of waveforms before and after cross-correlation at station LEM
Time (s)
0
0.1
0.2
0.3
0.4
0.5
0.6
0.7
0.8
0.9
1
2
3
4
event number
1
0.8
0.6
0.4
0.2
0
-0.2
-0.4
-0.6

Cluster 11 Error Margins

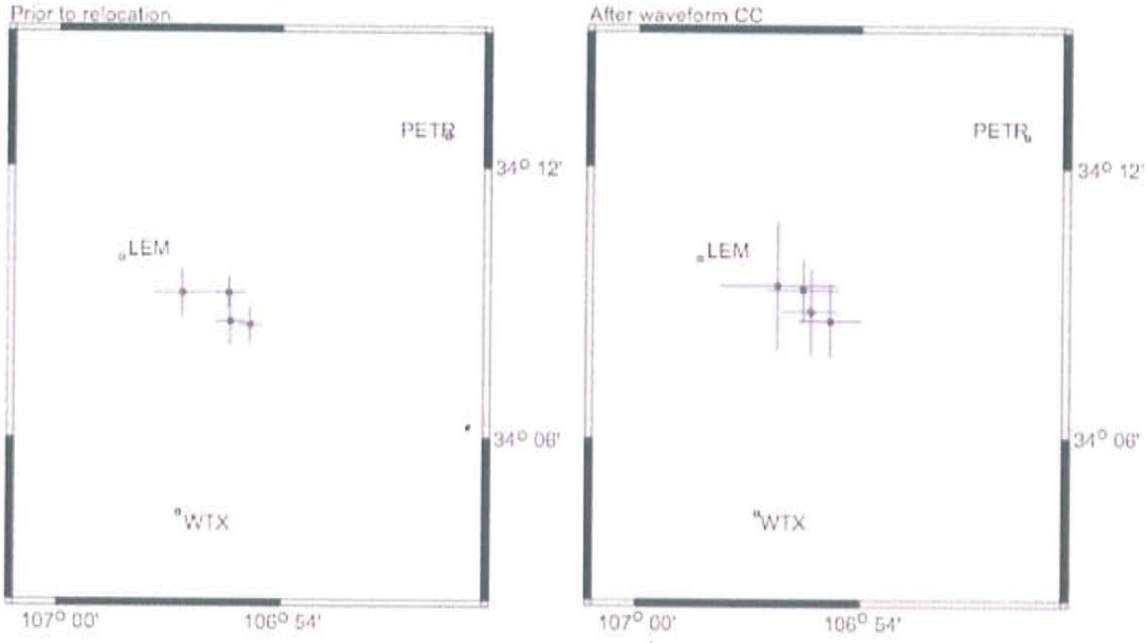

Cluster 11 prior to relocation

ind	lat	lstd	long	lstd	depth	lstd	yyyy	mm	dd	hh	mm	orig	lstd	mag	rms	stats	picks	refls
60	34.15317	0.53	-106.94450	0.78	4.30	0.59	2005	1	27	1	3	49.69	0.06	0.55	0.40	4	8	1
152	34.14167	0.40	-106.91417	0.34	4.62	1.16	2005	6	14	5	38	41.66	0.07	0.52	0.05	6	8	0
153	34.14283	0.53	-106.92317	0.41	7.12	0.50	2005	6	14	5	47	52.49	0.07	0.08	0.20	4	9	2
233	34.15333	0.35	-106.92367	0.45	4.23	1.30	2006	1	11	17	20	51.91	0.10	0.63	0.23	6	12	0

Cluster 11 after waveform CC

ind	lat	lstd	long	lstd	depth	lstd	yyyy	mm	dd	hh	mm	orig	lstd	mag	rms	stats	picks	refls
60	34.15633	1.46	-106.93717	1.57	5.54	0.92	2005	1	27	1	3	49.44	0.10	0.00	0.35	4	8	1
152	34.14317	0.85	-106.91383	0.85	4.50	2.64	2005	6	14	5	38	41.67	0.18	0.00	0.05	6	8	0
153	34.14650	0.99	-106.92233	0.81	7.27	0.70	2005	6	14	5	47	52.48	0.09	0.00	0.19	4	9	2
233	34.15467	0.73	-106.92583	0.98	3.00	3.83	2006	1	11	17	20	52.06	0.23	0.00	0.24	6	12	0

Cluster 12

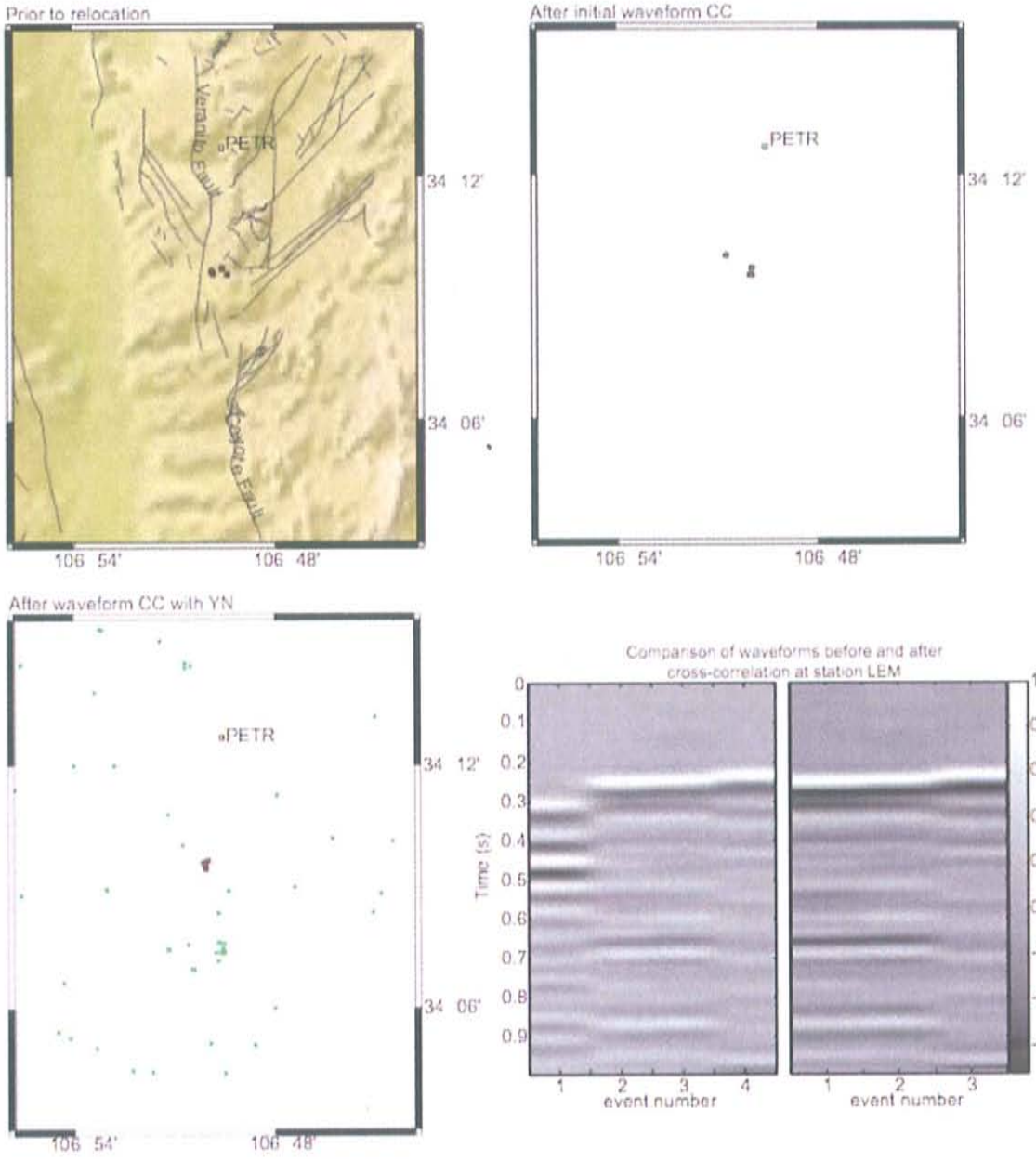
Prior to relocation
PETR
Verano Fault
Loma Fault
34 12'
34 06'
106 54'
106 48'
After initial waveform CC
PETR
34 12'
34 06'
106 54'
106 48'
After waveform CC with YN
PETR
34 12'
34 06'
106 54'
106 48'
Comparison of waveforms before and after cross-correlation at station LEM
Time (s)
0
0.1
0.2
0.3
0.4
0.5
0.6
0.7
0.8
0.9
1
2
3
4
event number
1
2
3
event number
1
0.8
0.6
0.4
0.2
0
-0.2
-0.4
-0.6

Cluster 12 Error Margins

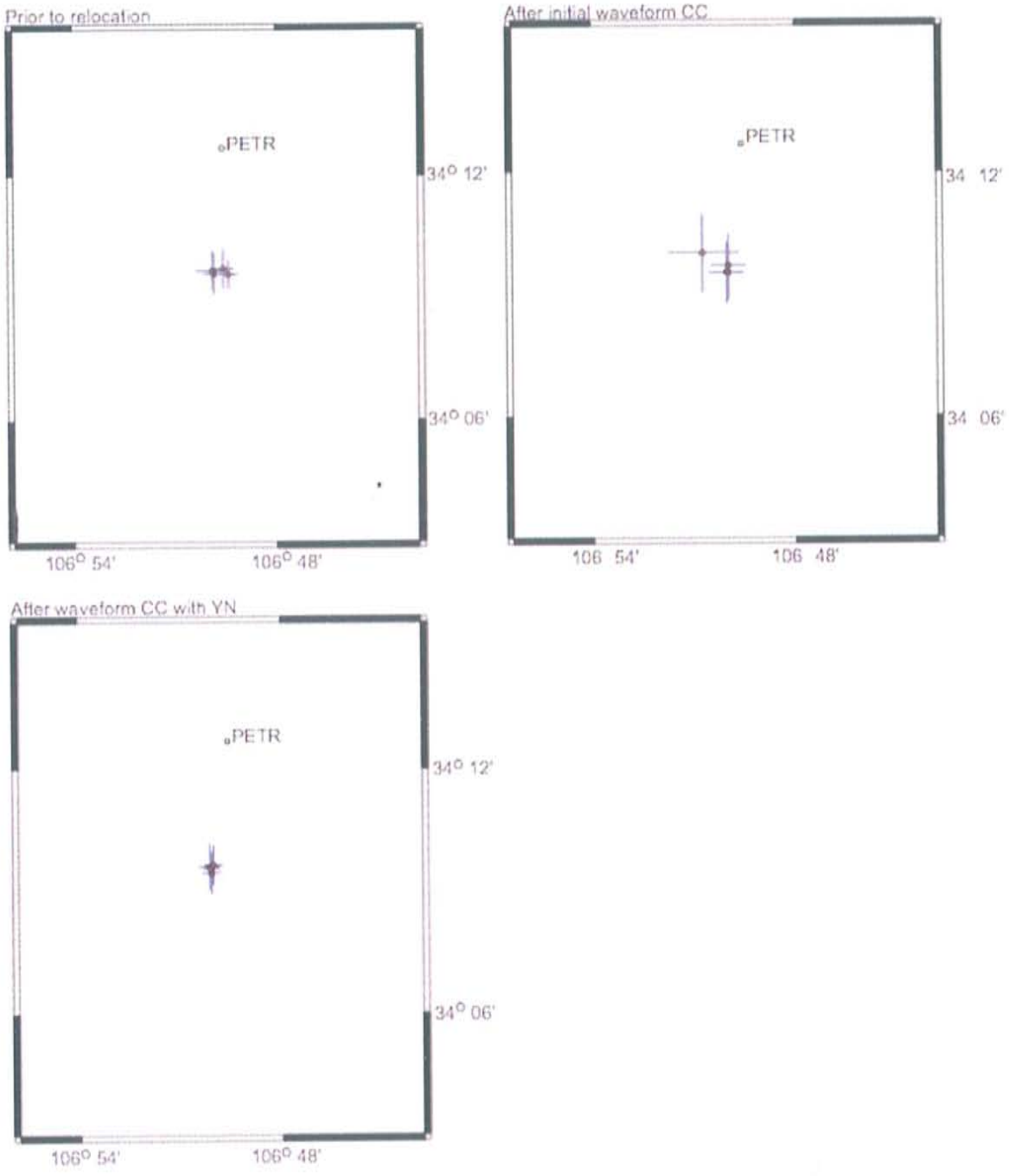

Cluster 12 prior to relocation

ind	lat	lstd	long	lstd	depth	lstd	yyyy	mm	dd	hh	mm	orig	lstd	mag	rms	stats	picks	refls
256	34.16217	0.54	-106.82617	0.32	4.88	0.88	2006	4	25	4	31	10.38	0.07	0.22	0.23	4	8	1
258	34.16000	0.54	-106.83067	0.32	8.90	0.57	2006	4	25	4	45	41.77	0.07	-0.07	0.39	5	10	2
259	34.16133	0.53	-106.83150	0.50	6.31	3.23	2006	4	25	5	9	8.52	0.19	-0.25	0.13	4	6	0
260	34.15967	0.37	-106.82350	0.27	4.29	0.87	2006	4	25	7	33	37.50	0.05	-0.12	0.14	5	11	1

Cluster 12 after waveform CC

ind	lat	lstd	long	lstd	depth	lstd	yyyy	mm	dd	hh	mm	orig	lstd	mag	rms	stats	picks	refls
256	34.15883	0.74	-106.83383	0.51	5.06	1.20	2006	4	25	4	31	10.36	0.11	0.00	0.31	4	8	1
258	34.16150	0.76	-106.83283	0.52	8.88	0.83	2006	4	25	4	45	41.77	0.10	0.00	0.39	5	10	2
259	34.16667	0.95	-106.84550	1.06	6.36	4.46	2006	4	25	5	9	8.32	0.21	0.00	0.12	4	6	0
260	34.15867	0.68	-106.83283	0.44	5.21	1.13	2006	4	25	7	33	37.50	0.10	0.00	0.23	5	11	1

Cluster 12 after waveform CC with YN

ind	lat	lstd	long	lstd	depth	lstd	yyyy	mm	dd	hh	mm	orig	lstd	mag	rms	stats	picks	refls
256	34.15750	0.51	-106.83433	0.33	6.09	1.00	2006	4	25	4	31	10.31	0.08	0.00	0.32	6	11	1
258	34.16083	0.51	-106.83333	0.33	9.14	0.72	2006	4	25	4	45	41.75	0.07	0.00	0.35	7	13	2
259	34.16000	0.58	-106.83567	0.38	9.76	1.59	2006	4	25	5	9	8.25	0.15	0.00	0.17	6	8	0
260	34.15917	0.43	-106.83450	0.29	6.19	0.93	2006	4	25	7	33	37.43	0.08	0.00	0.28	7	13	1

Cluster 13

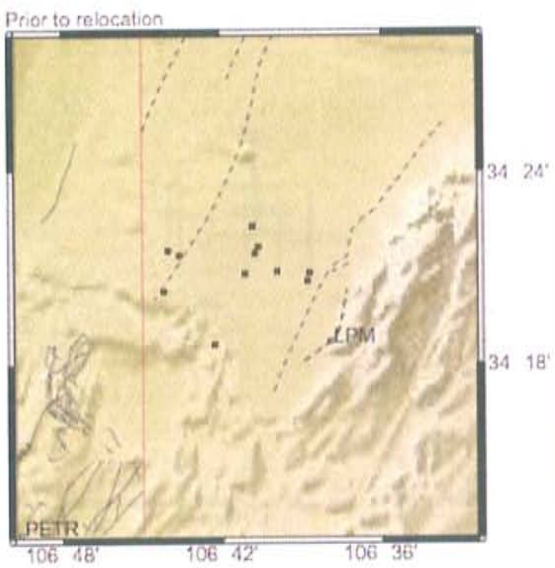
Prior to relocation
34 24'
34 18'
LPM
PETR
106 48'
106 42'
106 36'

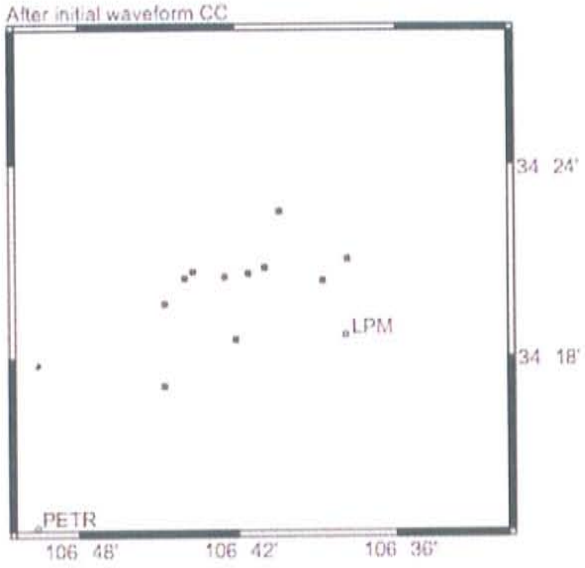
After initial waveform CC
34 24'
34 18'
LPM
PETR
106 48'
106 42'
106 36'

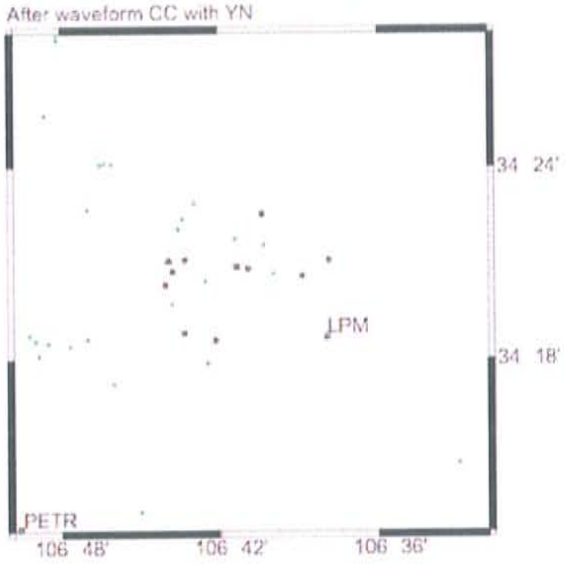
After waveform CC with YN
34 24'
34 18'
LPM
PETR
106 48'
106 42'
106 36'

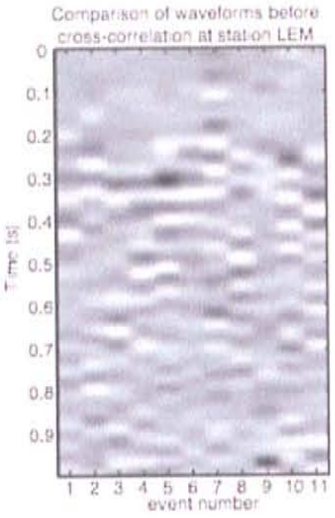
Comparison of waveforms before
cross-correlation at station LEM
0
0.1
0.2
0.3
0.4
0.5
0.6
0.7
0.8
0.9
1 2 3 4 5 6 7 8 9 10 11
event number

Cluster 13 Error Margins

Prior to relocation

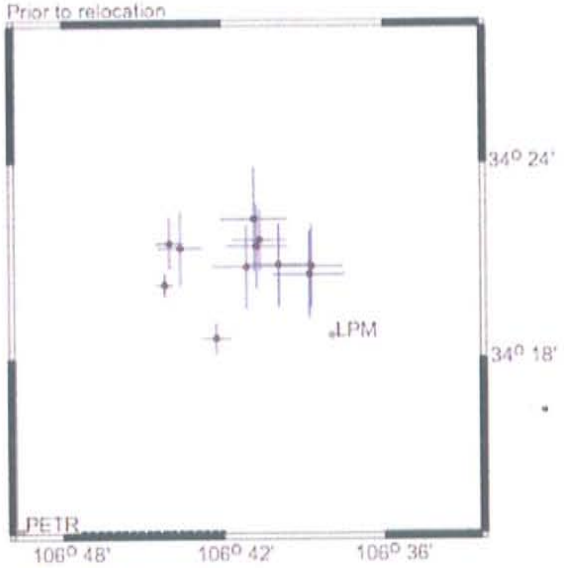

After initial waveform CC

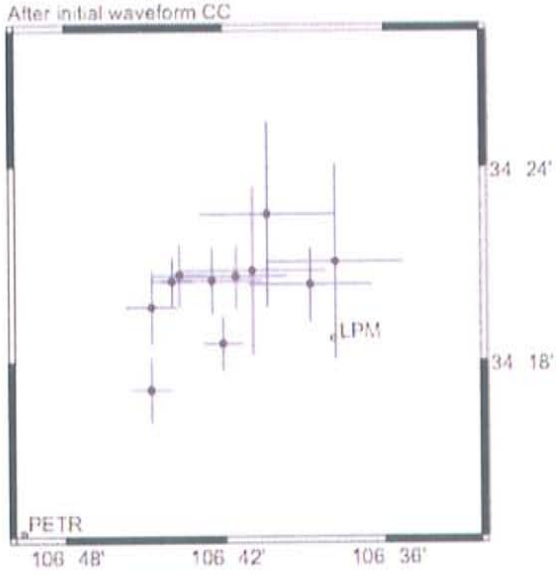

After waveform CC with YN

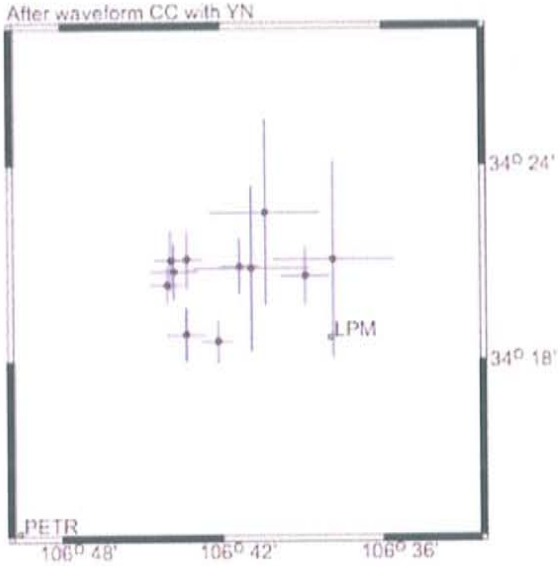

Cluster 13 prior to relocation

ind	lat	lstd	long	lstd	depth	lstd	yyyy	mm	dd	hh	mm	orig	lstd	mag	rms	stats	picks	refls
18	34.33750	0.36	-106.73617	0.33	5.00	0.00	2004	10	24	10	41	8.41	0.05	0.88	0.33	6	10	0
66	34.34667	1.29	-106.68517	1.29	14.60	2.66	2005	2	11	9	25	42.58	0.40	0.58	0.05	4	5	0
95	34.31017	0.49	-106.70433	0.56	5.06	2.23	2005	4	29	18	46	19.89	0.14	0.76	0.16	7	10	0
100	34.35883	0.82	-106.73333	0.54	3.76	3.07	2005	5	2	6	23	10.40	0.17	0.39	0.17	5	9	0
160	34.34717	1.29	-106.64483	1.19	8.65	1.82	2005	7	23	0	33	45.36	0.31	0.72	0.06	6	7	0
168	34.37133	1.62	-106.68067	1.26	11.20	3.13	2005	8	25	5	21	45.04	0.47	0.16	0.05	4	5	0
169	34.34783	1.28	-106.66533	1.24	9.39	2.06	2005	8	27	21	2	48.41	0.31	0.06	0.03	4	5	0
264	34.35617	1.17	-106.72667	0.84	5.01	3.08	2006	6	23	20	58	39.64	0.24	0.58	0.21	4	6	0
266	34.35733	1.31	-106.67900	1.17	9.50	2.22	2006	6	25	14	30	19.82	0.31	0.25	0.01	4	5	0
268	34.34300	1.34	-106.64617	1.36	8.05	1.87	2006	6	27	23	35	5.38	0.32	0.66	0.05	4	5	0
269	34.36067	0.95	-106.67717	1.01	10.58	1.53	2006	6	28	17	41	37.66	0.25	0.59	0.12	4	7	0

Cluster 13 after waveform CC

ind	lat	lstd	long	lstd	depth	lstd	yyyy	mm	dd	hh	mm	orig	lstd	mag	rms	stats	picks	refls
18	34.34117	0.76	-106.73317	0.77	5.00	0.00	2004	10	24	10	41	8.36	0.12	0.00	0.33	6	10	0
66	34.34667	2.59	-106.68267	2.76	15.00	4.98	2005	2	11	9	25	42.53	0.73	0.00	0.03	4	5	0
95	34.30917	0.84	-106.70100	0.75	5.00	0.00	2005	4	29	18	46	19.95	0.15	0.00	0.16	7	10	0
100	34.34450	0.98	-106.72817	1.02	2.86	5.92	2005	5	2	6	23	10.64	0.20	0.00	0.22	5	9	0
160	34.35117	3.02	-106.63083	2.57	10.82	4.64	2005	7	23	0	33	45.05	0.78	0.00	0.08	6	7	0
168	34.37583	2.88	-106.67350	2.54	13.71	5.06	2005	8	25	5	21	44.71	0.75	0.00	0.01	4	5	0
169	34.28517	1.04	-106.74600	0.77	5.00	0.00	2005	8	27	21	2	50.02	0.17	0.00	0.90	4	5	0
264	34.34167	1.03	-106.70783	1.92	3.88	5.28	2006	6	23	20	58	40.07	0.23	0.00	0.35	4	6	0
266	34.32783	1.15	-106.74583	0.96	5.00	0.00	2006	6	25	14	30	20.55	0.19	0.00	0.37	4	5	0
268	34.33967	1.14	-106.64617	2.33	8.99	2.23	2006	6	27	23	35	5.31	0.24	0.00	0.03	4	5	0
269	34.34367	1.00	-106.69300	1.97	8.68	2.47	2006	6	28	17	41	38.09	0.22	0.00	0.17	4	7	0

Cluster 13 after waveform CC with YN

ind	lat	lstd	long	lstd	depth	lstd	yyyy	mm	dd	hh	mm	orig	lstd	mag	rms	stats	picks	refls
18	34.33867	0.59	-106.73400	0.63	5.00	0.00	2004	10	24	10	41	8.40	0.09	0.00	0.33	6	10	0
66	34.34717	2.53	-106.68167	2.17	15.16	4.51	2005	2	11	9	25	42.50	0.71	0.00	0.03	4	5	0
95	34.31000	0.65	-106.70250	0.59	5.00	0.00	2005	4	29	18	46	19.92	0.11	0.00	0.15	7	10	0
100	34.34567	0.86	-106.72967	0.89	1.85	8.58	2005	5	2	6	23	10.63	0.20	0.00	0.22	5	9	0
160	34.35167	3.01	-106.63067	2.29	10.62	4.11	2005	7	23	0	33	45.06	0.77	0.00	0.07	6	7	0
168	34.37583	2.85	-106.67300	2.06	13.64	4.51	2005	8	25	5	21	44.72	0.74	0.00	0.01	4	5	0
169	34.31367	0.83	-106.72217	0.76	5.00	0.00	2005	8	27	21	2	49.59	0.14	0.00	0.65	4	5	0
264	34.35183	0.90	-106.72183	0.58	5.00	0.00	2006	6	23	20	58	39.72	0.15	0.00	0.23	6	8	0
266	34.35117	0.95	-106.73183	0.64	4.52	3.48	2006	6	25	14	30	20.20	0.20	0.00	0.30	6	7	0
268	34.34350	0.90	-106.64783	0.92	9.04	1.54	2006	6	27	23	35	5.25	0.20	0.00	0.12	6	8	0
269	34.34817	0.86	-106.68900	0.75	9.04	1.51	2006	6	28	17	41	38.00	0.19	0.00	0.16	6	10	0

Cluster 14

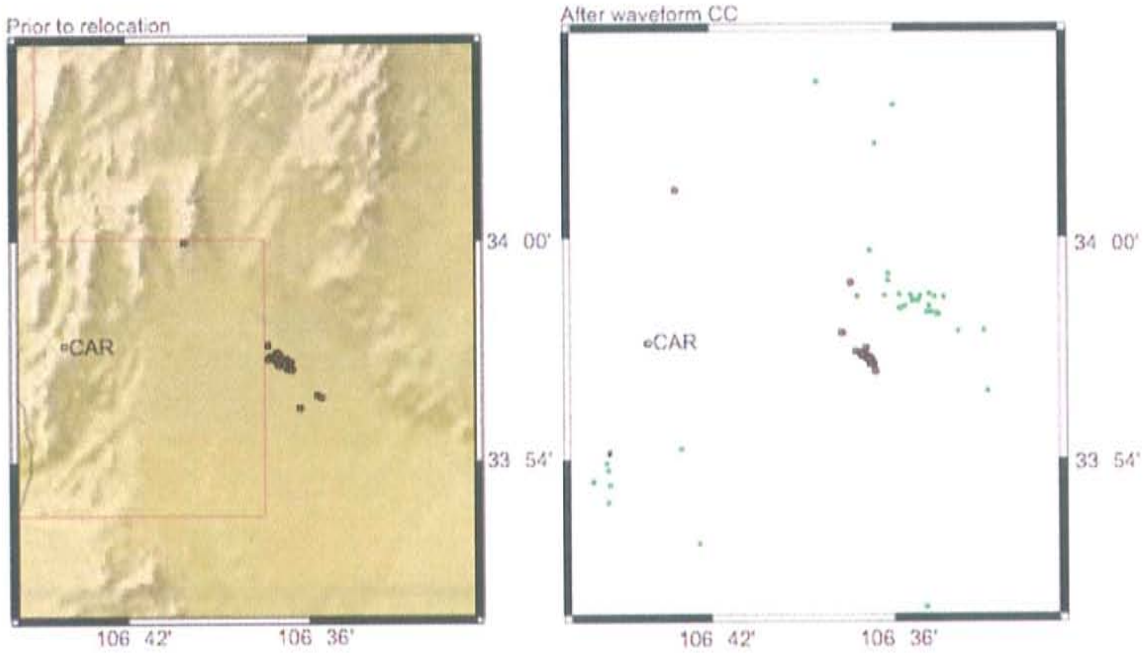
Prior to relocation
After waveform CC
CAR
CAR
34 00'
33 54'
34 00'
33 54'
106 42'
106 36'
106 42'
106 36'

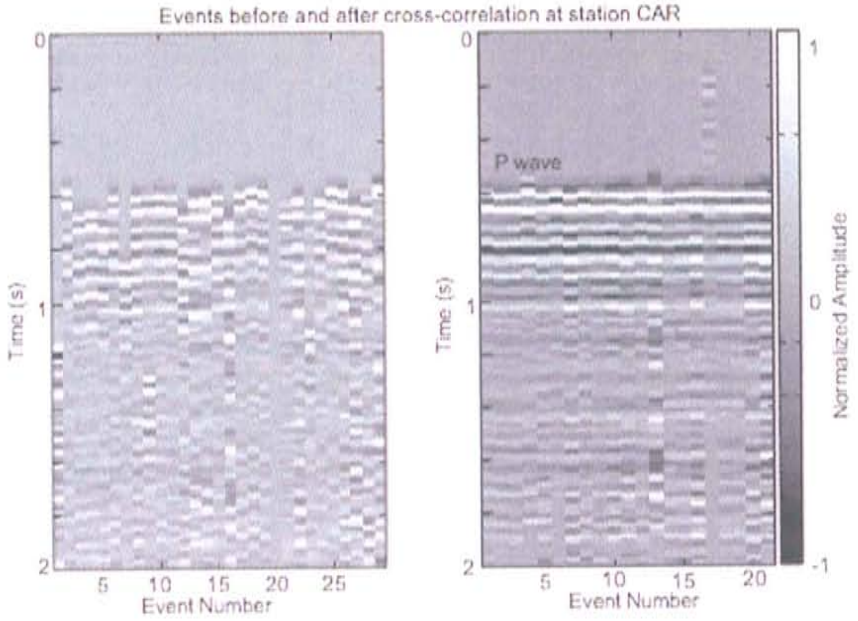
Events before and after cross-correlation at station CAR
P wave
Time (s)
Event Number
Normalized Amplitude

Cluster 14 Error Margins

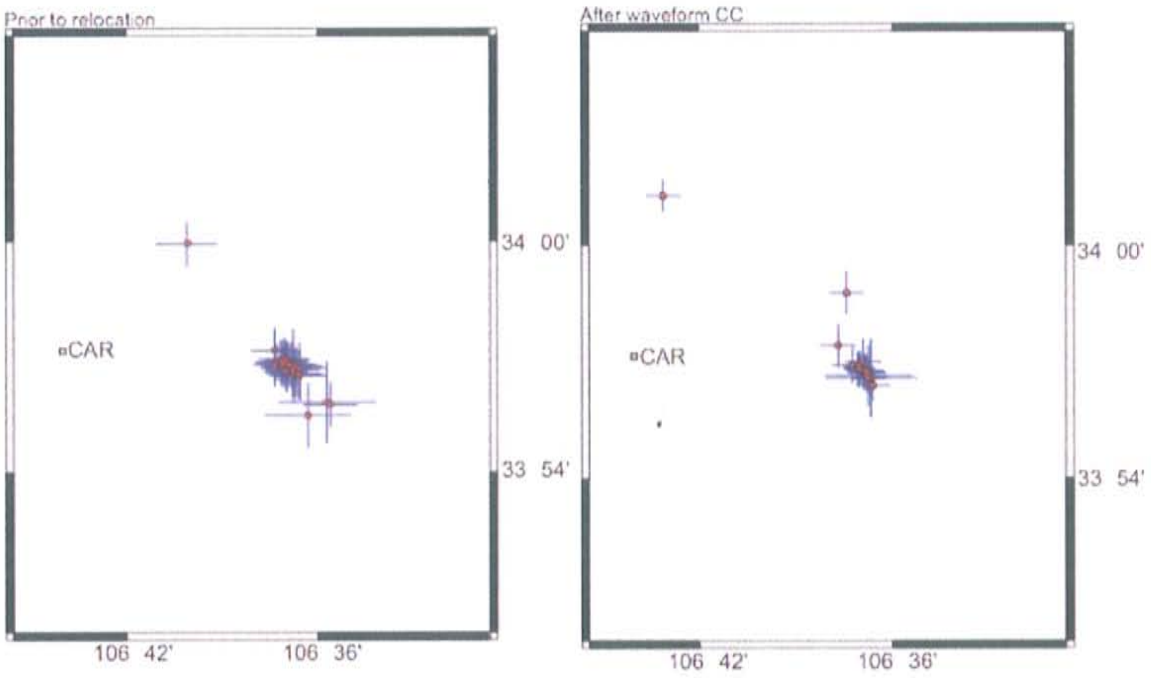

Cluster 14 prior to relocation

ind	lat	lstd	long	lstd	depth	lstd	yyyy	mm	dd	hh	mm	orig	lstd	mag	rms	stats	picks	refls
119	33.94633	0.64	-106.61367	0.87	5.85	2.31	2005	6	4	2	15	0.24	0.16	0.50	0.01	4	6	0
120	33.94550	0.52	-106.61783	0.69	5.03	2.23	2005	6	4	13	13	58.10	0.14	0.65	0.04	5	8	0
121	33.94533	0.52	-106.61650	0.70	5.20	2.20	2005	6	4	21	5	11.27	0.14	0.64	0.04	5	8	0
122	33.94217	0.60	-106.61100	0.84	4.21	2.76	2005	6	4	21	7	6.75	0.15	0.51	0.02	5	7	0
123	33.94500	0.63	-106.61617	0.84	5.97	2.24	2005	6	4	21	26	30.81	0.16	0.69	0.10	4	7	0
124	33.94233	0.64	-106.61217	0.85	5.10	2.63	2005	6	4	22	53	16.30	0.16	0.63	0.11	4	7	0
125	33.94733	0.52	-106.61600	0.70	6.21	1.94	2005	6	4	23	7	3.11	0.14	0.66	0.05	5	8	0
126	33.94483	0.70	-106.60983	0.88	5.26	2.66	2005	6	5	1	32	28.50	0.16	0.47	0.05	4	5	0
127	33.94617	0.96	-106.61283	0.94	5.10	2.57	2005	6	5	2	0	33.73	0.24	0.74	0.01	4	6	0
128	33.94583	0.52	-106.61167	0.71	5.70	2.13	2005	6	5	3	8	30.23	0.14	0.65	0.05	5	8	0
129	33.94367	0.52	-106.61650	0.70	4.56	2.44	2005	6	5	4	6	23.60	0.14	0.85	0.05	5	8	0
130	33.94600	0.52	-106.61483	0.70	6.83	1.84	2005	6	5	4	38	39.17	0.14	1.01	0.06	5	8	0
131	33.94917	0.57	-106.61767	0.80	6.29	1.89	2005	6	5	7	0	28.70	0.15	0.99	0.03	5	8	0
132	33.94683	0.56	-106.61900	0.70	6.52	1.93	2005	6	5	8	8	24.39	0.14	0.79	0.02	5	7	0
133	33.94767	0.49	-106.62100	0.61	5.36	1.92	2005	6	5	10	19	28.64	0.13	1.38	0.11	6	11	0
134	33.94183	0.64	-106.60950	0.86	5.15	2.67	2005	6	5	10	42	9.97	0.16	0.75	0.05	4	7	0
135	33.94417	0.68	-106.61300	0.85	5.32	2.57	2005	6	5	11	11	14.29	0.16	0.50	0.03	4	6	0
137	33.94783	0.57	-106.61917	0.80	6.89	1.77	2005	6	5	13	26	14.13	0.16	0.73	0.02	5	8	0
138	33.95283	0.61	-106.62250	0.75	10.65	1.06	2005	6	5	13	29	54.37	0.15	0.43	0.50	5	9	0
139	33.93017	1.08	-106.59533	1.53	4.40	3.74	2005	6	5	15	26	44.79	0.23	0.70	0.00	4	4	0
140	33.94667	0.59	-106.61483	0.83	5.63	2.10	2005	6	5	15	51	27.74	0.15	0.98	0.05	5	7	0
141	33.92450	0.86	-106.60500	1.36	5.00	0.00	2005	6	5	17	28	14.17	0.21	0.63	0.17	4	5	0
142	33.92917	0.60	-106.59333	0.86	5.00	0.00	2005	6	5	21	14	11.89	0.15	0.73	0.40	5	8	0
143	33.94200	0.64	-106.60950	0.86	5.67	2.47	2005	6	5	22	16	20.05	0.16	0.34	0.03	4	7	0
144	33.94867	0.52	-106.61650	0.70	6.95	1.79	2005	6	6	0	27	58.92	0.14	0.57	0.09	5	8	0
145	33.94650	0.57	-106.62250	0.69	5.43	1.91	2005	6	6	0	48	17.81	0.14	0.82	0.09	6	9	0
147	33.94700	0.62	-106.61800	0.88	6.00	2.13	2005	6	8	9	23	23.71	0.16	0.42	0.03	4	5	0
165	33.99950	0.61	-106.66817	0.97	6.47	1.55	2005	8	14	13	49	15.36	0.15	0.46	0.20	5	7	0

Cluster 14 after waveform CC

ind	lat	lstd	long	lstd	depth	lstd	yyyy	mm	dd	hh	mm	orig	lstd	mag	rms	stats	picks	refls
119	33.94517	0.47	-106.61417	0.55	6.16	2.16	2005	6	4	2	15	0.20	0.14	0.00	0.01	4	6	0
120	33.94750	0.40	-106.61750	0.45	6.62	1.73	2005	6	4	13	13	58.06	0.12	0.00	0.04	5	8	0
121	33.94700	0.40	-106.61667	0.45	6.73	1.72	2005	6	4	21	5	11.22	0.12	0.00	0.04	5	8	0
122	33.94600	0.46	-106.61467	0.55	6.41	1.83	2005	6	4	21	7	6.78	0.13	0.00	0.02	5	7	0
123	33.94533	0.43	-106.61300	0.54	5.84	2.23	2005	6	4	21	26	30.83	0.14	0.00	0.02	4	7	0
124	33.94500	0.43	-106.61250	0.55	6.33	2.11	2005	6	4	22	53	16.28	0.14	0.00	0.02	4	7	0
125	33.94683	0.40	-106.61733	0.45	6.49	1.76	2005	6	4	23	7	3.12	0.12	0.00	0.03	5	8	0
126	33.97967	0.55	-106.62367	0.56	10.93	1.89	2005	6	5	1	32	28.77	0.20	0.00	0.05	4	5	0
127	33.95000	0.59	-106.61517	0.58	5.00	0.00	2005	6	5	2	0	33.96	0.13	0.00	0.33	4	6	0
128	33.94667	0.40	-106.61700	0.45	6.60	1.74	2005	6	5	3	8	30.25	0.12	0.00	0.04	5	8	0
129	33.94717	0.40	-106.61650	0.45	6.67	1.73	2005	6	5	4	6	23.55	0.12	0.00	0.04	5	8	0
130	33.94750	0.40	-106.61733	0.45	6.53	1.75	2005	6	5	4	38	39.28	0.12	0.00	0.04	5	8	0
131	33.94517	0.41	-106.61300	0.54	6.12	1.88	2005	6	5	7	0	28.67	0.13	0.00	0.02	5	8	0
132	33.94667	0.47	-106.61700	0.50	6.46	1.94	2005	6	5	8	8	24.38	0.12	0.00	0.04	5	7	0
133	33.94783	0.34	-106.61733	0.44	6.77	1.65	2005	6	5	10	19	28.60	0.12	0.00	0.10	6	11	0
134	33.94600	0.43	-106.61350	0.54	5.91	2.20	2005	6	5	10	42	10.00	0.14	0.00	0.02	4	7	0
135	33.94567	0.47	-106.61317	0.56	5.91	2.36	2005	6	5	11	11	14.24	0.14	0.00	0.02	4	6	0
137	33.94517	0.41	-106.61233	0.54	6.10	1.89	2005	6	5	13	26	14.10	0.13	0.00	0.02	5	8	0
138	33.95700	0.56	-106.62817	0.57	14.34	1.29	2005	6	5	13	29	54.35	0.15	0.00	0.76	5	7	0
139	33.94300	1.01	-106.61083	1.43	5.97	2.42	2005	6	5	15	26	45.01	0.22	0.00	0.00	4	4	0
140	33.94333	0.42	-106.61150	0.55	5.00	0.00	2005	6	5	15	51	27.84	0.11	0.00	0.28	5	7	0
141	33.94400	0.80	-106.61233	1.37	5.85	2.34	2005	6	5	17	28	14.57	0.20	0.00	0.01	4	5	0
142	33.93967	0.39	-106.61000	0.55	5.00	0.00	2005	6	5	21	14	12.19	0.11	0.00	0.62	5	8	0
143	33.94533	0.43	-106.61283	0.54	5.76	2.26	2005	6	5	22	16	20.10	0.14	0.00	0.02	4	7	0
144	33.94683	0.40	-106.61667	0.45	6.43	1.78	2005	6	6	0	27	58.97	0.12	0.00	0.04	5	8	0
145	33.94283	0.42	-106.61233	0.54	5.00	0.00	2005	6	6	0	48	17.83	0.10	0.00	0.31	6	9	0
147	33.94867	0.48	-106.62067	0.62	6.89	1.91	2005	6	8	9	23	23.70	0.14	0.00	0.01	4	5	0
165	34.02167	0.42	-106.71900	0.55	5.00	0.00	2005	8	14	13	49	15.59	0.05	0.00	0.13	5	7	0

Appendix C: Focal Mechanism Solutions

Focal mechanisms are determined with the program focmec allowing for one error in pick polarity. Where more than one acceptable solution is possible, alternative interpretations are provided. Where no acceptable solutions have been found, stereonets are plotted without solutions.

ind = index	lat = latitude	1std = 1st standard deviation	dep = depth	yyyy = year
m = month	d = day	h = hour	mi = minute	orig = origin time
mag = magnitude	rms = root mean square error	sta = initial stations	pic = initial picks	ref = reflections

For each event, dip, strike, and rake are provided for a possible focal mechanism solution.

ind	lat	long	dep	yyyy	m	d	h	m	orig	mag	sta	pic	dip	strike	rake
5	34.51417	-107.15633	5	2004	9	21	5	15	51.39	1.73	9	12	85.00	5.00	85.00
29	34.464	-107.05667	2.96	2004	12	4	22	4	53.28	1.26	9	12	56.40	179.68	54.99
82	34.06883	-107.0015	4.41	2005	4	2	16	53	14.83	0.60	9	18	31.92	319.53	-85.51
85	34.07333	-107.004	6.07	2005	4	2	22	48	5.98	1.36	10	11	85.00	185.00	90.00
116	34.3135	-106.96933	12.99	2005	6	2	9	33	59.49	0.93	8	9	35.48	177.73	67.00
181	34.433	-106.77667	5	2005	10	7	18	37	33.6	1	9	13			
184	34.12867	-106.8435	4.13	2005	10	16	17	40	46.49	0.91	9	14	75.00	180.00	90.00
185	34.02067	-106.87467	5	2005	10	17	7	47	53.37	0.73	9	14			
200	34.0565	-106.95533	7.07	2005	10	30	2	57	35.18	2.33	10	10	85.00	350.00	-85.00
225	34.07	-106.96117	6.55	2005	11	8	18	20	52.53	1.47	10	14	53.07	231.66	-71.07
227	34.44933	-107.14067	5	2005	12	22	11	55	42.82	0.75	9	9	56.64	118.07	10.41
229	34.03183	-107.00183	4.17	2006	1	2	2	1	57.51	0.64	9	18	75.22	79.23	-49.55
243	34.17917	-106.87717	3.04	2006	3	29	4	23	0.32	0.88	10	12	42.37	251.52	-86.79
246	34.1855	-106.88233	5.16	2006	3	29	10	56	14.76	0.89	10	16	35.63	218.43	-43.66
250	34.25117	-106.8755	5	2006	4	3	3	9	29.41	0.95	10	14	58.08	180.41	6.75
252	34.4085	-107.00367	5	2006	4	4	8	13	35.25	0.53	9	12	82.85	63.39	79.41
267	33.97683	-106.92883	5	2006	6	25	18	0	24.41	0.72	9	15	56.28	25.69	-42.75
271	33.96033	-106.9985	6.76	2006	7	10	21	50	42.39	0.66	9	13	75.00	315.00	90.00
294	34.328	-106.83933	5	2006	12	31	2	44	31.18	0.91	8	14	35.89	250.92	19.27
302	34.03633	-107.0435	8.45	2007	1	30	12	16	15.13	0.58	10	16	45.86	227.17	-81.68
304	34.03683	-107.049	8.51	2007	1	30	12	19	50.16	0.33	9	13	45.24	222.20	-81.42
312	34.3725	-106.8065	5	2007	2	27	13	18	29.29	0.72	10	12	35.02	137.11	-88.27
315	34.33917	-106.91667	1.88	2007	3	8	11	58	57.42	0.95	9	11	49.64	266.71	-

															69.23
330	34.06017	-107.02983	5.65	2007	5	22	17	25	49.67	1.22	10	13	31.78	194.71	-86.38
333	34.0605	-107.02983	5.51	2007	5	23	3	20	51.47	1.28	10	11			
337	34.06033	-107.0295	5.82	2007	5	23	5	16	54.91	2.91	10	10			
344	34.06067	-107.02567	6.75	2007	5	24	17	15	55.26	0.65	10	20	79.82	109.00	29.55

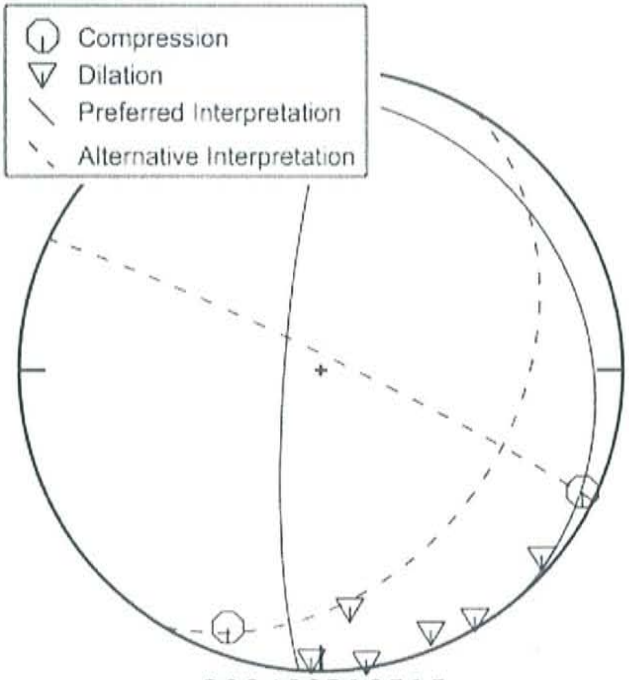

200409210515

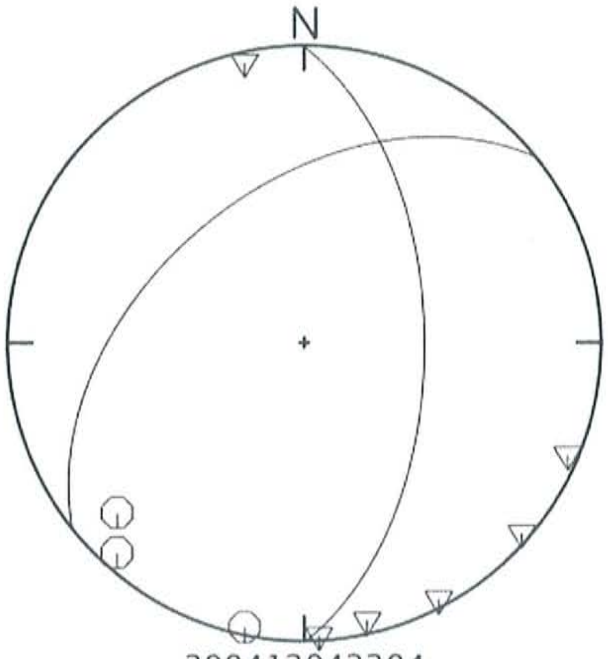

200412042204

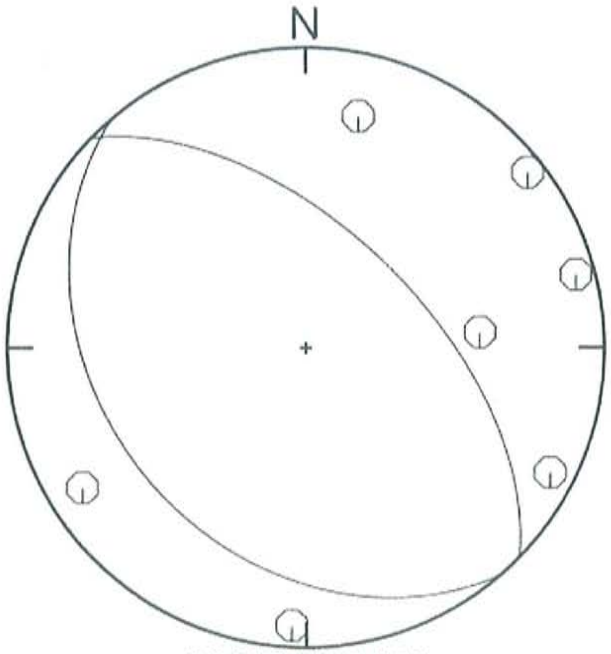

200504021653

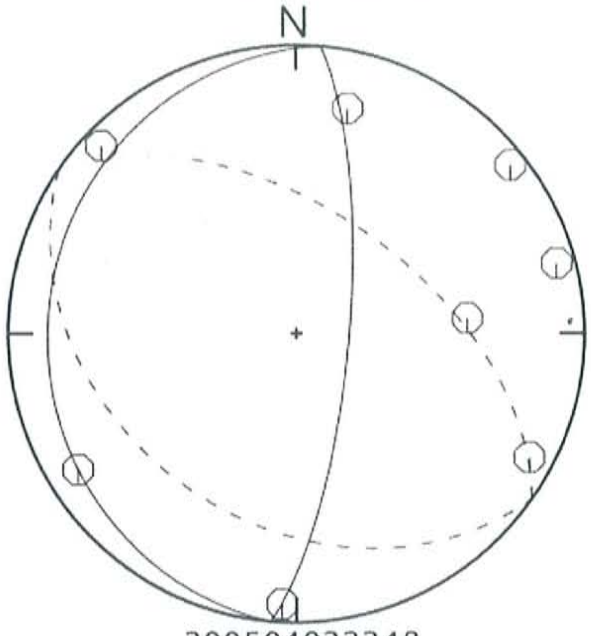

200504022248

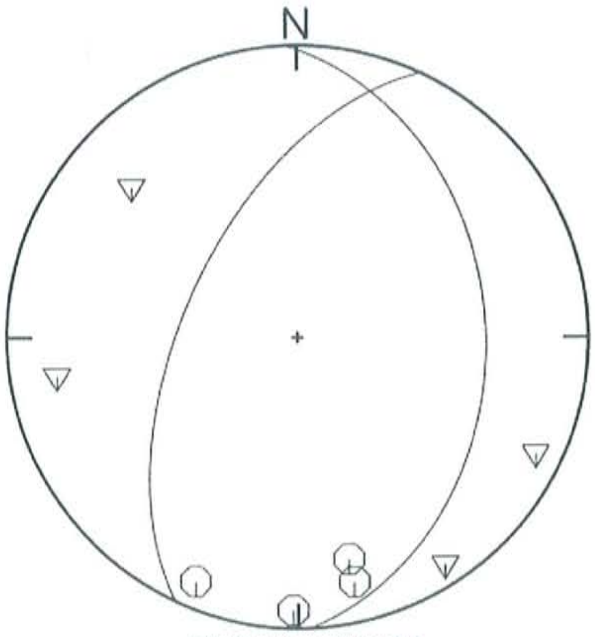

200506020933

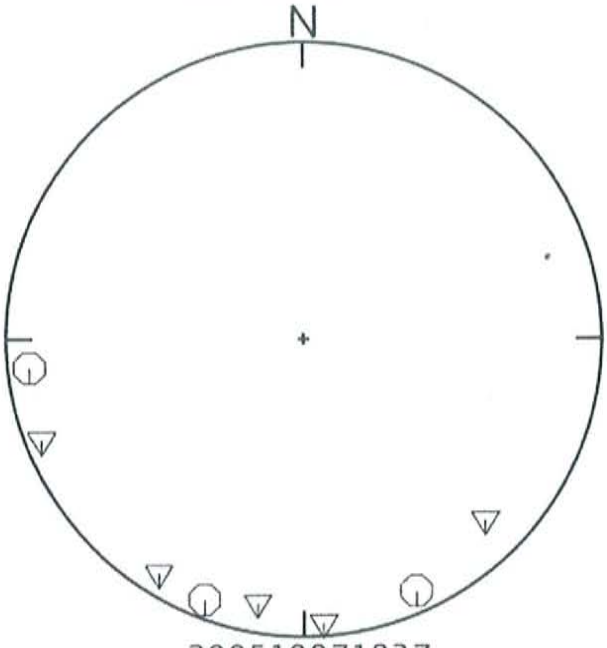

200510071837

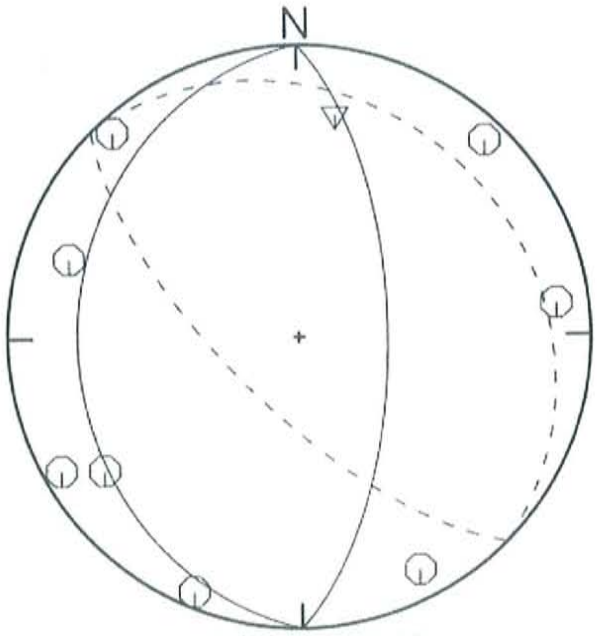

200510161740

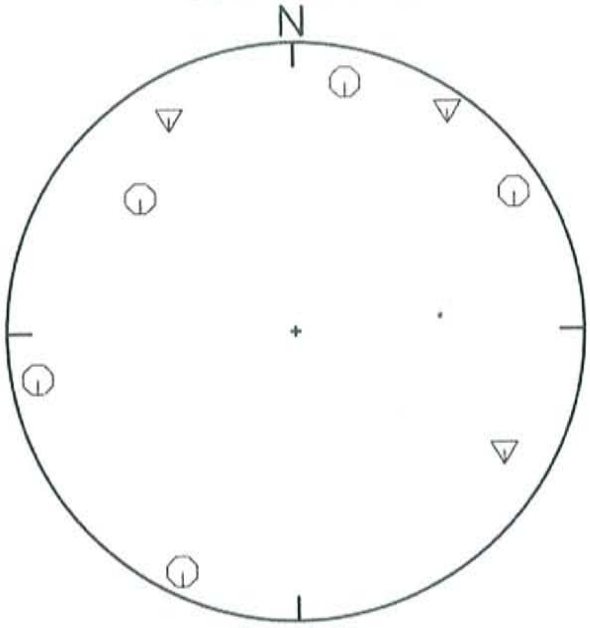

200510170747

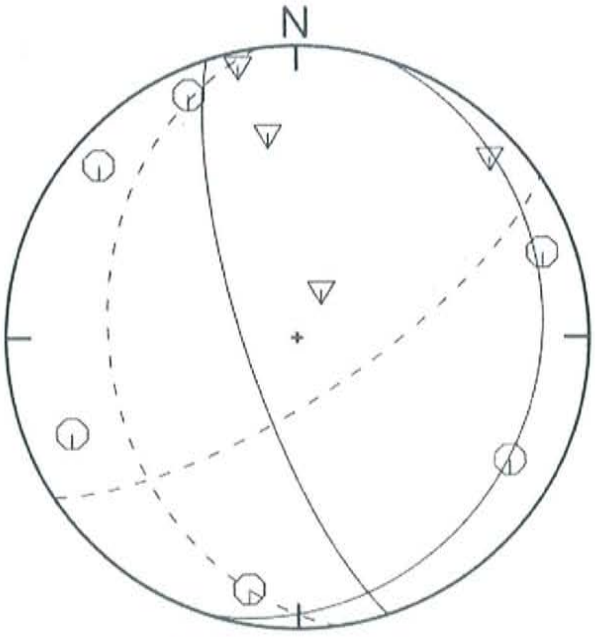

200510300257

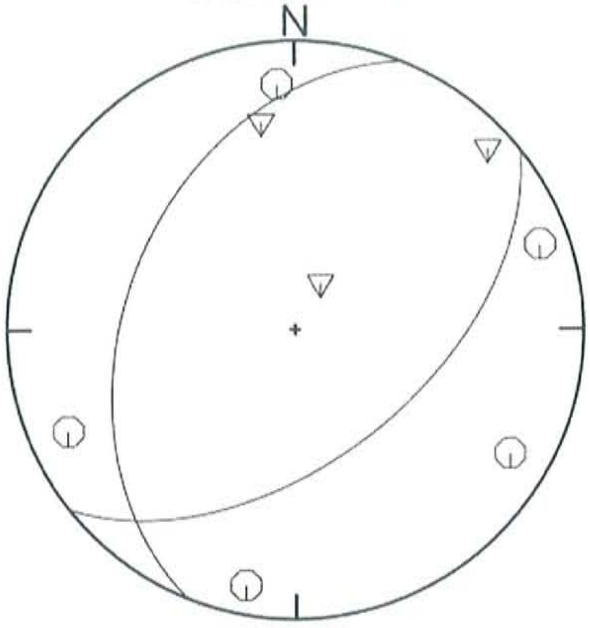

200511081820

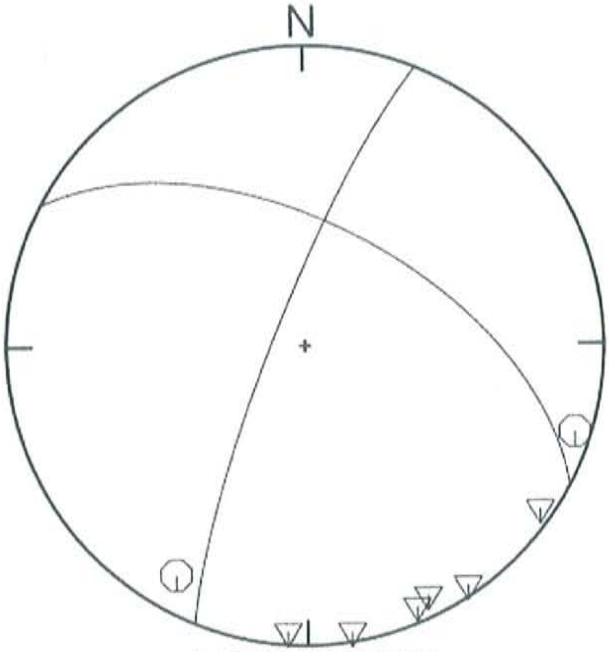

200512221155

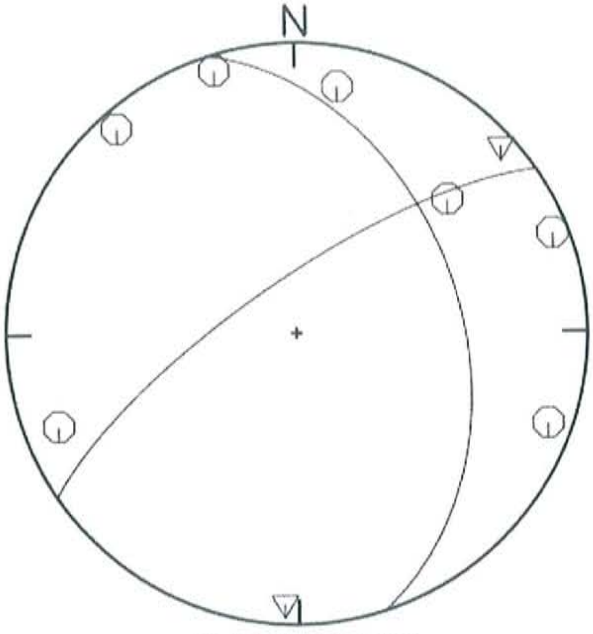

200601020201

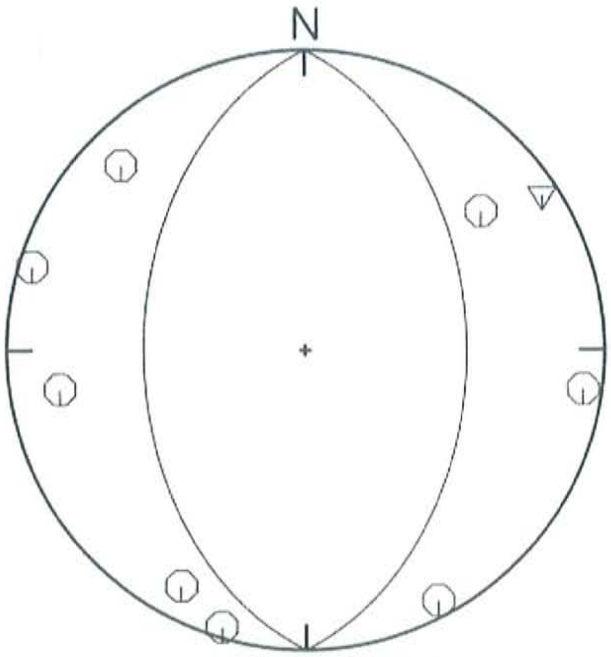

200603290423

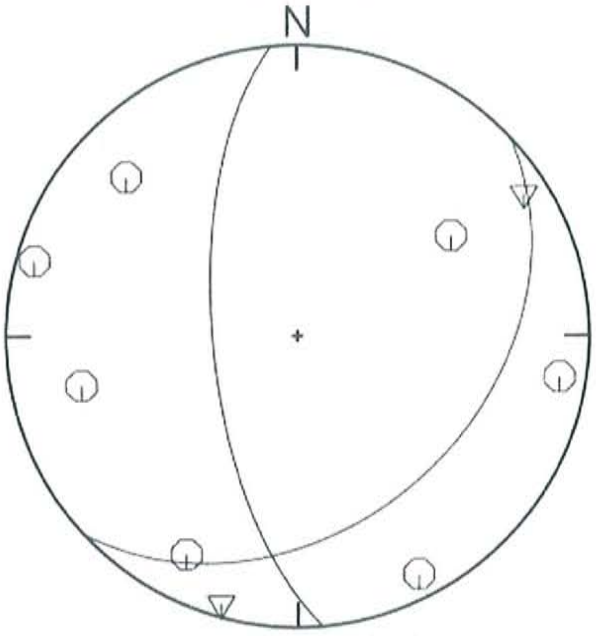

200603291056

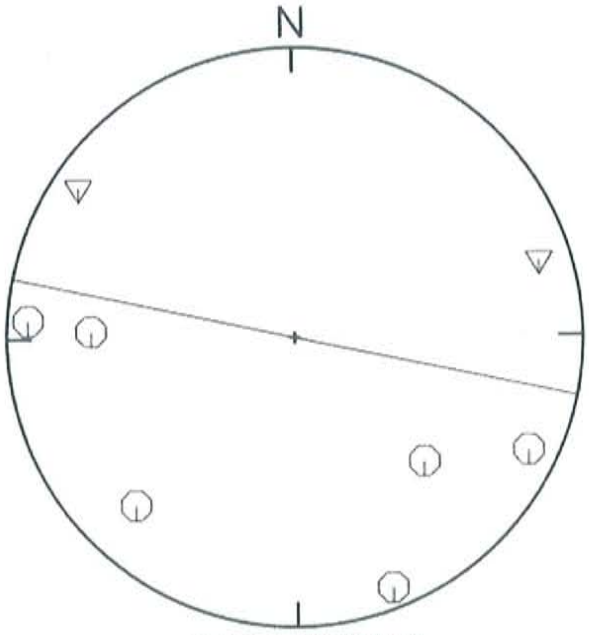

200604030309

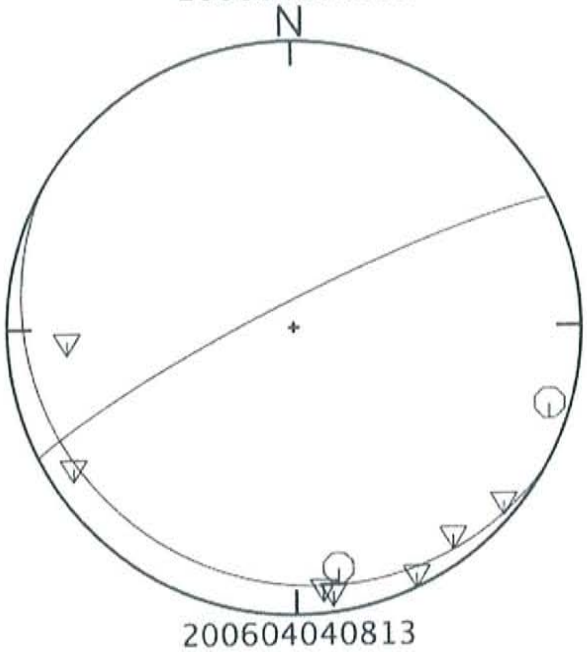

200604040813

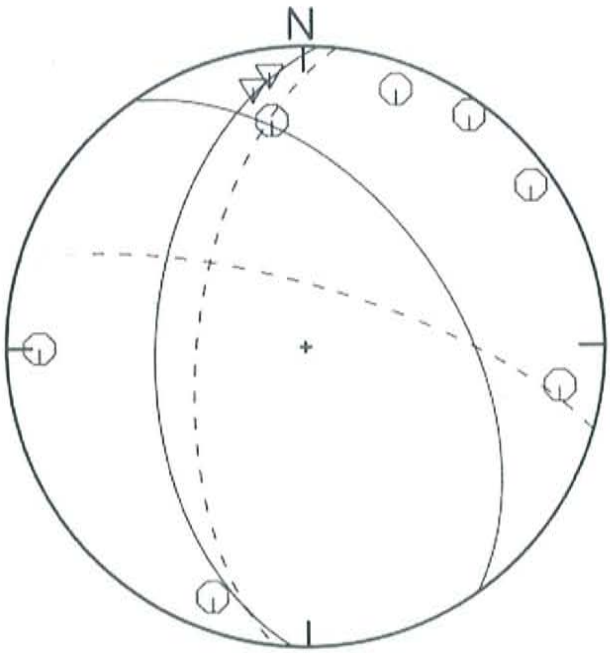

200606251800

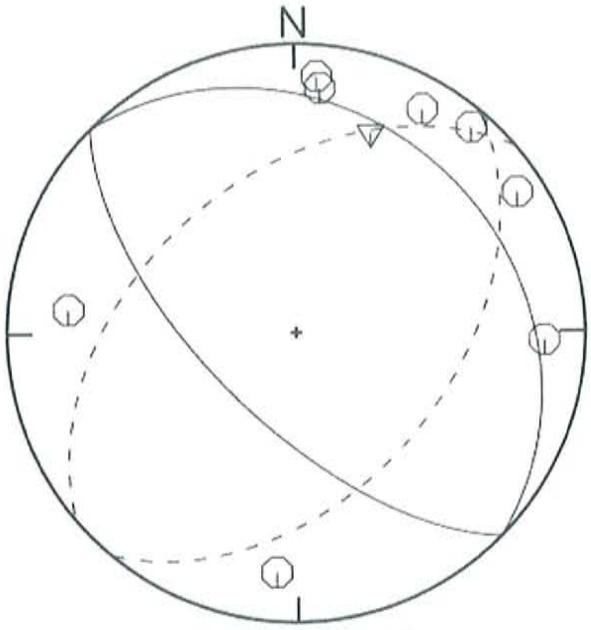

200607102150

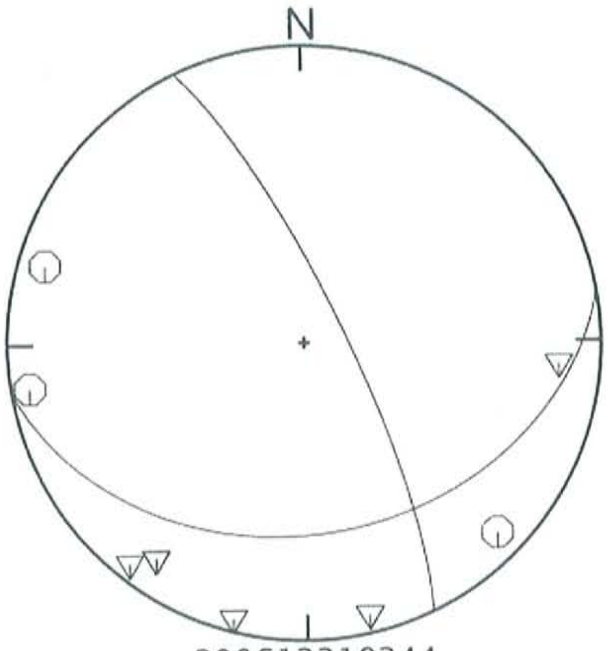

200612310244

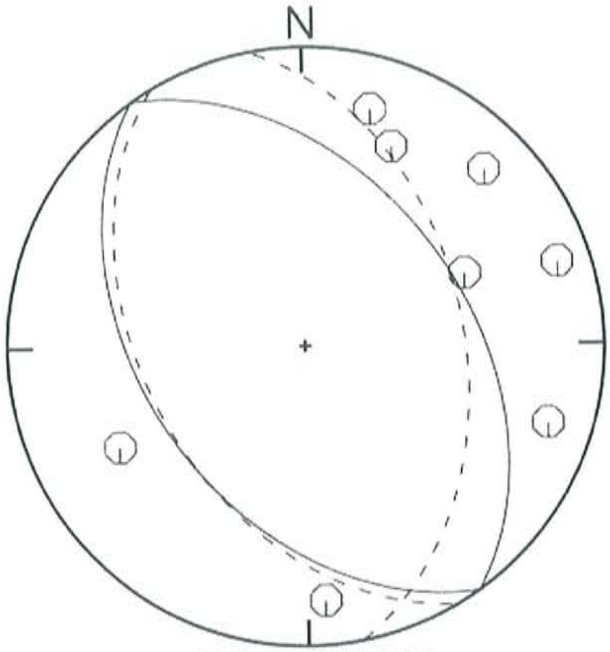

200701301216

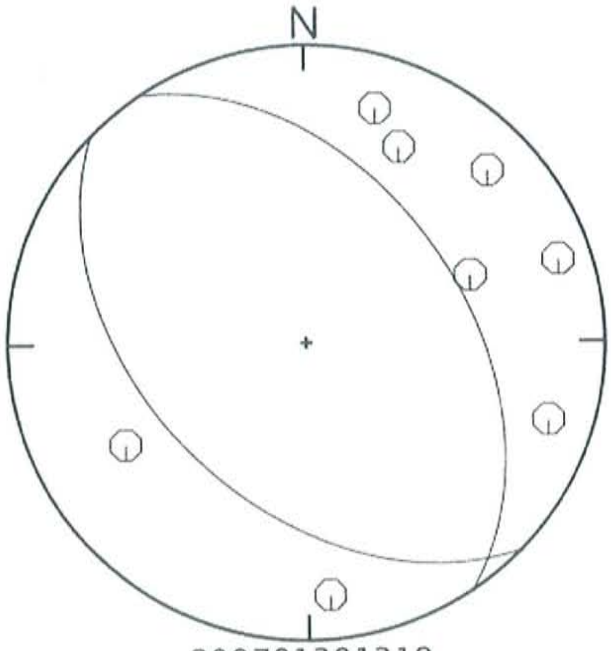

200701301219

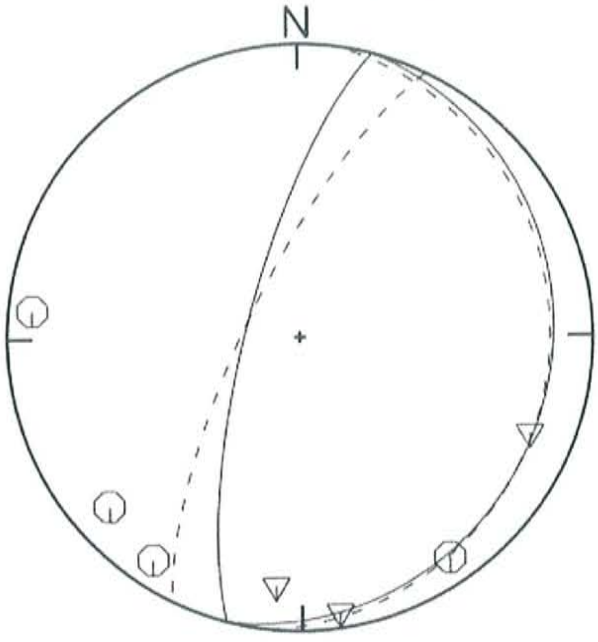

200702271318

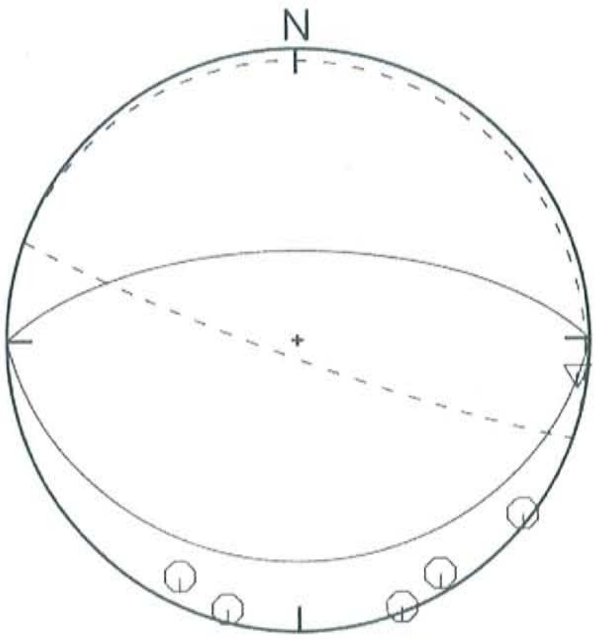

200703081158

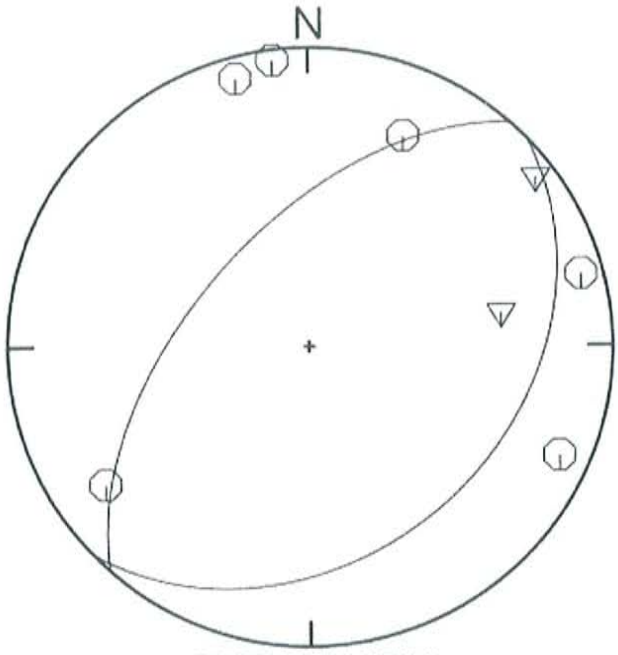

200705221725

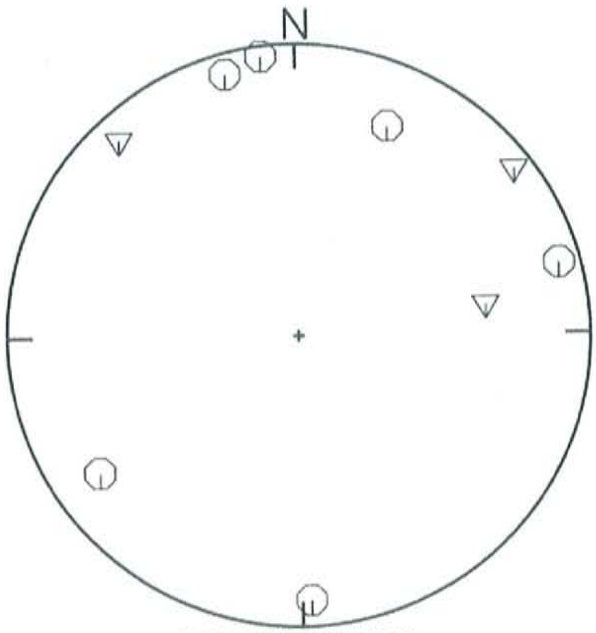

200705230320

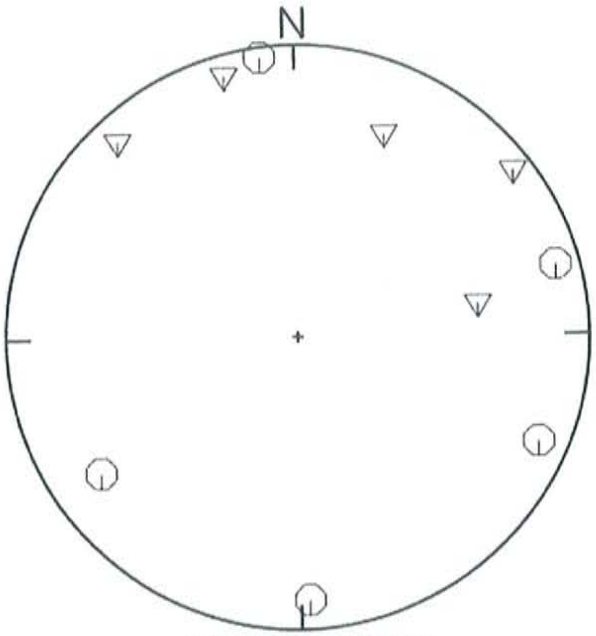

200705230516

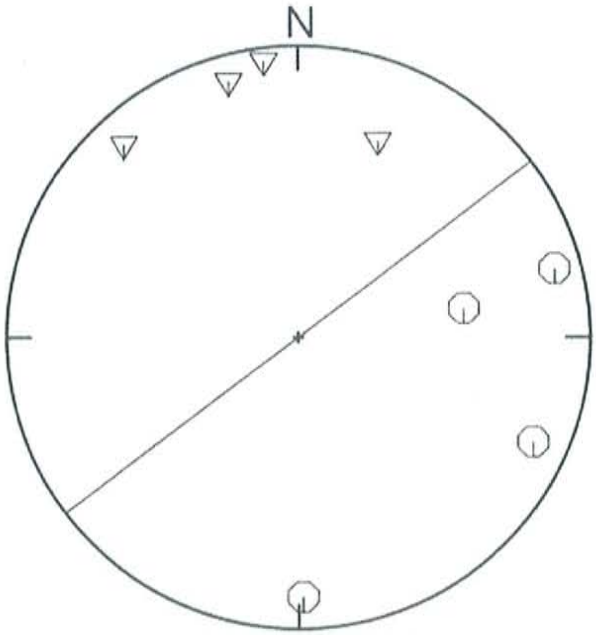

200705241715

Appendix D: Fully Relocated Earthquake Catalogue

ind = index	lat = latitude	1std = 1st standard deviation	dep = depth	yyyy = year
m = month	d = day	h = hour	m = minute	orig = origin time
mag = magnitude	rms = root mean square error	sta = initial stations	pic = initial picks	ref = reflections

Relocations are categorized in one of four ways in the last column F.
O = original location. No relocation was available for this event.
C = cluster location. Event was included in a cluster and relocation was performed.
Y = YN location. Event includes YN data. YN locations supersede cluster locations
B = cluster and YN location. Event is included in a cluster that contains events with YN data and was relocated. Locations that use both YN and clustering supersede all other locations.

ind	lat	1std	long	1std	dep	1std	yyyy	m	d	h	m	orig	1std	mag	rms	sta	pic	ref	F
1	34.03483	0.4	-106.85517	0.38	5	0	2004	9	3	22	41	2.34	0.07	0.96	0.25	6	9	0	O
2	33.94717	0.31	-106.923	0.34	5	0	2004	9	7	10	58	48.87	0.05	1.11	0.23	7	13	0	O
3	34.24583	1.48	-105.82583	1.03	5	0	2004	9	10	0	8	52.45	0.2	1.3	0.31	5	9	0	O
4	34.06117	0.36	-106.8405	0.35	5	0	2004	9	20	15	12	4.74	0.05	0.94	0.17	5	9	0	O
5	34.51417	0.31	-107.15633	0.44	5	0	2004	9	21	5	15	51.39	0.05	1.73	0.13	9	12	0	O
6	34.04133	0.29	-106.79333	0.37	5	0	2004	9	22	1	29	6.66	0.04	0.85	0.15	5	8	0	O
7	33.956	0.97	-106.58633	0.97	5	0	2004	9	25	10	5	46.75	0.18	0.51	0.02	4	4	0	O
8	34.29567	0.65	-106.70633	0.52	8.93	1.04	2004	9	27	7	44	40.31	0.12	0.33	0.45	4	7	1	O
9	34.277	0.5	-106.77	0.37	5	0	2004	9	28	12	40	39.2	0.07	-0.03	0.13	4	8	0	O
10	34.11083	0.35	-106.71133	0.44	5	0	2004	10	5	7	16	58.7	0.05	0.41	0.26	4	7	0	O
11	34.0705	2.18	-107.03383	0.68	8.07	2.39	2004	10	5	12	30	0.44	0.21	1.58	0.02	4	5	0	O
12	33.97217	0.65	-106.93467	0.62	5	0	2004	10	9	7	2	34.43	0.13	0.62	0.23	4	8	0	O
13	34.4465	1.45	-106.88533	0.39	5	0	2004	10	14	13	55	0.58	0.17	0.35	0.02	5	5	0	O

14	34.4525	1.18	-106.88767	0.39	5	0	2004	10	14	19	24	57.56	0.13	0.36	0.12	4	6	0	O
15	34.45633	0.38	-106.881	0.37	5	0	2004	10	16	0	52	5.72	0.05	0.57	0.04	7	8	0	O
16	34.14067	0.36	-106.78183	0.27	5	0	2004	10	21	4	50	27.74	0.05	0.32	0.19	4	7	0	O
17	33.75283	0.68	-107.27133	0.75	9.71	1.72	2004	10	22	1	11	18.86	0.16	0.58	0.14	5	10	0	O
18	34.33867	0.59	-106.734	0.63	5	0	2004	10	24	10	41	8.4	0.09	0.88	0.33	6	10	0	B
19	34.09633	0.25	-107.03133	0.27	8.05	1.3	2004	10	24	13	43	26.64	0.08	0.84	0.24	8	15	0	O
20	34.5225	0.49	-106.23433	1.12	5	0	2004	10	25	9	19	11.31	0.18	1.1	0.29	5	9	0	O
21	34.10333	0.75	-107.024	0.95	9.76	0.83	2004	10	31	9	1	14.87	0.15	0.1	0.22	3	7	1	O
22	34.08967	0.83	-107.016	1.18	5.69	3.29	2004	10	31	15	28	22.74	0.27	0.21	0.38	4	8	0	B
23	34.11433	0.34	-107.23817	0.49	5	0	2004	11	1	1	24	19.01	0.07	0.13	0.15	5	8	0	O
24	34.05933	0.3	-107.02883	0.49	5	0	2004	11	11	19	30	7.94	0.06	0.42	0.31	7	11	0	O
25	34.355	0.28	-106.9395	0.24	5	0	2004	11	16	21	12	28.42	0.04	1.08	0.25	8	13	0	C
26	34.33983	0.43	-106.94467	0.41	5	0	2004	11	16	22	6	8.81	0.07	0.38	0.24	5	7	0	C
27	33.95367	0.31	-106.9205	0.31	5	0	2004	11	20	1	27	0.25	0.04	1.31	0.3	8	11	0	O
28	34.3385	0.27	-106.94	0.25	5	0	2004	11	25	21	9	44.5	0.04	1.33	0.2	8	11	0	C
29	34.464	0.31	-107.05667	0.43	2.96	3.42	2004	12	4	22	4	53.28	0.07	1.26	0.15	9	12	0	O
30	34.1505	0.57	-106.87433	0.39	4.85	1.1	2004	12	5	0	14	33.52	0.07	0.50	0.13	5	10	1	B
31	34.375	0.88	-106.993	0.72	6.49	1.39	2004	12	5	2	31	4.65	0.17	0.49	0.13	4	9	1	O
32	34.02717	1.12	-106.99	1.01	5	0	2004	12	14	6	59	27.55	0.16	0.36	0.03	4	6	0	C
33	34.338	0.27	-106.945	0.32	5	0	2004	12	18	17	37	20.37	0.04	0.79	0.22	8	11	0	C
34	34.29417	1.62	-106.906	1.3	5	0	2004	12	21	0	50	13.68	0.24	0.47	0.17	4	6	0	B
35	34.4195	0.59	-107.06183	0.37	5	0	2004	12	21	12	2	8.99	0.08	0.58	0.17	5	8	0	O
36	34.4125	0.31	-107.06733	0.32	5	0	2004	12	21	12	6	39.4	0.04	0.76	0.12	8	12	0	O
37	34.412	0.31	-107.066	0.33	5	0	2004	12	21	21	31	52.64	0.04	1.17	0.11	8	11	0	O
38	34.41283	0.68	-107.06167	0.45	5	0	2004	12	22	20	48	56.13	0.11	1.63	0.07	6	8	0	O
39	34.41317	1.51	-107.05717	0.53	5	0	2004	12	22	21	15	17.38	0.21	0.71	0.06	4	5	0	O
40	34.39967	0.64	-107.016	0.32	5	0	2004	12	29	8	43	27.29	0.07	0.62	0.18	6	8	0	O
41	34.30717	0.36	-106.90167	0.33	7.5	1.06	2005	1	6	12	7	3.57	0.07	0.28	0.19	6	9	1	C
42	34.30517	0.31	-106.93033	0.31	4.96	1.13	2005	1	9	14	60	53.46	0.06	0.67	0.53	8	15	1	C
43	34.27717	0.76	-106.8825	0.54	7.92	0.87	2005	1	11	7	51	55.48	0.11	-0.14	0.33	5	10	2	B
44	34.27317	0.25	-106.95283	0.35	6.53	0.79	2005	1	14	21	7	18.2	0.05	0.51	0.15	8	13	1	O

45	34.06517	0.53	-107.01183	0.85	5	0	2005	1	15	9	54	58.66	0.1	0.55	0.24	5	9	0	B
46	34.1055	0.3	-106.86667	0.36	4.52	0.87	2005	1	15	14	28	22.8	0.05	0.31	0.22	4	9	1	O
47	34.09567	0.34	-106.8055	0.41	5	0	2005	1	17	23	31	36.27	0.05	0.7	0.07	4	6	0	O
48	34.07533	0.72	-106.89967	0.68	5	0	2005	1	18	19	33	25.59	0.1	0.47	0.18	5	6	0	C
49	34.06917	0.67	-106.90533	0.67	5	0	2005	1	18	20	56	54.28	0.09	0.48	0.37	4	6	0	C
50	34.07583	0.56	-106.89833	0.68	5	0	2005	1	19	1	13	51.98	0.08	0.36	0.34	5	7	0	C
51	34.07283	0.48	-106.89817	0.64	5	0	2005	1	19	2	52	29.22	0.07	0.90	0.43	7	10	0	C
52	34.06983	0.58	-106.90183	0.64	5	0	2005	1	19	6	19	10.8	0.09	0.58	0.22	4	8	0	C
53	34.0745	0.67	-106.9055	0.63	5	0	2005	1	19	12	1	0.25	0.09	0.38	0.3	5	7	0	C
54	34.04067	0.39	-106.95517	0.44	5	0	2005	1	19	21	46	56.41	0.05	0.05	0.16	4	7	0	B
55	34.00267	0.42	-106.955	0.42	5	0	2005	1	19	23	56	5.46	0.05	0.26	0.29	4	6	0	B
56	34.07117	0.47	-106.95567	0.43	5	0	2005	1	20	3	16	32.87	0.05	0.45	0.43	5	7	0	B
57	34.066	0.65	-106.90067	0.69	5	0	2005	1	21	3	26	7.64	0.09	0.34	0.08	4	6	0	C
58	34.0465	0.8	-106.99617	1.12	6.78	1.22	2005	1	22	0	53	41.15	0.13	0.55	0.15	4	8	1	C
59	34.30683	0.35	-106.90167	0.36	7	1.09	2005	1	25	1	51	16.76	0.08	0.26	0.21	4	8	1	C
60	34.15633	1.46	-106.93717	1.57	5.54	0.92	2005	1	27	1	3	49.44	0.1	0.45	0.35	4	8	1	C
61	34.07033	0.6	-106.89817	0.65	5	0	2005	2	1	8	23	20.23	0.09	0.34	0.32	4	7	0	C
62	34.39933	0.37	-107.04983	0.62	2.73	1.24	2005	2	4	0	35	28.37	0.06	0.29	0.17	4	8	1	O
63	34.4085	0.33	-107.0635	0.29	1.99	1.17	2005	2	4	1	20	30.41	0.05	0.47	0.12	6	12	1	O
64	34.44667	0.38	-106.88817	0.32	5	0	2005	2	9	4	53	27.78	0.05	0.39	0.13	5	9	0	O
65	34.45	0.34	-106.90117	0.35	5	0	2005	2	9	10	40	21.5	0.05	0.86	0.46	6	10	0	O
66	34.34717	2.53	-106.68167	2.17	15.16	4.51	2005	2	11	9	25	42.5	0.71	0.58	0.03	4	5	0	B
67	34.4375	0.42	-106.88883	0.41	5	0	2005	2	16	6	12	46.78	0.05	0.85	0.06	5	6	0	O
68	34.3395	0.35	-106.94	0.28	5	0	2005	2	21	16	49	24.67	0.06	0.31	0.36	5	12	2	C
69	34.3085	0.6	-107.006	0.71	6.38	3.7	2005	2	23	18	18	5.93	0.21	1.82	0.06	8	8	0	C
70	33.81733	0.47	-106.684	0.75	5	0	2005	2	28	9	57	28.49	0.09	0.47	4.15	3	6	0	O
71	34.142	0.42	-106.65317	0.6	5	0	2005	3	4	3	7	3.13	0.07	0.53	0.39	4	7	0	O
72	34.30917	0.34	-106.90367	0.35	6.41	1.1	2005	3	5	0	48	13.69	0.07	-0.11	0.32	5	9	1	C
73	34.19117	0.91	-106.9615	1.1	5	0	2005	3	5	16	16	1.7	0.12	0.73	0.19	5	5	0	B
74	34.1405	0.42	-106.64467	0.69	5	0	2005	3	7	18	52	13.19	0.08	0.24	0.12	3	5	0	O
75	34.50383	0.3	-106.87533	0.34	5	0	2005	3	20	12	59	13.88	0.05	1.13	0.2	8	15	1	O

76	34.33833	0.27	-106.94133	0.27	5	0	2005	3	20	14	4	8.97	0.04	1.06	0.21	8	12	0	C
77	34.044	0.36	-106.97567	0.35	6.53	0.87	2005	3	29	14	6	33.52	0.06	0.53	0.25	7	14	2	B
78	34.4995	0.39	-106.88317	0.37	5	0	2005	3	31	17	31	42.31	0.06	0.37	0.13	5	8	0	O
79	34.5265	0.96	-106.87167	0.42	5	0	2005	3	31	20	30	26.22	0.15	0.46	0.7	4	8	1	O
80	33.99133	0.78	-107.06117	0.83	8.14	0.73	2005	4	1	4	45	6.57	0.11	0.05	0.14	5	13	3	C
81	34.06933	0.47	-107.00233	0.36	5.66	1.03	2005	4	2	11	3	4.01	0.07	0.81	0.06	8	14	1	B
82	34.06883	0.42	-107.0015	0.35	4.41	0.63	2005	4	2	16	53	14.83	0.05	0.60	0.34	9	18	4	B
83	34.06433	0.67	-106.99717	0.52	4.4	0.99	2005	4	2	17	22	53.21	0.07	0.26	0.21	6	12	1	B
84	34.07833	0.69	-106.98717	1.01	5.39	0.9	2005	4	2	21	44	12.08	0.13	0.22	0.22	4	8	1	B
85	34.07333	0.45	-107.004	0.38	6.07	1.87	2005	4	2	22	48	5.98	0.09	1.36	0.13	10	11	0	B
86	34.07	0.48	-107.00317	0.36	4.54	1.62	2005	4	2	23	41	15.55	0.08	0.81	0.15	8	13	0	B
87	34.02083	0.92	-107.03667	0.83	8.72	0.77	2005	4	11	14	1	33.84	0.11	0.35	0.08	7	14	2	C
88	33.98833	0.59	-106.95367	0.56	6.73	2.69	2005	4	15	10	44	18.4	0.17	0.64	0.11	7	13	0	C
89	34.23	0.26	-106.85033	0.31	5	0	2005	4	17	8	55	22.55	0.04	0.69	0.14	7	11	0	O
90	34.23217	0.37	-106.84867	0.34	5	0	2005	4	17	9	11	57.84	0.05	0.63	0.06	6	8	0	O
91	34.30467	0.41	-107.01083	0.45	5	0	2005	4	22	21	44	20.24	0.05	0.24	0.08	6	8	0	C
92	34.28967	1.11	-106.893	0.93	8.73	1.89	2005	4	23	12	24	31.93	0.22	0.68	0.29	5	8	0	B
93	34.06733	1.03	-107.03417	2.48	8.12	2.4	2005	4	23	19	15	25.22	0.44	0.14	0.23	4	6	0	B
94	34.065	0.63	-107.0055	0.65	12.64	1.75	2005	4	24	4	53	58.43	0.18	0.93	0.33	7	10	0	B
95	34.31	0.65	-106.7025	0.59	5	0	2005	4	29	18	46	19.92	0.11	0.76	0.15	7	10	0	B
96	34.024	0.39	-106.711	0.62	5	0	2005	4	30	3	16	7.61	0.05	1	0.13	5	6	0	O
97	33.918	0.33	-107.06483	0.72	5	0	2005	5	1	6	3	9.96	0.08	0.36	0.05	4	7	0	O
98	33.9175	0.37	-107.06367	1.19	5	0	2005	5	1	7	26	8.61	0.12	0.49	0.1	3	6	0	O
99	33.91617	0.31	-107.06567	0.64	5	0	2005	5	1	7	37	46.58	0.08	0.5	0.11	5	9	0	O
100	34.34567	0.86	-106.72967	0.89	1.85	8.58	2005	5	2	6	23	10.63	0.2	0.39	0.22	5	9	0	B
101	33.85967	0.64	-107.21933	1.19	5	0	2005	5	3	11	59	39.71	0.19	0.13	0.73	4	6	1	O
102	34.27383	0.3	-106.71583	0.28	5	0	2005	5	4	7	3	31.19	0.04	1.28	0.19	9	13	0	O
103	34.27867	0.34	-106.71217	0.62	4.51	2.46	2005	5	4	7	6	24.95	0.12	0.49	0.09	8	9	0	O
104	34.27817	0.29	-106.71283	0.3	5	0	2005	5	4	7	8	30.06	0.04	1.02	0.29	8	12	0	O
105	34.27817	0.3	-106.71267	0.32	5	0	2005	5	4	12	3	59.21	0.04	1.13	0.2	9	11	0	O
106	34.30983	0.46	-107.07567	0.65	5	0	2005	5	8	11	13	42.45	0.05	0.53	0.33	7	10	1	B

107	34.00883	0.81	-106.98983	0.92	5	0	2005	5	11	16	48	18.38	0.14	1.27	0.83	8	13	0	C
108	33.993	2.23	-106.9675	2.48	6.67	3.57	2005	5	11	16	50	32.3	0.29	0.73	0.03	4	7	0	C
109	34.00483	1.35	-107.02383	1.68	11	3.02	2005	5	11	19	48	7.14	0.31	0.58	0.22	4	7	0	C
110	34.30967	0.45	-107.00783	0.46	4.59	2.43	2005	5	12	13	31	24.89	0.09	0.76	0.25	8	12	0	C
111	33.93817	0.34	-106.90767	0.39	5	0	2005	5	15	5	48	38.89	0.05	0.85	0.08	6	8	0	O
112	34.0275	0.49	-106.766	0.39	5	0	2005	5	24	5	52	48.88	0.05	0.34	0.05	4	6	0	O
113	34.31017	0.59	-107.01683	0.46	5	0	2005	6	1	11	27	18.21	0.09	0.15	0.18	5	7	0	C
114	34.28617	0.45	-107.05517	0.48	5	0	2005	6	1	14	5	45.37	0.05	0.39	0.31	7	11	1	C
115	34.09883	0.6	-106.7005	0.58	5	0	2005	6	2	3	38	51.78	0.06	0.61	0.02	4	4	0	O
116	34.3135	0.58	-106.96933	0.55	12.99	1.39	2005	6	2	9	33	59.49	0.12	0.93	0.31	8	9	0	C
117	34.24083	0.85	-106.91483	0.52	5	0	2005	6	3	5	20	41.52	0.14	0.75	0.23	4	7	0	O
118	34.255	0.42	-106.9275	0.45	5.36	1.69	2005	6	4	0	34	13.58	0.07	0.64	0.06	7	9	0	O
119	33.94517	0.47	-106.61417	0.55	6.16	2.16	2005	6	4	2	15	0.2	0.14	0.50	0.01	4	6	0	C
120	33.9475	0.4	-106.6175	0.45	6.62	1.73	2005	6	4	13	13	58.06	0.12	0.65	0.04	5	8	0	C
121	33.947	0.4	-106.61667	0.45	6.73	1.72	2005	6	4	21	5	11.22	0.12	0.64	0.04	5	8	0	C
122	33.946	0.46	-106.61467	0.55	6.41	1.83	2005	6	4	21	7	6.78	0.13	0.51	0.02	5	7	0	C
123	33.94533	0.43	-106.613	0.54	5.84	2.23	2005	6	4	21	26	30.83	0.14	0.69	0.02	4	7	0	C
124	33.945	0.43	-106.6125	0.55	6.33	2.11	2005	6	4	22	53	16.28	0.14	0.63	0.02	4	7	0	C
125	33.94683	0.4	-106.61733	0.45	6.49	1.76	2005	6	4	23	7	3.12	0.12	0.66	0.03	5	8	0	C
126	33.97967	0.55	-106.62367	0.56	10.93	1.89	2005	6	5	1	32	28.77	0.2	0.47	0.05	4	5	0	C
127	33.95	0.59	-106.61517	0.58	5	0	2005	6	5	2	60	33.96	0.13	0.74	0.33	4	6	0	C
128	33.94667	0.4	-106.617	0.45	6.6	1.74	2005	6	5	3	8	30.25	0.12	0.65	0.04	5	8	0	C
129	33.94717	0.4	-106.6165	0.45	6.67	1.73	2005	6	5	4	6	23.55	0.12	0.85	0.04	5	8	0	C
130	33.9475	0.4	-106.61733	0.45	6.53	1.75	2005	6	5	4	38	39.28	0.12	1.01	0.04	5	8	0	C
131	33.94517	0.41	-106.613	0.54	6.12	1.88	2005	6	5	7	60	28.67	0.13	0.99	0.02	5	8	0	C
132	33.94667	0.47	-106.617	0.5	6.46	1.94	2005	6	5	8	8	24.38	0.12	0.79	0.04	5	7	0	C
133	33.94783	0.34	-106.61733	0.44	6.77	1.65	2005	6	5	10	19	28.6	0.12	1.38	0.1	6	11	0	C
134	33.946	0.43	-106.6135	0.54	5.91	2.2	2005	6	5	10	42	10	0.14	0.75	0.02	4	7	0	C
135	33.94567	0.47	-106.61317	0.56	5.91	2.36	2005	6	5	11	11	14.24	0.14	0.50	0.02	4	6	0	C
136	33.89417	0.81	-106.49017	2.12	5	0	2005	6	5	12	36	37.64	0.35	0.39	1.51	4	6	0	O
137	33.94517	0.41	-106.61233	0.54	6.1	1.89	2005	6	5	13	26	14.1	0.13	0.73	0.02	5	8	0	C

138	33.957	0.56	-106.62817	0.57	14.34	1.29	2005	6	5	13	29	54.35	0.15	0.43	0.76	5	7	0	C
139	33.943	1.01	-106.61083	1.43	5.97	2.42	2005	6	5	15	26	45.01	0.22	0.7	0	4	4	0	C
140	33.94333	0.42	-106.6115	0.55	5	0	2005	6	5	15	51	27.84	0.11	0.98	0.28	5	7	0	C
141	33.944	0.8	-106.61233	1.37	5.85	2.34	2005	6	5	17	28	14.57	0.2	0.63	0.01	4	5	0	C
142	33.93967	0.39	-106.61	0.55	5	0	2005	6	5	21	14	12.19	0.11	0.73	0.62	5	8	0	C
143	33.94533	0.43	-106.61283	0.54	5.76	2.26	2005	6	5	22	16	20.1	0.14	0.34	0.02	4	7	0	C
144	33.94683	0.4	-106.61667	0.45	6.43	1.78	2005	6	6	0	27	58.97	0.12	0.57	0.04	5	8	0	C
145	33.94283	0.42	-106.61233	0.54	5	0	2005	6	6	0	48	17.83	0.1	0.82	0.31	6	9	0	C
146	34.236	0.98	-106.91567	0.51	5	0	2005	6	8	6	31	32.23	0.15	0.56	0.2	4	6	0	O
147	33.94867	0.48	-106.62067	0.62	6.89	1.91	2005	6	8	9	23	23.7	0.14	0.42	0.01	4	5	0	C
148	34.0075	1.07	-107.00767	1.44	4.2	5.03	2005	6	11	10	18	55.56	0.26	0.27	0.04	5	8	0	C
149	34.05333	0.38	-107.0415	0.39	5	0	2005	6	11	15	57	1.9	0.05	0.39	0.1	6	8	0	O
150	34.29133	0.96	-106.8905	0.69	2.56	6.2	2005	6	13	20	22	50.18	0.15	0.42	0.18	6	8	0	C
151	34.06067	0.83	-106.952	0.97	5.61	0.82	2005	6	14	3	51	55.56	0.14	0.13	0.1	4	7	1	B
152	34.14317	0.85	-106.91383	0.85	4.5	2.64	2005	6	14	5	38	41.67	0.18	0.52	0.05	6	8	0	C
153	34.1465	0.99	-106.92233	0.81	7.27	0.7	2005	6	14	5	47	52.48	0.09	0.08	0.19	4	9	2	C
154	34.45167	0.35	-106.89033	0.37	5	0	2005	6	19	3	49	20.27	0.05	0.78	0.25	7	11	0	O
155	34.37217	0.51	-107.00367	0.42	5	0	2005	6	23	6	42	12.96	0.07	0.62	0.12	8	12	0	O
156	34.24633	1	-106.90633	0.52	5	0	2005	6	30	14	46	50.88	0.15	0.39	0.19	4	6	0	O
157	34.3515	1.29	-106.9785	1.19	5	0	2005	7	4	3	28	14.24	0.24	0.55	0.07	4	6	0	O
158	33.95983	0.31	-106.9745	0.31	5	0	2005	7	12	8	34	49.97	0.04	0.76	0.25	7	10	0	O
159	34.19633	0.89	-106.90717	0.6	5	0	2005	7	12	11	49	39.62	0.15	0.79	0.48	4	7	0	O
160	34.35167	3.01	-106.63067	2.29	10.62	4.11	2005	7	23	0	33	45.06	0.77	0.72	0.07	6	7	0	B
161	34.067	0.42	-106.99417	0.35	4.89	0.77	2005	8	5	12	44	58.34	0.05	0.69	0.35	10	17	2	B
162	34.26333	0.73	-106.83083	0.46	5	0	2005	8	6	6	44	30.84	0.08	0.37	0.02	5	7	0	O
163	34.02017	1.15	-107.02367	1.02	10.02	4.51	2005	8	7	17	11	21.51	0.42	0.71	0.05	7	9	0	C
164	34.12167	0.44	-106.851	0.34	5.62	2.05	2005	8	10	2	4	1.82	0.1	0.63	0.07	6	8	0	O
165	34.02167	0.42	-106.719	0.55	5	0	2005	8	14	13	49	15.59	0.05	0.46	0.13	5	7	0	C
166	34.38367	0.32	-107.01433	0.31	5	0	2005	8	16	20	58	48	0.04	0.51	0.11	7	10	0	O
167	33.98617	0.75	-106.9635	0.9	5.82	3.34	2005	8	22	14	49	14.38	0.19	0.65	0.09	6	9	0	C
168	34.37583	2.85	-106.673	2.06	13.64	4.51	2005	8	25	5	21	44.72	0.74	0.16	0.01	4	5	0	B

169	34.31367	0.83	-106.72217	0.76	5	0	2005	8	27	21	2	49.59	0.14	0.06	0.65	4	5	0	B
170	34.24017	0.82	-106.9455	0.84	9.68	1.47	2005	8	27	23	9	29.5	0.19	0.67	0.15	4	6	0	O
171	34.45233	0.41	-106.881	0.44	5	0	2005	9	1	9	38	1.68	0.05	0.64	0.04	7	7	0	O
172	34.31033	1	-106.90783	0.79	5	0	2005	9	1	16	50	55.11	0.17	0.44	0.15	5	7	0	C
173	34.32517	1.08	-106.93333	0.96	10.39	1.97	2005	9	4	11	25	14.57	0.23	0.28	0.59	5	7	0	C
174	34.01183	0.56	-106.69683	1.01	5.86	1.38	2005	9	18	10	59	35.77	0.13	0.28	0.1	5	8	0	Y
175	34.12417	0.34	-106.82783	0.31	5	0	2005	9	20	9	59	39.92	0.04	0.6	0.07	8	9	0	Y
176	34.12483	0.31	-106.82833	0.34	5	0	2005	9	20	17	40	54.06	0.04	0.57	0.03	7	8	0	Y
177	34.256	1.07	-106.84617	0.61	5.63	2.12	2005	9	20	18	22	32.26	0.19	0.50	0.15	5	6	0	B
178	34.07667	0.52	-107.04467	0.55	5	0	2005	9	25	13	8	14.53	0.05	-0.01	0.06	5	6	0	Y
179	33.9915	0.49	-106.53267	1.2	5.65	0.73	2005	10	2	18	23	5.82	0.17	0.51	0.09	4	8	1	O
180	34.32083	0.81	-106.44767	1.67	5.99	5.08	2005	10	5	23	37	56.61	0.23	0.42	0.13	4	7	0	O
181	34.433	0.25	-106.77667	0.24	5	0	2005	10	7	18	37	33.6	0.04	1	0.16	9	13	0	Y
182	34.1835	0.55	-106.87733	0.38	3.98	0.75	2005	10	12	18	54	46.25	0.06	0.57	0.29	6	12	2	B
183	34.05067	0.32	-106.85283	0.34	3.67	0.65	2005	10	15	19	23	11.71	0.04	0.98	0.1	6	9	1	Y
184	34.12867	0.3	-106.8435	0.22	4.13	0.45	2005	10	16	17	40	46.49	0.03	0.91	0.14	9	14	2	Y
185	34.02067	0.27	-106.87467	0.23	5	0	2005	10	17	7	47	53.37	0.03	0.73	0.24	9	14	0	Y
186	34.13833	0.41	-106.84533	0.31	4.05	0.45	2005	10	18	5	17	27.74	0.04	0.6	0.06	6	10	2	Y
187	34.05733	0.61	-106.95617	0.41	6.66	0.59	2005	10	21	8	11	36.51	0.06	-0.21	0.16	6	11	2	B
188	34.05333	0.89	-106.95733	0.46	6.6	1.23	2005	10	21	8	29	56.02	0.12	-0.91	0.13	5	7	0	B
189	34.0505	0.47	-106.95883	0.43	4.46	0.68	2005	10	24	18	14	11.76	0.06	-0.34	0.52	5	11	2	B
190	34.05817	0.35	-106.9585	0.38	6.31	0.35	2005	10	24	18	16	27.44	0.05	-0.88	0.19	4	8	2	O
191	34.1225	0.56	-106.99783	0.59	5	0	2005	10	24	18	27	53.57	0.06	-0.41	0.47	4	7	0	B
192	33.84283	0.44	-107.10417	0.44	7.84	1.3	2005	10	25	18	6	53.49	0.14	0.05	0.06	6	8	0	O
193	34.06133	0.46	-106.978	0.42	5.5	0.64	2005	10	26	23	28	18.04	0.06	0.16	0.32	7	13	2	B
194	34.04733	0.73	-106.9635	0.75	6.98	0.47	2005	10	27	4	29	51.25	0.09	-0.94	0.24	4	6	1	O
195	34.0175	0.74	-107.02433	0.56	5.96	0.59	2005	10	29	0	31	12.73	0.1	-0.93	0.26	4	7	1	O
196	34.05517	0.28	-106.958	0.34	7.08	0.34	2005	10	30	1	56	49.98	0.04	1.15	0.19	7	14	3	O
197	34.052	0.46	-106.95483	0.39	6.56	0.6	2005	10	30	2	5	25.18	0.06	0.06	0.18	7	13	2	B
198	34.29933	0.85	-106.7815	0.4	5	0	2005	10	30	2	5	0.13	0.13	0.05	0.11	4	8	0	O
199	34.05633	0.42	-106.95633	0.36	6.47	0.33	2005	10	30	2	9	18.76	0.04	0.56	0.19	6	14	3	O

200	34.0565	0.31	-106.95533	0.32	7.07	0.79	2005	10	30	2	57	35.18	0.06	2.33	0.07	10	10	0	O
201	34.05817	0.54	-106.95983	0.48	7.42	0.29	2005	10	30	2	59	24.5	0.05	0.00	0.37	4	7	3	O
202	34.05717	0.33	-106.95867	0.33	6.37	0.34	2005	10	30	3	3	38	0.04	0.00	0.28	7	17	3	O
203	34.05733	0.39	-106.957	0.33	5.9	0.24	2005	10	30	3	6	50.79	0.04	0.4	0.18	5	12	3	O
204	34.05517	0.49	-106.956	0.38	5.71	0.27	2005	10	30	3	7	25.96	0.04	0.29	0.16	5	8	3	O
205	34.062	0.59	-106.95767	0.5	7.88	0.81	2005	10	30	3	14	32.58	0.08	-0.51	0.04	4	5	1	B
206	34.062	0.59	-106.95767	0.5	7.88	0.81	2005	10	30	3	14	32.58	0.08	0.11	0.04	0	0	0	B
207	34.05817	0.52	-106.9585	0.39	6.69	0.57	2005	10	30	3	19	55.74	0.06	-0.21	0.15	6	9	3	B
208	34.059	0.51	-106.95817	0.4	6.54	0.62	2005	10	30	3	26	37.41	0.06	0.21	0.2	6	8	2	B
209	34.04767	0.53	-106.97433	0.4	6.82	0.59	2005	10	30	4	43	6.45	0.06	0.11	0.23	6	9	3	B
210	34.06	0.53	-106.95783	0.4	7.39	0.66	2005	10	30	4	45	20.85	0.06	-0.01	0.14	6	8	2	B
211	34.058	0.54	-106.95767	0.4	6.68	0.57	2005	10	30	4	50	47.47	0.06	0.22	0.19	5	8	3	B
212	34.062	1.21	-106.95517	1.75	7.04	0.89	2005	10	30	5	1	23.95	0.18	-0.63	0.02	4	5	1	B
213	34.02517	0.51	-107.0245	0.46	8.53	1.17	2005	10	30	5	26	15.71	0.1	-0.26	0.18	5	6	1	Y
214	34.05	0.39	-106.95583	0.45	6.54	0.59	2005	11	1	9	28	12.9	0.05	0.62	0.18	7	10	3	B
215	34.05467	0.66	-106.9575	0.43	6.33	0.57	2005	11	3	14	58	57.23	0.07	0.28	0.16	5	11	3	B
216	34.05467	0.66	-106.9575	0.43	6.33	0.57	2005	11	3	14	58	57.23	0.07	0.28	0.16	5	11	3	B
217	34.06333	0.26	-106.94383	0.27	5	0	2005	11	4	22	15	43.34	0.04	0.28	0.74	6	13	2	O
218	34.06083	0.5	-106.96467	0.52	6.06	0.4	2005	11	4	22	26	17.8	0.07	-0.27	0.16	4	10	2	O
219	34.05983	0.42	-106.95783	0.32	6.9	0.42	2005	11	4	23	26	41	0.05	0.24	0.09	5	11	2	O
220	34.08267	0.45	-106.96667	0.37	6.12	0.53	2005	11	5	2	9	33.82	0.06	0.30	0.35	6	15	3	B
221	34.059	0.46	-106.95683	0.46	7.43	1.08	2005	11	6	12	33	43.35	0.1	1.25	0.03	7	7	0	O
222	34.0575	0.4	-106.95633	0.46	6.37	0.64	2005	11	6	12	45	19.64	0.06	0.47	0.18	6	9	2	B
223	34.03867	0.39	-106.95217	0.46	6.12	0.69	2005	11	6	13	16	28.74	0.06	0.44	0.33	6	8	2	B
224	34.054	0.41	-106.953	0.35	6.15	0.41	2005	11	6	14	33	23.75	0.05	0.5	0.14	6	12	2	O
225	34.07	0.35	-106.96117	0.36	6.55	0.54	2005	11	8	18	20	52.53	0.05	1.47	0.25	10	14	3	B
226	34.07667	0.91	-106.8925	0.69	5	0	2005	12	12	4	36	58.5	0.12	1.02	0.23	5	5	0	C
227	34.44933	1.44	-107.14067	0.71	5	0	2005	12	22	11	55	42.82	0.22	0.75	0.13	9	9	0	O
228	34.0755	0.97	-106.87583	0.86	7.98	2.4	2005	12	29	2	31	27.55	0.25	-0.61	0.1	4	8	0	O
229	34.03183	0.27	-107.00183	0.28	4.17	1	2006	1	2	2	1	57.51	0.05	0.64	0.17	9	18	1	O
230	34.0285	0.82	-106.9945	1.2	5.19	1.14	2006	1	2	15	27	37.6	0.13	-0.02	0.04	4	9	1	C

231	34.02667	0.73	-107.0195	1.23	4.22	1.3	2006	1	3	6	8	24.27	0.17	0.43	0.16	5	11	1	C
232	34.03867	1.1	-106.99633	0.91	4.02	1.16	2006	1	5	11	17	10.29	0.13	0.41	0.3	5	9	1	C
233	34.15467	0.73	-106.92583	0.98	3	3.83	2006	1	11	17	20	52.06	0.23	0.63	0.24	6	12	0	C
234	34.03	1.19	-107.0585	0.91	9.2	0.79	2006	1	20	22	14	19.22	0.13	-0.69	0.28	4	10	2	C
235	34.251	0.43	-106.7555	0.34	5	0	2006	1	21	7	57	40.8	0.05	0.43	1.29	5	12	2	O
236	34.01433	0.81	-107.02067	0.7	8.43	0.56	2006	1	24	12	2	52.61	0.1	-0.87	0.09	4	8	1	O
237	34.33517	0.58	-107.06467	0.82	5	0	2006	2	9	21	60	34.5	0.06	0.07	0.37	4	7	0	B
238	34.28517	0.44	-106.70217	0.29	3.94	0.81	2006	3	10	3	51	26.18	0.06	0.23	0.24	7	12	1	Y
239	33.98467	0.31	-106.81917	0.34	5	0	2006	3	10	8	10	17.66	0.04	1.2	0.14	8	11	0	Y
240	34.386	0.81	-107.00383	0.72	5	0	2006	3	28	4	14	8.73	0.1	-0.1	0.05	6	8	0	Y
241	34.181	0.44	-106.87817	0.33	3.14	2.08	2006	3	29	3	33	13.35	0.09	0.70	0.05	8	9	0	B
242	34.17367	0.4	-106.88367	0.32	5	0	2006	3	29	3	53	22.49	0.04	0.60	0.39	8	12	0	B
243	34.17917	0.4	-106.87717	0.3	3.04	1.97	2006	3	29	4	23	0.32	0.08	0.88	0.14	10	12	0	B
244	34.18133	0.45	-106.87817	0.31	3.05	1.89	2006	3	29	6	27	48.34	0.09	0.19	0.07	7	10	0	B
245	34.18383	0.45	-106.8795	0.32	2.7	2.27	2006	3	29	8	56	5.42	0.09	-0.17	0.14	7	9	0	B
246	34.1855	0.39	-106.88233	0.3	5.16	0.84	2006	3	29	10	56	14.76	0.06	0.89	0.23	10	16	1	B
247	34.1805	0.42	-106.87733	0.45	2.21	5.87	2006	3	29	11	27	41.48	0.15	0.96	0.14	7	11	0	B
248	34.17633	0.44	-106.87333	0.32	5	0	2006	3	29	11	29	31.36	0.04	0.27	0.21	7	10	0	B
249	34.18383	0.42	-106.87867	0.31	2.49	2.34	2006	3	29	12	30	8.81	0.09	0.35	0.13	8	11	0	B
250	34.25117	0.32	-106.8755	0.26	5	0	2006	4	3	3	9	29.41	0.04	0.95	0.21	10	14	0	Y
251	34.412	0.65	-107.00317	0.36	5	0	2006	4	3	21	36	0.68	0.08	0.32	0.27	6	8	0	Y
252	34.4085	0.53	-107.00367	0.31	5	0	2006	4	4	8	13	35.25	0.07	0.53	0.15	9	12	0	Y
253	34.36133	0.66	-107.008	0.54	5	0	2006	4	4	16	47	43.97	0.07	0.55	0.13	6	8	0	Y
254	34.25533	1.61	-106.85667	0.81	5	0	2006	4	18	1	8	40.21	0.16	0.54	0.41	5	6	0	B
255	34.27267	2.19	-106.86883	1.14	5	0	2006	4	18	1	32	0.41	0.22	0.30	0.14	4	4	0	B
256	34.1575	0.51	-106.83433	0.33	6.09	1	2006	4	25	4	31	10.31	0.08	0.22	0.32	6	11	1	B
257	34.1505	0.39	-106.84133	0.34	7.27	1.57	2006	4	25	4	33	44.13	0.11	0.77	0.15	8	9	0	Y
258	34.16083	0.51	-106.83333	0.33	9.14	0.72	2006	4	25	4	45	41.75	0.07	-0.07	0.35	7	13	2	B
259	34.16	0.58	-106.83567	0.38	9.76	1.59	2006	4	25	5	9	8.25	0.15	-0.25	0.17	6	8	0	B
260	34.15917	0.43	-106.8345	0.29	6.19	0.93	2006	4	25	7	33	37.43	0.08	-0.12	0.28	7	13	1	B
261	34.12917	0.36	-106.666	0.55	4.86	1.7	2006	4	30	10	3	31.15	0.13	0.45	0.33	7	9	0	Y

262	34.4055	0.34	-107.04033	0.34	5	0	2006	5	2	11	33	11.71	0.04	0.66	0.12	10	11	0	Y
263	34.08583	0.46	-107.01133	0.42	1.62	0.93	2006	5	6	10	59	0.22	0.06	0.81	0.22	9	15	2	B
264	34.35183	0.9	-106.72183	0.58	5	0	2006	6	23	20	58	39.72	0.15	0.58	0.23	6	8	0	B
265	34.36667	0.75	-106.8685	0.42	5	0	2006	6	24	12	25	28.68	0.12	0.34	0.12	6	10	0	Y
266	34.35117	0.95	-106.73183	0.64	4.52	3.48	2006	6	25	14	30	20.2	0.2	0.25	0.3	6	7	0	B
267	33.97683	0.26	-106.92883	0.28	5	0	2006	6	25	18	0	24.41	0.04	0.72	0.15	9	15	0	Y
268	34.3435	0.9	-106.64783	0.92	9.04	1.54	2006	6	27	23	35	5.25	0.2	0.66	0.12	6	8	0	B
269	34.34817	0.86	-106.689	0.75	9.04	1.51	2006	6	28	17	41	38	0.19	0.59	0.16	6	10	0	B
270	33.9605	0.42	-106.77783	0.42	3.85	1.56	2006	7	1	14	28	51.6	0.09	0.7	0.35	8	11	0	Y
271	33.96033	0.3	-106.9985	0.41	6.76	2.05	2006	7	10	21	50	42.39	0.11	0.66	0.08	9	13	0	Y
272	34.10117	0.31	-107.03317	0.71	5	0	2006	7	11	20	52	32.31	0.08	0.72	0.2	7	9	0	Y
273	34.09917	0.26	-106.7875	0.31	5	0	2006	7	12	19	1	46.15	0.04	0.53	0.06	7	11	0	Y
274	34.29717	0.8	-106.914	0.97	5	0	2006	7	24	12	38	16.42	0.18	0.59	10.37	7	11	1	Y
275	33.68267	0.58	-107.72617	0.69	5	0	2006	7	24	14	14	7.84	0.11	0.28	10.73	7	10	1	Y
276	34.32333	0.64	-107.05133	1.01	5	0	2006	7	25	17	21	8.69	0.06	0.14	0.16	4	6	0	B
277	33.45967	11.25	-106.9525	5.3	5	0	2006	7	26	20	6	12.52	0.66	-1.71	25.08	5	9	0	Y
278	34.23367	0.32	-106.83817	0.25	4.16	0.53	2006	7	31	8	19	50.18	0.04	0.46	0.24	9	15	2	O
279	34.22817	0.3	-106.83983	0.24	3.44	0.54	2006	7	31	8	20	59.42	0.04	0.63	0.33	9	16	2	O
280	34.0005	0.39	-106.7085	0.66	6.72	1.39	2006	8	6	10	58	31.64	0.13	0.64	0.14	7	9	0	O
281	34.32233	0.92	-106.67567	0.55	7.22	0.66	2006	8	8	8	31	52.78	0.11	-0.14	0.07	4	6	1	O
282	34.0335	0.33	-107.06067	0.43	8.08	0.7	2006	8	29	14	41	57.65	0.06	0.48	0.1	8	13	1	O
283	34.00667	0.29	-107.0175	0.37	7.16	0.49	2006	9	2	3	39	17.65	0.05	0.73	0.65	9	15	3	O
284	34.417	0.49	-106.9935	0.32	5	0	2006	9	5	8	30	43.46	0.07	0.82	0.21	8	14	1	O
285	34.4085	0.54	-107.01867	0.34	5	0	2006	9	6	12	9	0.67	0.07	0.55	0.07	6	10	0	O
286	34.28283	0.5	-106.70117	0.32	5	0	2006	10	7	13	48	31.19	0.05	0.17	0.95	4	9	2	O
287	34.29567	0.55	-106.69717	0.45	10.17	0.89	2006	10	7	13	52	59.33	0.13	0.59	0.09	8	13	1	O
288	34.51583	1.25	-106.26083	1.17	5	0	2006	10	10	6	10	38.32	0.22	1.02	0.12	6	8	0	O
289	34.332	0.72	-106.81783	0.43	5	0	2006	11	10	7	37	38.83	0.11	0.28	0.11	6	9	0	O
290	34.2575	0.51	-106.81067	0.36	5	0	2006	12	6	2	5	31.93	0.07	0.08	0.08	4	8	0	O
291	34.25667	0.31	-106.81383	0.25	5	0	2006	12	6	5	12	14.28	0.04	0.84	0.1	7	13	0	O
292	34.26417	0.48	-106.78283	0.36	5	0	2006	12	23	8	5	19.07	0.07	0.39	0.07	5	9	0	O

293	33.5765	1.64	-107.06333	0.69	7.25	3.16	2006	12	29	17	37	9.14	0.27	1.66	0.07	8	9	0	O
294	34.328	0.38	-106.83933	0.28	5	0	2006	12	31	2	44	31.18	0.05	0.91	0.12	8	14	1	O
295	34.28267	0.67	-106.874	0.52	2.01	6.59	2006	12	31	13	3	4.16	0.11	1.05	0.26	7	9	0	B
296	33.98367	0.66	-106.9465	0.65	5	0	2006	12	31	13	49	44.15	0.09	0.77	0.25	6	10	0	C
297	34.409	0.91	-107.16517	1.12	5	0	2007	1	1	20	47	27.63	0.18	0.39	0.18	6	6	0	O
298	34.07833	0.45	-106.946	0.63	3.13	0.63	2007	1	2	7	12	2.39	0.07	0.25	0.17	4	6	0	O
299	34.08683	0.23	-106.8555	0.28	8.98	0.77	2007	1	28	4	5	16.74	0.08	0.09	0.17	7	11	0	Y
300	34.02517	0.4	-107.04133	0.41	4.26	0.56	2007	1	29	2	14	11.46	0.06	-0.53	0.58	7	14	3	Y
301	34.01733	0.58	-107.0355	0.64	9.21	2.38	2007	1	29	2	15	19.67	0.2	-0.49	0.05	5	6	0	O
302	34.03633	0.31	-107.0435	0.37	8.45	0.38	2007	1	30	12	16	15.13	0.04	0.58	0.1	10	16	2	Y
303	34.0425	0.38	-107.049	0.81	8.29	1.23	2007	1	30	12	18	15.33	0.1	-0.13	0.08	6	8	0	Y
304	34.03683	0.33	-107.049	0.38	8.51	1.08	2007	1	30	12	19	50.16	0.09	0.33	0.12	9	13	0	Y
305	34.0385	0.36	-107.04867	0.48	8.99	1.1	2007	1	30	12	22	3.61	0.09	0.35	0.1	8	12	0	Y
306	34.0375	0.37	-107.04867	0.51	8.46	1.64	2007	1	30	13	10	21.2	0.13	0.65	0.12	8	12	0	Y
307	34.66933	0.3	-107.10367	0.61	5	0	2007	1	30	21	23	21.28	0.07	1.47	3.8	12	18	0	Y
308	34.07533	0.4	-106.99567	0.49	5	0	2007	1	30	22	1	1.42	0.06	1.69	0.09	6	6	0	O
309	34.06817	0.36	-107.01067	0.36	5	0	2007	1	30	22	40	40.9	0.04	1.3	0.17	7	7	0	O
310	34.05967	0.49	-106.996	0.42	6.59	0.8	2007	2	12	18	51	20.06	0.07	0.92	0.21	7	10	1	O
311	34.21783	0.32	-106.89183	0.26	5	0	2007	2	26	0	0	50.35	0.04	0.69	0.11	9	11	0	Y
312	34.3725	0.53	-106.8065	0.31	5	0	2007	2	27	13	18	29.29	0.07	0.72	0.14	10	12	0	Y
313	34.03433	0.26	-107.01467	0.29	1.04	5.35	2007	3	4	7	47	34.87	0.06	0.97	0.22	12	13	0	Y
314	34.58167	0.42	-106.859	0.47	5	0	2007	3	5	7	55	55.67	0.07	1.41	0.09	10	11	0	Y
315	34.33917	0.45	-106.91667	0.31	1.88	3.81	2007	3	8	11	58	57.42	0.07	0.95	0.08	9	11	0	Y
316	34.33933	1.46	-106.71867	2.09	1.38	18.83	2007	3	9	2	0	59.54	0.33	0.95	0.13	4	6	0	O
317	34.02317	0.3	-107.045	0.32	8.66	0.46	2007	3	12	17	5	11.78	0.05	0.79	0.08	8	13	3	O
318	34.36233	0.64	-107.1065	0.76	6.02	1.27	2007	3	27	16	34	7.04	0.13	0.76	0.63	4	7	1	O
319	33.969	0.33	-106.973	0.32	5	0	2007	4	2	23	42	41.63	0.04	0.84	0.22	7	10	0	O
320	34.54333	0.33	-107.13417	0.5	4.8	2.82	2007	4	22	10	21	40.12	0.09	0.84	0.07	6	11	0	O
321	34.351	0.46	-106.72683	0.38	9.27	0.97	2007	5	9	1	41	8.07	0.1	1.15	0.18	8	15	1	O
322	34.32117	0.4	-106.86883	0.3	5	0	2007	5	11	17	42	20.93	0.05	1.1	0.04	8	10	0	O
323	34.30133	0.4	-106.8995	0.3	8.19	0.87	2007	5	14	22	52	19.59	0.06	0.53	0.13	7	11	1	O

324	34.04533	0.29	-107.03217	0.31	5	0	2007	5	15	2	16	48.24	0.04	0.72	0.46	7	11	1	0
325	34.304	0.67	-106.89383	0.45	8.75	0.77	2007	5	15	19	45	37.72	0.1	0.37	0.22	5	10	2	0
326	34.306	0.38	-106.89933	0.29	5	0	2007	5	15	21	5	56.33	0.05	0.46	0.09	7	10	0	0
327	34.363	0.44	-106.83033	0.25	5	0	2007	5	19	0	48	11.27	0.06	1.05	0.17	8	14	0	0
328	34.36633	0.47	-106.82767	0.29	5	0	2007	5	19	4	17	33.55	0.06	0.58	0.16	6	12	1	0
329	34.378	0.86	-106.718	0.95	6.43	2.7	2007	5	22	2	38	17.6	0.21	0.3	0.97	5	8	0	0
330	34.06017	0.27	-107.02983	0.26	5.65	0.97	2007	5	22	17	25	49.67	0.05	1.22	0.06	10	13	0	0
331	34.0585	0.32	-107.02817	0.36	6.5	0.36	2007	5	23	3	0	53.24	0.04	0.2	0.29	8	17	5	0
332	34.06067	0.27	-107.031	0.26	6.55	0.38	2007	5	23	3	5	38.15	0.04	0.48	0.07	8	16	4	0
333	34.0605	0.28	-107.02983	0.28	5.51	1.29	2007	5	23	3	20	51.47	0.07	1.28	0.06	10	11	0	0
334	34.062	0.28	-107.028	0.27	6.8	0.45	2007	5	23	3	41	43.91	0.04	0.24	0.08	8	14	3	0
335	34.062	0.27	-107.02983	0.26	6.85	0.4	2007	5	23	3	42	6.61	0.04	0.36	0.06	8	15	3	0
336	34.05633	0.43	-107.02717	0.38	6.72	0.33	2007	5	23	3	57	27.47	0.05	0.02	0.06	4	10	3	0
337	34.06033	0.29	-107.0295	0.31	5.82	1.26	2007	5	23	5	16	54.91	0.06	2.91	0.06	10	10	0	0
338	34.06017	0.41	-107.03117	0.38	6.67	0.75	2007	5	23	6	55	17.93	0.07	0.29	0.07	6	10	1	0
339	34.06	0.24	-107.02683	0.2	7.04	0.37	2007	5	23	7	38	2.49	0.04	0.54	0.07	10	18	3	0
340	34.061	0.25	-107.03033	0.25	5.49	1.09	2007	5	23	10	46	43.46	0.06	1.15	0.09	11	16	0	0
341	34.05933	0.49	-107.02967	0.35	6.42	0.53	2007	5	23	11	45	41.68	0.06	0.1	0.08	6	13	2	0
342	34.0595	0.34	-107.0305	0.43	6.38	0.51	2007	5	23	21	35	51.46	0.06	0.59	0.09	7	13	3	0
343	34.06133	0.44	-107.028	0.43	6.05	1.26	2007	5	23	22	21	43.32	0.09	0.61	0.05	8	8	0	0
344	34.06067	0.27	-107.02567	0.3	6.75	0.4	2007	5	24	17	15	55.26	0.04	0.65	0.12	10	20	4	0
345	34.06333	0.35	-107.03283	0.36	6.7	0.41	2007	5	28	11	24	3.05	0.05	0.24	0.12	6	13	3	0
346	34.13633	0.29	-106.808	0.25	5	0	2007	5	31	6	4	59.5	0.04	0.58	0.25	7	13	1	0